Міністерство освіти і науки України
Національний університет «Одеська політехніка»

Праці
ОДЕСЬКОГО ПОЛІТЕХНІЧНОГО УНІВЕРСИТЕТУ

Вип. 2(72), 2025

Науковий та науково-виробничий збірник

Виходить два рази на рік

Заснований у лютому 1996 року

Одеса, 2025

Праці Одеського політехнічного університету: Науковий та науково-виробничий збірник. Одеса, 2025. Вип. 1(71). 204 с. Мова: англ., укр.

Рекомендується до друку вченою радою Національного університету «Одеська політехніка», протокол № 8 від 24.12.2025

Комп'ютерна версія опублікованих матеріалів за адресою: https://pratsi.op.edu.ua

Основна назва: **Праці Одеського політехнічного університету; Proceedings of Odessa Polytechnic University.**

Варіанти назви: **Труды Одесского политехнического университета; Trudy Odesskogo politehničeskogo universiteta; Odes'kyi Politechnichnyi Universytet. Pratsi.**

ISSN 2076-2429 (print)
ISSN 2223-3814 (online)

Ministry of Education, Science of Ukraine
Odessa Polytechnic National University

Proceedings
OF ODESSA POLYTECHNIC UNIVERSITY

Issue 2(72), 2025

Scientific, science and technology collected articles

Publication Frequency: 2 issues per year

Established in February 1996

Odesa, 2025

Proceedings of Odessa Polytechnic University: Scientific, science and technology collected articles. Odesa, 2025. Issue 2(72). 204 p. Language: ENG-UKR.

Recommended for publication by the Scientific Council of the Odessa Polytechnic National University, minutes No. 8, December 24, 2025

Free online access to printed materials at: https://pratsi.op.edu.ua

Key title: **Proceedings of Odessa Polytechnic University;**
Праці Одеського політехнічного університету.
Variant title: **Trudy Odesskogo politehničeskogo universiteta;**
Труды Одесского политехнического университета;
Odes'kyi Politechnichnyi Universytet. Pratsi.

ISSN 2076-2429 (print)
ISSN 2223-3814 (online)

ЗМІСТ / CONTENTS

МАШИНОБУДУВАННЯ / MACHINE BUILDING

ЕНЕРГЕТИКА / ENERGETICS

ІНФОРМАЦІЙНІ ТЕХНОЛОГІЇ / INFORMACION TECHNOLOGY

ISSN 2076-2429 (print)
ISSN 2223-3814 (online)

МАШИНОБУДУВАННЯ

MACHINE BUILDING

UDC 519.711, 519.2, 621.9.015

M. Kunitsyn, PhD, Assoc. Prof.,
A. Usov, DSc, Prof.,
Yu. Sikirash
Odessa Polytechnic National University, Shevchenko Ave. 1, Odesa, Ukraine, 65044, e-mail: usov.anatolij.ua@gmail.com

STOCHASTIC MODELING OF NONLINEAR DYNAMICS OF THE MACHINE-TOOL-WORKPIECE SYSTEM AND ITS INFLUENCE ON THE FORMATION OF SURFACE TOPOGRAPHY DURING FINISHING

М. Куніцин, А. Усов, Ю. Сікіраш. **Стохастичне моделювання нелінійної динаміки системи верстат-інструмент-деталь та її вплив на формування топографії поверхні при фінішній обробці.** Забезпечення стабільної якості поверхні при фінішній обробці є критичним завданням сучасного машинобудування, проте традиційні детерміністичні моделі динаміки різання нездатні повною мірою відтворити статистичну природу топографії, що формується в реальних виробничих умовах. Це суттєве обмеження зумовлене ігноруванням випадкових факторів, таких як мікроструктурна неоднорідність оброблюваного матеріалу, флуктуації зносу інструменту та зовнішні вібраційні збурення. У даній роботі запропоновано нову нелінійну стохастичну модель динамічної системи «верстат-пристосування-інструмент-деталь», яка дозволяє ефективно подолати цей розрив між теорією та практикою. Математично система описується стохастичним диференціальним рівнянням із запізненням, що комплексно враховує регенеративний ефект сил різання, нелінійну кубічну жорсткість конструкції та адитивні стохастичні збурення типу білого шуму. Чисельна реалізація моделі виконана з використанням методу Ейлера-Маруями в рамках алгоритму Монте-Карло (N=50). Результати моделювання показали, що стабільна система під дією шуму формує стохастичний атрактор, генеруючи обмежені неперіодичні коливання. Головним науковим результатом є побудова повної функції розподілу ймовірностей для прогнозованої середньоквадратичної шорсткості із середнім значенням μ=14,14 мкм, що дозволяє перейти до ймовірнісного прогнозування якості поверхні замість використання єдиного детермінованого значення. Проведена валідація адекватності моделі продемонструвала високий коефіцієнт детермінації (R^2=0,9999) між дисперсією вхідного шуму та вихідною дисперсією зміщення, що підтверджує фізичну коректність запропонованого підходу. Розроблена методологія створює надійну основу для прогнозування невизначеності технологічного процесу, оцінки надійності обробки та мінімізації браку на відповідальних фінішних операціях.

Ключові слова: стохастичне моделювання, нелінійна динаміка, механічна обробка, топографія поверхні, стохастичне диференціальне рівняння із запізненням, симуляція Монте-Карло, регенеративний ефект

M. Kunitsyn, A. Usov, Yu. Sikirash. **Stochastic modeling of nonlinear dynamics of the machine-tool-workpiece system and its influence on the formation of surface topography during finishing.** Ensuring stable surface quality during finishing operations is a critical task in mechanical engineering; however, traditional deterministic models of machining dynamics fail to fully capture the statistical nature of surface topography formed under real-world conditions. This limitation arises from neglecting random factors such as microstructural material inhomogeneity, tool wear fluctuations, and external vibrational disturbances. This paper proposes a novel nonlinear stochastic model of the "machine-tool-workpiece" dynamic system to bridge this gap between theory and practice. Mathematically, the system is formulated as a Stochastic Differential Delay Equation, which comprehensively incorporates the regenerative effect of cutting forces, nonlinear cubic structural stiffness, and additive stochastic perturbations modeled as white noise. The numerical implementation of the model was performed using the Euler-Maruyama scheme within a Monte Carlo framework (N=50). Simulation results demonstrated that the stable system, under the influence of noise, forms a stochastic attractor, generating bounded non-periodic oscillations. The primary contribution of this study is the derivation of a full Probability Density Function for the predicted Root Mean Square surface roughness, with a mean value of μ=14.14 μm. This enables a shift from single-point deterministic predictions to probabilistic forecasting of surface quality. A rigorous model adequacy validation was conducted, yielding a near-perfect coefficient of determination (R^2=0.9999) between the input noise variance and the output displacement variance, confirming the physical consistency of the proposed approach. The developed methodology provides a robust framework for predicting process uncertainty, assessing machining reliability, and minimizing scrap rates in high-precision finishing operations.

Keywords: stochastic modeling, nonlinear dynamics, machining, surface topography, Stochastic Differential Delay Equation, Monte Carlo simulation, regenerative effect

Introduction

Stochastic fluctuations in cutting force and material properties can amplify nonlinear vibrations and degrade surface quality in machine-tool-workpiece systems during finishing operations. These

DOI: 10.15276/opu.2.72.2025.01

ISSN 2076-2429 (print)
ISSN 2223-3814 (online)

fluctuations-such as random variations in cutting force or material heterogeneity-act as external disturbances that interact with the inherent nonlinearities of the system, arising from joint friction, structural flexibility, and regenerative effects [1, 2, 3]. When subjected to such fluctuations, the system can exhibit periodic, quasi-periodic, and chaotic vibrations, especially near resonance [2, 3]. The amplitude and frequency content of these vibrations are strongly influenced by the magnitude and spectral characteristics of the stochastic inputs [4, 5].

Surface quality is most affected by roughness and defects [4, 6], dynamic instability [7], and noise-induced effects [4]. The statistical properties of vibrations are linked to surface topography parameters (e.g., R_a, R_q) through regression, spectral analysis, or machine learning. Linear and nonlinear regression models predict roughness from vibration RMS [8, 9]. Spectral and principal component analysis extract correlated vibration features [10]. Physics-based models simulate topography by superimposing vibrations on the tool path [11]. Machine learning uses vibration features for high-accuracy predictions [12].

Analysis of recent research and publications

Deterministic models of nonlinear vibrations fail to predict actual surface quality accurately because they neglect random disturbances such as material inhomogeneity, tool wear, and environmental fluctuations, leading to discrepancies between predicted and measured profiles [13]. These models are typically validated under controlled laboratory conditions and lose predictive accuracy when applied to industrial settings with varying machines, materials, or process parameters [13].

Idealized assumptions in deterministic models inadequately capture key nonlinearities, including friction, tool disengagement, and regenerative chatter effects, which significantly influence surface formation [14]. Deterministic approaches struggle to model multi-axis vibrations and high-frequency phenomena in advanced processes like ultrasonic vibration-assisted machining, resulting in errors in roughness prediction [15].

The Fokker-Planck equation models the probabilistic evolution of system states in stochastic cutting dynamics, with recent deep learning solvers enabling solutions for high-dimensional cases [16]. Monte Carlo simulations propagate uncertainties from process parameters through cutting force models to predict surface roughness and optimize robustness [17].

Spectral analysis using Gaussian processes simulates random cutting force fluctuations and distinguishes stochastic noise from deterministic chatter in vibration signals [18]. Stochastic differential equations incorporate Gaussian white noise into deterministic cutting models, capturing high-frequency fluctuations for more realistic dynamic simulations [19].

Surrogate models like stochastic kriging approximate stability boundaries under uncertainty, offering computational efficiency over full Monte Carlo methods [17]. High-dimensional stochastic models remain limited for multi-physics cutting systems, lacking scalable methods for coupled vibrations and surface formation [20].

Real-time integration of sensor data with stochastic models for adaptive control or online topography prediction is underexplored [19]. Stochastic defects in materials, modeled as random variables with probabilistic distributions, are integrated into dynamic response predictions using Monte Carlo and statistical finite element methods [21].

Cubic structural stiffness introduces nonlinear effects like hardening/softening and jump phenomena, amplifying vibrations under stochastic inputs [22]. Regenerative cutting forces, dependent on delayed vibrations, are the primary source of chatter instability in nonlinear machining dynamics [22].

Nonlinear friction in tool-workpiece interfaces exhibits velocity-dependent behavior, influencing both vibration excitation and suppression [23].

Problem. Most cutting dynamics models are deterministic. They can predict the stability limit (the onset of “chipping”), but cannot adequately describe the statistical nature of surface roughness, which is formed in real conditions under the influence of random factors. Existing models describe nonlinear oscillations, but not their stochastic nature.

Hypothesis. The introduction of stochastic disturbances into a nonlinear differential model of the dynamics of the machine-tool-workpiece system will allow not only to determine the limits of stability, but also to obtain a statistically reliable forecast of the parameters of the topography of the machined surface, which is more consistent with experimental data than purely deterministic models.

The purpose and objectives of the research

To develop a mathematical model for analyzing the influence of stochastic disturbances in the nonlinear dynamic machine-tool-workpiece system on the probabilistic characteristics of the quality (topography) of the surface layer during finishing operations.

Research Methodology

Stochastic differential equations (SDEs) and high-dimensional probabilistic modeling are suited for coupling nonlinear vibrations with random surface topography, while probabilistic cellular automata are specialized for discrete microstructure evolution [24, 25]. SDEs model nonlinear instabilities under stochastic influences, extendable to spatial effects via random fields [24, 26]. SDE-based models predict fluctuation propagation to surface topography when coupled with statistical analysis [27].

High-dimensional methods like probability density evolution handle joint uncertainties in dynamic response and surface formation [28]. Numerical integration via Euler-Maruyama or Monte Carlo is standard for nonlinear machining SDEs, as analytical Fokker-Planck solutions are limited [29, 30].

Model Definition. Dominant nonlinear forces include cubic structural stiffness causing hardening/softening and jump phenomena [22], regenerative cutting force inducing chatter, nonlinear friction with velocity dependence [23], process damping at low speeds [22], and non-smooth contact at large amplitudes [31].

Main stochasticity sources are random material properties varying cutting forces [32], friction fluctuations from wear [23], tool wear progression [32], abrasive grain distribution [33], and external noise as Gaussian processes [34].

To bridge the sources of stochasticity with the governing dynamics, these random effects are incorporated into the cutting force $\mathbf{F}_c(\mathbf{q},t)$ and as an additive stochastic term $\mathbf{\Gamma}(t)$, transforming the deterministic equation of motion into a system of stochastic differential equations [18, 19].

The system for relative displacement $\mathbf{q}(t)$ is:

$$\mathbf{M}\ddot{\mathbf{q}}(t)+\mathbf{C}\dot{\mathbf{q}}(t)+\mathbf{K}\mathbf{q}(t)=\mathbf{F}_c(\mathbf{q},t)+\mathbf{\Gamma}(t),$$

with $\mathbf{\Gamma}(t)$ as stochastic noise [18, 19].

Inputs: stiffness $\mathbf{K}$, damping $\mathbf{C}$, cutting coefficients (stochastic), noise variance σ^2, mass $\mathbf{M}$, process parameters [35].

Outputs: displacement time series, surface topography via tool path integration, statistical moments (e.g., S_a, S_q), stability indicators [18, 19, 27].

Theoretical Basis and Model Formulation

Physical Formulation and Basic Model. The aim of this study is to perform stochastic modeling of the dynamics of the "machine-tool-workpiece" (MTW) system to predict the statistical characteristics of surface topography. The key indicator that directly shapes the micro-relief is the vector of relative displacement between the cutting tool and the workpiece in a plane perpendicular to the cutting axis.

Let us denote this vector as $\mathbf{q}(t)\in R^n$ (where n is the number of degrees of freedom, usually $n=2$). In the most general form, the dynamics of this system are described by the classical Langevin equation (equation of motion):

$$\mathbf{M}\ddot{\mathbf{q}}(t)+\mathbf{C}\dot{\mathbf{q}}(t)+\mathbf{K}\mathbf{q}(t)=\mathbf{F}_c(t), \quad (1)$$

where $\mathbf{M}$ is the system mass matrix ($n\times n$), $\mathbf{C}$ is the damping matrix ($n\times n$), $\mathbf{K}$ is the stiffness matrix ($n\times n$), $\mathbf{F}_c(t)$ is the vector of external forces, primarily cutting forces ($n\times 1$).

This deterministic linear model (1) is unable to describe two key aspects of real processing noted in the problem statement: nonlinear effects (vibration generation, "crushing") and stochastic nature (random nature of topography).

Introduction of nonlinearities. Model (1) is refined by introducing dominant nonlinear factors identified in the literature review.

1. Structural nonlinearity (cubic stiffness): The actual stiffness of machine tool components is not linear. The elastic resistance force $\mathbf{F}_s$ is more accurately described as a nonlinear displacement function. By introducing dominant cubic nonlinearity (hardening/softening effects), we replace the linear term $\mathbf{K}\mathbf{q}(t)$:

$$\mathbf{F}_s(\mathbf{q})=\mathbf{K}\mathbf{q}(t)+\mathbf{F}_{nl}(\mathbf{q}), \quad (2)$$

where $\mathbf{F}_{nl}(\mathbf{q})$ is a vector of nonlinear forces, whose components are usually cubic polynomials of the components $\mathbf{q}$ (e.g., $\sim k_{nl}q_i^3$).

ISSN 2076-2429 (print)
ISSN 2223-3814 (online)

2. Nonlinearity of the process (regenerative effect): A key source of dynamic instability (chatter). The cutting force $\mathbf{F}_c$ depends not on the absolute position of the tool, but on the current thickness of the layer being cut. This thickness, in turn, is the difference between the current position of the tool $\mathbf{q}(t)$ and the position of the tool on the previous revolution $\mathbf{q}(t-T)$, where T is the period of one revolution of the workpiece:

$$\Delta\mathbf{q}(t)=\mathbf{q}(t)-\mathbf{q}(t-T). \tag{3}$$

The cutting force $\mathbf{F}_c$ also depends nonlinearly on the cutting speed $\dot{\mathbf{q}}(t)$ (nonlinear damping of the process). Thus, the deterministic cutting force becomes a nonlinear function with a delay:

$$\mathbf{F}_c(t)\to\mathbf{F}_c(\Delta\mathbf{q}(t),\dot{\mathbf{q}}(t))=\mathbf{F}_c(\mathbf{q}(t)-\mathbf{q}(t-T),\dot{\mathbf{q}}(t)). \tag{1}$$

Combining (1), (2), and (4), we obtain a deterministic nonlinear model with delay:

$$\mathbf{M}\ddot{\mathbf{q}}(t)+\mathbf{C}\dot{\mathbf{q}}(t)+\mathbf{K}\mathbf{q}(t)+\mathbf{F}_{nl}(\mathbf{q})=\mathbf{F}_c(\mathbf{q}(t)-\mathbf{q}(t-T),\dot{\mathbf{q}}(t)). \tag{5}$$

Introduction of stochastic factors. Model **Ошибка! Источник ссылки не найден.** is still deterministic and will only predict convergence to a point or limit cycles (stable "fragmentation"). To describe the statistical nature of the topography, we introduce stochastic (random) perturbations using the space (Ω, F, P).

1. Additive noise (external fluctuations): Models unaccounted for high-frequency fluctuations in the process: fluctuations in drives, random shocks, etc. Introduced as an additive force term $\mathbf{\Gamma}(t,\omega)$.

2. Parametric/Multiplicative noise (Internal fluctuations): This is the core of the hypothesis. The parameters of the system itself are random processes:

– Material randomness: Heterogeneities (ω_m) cause the cutting force coefficients $\mathbf{F}_c$ to fluctuate over time.

– Tool wear: The random wear process (ω_w) causes a slow random "drift" of the stiffness $\mathbf{K}$ and damping $\mathbf{C}$ parameters.

Thus, the deterministic matrices and functions from (5) are replaced by their stochastic analogues:

$$\mathbf{C}\to\mathbf{C}(t,w_w),$$

$$\mathbf{K}\to\mathbf{K}(t,w_w),$$

$$\mathbf{F}_c(\ldots)\to\mathbf{F}_c(\ldots,w_m).$$

Final Stochastic Model. Combining all components, we obtain a system of nonlinear stochastic differential equations with delay and stochastic coefficients:

$$\mathbf{M}\ddot{\mathbf{q}}(t)+\mathbf{C}(t,w)\dot{\mathbf{q}}(t)+\mathbf{K}(t,w)\mathbf{q}(t)+\mathbf{F}_{nl}(\mathbf{q})=\mathbf{F}_c(\mathbf{q}(t)-\mathbf{q}(t-T),\dot{\mathbf{q}}(t),\omega)\mathbf{\Gamma}(t,\omega). \tag{6}$$

Physical meaning of variables in the final model (6):

– $\mathbf{q}(t)$: ($n\times1$) Relative displacement vector (instrument-part) – the quantity of interest;

– $\mathbf{M}$: ($n\times n$) Mass matrix (deterministic).

– $\mathbf{C}(t,\omega)$: ($n\times n$) Stochastic damping matrix (includes deterministic part and wear fluctuations).

– $\mathbf{K}(t,\omega)$: ($n\times n$) Stochastic linear stiffness matrix (includes deterministic part and wear fluctuations).

– $\mathbf{F}_{nl}(\mathbf{q})$: ($n\times1$) Vector of nonlinear structural stiffness forces (e.g., cubic).

– $\mathbf{F}_c(\ldots,\omega)$: ($n\times1$) Vector of nonlinear cutting force depending on:

  – $\mathbf{q}(t)-\mathbf{q}(t-T)$: Vector of lagging displacement (regenerative effect).

  – $\dot{\mathbf{q}}(t)$: Vector of velocity (nonlinear damping).

  – ω: Random fluctuations (material heterogeneity).

– T: Period of one revolution (scalar, delay time).

– $\mathbf{\Gamma}(t,\omega)$: ($n\times1$) Additive noise vector (external fluctuations).

Reduction to a form suitable for numerical solution. Equation (6) is a second-order system, which is inconvenient for integrators. For numerical implementation, it must be converted to a first-order system.

Let us introduce the state vector $\mathbf{x}(t) \in \mathbf{R}^{2n}$:

$$\mathbf{x}(t) = \begin{bmatrix} \mathbf{q}(t) \\ \dot{\mathbf{q}}(t) \end{bmatrix} \begin{bmatrix} \mathbf{x}_1(t) \\ \mathbf{x}_2(t) \end{bmatrix}. \tag{7}$$

Then the derivative $\dot{\mathbf{x}}(t)$ will be:

$$\dot{\mathbf{x}}(t) = \begin{bmatrix} \dot{\mathbf{q}}(t) \\ \ddot{\mathbf{q}}(t) \end{bmatrix} = \begin{bmatrix} \mathbf{x}_2(t) \\ \mathbf{M}^{-1}[\mathbf{F}_{\text{total}}] \end{bmatrix}, \tag{8}$$

where $\mathbf{F}_{\text{total}}$ is the sum of all forces from the right and left parts of (6) transferred to the right (except for $\mathbf{M}\ddot{\mathbf{q}}$).

Writing the stochastic terms in canonical Ito form (where $d\mathbf{W}(t)$ is a Wiener process), we reduce (6) to the standard form of a Stochastic Delay Differential Equation (SDDE):

$$d\mathbf{x}(t) = \mathbf{f}(\mathbf{x}(t), \mathbf{x}(t-T), t)dt + \mathbf{G}(\mathbf{x}(t), \mathbf{x}(t-T), t)d\mathbf{W}(t). \tag{9}$$

This form (9) is the final result, where $\mathbf{f}(\ldots)$ is the deterministic drift term containing all nonlinear and deterministic forces; $\mathbf{G}(\ldots)$ is the diffusion matrix containing all additive and multiplicative stochastic coefficients; $d\mathbf{W}(t)$ is the vector Wiener process.

Feasibility check. The model in form (9) is completely ready for numerical solution. It can be implemented using numerical integrator by modified Euler-Maruyama method or stochastic Runge-Kutta for SDDE; or Monte Carlo simulations by repeatedly (thousands of times) numerically integrating (9) with different realizations of $d\mathbf{W}(t)$ to obtain an ensemble of trajectories $\mathbf{x}(t)$; or by topography analysis where each trajectory $\mathbf{q}(t) = \mathbf{x}_1(t)$ from the ensemble represents one random realization of the surface topography. Analysis of this ensemble (calculation of R_a, R_q, asymmetry) will give the desired statistical prediction of surface quality.

Research results

The stochastic differential delay equation (SDDE) model, as formulated in (9), was solved numerically to investigate the system's dynamic behavior and its resultant impact on surface topography. The simulation was performed using a 1-DoF model with parameters representative of a stable finishing process on AISI 1045 steel, as detailed in the simulation code.

Numerical Simulation Algorithm. The complex, non-linear, and stochastic-delay nature of the final model (9) precludes a closed-form analytical solution. Therefore, a numerical approach based on the Euler-Maruyama integration scheme was implemented in Python with a time step of $dt = 1 \times 10^{-6}$ s, accelerated using Numba for JIT-compilation. The core computational process is divided into two main algorithms, as illustrated in the flowcharts below: the primary Monte Carlo simulation for topography prediction and a secondary adequacy test for model validation.

Next diagram (Fig. 1) illustrates the main simulation loop ($N = 50$) used to solve the SDDE and aggregate the statistical results for surface topography (as shown later in Fig. 6).

Next diagram (Fig. 2) shows the validation process ($N = 20$ runs per level) used to test the model's physical consistency by correlating input noise power with output system power (as shown later in Fig. 7).

The analysis in the following sections is presented based on the outputs of these two core algorithms. The analysis is presented in three parts: first, an examination of the system's steady-state dynamics from individual simulation runs; second, the aggregated statistical findings from a Monte Carlo analysis; and third, a crucial validation of the model's physical adequacy.

Single-Run Dynamic Analysis. To understand the fundamental behavior of the system, individual simulation trajectories were analyzed after the initial transient period ($t > 0.25$ s).

Fig. 3 illustrates the relative displacement $\mathbf{q}(t)$ during the steady-state phase for three distinct simulations. The trajectories confirm that the system, governed by the selected stable parameters (e.g., k, c, k_{n_1}, and K_r), does not diverge. Instead, it settles into bounded, non-periodic oscillations. This behavior is characteristic of a stable nonlinear system under persistent stochastic excitation. The amplitude of these vibrations, which directly dictates the kinematic component of surface roughness, is dynamically constrained by the interplay of the linear damping (c) and the nonlinear "hardening"

ISSN 2076-2429 (print)
ISSN 2223-3814 (online)

stiffness (k_{n_1}). The non-periodic, chaotic-like nature is a direct consequence of the persistent stochastic force term $\mathbf{\Gamma}(t,\omega)$, which models the physical randomness of the process.

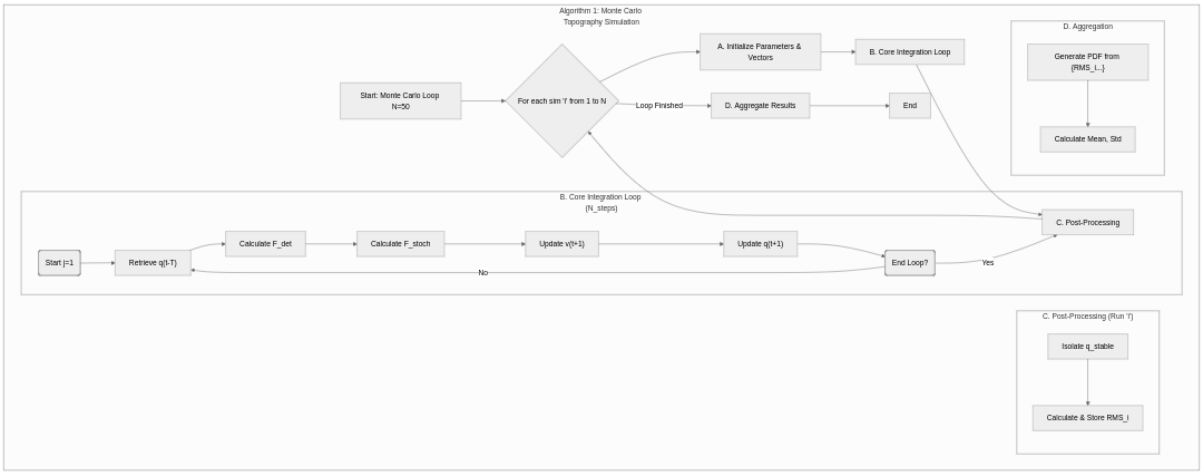

Fig. 1. Algorithm of the Monte Carlo topography simulation

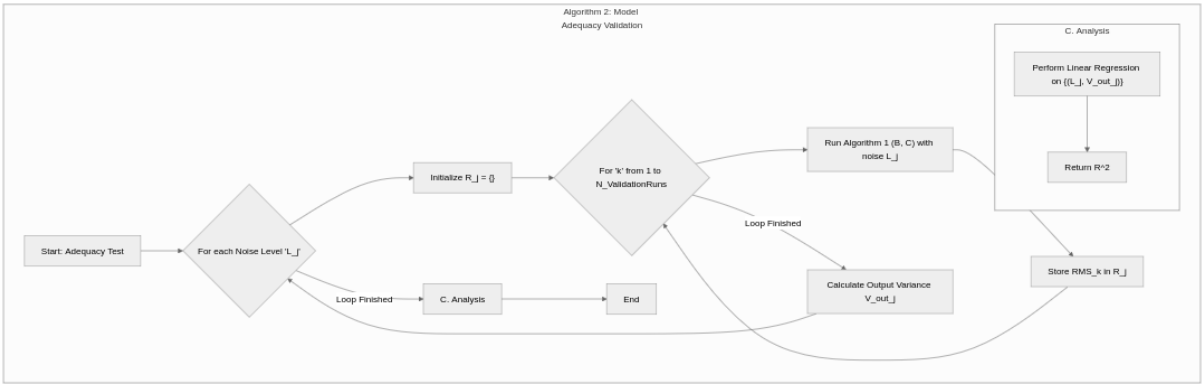

Fig. 2. Algorithm of the model adequacy validation

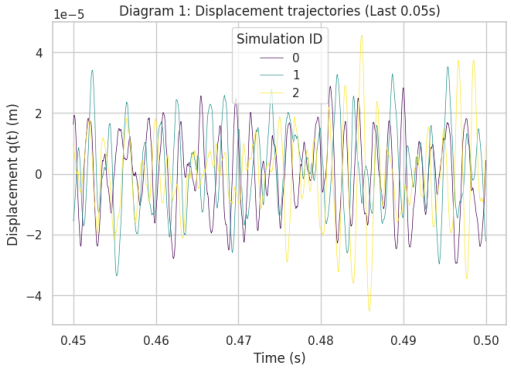

Fig. 3. Steady-state displacement trajectories for three independent simulation runs (last 0.05 s)

Fig. 4 presents the corresponding steady-state phase portrait, plotting system velocity $\dot{\mathbf{q}}(t)$ against displacement $\mathbf{q}(t)$. In a classical deterministic system, a stable process would converge to a fixed point (no vibration) or a clean limit cycle (periodic chatter). However, the introduction of stochasticity transforms this behavior. The system converges not to a simple geometric line, but to a stochastic attractor. This bounded, cloud-like distribution in the phase plane represents the probability density of the system's state. The stochastic force term continuously perturbs the system's trajectory, causing it to densely explore this bounded region. The dimensions of this attractor define the maximum extents of displacement and velocity, providing a clear visual representation of the system's dynamic stability and energy.

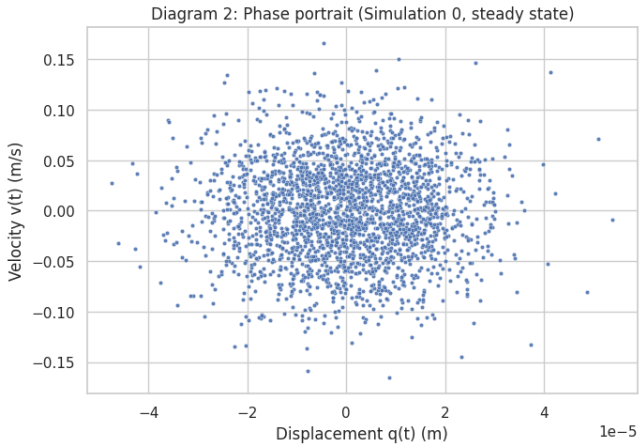

Fig. 4. Steady-state phase portrait for a single simulation run (Simulation 0, $t > 0.25$ s)

Fig. 5 displays a high-resolution fragment of the input stochastic force, $\mathbf{\Gamma}(t,\omega)$, which serves as the primary random excitation in the model. This term, modeled numerically as scaled Gaussian white noise, represents the aggregation of all unmodeled, high-frequency disturbances inherent in the cutting process, such as material micro-inhomogeneities, grain-boundary interactions, and high-frequency force fluctuations. This persistent stochastic input is the fundamental driver that propagates through the nonlinear and delayed dynamics of the system (6) to generate the stochastic response observed in Fig. 3 and Fig. 4.

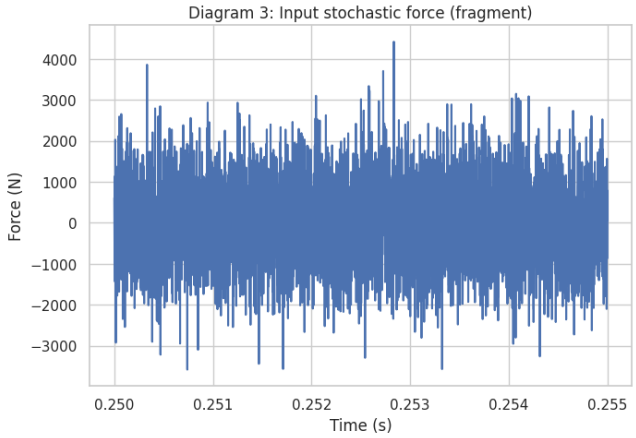

Fig. 5. Representative fragment of the input stochastic force $\mathbf{\Gamma}(t,\omega)$ (Simulation 0)

Monte Carlo Statistical Analysis. The primary objective of this study is to move beyond singular trajectories and provide a probabilistic forecast of surface quality. To achieve this, a Monte Carlo analysis ($N = 50$) was performed.

Fig. 6 presents the principal result of the stochastic simulation. The histogram depicts the probability density function (PDF) of the predicted Root Mean Square (RMS) surface roughness, calculated from the steady-state portion of 50 independent simulation runs. This result eschews a single, deterministic prediction in favor of a statistically robust forecast.

The distribution, which approximates a Gaussian profile, is centered at a mean value μ of 14.14 μm, with a standard deviation σ of approximately 0.72 μm. This mean value represents the expected surface roughness for the given process parameters. The variance quantifies the inherent process variability, providing a confidence interval for the achievable surface quality. This probabilistic approach is a significant advancement over deterministic models, as it allows for the quantification of process uncertainty and reliability.

Model Adequacy Validation. Finally, a critical test was performed to validate the physical and numerical adequacy of the model. According to stochastic systems theory, for a stable linear or weakly nonlinear system, the output power (variance) should be directly proportional to the input power (variance of the noise).

ISSN 2076-2429 (print)
ISSN 2223-3814 (online)

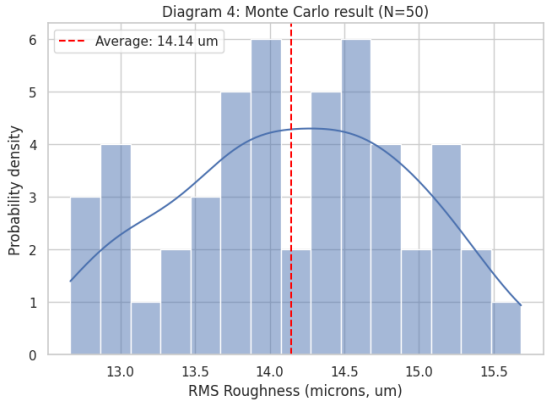

Fig. 6. Probability density function of predicted RMS surface roughness from Monte Carlo analysis ($N = 50$)

Fig. 7 plots the mean output displacement variance (RMS²) as a function of the input noise variance (defined by noise strength). The simulation was run 20 times at each of 6 distinct noise levels. The resulting data points demonstrate a clear and strong linear relationship.

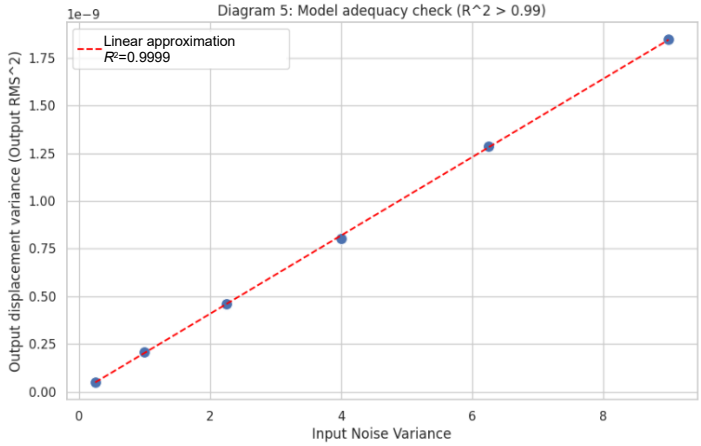

Fig. 7. Output displacement variance (RMS²) versus input noise variance

A linear regression fitted to this data yields a coefficient of determination $R^2 = 0.9999$. This near-perfect linear correlation confirms that the model is adequate, stable, and physically consistent. It validates that the numerical simulation does not suffer from divergence or artifact-inducing numerical errors, and that the system's response to stochastic excitation is well-behaved and predictable in a statistical sense. This validation provides high confidence in the statistical results presented in Fig. 6.

Conclusions

In this study, a nonlinear stochastic dynamic model of the MFTW system was developed and numerically implemented to bridge the gap between theoretical dynamics and practical machining quality assurance. The following conclusions and practical recommendations are drawn:

1. The dynamic analysis demonstrated that under finishing conditions, the interplay of regenerative feedback and stochastic noise transforms the system's behavior from a simple limit cycle to a stochastic attractor. This results in bounded, non-periodic vibrations that cannot be predicted by deterministic models alone.

2. The application of the Monte Carlo method ($N = 50$) allowed for the generation of a Probability Density Function (PDF) for the RMS surface roughness. It was established that the roughness follows a distribution with a mean of $\mu = 14.14$ μm and a standard deviation of $\sigma = 0.72$ μm.

3. The model's adequacy was rigorous validated ($R^2 = 0.9999$), confirming a linear relationship between input noise variance and output topography variance, which proves the physical consistency of the proposed SDDE formulation.

Based on the simulation results, the following guidelines are proposed for industrial application to minimize scrap rates due to random disturbances:

1. Engineers should abandon single-value roughness predictions. Instead, the "3-sigma" rule should be applied based on the model's PDF output. For the modeled parameters, to ensure a 99.7% yield (scrap rate < 0.3%), the process tolerance should be set not at the mean (14.14 μm), but at the upper statistical limit ($\mu + 3\sigma \approx 16.3$ μm).

2. To suppress the stochastic nonlinear effects identified in the phase portrait (Fig. 4), it is recommended to select equipment where the static stiffness k exceeds the process regenerative stiffness K_r by a safety factor of at least 2.5. This prevents the system from entering the "unstable" zone where stochastic resonance can amplify microscopic external vibrations.

3. Since the adequacy test (Fig. 7) proved the direct transfer of input noise to output roughness, effective isolation of the finishing machine from external floor vibrations and thermal fluctuations in the workshop is critical. Reducing the external noise variance by 50% leads to a proportional reduction in the dispersion of the final surface topography, directly improving process capability (C_{pk}).

Література

1. Nonlinear dynamic modeling and vibration analysis of whole machine tool / H. Miao et al. *International Journal of Mechanical Sciences*. 2023. Vol. 245. P. 108122. DOI: 10.1016/j.ijmecsci.2023.108122.
2. Chanda A., Dwivedy S. K. Nonlinear dynamic analysis of flexible workpiece and tool in turning operation with delay and internal resonance. *Journal of Sound and Vibration*. 2018. Vol. 434. P. 358–378. DOI: 10.1016/j.jsv.2018.05.043.
3. Systematic approach for reducing micro-crack formation in Inconel 713LC components fabricated by laser powder bed fusion / H.-Y. Wang et al. *Rapid Prototyping Journal*. 2021. Vol. 27, No. 8. P. 1548–1561. DOI: 10.1108/RPJ-11-2020-0282.
4. Surface Quality of a Work Material's Influence on the Vibrations of the Cutting Process / J. Lipski et al. *Journal of Sound and Vibration*. 2002. Vol. 252, No. 4. P. 729–737. DOI: 10.1006/jsvi.2001.3943.
5. Youla parameterized adaptive vibration control against deterministic and band-limited random signals / F. Qian et al. *Mechanical Systems and Signal Processing*. 2019. Vol. 134. P. 106359. DOI: 10.1016/j.ymssp.2019.106359.
6. Usov A., Kunitsyn M. Modeling the impact of nonlinear oscillations on the quality of the working surface of parts in finishing operations. *Cutting & Tools in Technological System*. 2025. No. 102. P. 20–36. DOI: 10.20998/2078-7405.2025.102.02.
7. Investigation of Dynamic Behavior and Process Stability at Turning of Thin-Walled Tubular Workpieces Made of 42CrMo4 Steel Alloy / K. Mehdi et al. *Machines*. 2024. Vol. 12, No. 2. P. 120. DOI: 10.3390/machines12020120.
8. Bouchama R., Bouhalais M. L., Cherfia A. Surface roughness and tool wear monitoring in turning processes through vibration analysis using PSD and GRMS. *The International Journal of Advanced Manufacturing Technology*. 2024. Vol. 130, No. 7–8. P. 3537–3552. DOI: 10.1007/s00170-023-12742-x.
9. Abouelatta O. B., Mádl J. Surface roughness prediction based on cutting parameters and tool vibrations in turning operations. *Journal of Materials Processing Technology*. 2001. Vol. 118, No. 1–3. P. 269–277. DOI: 10.1016/S0924-0136(01)00959-1.
10. García Plaza E., Núñez López P. J. Surface roughness monitoring by singular spectrum analysis of vibration signals. *Mechanical Systems and Signal Processing*. 2017. Vol. 84. P. 516–530. DOI: 10.1016/j.ymssp.2016.06.039.
11. Surface topography prediction in peripheral milling of thin-walled parts considering cutting vibration and material removal effect / Y. Zhuo et al. *International Journal of Mechanical Sciences*. 2021. Vol. 211. P. 106797. DOI: 10.1016/j.ijmecsci.2021.106797.
12. Lin C.-J., Jhang J.-Y., Young K.-Y. Parameter Selection and Optimization of an Intelligent Ultrasonic-Assisted Grinding System for SiC Ceramics. *IEEE Access*. 2020. Vol. 8. P. 195721–195732. DOI: 10.1109/ACCESS.2020.3033884.
13. Novel Framework for Quality Control in Vibration Monitoring of CNC Machining / G. Apostolou et al. *Sensors*. 2024. Vol. 24, No. 1. P. 307. DOI: 10.3390/s24010307.
14. Kibbou E. M., Dellagi S., Majdouline I., Moufki A. Prediction of Surface Quality Based on the Non-Linear Vibrations in Orthogonal Cutting Process: Time Domain Modeling. *Journal of Manufacturing and Materials Processing*. 2019. Vol. 3, No. 3. P. 53. DOI: 10.3390/jmmp3030053.
15. Theoretical Modeling and Surface Roughness Prediction of Microtextured Surfaces in Ultrasonic Vibration-Assisted Milling / C. Ni et al. *Chinese Journal of Mechanical Engineering*. 2024. Vol. 37, No. 1. P. 51. DOI: 10.1186/s10033-024-01033-5.

ISSN 2076-2429 (print)
ISSN 2223-3814 (online)

16. Solving Fokker–Planck equations using deep KD-tree with a small amount of data / H. Zhang et al. *Nonlinear Dynamics*. 2022. Vol. 108, No. 4. P. 4029–4043. DOI: 10.1007/s11071-022-07361-2.
17. Wan J., Che Y., Wang Z., Cheng C. Uncertainty Quantification and Optimal Robust Design for Machining Operations. *Journal of Computing and Information Science in Engineering*. 2023. Vol. 23, No. 1. P. 011005. DOI: 10.1115/1.4055039.
18. Fodor G., Sykora H. T., Bachrathy D. Stochastic modeling of the cutting force in turning processes. *The International Journal of Advanced Manufacturing Technology*. 2020. Vol. 111, No. 1–2. P. 213–226. DOI: 10.1007/s00170-020-05877-8.
19. Liu Y., Xiong Z., Liu Z. Stochastic Cutting Force Modeling and Prediction in Machining. *Journal of Manufacturing Science and Engineering*. 2020. Vol. 142, No. 12. P. 121004. DOI: 10.1115/1.4047626.
20. Adaptive normalizing flows for solving Fokker–Planck equation / W. Xu et al. *Chaos: An Interdisciplinary Journal of Nonlinear Science*. 2025. Vol. 35, No. 8. P. 083116. DOI: 10.1063/5.0273776.
21. Modeling the effect of stochastic defects formed in products during machining on the loss of their functional dependencies / A. Usov et al. *Proceedings of Odessa Polytechnic University*. 2022. Vol. 1, No. 65. P. 16–29. DOI: 10.15276/opu.1.65.2022.02.
22. Moradi H., Vossoughi G., Movahhedy M. R. Experimental dynamic modelling of peripheral milling with process damping, structural and cutting force nonlinearities. *Journal of Sound and Vibration*. 2013. Vol. 332, No. 19. P. 4709–4731. DOI: 10.1016/j.jsv.2013.03.029.
23. Time domain coupled simulation of machine tool dynamics and cutting forces considering the influences of nonlinear friction characteristics and process damping / R. Sato et al. *Precision Engineering*. 2020. Vol. 61. P. 103–109. DOI: 10.1016/j.precisioneng.2019.10.010.
24. O'Leary J., Paulson J. A., Mesbah A. Stochastic physics-informed neural ordinary differential equations. *Journal of Computational Physics*. 2022. Vol. 468. P. 111466. DOI: 10.1016/j.jcp.2022.111466.
25. Soize C., Ghanem R. Probabilistic-learning-based stochastic surrogate model from small incomplete datasets for nonlinear dynamical systems. *Computer Methods in Applied Mechanics and Engineering*. 2024. Vol. 418. P. 116498. DOI: 10.1016/j.cma.2023.116498.
26. Soize C., Farhat C. A nonparametric probabilistic approach for quantifying uncertainties in low-dimensional and high-dimensional nonlinear models. *International Journal for Numerical Methods in Engineering*. 2017. Vol. 109, No. 6. P. 837–888. DOI: 10.1002/nme.5312.
27. Modelling of machined surface topography and anisotropic texture direction considering stochastic tool grinding error and wear in peripheral milling / C. Cai et al. *Journal of Materials Processing Technology*. 2021. Vol. 292. P. 117065. DOI: 10.1016/j.jmatprotec.2021.117065.
28. A decoupled approach for determination of the joint probability density function of a high-dimensional nonlinear stochastic dynamical system via the probability density evolution method / M.-Z. Lyu et al. *Computer Methods in Applied Mechanics and Engineering*. 2024. Vol. 418. P. 116443. DOI: 10.1016/j.cma.2023.116443.
29. Kloeden P. E., Platen E. Numerical Solution of Stochastic Differential Equations. Berlin ; Heidelberg : Springer Berlin Heidelberg, 1992. DOI: 10.1007/978-3-662-12616-5.
30. Multi-level Monte Carlo methods with the truncated Euler–Maruyama scheme for stochastic differential equations / Q. Guo et al. *International Journal of Computer Mathematics*. 2018. Vol. 95, No. 9. P. 1715–1726. DOI: 10.1080/00207160.2017.1329533.
31. Mohammadi Y., Ahmadi K. Finite-amplitude stability in regenerative chatter: The effect of process damping nonlinearity and intermittent cutting in turning. *Journal of Sound and Vibration*. 2022. Vol. 537. P. 117158. DOI: 10.1016/j.jsv.2022.117158.
32. Zhang X., Yu T., Zhao J. An analytical approach on stochastic model for cutting force prediction in milling ceramic matrix composites. International Journal of Mechanical Sciences. 2020. Vol. 168. P. 105314. DOI: 10.1016/j.ijmecsci.2019.105314.
33. Lv D., Yan C., Chen G., Liu D., Wu X., Zhu Y. Mechanistic prediction for cutting force in rotary ultrasonic machining of BK7 glass based on probability statistics. *Ultrasonics.* 2020. Vol. 101. P. 106006. DOI: 10.1016/j.ultras.2019.106006.
34. Sykora H.T., Hajdu D., Dombovari Z., Bachrathy D. Chatter formation during milling due to stochastic noise-induced resonance. *Mechanical Systems and Signal Processing.* 2021. Vol. 161. P. 107987. DOI: 10.1016/j.ymssp.2021.107987.
35. Liu J., Niu Y., Zhao Y., Zhang L., Zhao Y. Prediction of Surface Topography in Robotic Ball-End Milling Considering Tool Vibration. *Actuators.* 2024. Vol. 13, No. 2. P. 72. DOI: 10.3390/act13020072.

References

1. Miao, H., Wang, C., Li, C., Song, W., Zhang, X., & Xu, M. (2023). Nonlinear dynamic modeling and vibration analysis of whole machine tool. *International Journal of Mechanical Sciences*, *245*, Article 108122. DOI: 10.1016/j.ijmecsci.2023.108122.
2. Chanda, A., & Dwivedy, S. K. (2018). Nonlinear dynamic analysis of flexible workpiece and tool in turning operation with delay and internal resonance. *Journal of Sound and Vibration*, *434*, 358–378. DOI: 10.1016/j.jsv.2018.05.043.
3. Wang, H.-Y., Lo, Y.-L., Tran, H.-C., Raza, M. M., & Le, T.-N. (2021). Systematic approach for reducing micro-crack formation in Inconel 713LC components fabricated by laser powder bed fusion. *Rapid Prototyping Journal*, *27*(8), 1548–1561. DOI: 10.1108/RPJ-11-2020-0282.
4. Lipski, J., Litak, G., Rusinek, R., Szabelski, K., Teter, A., Warmiński, J., & Zaleski, K. (2002). Surface quality of a work material's influence on the vibrations of the cutting process. *Journal of Sound and Vibration*, *252*(4), 729–737. DOI: 10.1006/jsvi.2001.3943.
5. Qian, F., Wu, Z., Zhang, M., Wang, T., Wang, Y., & Yue, T. (2019). Youla parameterized adaptive vibration control against deterministic and band-limited random signals. *Mechanical Systems and Signal Processing*, *134*, Article 106359. DOI: 10.1016/j.ymssp.2019.106359.
6. Usov, A., & Kunitsyn, M. (2025). Modeling the impact of nonlinear oscillations on the quality of the working surface of parts in finishing operations. *Cutting & Tools in Technological System*, (102), 20–36. DOI: 10.20998/2078-7405.2025.102.02.
7. Mehdi, K., Monka, P. P., Monkova, K., Sahraoui, Z., Glaa, N., & Kascak, J. (2024). Investigation of dynamic behavior and process stability at turning of thin-walled tubular workpieces made of 42CrMo4 steel alloy. *Machines*, *12*(2), Article 120. DOI: 10.3390/machines12020120.
8. Bouchama, R., Bouhalais, M. L., & Cherfia, A. (2024). Surface roughness and tool wear monitoring in turning processes through vibration analysis using PSD and GRMS. *The International Journal of Advanced Manufacturing Technology*, *130*(7–8), 3537–3552. DOI: 10.1007/s00170-023-12742-x.
9. Abouelatta, O. B., & Mádl, J. (2001). Surface roughness prediction based on cutting parameters and tool vibrations in turning operations. *Journal of Materials Processing Technology*, *118*(1–3), 269–277. DOI: 10.1016/S0924-0136(01)00959-1.
10. García Plaza, E., & Núñez López, P. J. (2017). Surface roughness monitoring by singular spectrum analysis of vibration signals. *Mechanical Systems and Signal Processing*, *84*, 516–530. DOI: 10.1016/j.ymssp.2016.06.039.
11. Z Zhuo, Y., Han, Z., An, D., & Jin, H. (2021). Surface topography prediction in peripheral milling of thin-walled parts considering cutting vibration and material removal effect. *International Journal of Mechanical Sciences*, *211*, Article 106797. DOI: 10.1016/j.ijmecsci.2021.106797.
12. Lin, C.-J., Jhang, J.-Y., & Young, K.-Y. (2020). Parameter selection and optimization of an intelligent ultrasonic-assisted grinding system for SiC ceramics. *IEEE Access*, *8*, 195721–195732. DOI: 10.1109/ACCESS.2020.3033884.
13. Apostolou, G., Ntemi, M., Paraschos, S., Gialampoukidis, I., Rizzi, A., Vrochidis, S., & Kompatsiaris, I. (2024). Novel framework for quality control in vibration monitoring of CNC machining. *Sensors*, *24*(1), Article 307. DOI: 10.3390/s24010307.
14. Kibbou, E. M., Dellagi, S., Majdouline, I., & Moufki, A. (2019). Prediction of surface quality based on the non-linear vibrations in orthogonal cutting process: Time domain modeling. *Journal of Manufacturing and Materials Processing*, *3*(3), Article 53. DOI: 10.3390/jmmp3030053.
15. Ni, C., Zhu, J., Wang, Y., Liu, D., Wang, X., & Zhu, L. (2024). Theoretical modeling and surface roughness prediction of microtextured surfaces in ultrasonic vibration-assisted milling. *Chinese Journal of Mechanical Engineering*, *37*(1), Article 51. DOI: 10.1186/s10033-024-01033-5.
16. Zhang, H., Xu, Y., Liu, Q., Wang, X., & Li, Y. (2022). Solving Fokker–Planck equations using deep KD-tree with a small amount of data. *Nonlinear Dynamics*, *108*(4), 4029–4043. DOI: 10.1007/s11071-022-07361-2.
17. Wan, J., Che, Y., Wang, Z., & Cheng, C. (2023). Uncertainty quantification and optimal robust design for machining operations. *Journal of Computing and Information Science in Engineering*, *23*(1), Article 011005. DOI: 10.1115/1.4055039.
18. Fodor, G., Sykora, H. T., & Bachrathy, D. (2020). Stochastic modeling of the cutting force in turning processes. *The International Journal of Advanced Manufacturing Technology*, *111*(1–2), 213–226. DOI: 10.1007/s00170-020-05877-8.
19. Liu, Y., Xiong, Z., & Liu, Z. (2020). Stochastic cutting force modeling and prediction in machining. *Journal of Manufacturing Science and Engineering*, *142*(12), Article 121004. DOI: 10.1115/1.4047626.

20. Xu, W., Feng, J., Su, J., Guo, Q., & Han, Y. (2025). Adaptive normalizing flows for solving Fokker–Planck equation. *Chaos: An Interdisciplinary Journal of Nonlinear Science*, *35*(8), Article 083116. DOI: 10.1063/5.0273776.
21. Usov, A., Kunitsyn, M., Klymenko, D., & Davydiuk, V. (2022). Modeling the effect of stochastic defects formed in products during machining on the loss of their functional dependencies. *Proceedings of Odessa Polytechnic University*, *1*(65), 16–29. DOI: 10.15276/opu.1.65.2022.02.
22. Moradi, H., Vossoughi, G., & Movahhedy, M. R. (2013). Experimental dynamic modelling of peripheral milling with process damping, structural and cutting force nonlinearities. *Journal of Sound and Vibration*, *332*(19), 4709–4731. DOI: 10.1016/j.jsv.2013.03.029.
23. Sato, R., Noguchi, S., Hokazono, T., Nishida, I., & Shirase, K. (2020). Time domain coupled simulation of machine tool dynamics and cutting forces considering the influences of nonlinear friction characteristics and process damping. *Precision Engineering*, *61*, 103–109. DOI: 10.1016/j.precisioneng.2019.10.010.
24. O'Leary, J., Paulson, J. A., & Mesbah, A. (2022). Stochastic physics-informed neural ordinary differential equations. *Journal of Computational Physics*, *468*, Article 111466. DOI: 10.1016/j.jcp.2022.111466.
25. Soize, C., & Ghanem, R. (2024). Probabilistic-learning-based stochastic surrogate model from small incomplete datasets for nonlinear dynamical systems. *Computer Methods in Applied Mechanics and Engineering*, *418*, Article 116498. DOI: 10.1016/j.cma.2023.116498.
26. Soize, C., & Farhat, C. (2017). A nonparametric probabilistic approach for quantifying uncertainties in low-dimensional and high-dimensional nonlinear models. *International Journal for Numerical Methods in Engineering*, *109*(6), 837–888. DOI: 10.1002/nme.5312.
27. Cai, C., An, Q., Ming, W., & Chen, M. (2021). Modelling of machined surface topography and anisotropic texture direction considering stochastic tool grinding error and wear in peripheral milling. *Journal of Materials Processing Technology*, *292*, Article 117065. DOI: 10.1016/j.jmatprotec.2021.117065.
28. Lyu, M.-Z., Feng, D.-C., Chen, J.-B., & Li, J. (2024). A decoupled approach for determination of the joint probability density function of a high-dimensional nonlinear stochastic dynamical system via the probability density evolution method. *Computer Methods in Applied Mechanics and Engineering*, *418*, Article 116443. DOI: 10.1016/j.cma.2023.116443.
29. Kloeden, P. E., & Platen, E. (1992). *Numerical solution of stochastic differential equations*. Springer. DOI: 10.1007/978-3-662-12616-5.
30. Guo, Q., Liu, W., Mao, X., & Zhan, W. (2018). Multi-level Monte Carlo methods with the truncated Euler–Maruyama scheme for stochastic differential equations. *International Journal of Computer Mathematics*, *95*(9), 1715–1726. DOI: 10.1080/00207160.2017.1329533.
31. Mohammadi, Y., & Ahmadi, K. (2022). Finite-amplitude stability in regenerative chatter: The effect of process damping nonlinearity and intermittent cutting in turning. *Journal of Sound and Vibration*, *537*, Article 117158. DOI: 10.1016/j.jsv.2022.117158.
32. Zhang, X., Yu, T., & Zhao, J. (2020). An analytical approach on stochastic model for cutting force prediction in milling ceramic matrix composites. *International Journal of Mechanical Sciences*, *168*, Article 105314. DOI: 10.1016/j.ijmecsci.2019.105314.
33. Lv, D., Yan, C., Chen, G., Liu, D., Wu, X., & Zhu, Y. (2020). Mechanistic prediction for cutting force in rotary ultrasonic machining of BK7 glass based on probability statistics. *Ultrasonics*, *101*, Article 106006. DOI: 10.1016/j.ultras.2019.106006.
34. Sykora, H. T., Hajdu, D., Dombovari, Z., & Bachrathy, D. (2021). Chatter formation during milling due to stochastic noise-induced resonance. *Mechanical Systems and Signal Processing*, *161*, Article 107987. DOI: 10.1016/j.ymssp.2021.107987.
35. Liu, J., Niu, Y., Zhao, Y., Zhang, L., & Zhao, Y. (2024). Prediction of surface topography in robotic ball-end milling considering tool vibration. *Actuators*, *13*(2), Article 72. DOI: 10.3390/act13020072.

Куніцин Максим Володимирович; Maksym Kunitsyn, ORCID: https://orcid.org/0000-0003-1764-8922
Усов Анатолій Васильович; Anatolii Usov, ORCID: https://orcid.org/0000-0002-3965-7611
Сікіраш Юлія Євгеніївна, Yulia Sikirash, ORCID: https://orcid.org/0000-0003-0853-582X

Received November 02, 2025
Accepted November 29, 2025

UDC 621.01.519.17

V. Kurhan
Odessa Polytechnic National University, Shevchenko Ave. 1, Odesa, Ukraine, 65044, e-mail: 10127013@stud.op.edu.ua

ANALYSIS OF BUCKET ELEVATOR DRIVE MOUNTING STRUCTURES BASED ON GRAPH MODELS

В. Курган. **Аналіз конструкцій кріплення приводу ковшових елеваторів на основі графових моделей.** У статті наведено результати аналізу та синтезу приводів ковшових елеваторів на основі комбінованих графових моделей у механіці. Дослідження виконано з використанням теорії модифікованих кінематичних графів, що дозволяє подати приводи ковшових елеваторів у вигляді пружних механічних систем з механічним зворотним зв'язком. Запропонований підхід забезпечує формалізований аналіз структур існуючих приводів і створює підґрунтя для синтезу нових конструктивних рішень з розширеними функціональними можливостями. Проведено огляд та систематизацію основних типів графових моделей, що застосовуються для розв'язання задач механіки, зокрема кінематичних, силових та комбінованих графів. Показано доцільність використання модифікованих кінематичних графів для аналізу керованих пружних систем, що характеризуються негативною або нульовою рухомістю. Для оцінювання можливостей керування пружними характеристиками механізмів використано показники ступеня рухомості та цикломатичного числа. У роботі запропоновано критерій вибору оптимального конструктивного рішення на основі енергії модифікованого кінематичного графа, яка визначається з використанням спектральної теорії графів. Матриці суміжності формуються з урахуванням вагових коефіцієнтів, що відображають конструктивно-технологічні фактори та напрям дії пружних сил. На прикладі двох структур кріплення приводів ковшових елеваторів виконано порівняльний аналіз, який дозволив обґрунтувати вибір більш раціональної структури за критерієм мінімальної енергії графа. Отримані результати підтверджують ефективність застосування модифікованих кінематичних графів для формалізації та алгоритмізації процесів структурного аналізу й синтезу приводів ковшових елеваторів з урахуванням конструктивних і технологічних обмежень.

Ключові слова: ковшовий елеватор, привід, пружна система, модифікований кінематичний граф, механічний зворотний зв'язок

V. Kurhan. **Analysis of Bucket Elevator Drive Mounting Structures Based on Graph Models.** The paper presents the results of the analysis and synthesis of bucket elevator drives based on combined graph models in mechanics. The study is carried out using the theory of modified kinematic graphs, which makes it possible to represent bucket elevator drives as elastic mechanical systems with mechanical feedback. The proposed approach provides a formalized analysis of the structures of existing drives and creates a basis for the synthesis of new design solutions with extended functional capabilities. A review and systematization of the main types of graph models used to solve problems in mechanics is performed, including kinematic, force, and combined graphs. The expediency of using modified kinematic graphs for the analysis of controlled elastic systems characterized by negative or zero mobility is demonstrated. The degree of mobility and the cyclomatic number are used to assess the controllability of elastic characteristics of mechanisms. The paper proposes a criterion for selecting an optimal design solution based on the energy of a modified kinematic graph, which is determined using spectral graph theory. Adjacency matrices are formed taking into account weighting coefficients that reflect design and technological factors as well as the direction of elastic force action. Using the example of two bucket elevator drive mounting structures, a comparative analysis is performed, which substantiates the selection of a more rational structure according to the criterion of minimum graph energy. The obtained results confirm the effectiveness of using modified kinematic graphs for the formalization and algorithmization of structural analysis and synthesis processes of bucket elevator drives, taking into account design and technological constraints.

Keywords: bucket elevator, drive, elastic system, modified kinematic graph, mechanical feedback

1. Introduction

The development of the agro-industrial complex necessitates improving the efficiency of technological processes for transporting bulk materials. A significant role in these processes is played by bucket elevators, which are widely used in grain processing and related industries. Of particular interest are self-supporting bucket elevators, whose design features impose limitations on the mass and overall dimensions of the drive unit, thereby complicating efforts to increase their productivity.

One of the most heavily loaded operating modes of bucket elevators is the drive start-up mode, during which considerable dynamic loads and shock effects occur, adversely affecting the reliability and durability of the structure. Known technical solutions aimed at reducing dynamic loads, such as the use of frequency converters or fluid couplings, are not always appropriate due to increased structural complexity, higher costs, and elevated operating expenses.

In this regard, the development of passive mechanical systems capable of effectively attenuating start-up loads without significantly complicating the drive design is of particular relevance. One promising approach involves the use of elastic systems with mechanical feedback, which make it possible to form specified elastic characteristics and adapt the dynamic behavior of the drive during transient operating conditions.

DOI: 10.15276/opu.2.72.2025.02

ISSN 2076-2429 (print)
ISSN 2223-3814 (online)

The purpose of this study is to analyze and synthesize bucket elevator drive mounting structures based on graph models using the theory of modified kinematic graphs.

2. Literature analysis

Modern approaches to modeling mechanical systems increasingly rely on graph-based representations, which allow formalizing the structural, kinematic, and dynamic interactions of system components. Graph models can be classified according to the type of information they convey, and each type has been widely used in different areas of mechanical engineering.

For modeling energy interactions within mechanical systems, force graphs are commonly applied. These models have been successfully used by Schneider, Pfeiffer, and Borutsky [1, 2] in studies related to machine dynamics, hydraulics, and electromechanics. Force graphs provide a convenient tool for analyzing the transmission of forces and energy flows between system elements.

Stiffness graphs (or structural graphs) have been employed in the works of Uicker, Pennock, Shigley, and Tsai [3, 4] for modeling elastic systems and building structures. These graphs are particularly useful in evaluating the rigidity and deformation characteristics of mechanical assemblies, enabling the prediction of structural behavior under load.

Another widely used approach involves kinematic graphs, which describe the connectivity and mobility of mechanical systems. Pioneering studies by Jain, and Pennock. [5, 6] applied kinematic graphs to analyze mechanical and robotic systems, determining degrees of freedom, identifying redundant constraints, and synthesizing mechanisms with desired functional properties. Kinematic graphs provide a systematic framework for structural analysis and mechanism design.

Finally, constraint graphs have been utilized to model the dynamics of multi-body systems with interacting components. Jain and Karnopp [5, 7, 8] employed constraint graphs in studies of elastic and dissipative connections, effectively capturing the dynamic behavior of complex assemblies and facilitating the simulation of multi-body interactions.

Overall, the literature indicates that combining different types of graph models allows for a more comprehensive analysis of mechanical systems. By integrating kinematic, force, and stiffness information, hybrid graph models can support the design, optimization, and synthesis of mechanical systems, including drives for bucket elevators, where both structural compactness and dynamic performance are critical.

3. Purpose of research

The aim of the study is to test methods for representing mechanical systems in the form of graphs and to apply these methods for the analysis of existing and the synthesis of new bucket elevator drive designs. The research involves identifying structural and design differences between drives by highlighting the parameters that determine these differences, as well as developing features and criteria that allow an optimal choice among multiple possible solutions, ensuring structural compactness and maximum functional capabilities. In addition, the study focuses on the formulation and evaluation of criteria for selecting the optimal solution, which enables a reasoned determination of the most effective variant among available alternatives. Achieving this objective provides a systematic approach to formalizing the processes of structural analysis and synthesis of bucket elevator drives while taking into account design and technological constraints.

4. Research method

Based on the considered key types of graph models, it can be concluded that their application makes it possible to solve a wide range of engineering problems. Such problems include the structural analysis of mechanisms, in particular the determination of their mobility using the Chebyshev–Grübler–Kutzbach criterion, dynamic modeling of mechanical systems (Lagrange equations, bond graph method), optimization of mechanisms at the stage of their design implementation (elimination of redundant constraints, mass minimization), as well as the kinematic analysis of manipulators in robotic systems.

When designing mechanisms with prescribed functional characteristics, primary attention is paid to the initial structural analysis of existing analogues. This analysis, in turn, requires the use of various graph models, applied both individually and in certain combinations. Despite the diversity of mechanical problems, their relationship with the functional characteristics of a mechanism makes it possible to identify common patterns, which creates the prerequisites for formalizing the processes of analysis and synthesis based on graph theory.

In solving problems of analysis and synthesis in a mechanical formulation, the most commonly used models are kinematic graphs, which represent the structure of a mechanism and define kinematic

constraints between its links; force graphs, which are used to model the processes of force transmission between system elements; and functional graphs, which describe the laws of motion transformation. However, the complexity and non-standard nature of modern analysis and synthesis problems in mechanical engineering necessitate the development and application of combined graph models. Such combined models should take into account not only the existing topological constraints of the mechanical system but also ensure the compatibility of functional requirements, along with the possibility of automation and algorithmization of the search for optimal structural solutions.

The studies conducted in this chapter are based on a combined graph model developed by Professor I. I. Sydorenko, which establishes the theoretical foundations and corresponding methodologies for the analysis and synthesis of controlled elastic systems using a combined graph-based approach, referred to by the author as the modified kinematic graph [9, 10]. This theory represents a further development of the theory of analysis and synthesis of mechanisms based on kinematic graphs [11, 12, 13].

The results of studies related to the validation of the above-mentioned theory made it possible to formulate the basic principles of structural synthesis of elastic systems of this type [10 – 14].

According to one of the principles of the applied theory, an idealized representation of the structure of a conventional planar passive device having a single parameter (for example, the stiffness coefficient) subject to controlled variation is a modified kinematic graph (non-bipolar). Such a graph characterizes negative or zero mobility of the considered device, which is determined by the following equation:

$$W = 3 \cdot (p_{\Sigma} - 1) - 2q_5 - q_4 - q_c \le 0 , \tag{1}$$

where:

p_{Σ} – the total number of graph vertices corresponding to the number of rigid links of the device;

$q_{(i)}$ – the number of graph edges equal to the number of kinematic pairs of the i-th class;

q_c – the number of graph edges corresponding to the number of non-kinematic connections (elastic, dissipative, etc.) between the rigid links of the device, this component does not affect the kinematic characteristics of the device and can therefore be considered as a virtual kinematic pair of the 4th class.

According to another principle stated in the applied theory, the nature of kinematic control of the properties of a given device, when it is modeled using a modified kinematic graph, can be assessed by an indicator in the form of the cyclomatic number. For controlled elastic mechanisms, this indicator is defined as follows:

$$\sigma = q - p + 1 \ge 2 , \tag{2}$$

where:

q – the number of graph edges, regardless of their type;

p – the number of graph vertices, also regardless of their type.

Expressions (1) and (2) make it possible to analyze the device under consideration in order to assess the feasibility of controlling its elastic characteristic, and also provide the possibility of synthesizing such a device by adding to the model the required number of structural groups and elastic elements, guided by the specified indicators.

Considering that multiple alternative solutions are possible in the synthesis process, an indicator in the form of the energy of the modified kinematic graph is used to select the optimal synthesis option; for the optimal solution, this indicator should be minimal. The energy of a graph $E(G)$, as a quantity from spectral graph theory, is understood as the sum of the absolute values of the eigenvalues of its adjacency matrix. For a simple graph G with n vertices, its adjacency matrix A is a square matrix of size $n \times n$. Typically, the element A_{ij} is defined as follows: it equals (1) if vertex i is connected by an edge to vertex j, or 0 if vertices i and j are not connected (similarly for $i=j$, since the graph is simple). In the presented methodology, the use of the adjacency matrix is defined with the application of certain weighting coefficients that reflect a particular prevailing factor (from the standpoint of technology, durability, cost, etc.); moreover, the more significant the factor, the lower its weighting coefficient. Based on these conditions, the eigenvalues (roots of the characteristic polynomial) of the adjacency matrix A are determined according to the expression:

$$\varphi(\lambda) = \det(A - \lambda I) , \tag{3}$$

where: I – the identity matrix and det – the determinant.

ISSN 2076-2429 (print)
ISSN 2223-3814 (online)

Considering that for a graph with n vertices n eigenvalues can be obtained: $\lambda_1, \lambda_2, \ldots, \lambda_n$, then the energy of a graph is understood as the sum of the absolute values of all eigenvalues:

$$E(G) = \sum_{1}^{n} |\lambda_i| . \quad (4)$$

Let us consider the above-mentioned theory in application to the subject of this study. For this purpose, an analysis of two designs (Structure A and Structure B) of elastic mechanisms for fastening bucket elevator drives in different directions of force (Fig. 1) was conducted, and the most optimal of them was determined.

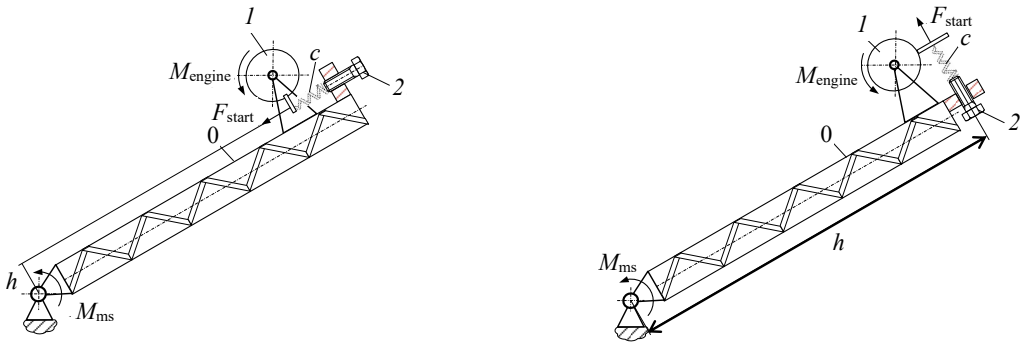

Fig. 1. Kinematic diagrams of the elastic mechanism for mounting bucket elevator drives: *a* – Structure A; *b* – Structure B; M_{engine} – is the engine torque; $F_{starting}$ – is the excitation force caused by the engine start; M_{ms} – is the torque of the metal structure; *c* – is the spring stiffness; *h* – is the lever arm; *1* – electric motor; *2* – elastic mechanism

Based on the kinematic schemes (Fig. 1), the corresponding models in the form of modified kinematic graphs (Fig. 2) are tripolar graphs and, therefore, can be analyzed using the methodology presented above.

Fig. 2. Models of the considered structures in the form of modified kinematic graphs: structure A (*a*); structure B (*b*)

The calculation of the degree of mobility according to expression (1) yields the same result in both cases and determines the mobility of the models:

$$W = 3 \cdot (3-1) - 2 \cdot 1 - 1 - 1 = 2 , \quad (5)$$

which, according to the adopted methodology, does not define the considered structures as self-controlled (the condition $W \leq 0$ is not met). However, control of the characteristic q_c is possible with the mutual displacement of the elements of the structures defined by the poles of the graph p_0 and p_2.

The statement about the absence of self-control, obtained in the above calculation, is also confirmed by the calculation of the cyclomatic number according to expression (2):

$$\sigma = 3 - 3 + 1 = 1 , \quad (6)$$

for self-controlled devices, this indicator must satisfy the condition $\sigma \geq 2$.

However, the adopted methodology allows us to choose the optimal solution among several existing ones. To do this, we will compile for the structure under consideration the corresponding adjacency matrices with the introduction of weight coefficients, which take into account both the direction of action of the elastic force relative to the longitudinal axis of the metal structure of the bucket elevator,

and the technological features associated with the manufacture of kinematic pairs of the 5-th and 4-th classes. Moreover, the direction of the elastic force along the longitudinal axis of the metal structure will be considered more preferable (the weight coefficient is minimal) than the direction of the elastic force perpendicular to the axis of the metal structure. The adopted values of the weight coefficients in the adjacency matrix of the structures under consideration are given in the corresponding table (Table 1).

Table 1

Determination of weight coefficients in the matrix of structures under consideration

Structure	Edge of a graph (poles)	Weighting factor	Explanation
A	$q_c(p_1–p_2)$	1 (min)	Elastic force along the longitudinal axis of the metal structure
B	$q_c(p_1–p_2)$	2 (max)	Elastic force perpendicular to the longitudinal axis of the metal structure
A – B	$q_5(p_0–p_1)$	1 (min)	Less technologically complex
A – B	$q_4(p_0–p_2)$	2 (max)	More technologically complex

Given that for a graph with three vertices, we can obtain three eigenvalues for the adjacency matrix:

– For structure A we obtained: $\lambda_{1A} = –2$; $\lambda_{2A} = –1.46$; $\lambda_{3A} = 2.73$;

– For structure B we obtained: $\lambda_{1A} = –1$; $\lambda_{2A} = –5.24$; $\lambda_{3A} = 6.24$.

Therefore, the calculated value of the graph energy according to expression (4) for Structure A is $E(A) = 6.19$, for Structure B it is $E(B) = 12.48$.

Taking into account the adopted weight coefficients, the adjacency matrices of the structures under consideration have the form (the matrices have the same structure, but different weighting coefficients):

$$\text{For Structure A} = \begin{array}{c|ccc} & p_0 & p_1 & p_2 \\ \hline p_0 & 0 & q_5 & q_c \\ p_1 & q_5 & 0 & q_4 \\ p_2 & q_c & q_4 & 0 \end{array} = \begin{array}{c|ccc} & p_0 & p_1 & p_2 \\ \hline p_0 & 0 & 1 & 1 \\ p_1 & 1 & 0 & 2 \\ p_2 & 1 & 2 & 0 \end{array} \tag{7}$$

$$\text{For Structure B} = \begin{array}{c|ccc} & p_0 & p_1 & p_2 \\ \hline p_0 & 0 & q_5 & q_c \\ p_1 & q_5 & 0 & q_4 \\ p_2 & q_c & q_4 & 0 \end{array} = \begin{array}{c|ccc} & p_0 & p_1 & p_2 \\ \hline p_0 & 0 & 1 & 2 \\ p_1 & 1 & 0 & 2 \\ p_2 & 2 & 2 & 0 \end{array} \tag{8}$$

Based on the results of the calculations $E(A) < E(B)$, the applied method indicates a more rational Structure A, which is actually confirmed by the analysis in Fig. 2, which shows that the elastic force shoulder $h_A < h_B$, which determines a smaller influence of the moment relative to the attachment point of the metal structure of the bucket elevator.

5. Conclusions

Based on the results of the conducted studies, the following conclusions have been drawn:

1. Despite the effectiveness of standard approaches to applying graph theory for the analysis and synthesis of technical systems, the ambiguity and multi-criteria nature of such problems make the development and implementation of combined graph models preferable. These hybrid structures, by integrating information on kinematics, forces, and functional interactions of the modeled mechanical systems, provide comprehensive system-level modeling and enhance the adequacy of decision-making.

2. The studies have validated the effectiveness of the adopted methodology using modified kinematic graphs for analyzing existing designs and synthesizing new configurations of bucket elevator drives, particularly with respect to optimizing their structure and functional capabilities.

3. As a criterion for selecting the optimal solution from a set of possible alternatives in the synthesis of elevator drives, the successful application of the graph energy $E(G)$, derived from spectral graph theory, was adopted. It was established that the optimal solution corresponds to the minimum

ISSN 2076-2429 (print)
ISSN 2223-3814 (online)

value of the graph energy. This approach allows formalizing the selection process while taking into account both structural and technological/design factors through weighted adjacency matrices.

4. The validation of the adopted methodology and the corresponding methods of representing a technical system via a modified kinematic graph, along with the availability of an effective criterion for optimal selection, enables the formalization and algorithmization of the structural analysis and synthesis processes of bucket elevator drives. This ensures the selection of solutions that combine structural compactness with maximal functional capabilities while considering design and technological constraints.

Література

1. Pfeiffer F. Mechanical System Dynamics (Lecture Notes in Applied and Computational Mechanics). Springer, 2008. DOI: https://doi.org/10.1007/978-3-540-79436-3.
2. Borutzky W. Bond Graph Methodology: Development and Analysis of Multidisciplinary Dynamic System Models. Springer, 2010. DOI: https://doi.org/10.1007/978-1-84882-882-7.
3. Uicker J. J., Pennock G. R., Shigley J. E. Theory of Machines and Mechanisms. 5th ed. New York : Oxford University Press, 2017. 936 p.
4. Tsai L. W. Mechanism Design: Enumeration of Kinematic Structures According to Function. Boca Raton, FL, USA : CRC Press, 2000. 320 p.
5. Jain A. Robot and Multibody Dynamics: Analysis and Algorithms. Springer New York, 2011. 510 p.
6. Pennock G. R. Kinematics and Dynamics of Mechanical Systems: Implementation in MATLAB® and Simscape Multibody™. 2nd Edition. Boca Raton : CRC Press, 2016. 640 p.
7. Karnopp D. C., Margolis D. L., Rosenberg R. C. System dynamics: Modeling, simulation, and control of mechatronic systems. 5th ed. John Wiley & Sons, 2012. 664 p.
8. Preumont A. Vibration Control of Active Structures: An Introduction. 4th Edition. Cham : Springer Nature, 2018. 466 p.
9. Synthesis Passive Pressure Reducing Valve Using Modified Kinematic Graphs / I. Sydorenko, V. Semenyuk, V. Lingur et al. // Advances Manufacturing Processes : InterPartner – 2020. Lecture Notes in Mechanical Engineering. Springer, Cham, 2021. P. 207–216. DOI: 10.1007/978-3-030-68014-5_21.
10. Сидоренко І. Структура і класифікаційні ознаки пасивних віброізолюючих пристроїв з механічним зворотним зв'язком. *Машинознавство*. 2006. № 12 (112–113). С. 24–28.
11. Lynch K. M., Park F. C. Modern Robotics: Mechanics, Planning, and Control. Cambridge : Cambridge University Press, 2017. 544 p.
12. McCarthy J. M., Soh G. S. Geometric Design of Linkages. 2nd Edition. New York : Springer, 2021. 444 p.
13. Norton R. L. Design of Machinery: An Introduction to the Synthesis and Analysis of Mechanisms and Machines. 6th Edition. New York : McGraw-Hill Education, 2020. 928 p.
14. Application of Modified Kinematic Graphs to Analyze the Structures of Passive Relaxation Shock Absorbers / I. Sydorenko, V. Kurgan, V. Semenyuk et al. Advanced Manufacturing Processes VI : Interpartner 2024. Lecture Notes in Mechanical Engineering. Springer, Cham, 2025. DOI: https://doi.org/10.1007/978-3-031-82746-4_12.

References

1. Pfeiffer, F. (2008). *Mechanical System Dynamics* (Lecture Notes in Applied and Computational Mechanics). Springer. DOI: https://doi.org/10.1007/978-3-540-79436-3.
2. Borutzky, W. (2010). *Bond Graph Methodology: Development and Analysis of Multidisciplinary Dynamic System Models*. Springer. DOI: https://doi.org/10.1007/978-1-84882-882-7.
3. Uicker, J. J., Pennock, G. R., & Shigley, J. E. (2017). *Theory of Machines and Mechanisms* (5th ed.). Oxford University Press.
4. Tsai, L. W. (2000). *Mechanism Design: Enumeration of Kinematic Structures According to Function*. CRC Press.
5. Jain, A. (2011). *Robot and Multibody Dynamics: Analysis and Algorithms*. Springer.
6. Pennock, G. R. (2016). *Kinematics and Dynamics of Mechanical Systems: Implementation in MATLAB® and Simscape Multibody™* (2nd ed.). CRC Press.
7. Karnopp, D. C., Margolis, D. L., & Rosenberg, R. C. (2012). *System Dynamics: Modeling, Simulation, and Control of Mechatronic Systems* (5th ed.). John Wiley & Sons.
8. Preumont, A. (2018). *Vibration Control of Active Structures: An Introduction* (4th ed.). Springer Nature. DOI: https://doi.org/10.1007/978-3-319-72296-2.

9. Sydorenko, I., Semenyuk, V., Lingur, V., Bovnegra, L., & Pavlyshko, O. (2021). Synthesis passive pressure reducing valve using modified kinematic graphs. In V. Tonkonogyi et al. (Eds.), *Advances in Manufacturing Processes. InterPartner – 2020* (Lecture Notes in Mechanical Engineering, pp. 207–216). Springer, Cham. DOI: 10.1007/978-3-030-68014-5_21.
10. Sidorenko, I. (2006). Structure and classification features of passive vibration-isolating devices with mechanical feedback. *Mashinostroenie*, (12), 24–28.
11. Lynch, K. M., & Park, F. C. (2017). *Modern Robotics: Mechanics, Planning, and Control*. Cambridge University Press.
12. McCarthy, J. M., & Soh, G. S. (2021). *Geometric Design of Linkages* (2nd ed.). Springer. DOI: https://doi.org/10.1007/978-1-4419-7892-9.
13. Norton, R. L. (2020). *Design of Machinery: An Introduction to the Synthesis and Analysis of Mechanisms and Machines* (6th ed.). McGraw-Hill Education.
14. Sydorenko, I., Kurgan, V., Semenyuk, V., et al. (2025). Application of Modified Kinematic Graphs to Analyze the Structures of Passive Relaxation Shock Absorbers. *Advanced Manufacturing Processes VI: Interpartner 2024* (Lecture Notes in Mechanical Engineering). Springer, Cham. DOI:https://doi.org/10.1007/978-3-031-82746-4_12.

Курган Володимир Олегович; Volodymyr Kurhan, ORCID: https://orcid.org/0009-0003-9816-5419

Received November 10, 2025

Accepted December 12, 2025

ISSN 2076-2429 (print)
ISSN 2223-3814 (online)

UDC 621.73

O. Vatrenko[1], DSc, Prof.,
Ya. Verkhivker[1], DSc, Prof.
I. Prokopovych[2], DSc, Prof.
[1] Odesa National University of Technology, Kanatnaya Str. 112, Odesa, Ukraine, e-mail: alexvatrenko@gmail.com
[2] Odessa Polytechnic National University, Shevchenko Ave. 1, Odesa, Ukraine, 65044

DEVELOPMENT OF A PACKAGE OF DIES FOR THE COVERS OF THE TWIST-OFF SYSTEM

О. Ватренко, Я. Верхівкер, І. Прокопович. **Розробка пакету штампів для кришок системи твіст-оф.** Холодне штампування металів широко використовується в машинобудуванні та інших галузях промисловості для виробництва деталей та виробів з тонколистового прокату. Перевагами цього методу є висока продуктивність обладнання та відносно невеликі витрати енергії. Штампування здійснюється на вертикальних або горизонтальних пресах з використанням змінного штампового оснащення. Світова тенденція у виробництві тари та упаковки спрямована на зменшення товщини пакувальних виробів та питомої частки упаковки в загальній масі упакованої продукції. Однак просто взяти і зменшити товщину жерсті існуючих виробів, наприклад, кришок системи твіст-оф неможливо, оскільки зменшення товщини металу одразу негативно вплине на надійність герметизації затвора. Необхідно вжити запобіжні заходи, які могли б адекватно компенсувати зменшення товщини металу. Ці заходи полягають в обов'язковому внесенні змін в існуючу конструкцію кришок, а отже, й в штампове оснащення. В статті розглянуто проєктування пакету штампів трансферного пресу для виробництва кришок системи твіст-оф для консервної скляної тари. Наводиться технологія виготовлення кришок та описується робота кожного штампу з пакету окремо. Показано конструкції кожного штампу, які входять в пакет, та послідовну розробку технічної документації на штампове оснащення. Наводяться конструкції найважливіших деталей штампів, які зазнали змін при переведенні виробництва кришок на жерсть зниженої товщини. Надається обгрунтування та пояснюються конструктивні зміни найважливіших деталей штампів.
Ключові слова: холодне штампування, жерсть, пакет штампів, пуансон, матриця, згинання

O. Vatrenko, Ya. Verkhivker, I. Prokopovych. **Development of a package of dies for the covers of the twist-off system.** Cold stamping of metals is widely used in mechanical engineering and other industries for the production of parts and products from thin plates. The advantages of this method are high productivity of equipment and relatively low energy consumption. Stamping is carried out on vertical or horizontal presses using interchangeable stamping equipment. However, it is not possible to simply take and reduce the thickness of the tin of existing products, for example, twist-off covers, since reducing the thickness of the metal will immediately negatively affect the reliability of the sealing of the seal. Precautions must be taken that could adequately compensate for the decrease in the thickness of the metal. These measures are mandatory changes to the existing design of the covers, and therefore to the stamping equipment. The article discusses the design of a package of transfer press dies for the production of twist-off system lids for tin glass containers. The technology for manufacturing lids is given and the operation of each stamp from the bag is described separately. The designs of each die included in the package and the sequential development of technical documentation for stamping equipment are shown. The designs of the most important parts of dies are given, which have undergone changes during the transfer of the production of covers to tinplate of reduced thickness. Justification is provided and structural changes in the most important parts of dies are explained.
Keywords: cold stamping, tin, die package, punch, die, bending

1. Introduction

Cold stamping of metals plays a key role in the production of metal packaging. The global trend in the production of packaging for the food industry is aimed at reducing its material consumption. Thus, the issue of reducing the level of consumption of material resources, reducing the cost of packaged products, reducing the harmful impact of used packaging on the external environment is solved. The rapid development of the production and use of packaging products has sharply exacerbated environmental problems. After all, after use, the packaging turns into garbage, which complicates the already difficult environmental situation.

Ukraine, as well as the whole world, faces the task of minimizing packaging. This can be achieved, for example, by reducing the thickness of the material for the manufacture of packaging products, making a change in their design and developing, accordingly, new stamping equipment. The most important and technically complex link in the technological process of production of twist-off (TO) lids is the stage of forming on a multi-position transfer press by cold stamping.

The lids of the twist-off system are mass-produced products and are made of white tin. It is known that metal packaging, along with glass, is the most energy-consuming and leaves a large carbon footprint, in addition, tinplate is not produced in Ukraine at all, but imported from abroad.

DOI: 10.15276/opu.2.72.2025.03

Based on the above, the development of stamping equipment designed for the mass production of metal products from tinplate of reduced thickness is not an easy and urgent task. The development of such equipment requires the production of high-precision parts of complex configuration and a long process of approbation of capping agents, with appropriate changes in the design of die parts, in the conditions of a real process of capping and subsequent sterilization of products to obtain high quality products.

2. Analysis of literature data and problem statement

Equipment and stamping equipment, as well as technological processes of cold stamping of thin plates are quite well covered in specialized literature [1, 2]. It provides data on the processes of sheet metal formation, classification of these processes, plastic deformation, stress, characteristics of types of presses, analyzes materials for molding. The main processes of sheet stamping, such as felling, bending, deep drawing, and others are described in [3, 4]. The paper [5] thoroughly considers the mechanics of formation processes and the interaction of the properties of metals with the processes of extraction.

The third part of the work [6] provides a methodology for designing and calculating the main parts of dies for the production of products of the most common configurations. In the paper [7], the stamp for the manufacture of hollow products from hard-to-form materials is considered, and in the work [8] the choice of the optimal rounding radius of the punch for the cold drawing process from pre-profiled sheet blanks is investigated.

The problems of forming products from thin-sheet rolled products of low-carbon steel by bending under the condition of a constant decrease in the thickness of rolled products are not sufficiently covered, or are not considered at all.

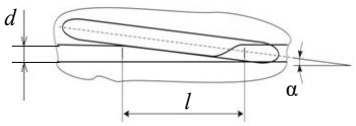

Fig. 1. Threaded gate element. *l* is the length of the threaded stop, *α* is the angle of lifting the thread, *d* is the diameter of the shoulder of the cover rigidity assembly

3. Purpose and objectives of the study

The purpose of this work is to develop stamping equipment for the formation of maintenance system covers from tinplate of reduced thickness. This stamping equipment is a three-position package of dies for a transfer press.

Research objectives.

Design of a package of dies, which consists of dies of the 1st, 2nd and 3rd operations, with their arrangement in one column block.

Production of stamping equipment and testing it on tin of reduced thickness.

Analysis of the resulting products, identification of shortcomings and making changes to the corresponding stamps operationally.

Final completion of the stamping equipment by approbation after making changes with the analysis of the resulting products.

Table 1

Mechanical properties of tin produced by USS Corporation at the plant in Slovakia (Košice)

Degree of hardness, strength class	Annealing	Hardness HR 30 T at tin thickness δ≤0.21, mm	Yield strength $\sigma_{0.2}$, MPa	Tensile strength $\sigma_в$, MPa
TS260	portioned	56±4	260±50	360±50
TS275	portioned	58±4	275±50	375±50
TH415	continuous	62±4	415±50	435±50
TH435	continuous	65±4	430±50	460±50
TH520	continuous	–	520±50	540±50
TS550	portioned	–	550±50	575±50
TH550	continuous	73±3	550±50	570±50
TH580	continuous	–	580±50	590±50
TH620	continuous	76±3	620±50	625±50

4. Materials and methods of research

The existing stamping equipment for the production of TO-82 covers was designed for tin with a thickness of δ=0.24 and δ=0.25 mm, the length of the threaded stops of which was *l*=13 mm. However, in order to remain competitive and in accordance with global trends, manufacturers had a need to reduce the thickness of the tin to δ=0.18...0.20 mm. A decrease in the thickness of the tin led to changes in the key geometric parameters of the covers – an increase in the length of their threaded stops to *l*=18 mm, Fig. 1. All this was the reason for the development of new stamp equipment.

However, the increase in the length of the threaded stops was not enough. It was also necessary to increase the hardness of the tin. Table 1 shows the mechanical properties of white and chrome-plated tin with a thickness of δ≤0.21 mm of Slovak manufacturers.

Consider the production line of the twist-off system covers, Fig. 2. The production of lids begins with cutting sheets of tin. In most cases, tin sheets are first calibrated on disc scissors. Consider a line with two-row checkerboard cutting of sheets. which is carried out using disc shears *1*, *2*.

ISSN 2076-2429 (print)
ISSN 2223-3814 (online)

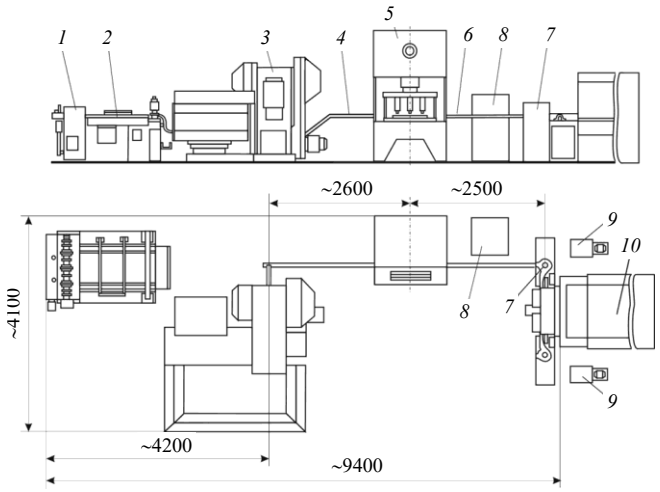

Fig. 2. Positional Cap Production Line: *1*, *2* – disc scissors; *3* – crank press; *4*, *6* – conveyors; *5* – transfer press: *7* – paste-laying machines; *8* – plastisol mixer; *9* – pumps for plastisol; *10* – conveyor oven

Fig. 3. Blanking the lid after stamping

The next operation is stamping blanks to make lids. The workpieces are stamped on a horizontal crank press machine *3*. Strips of prepared tin are laid in the press shop, from where they are automatically fed for stamping. The press is equipped with a 2-row single-position column die. During stamping, a round workpiece is cut out of the strip and during the same stroke of the slider, a cover blank with a fully formed field relief is stamped, Fig. 3.

Blanks of lids are fed to the transfer press *5* (Fig. 2) using conveyors *4*, which works on the principle of a vertical crank. The peculiarity of this press is that several dies are installed on it in a solid columnar block at once, in this case three, Fig. 4. The lid body is formed from the workpiece in three operations, Fig. 5. Each operation is performed on a separate stamp. The workpiece, moving from position to position, sequentially passes each die of the package and changes its configuration, taking the form of a finished lid body after the third operation.

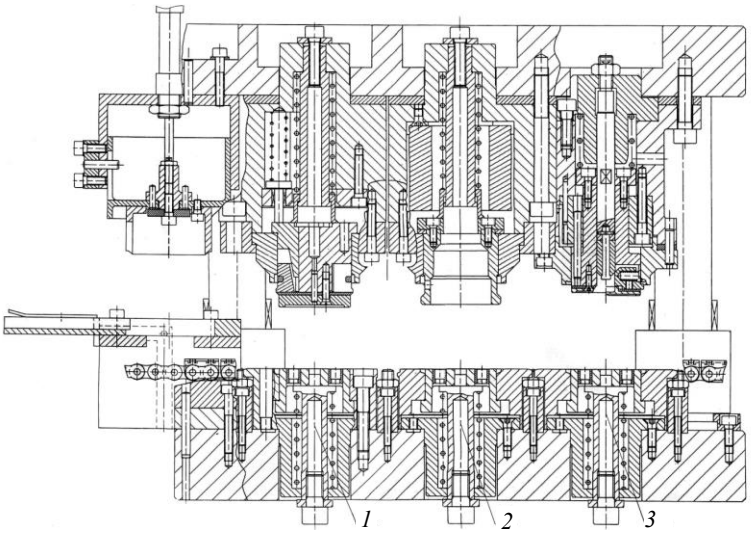

Fig. 4. A package of stamps for the cover of the twist-off system. *1* – stamp of the first operation; *2* – stamp of the second operation; *3* – stamp of the third operation

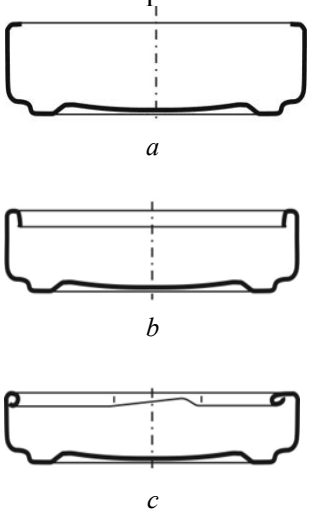

Fig. 5. Operationally forming of the lid body from the workpiece: *a* – the preparation of the first operation; *b* – preparation of the second operation; *c* – finished case

Consider the operation of a stamp package. The workpiece (Fig. 3), with the help of a stepper conveyor, in the “edge up” position, is installed on the spring-loaded Table 1 of the open die of the first operation, Fig. 6, and is fixed on it with magnets *2* and using a vacuum. When the die is closed, the spring-loaded clamp *3* enters the annular channel of the workpiece, centering the latter.

The presser *3* moves the workpiece downwards, until the stop of the table 1 in the glass *4* of the press plate underplate, fixing it in the lowest position. At the same time, the upper part of the die continues to move downwards and six spring-loaded wedges *5*, descending, spread the same number of sectors *6* pulled by a spring *7* from the axis of the die. The edge of the workpiece is fixed between the working surface of the matrix *8* from the outside and the working surfaces of the sectors from the in-

side and, as a result of their convergence, at the moment of closing the die, is bent to the angle determined by the matrix profile (Fig. 5*a*).

Having reached the lowest position, the die opens and its upper part begins to move upwards, lifting the wedges *5*. In this case, sectors *6* under the action of spring *7* are reduced to the axis of the die, freeing the molded workpiece, and the clamper *3* brings the latter out of the matrix *8*. The workpiece continues to be held by the magnets of the Table 1. Under the action of its spring, the Table 1 rises, setting the workpiece at the level of the upper plane of the lower part of the die package.

The workpiece, with the help of a stepper conveyor, is removed from the die table of the first operation, transferred to the spring-loaded Table 1 of the open die of the second operation, Fig. 7, and is fixed on it with magnets *2* and using a vacuum. When the die is closed, the spring-loaded clamp *3* enters the annular channel of the workpiece, centering the latter.

The clamp *3* moves the workpiece down, until the stop of table 1 in the glass *4* of the press plate under-stamp, fixing it in the lowest position. At the same time, the upper part of the die continues to move downwards and the workpiece is pressed with an edge against the working surface of the matrix *5*. As a result of their axial convergence, the edge of the workpiece is bent to the angle determined by the matrix profile (see Fig. 5*b*).

Having reached the lowest position, the stamp opens and its upper part begins to move upwards. At this time, the spring-loaded clamp *3* removes the workpiece from the matrix, which continues to be held by the magnets of the Table 1. The spring-loaded Table 1 rises, setting the workpiece at the level of the upper plane of the bottom of the die pack.

The workpiece, with the help of a stepper conveyor, is removed from the die table of the second operation, transferred to the spring-loaded table of the open die of the third operation, Fig. 8, and is fixed on it with magnets and using a vacuum. When the die is closed, the spring-loaded clamp *2* enters the annular channel of the workpiece, centering the latter.

The presser *2* moves the workpiece downwards, until the stop of the Table 1 into the glass *3* of the press under-die plate, fixing it in the lowest position.

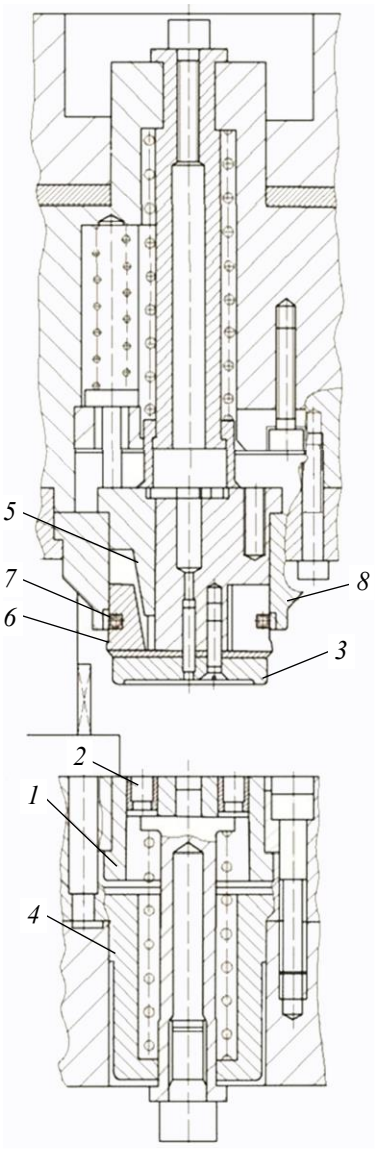

Fig. 6. Stamp of the first operation

At the same time, the upper part of the die continues to move downwards, and the pyramid-shaped hexagonal rod *4*, descending, spreads six spring-loaded crackers *5* from the axis of the die (according to the number of threaded stops of the covers). Each cracker with a forming part goes under the edge of the workpiece bent in the middle after the second operation, forming, so to speak, a small anvil.

On the sections of matrix 6 located opposite the crackers, special molding platforms for threaded stops are made. As a result of the axial convergence of the edge of the workpiece with the molding pads of the matrix, with simultaneous support on the forming parts of the crackers, threaded stops are formed. Formation occurs by pushing the bent edge of the workpiece into the gaps between the crackers and the forming pads of the matrix.

At the same time, when the crackers have gone under the bent edge of the workpiece and the threaded stops begin to form, and the upper part of the die continues to move downwards, the sections of the edge located between the stops are pressed against the working surface of the matrix 6. As a result of their axial convergence, the formation of the edge into a torus-shaped ring shoulder is completed. This completes the formation of the lid body (Fig. 5*b*).

ISSN 2076-2429 (print)
ISSN 2223-3814 (online)

Having reached the lowest position, the die opens and its upper part begins to move upwards, lifting the pyramidal rod *4*. In this case, the crackers *5*, under the action of springs *7*, are reduced to the axis of the die, freeing the molded body. Presser *2* brings the latter out of matrix *6*. The body is held in place by the magnets of the Table 1. Under the action of its spring, the table rises, setting the body at the level of the upper plane of the die package. The body, with the help of a stepper conveyor, is removed from the die table of the third operation and transferred to conveyor 6 (Fig. 2).

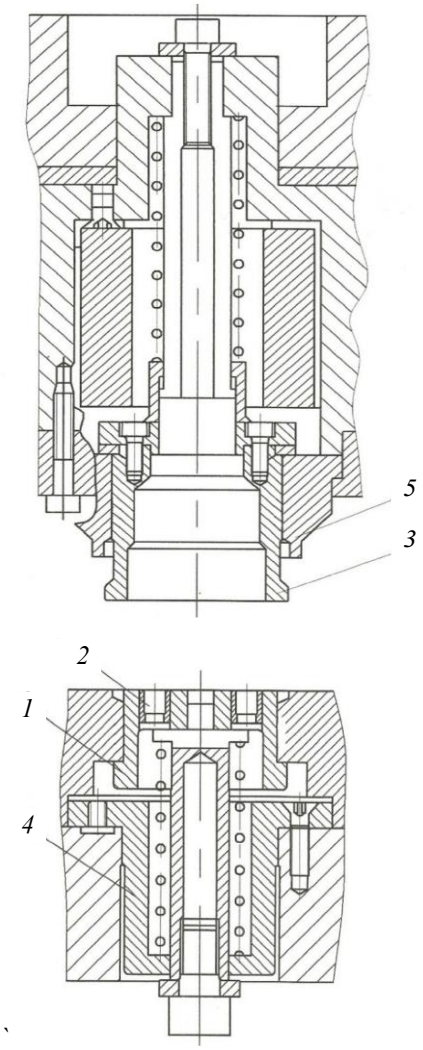

Fig. 7. Stamp of the second operation

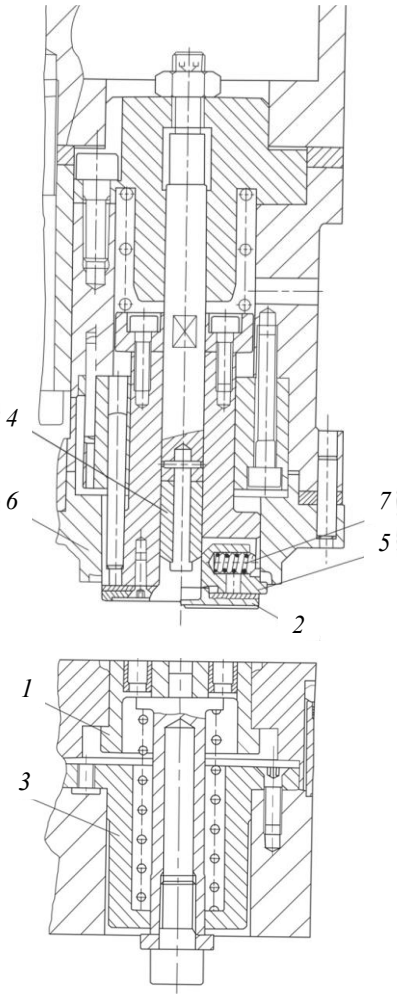

Fig. 8. Stamp of the third operation

5. Development of technical documentation for stamping equipment

On the stamp of the first operation with the transition to tin of reduced thickness, this problem was significantly exacerbated. Sectors *6*, which are involved in the formation of the edge of the workpiece (Fig. 6), are tightened by a coiled spring *7*. Due to the possible unevenness of the pitch of the spring turns *7*, as well as the difference in the contact of the spring with pairs of adjacent sectors in the places of the gaps between them (the spring coil falls into the gap and can cling to the sector, or the gap between the turns falls on the gap between the sectors), some distortion of the sectors may occur.

In this case, the equilibrium of the forces from the spring *7* arising at the points of contact of the spring with the sectors, which acts from the side of a separate sector on a separate wedge *5*, which dilutes this sector, will, passing through the axis of the wedge, be directed not to the axis of the die, but past it. So, when the wedges spread skewed sectors, then when forming a workpiece from thin tin, its edge is deformed unevenly, which leads to a lack of finished products.

It was possible to get rid of this problem by removing six coots *2* mm deep in the places between adjacent sectors, Fig. 9. Now there are no sharp edges of the sectors to which the spring would cling,

and the equilibrium of the above-mentioned forces, passing through the axes of the wedges, converge on the axis of the die. As a result, the edge of the workpiece on the die of the first operation is deformed evenly.

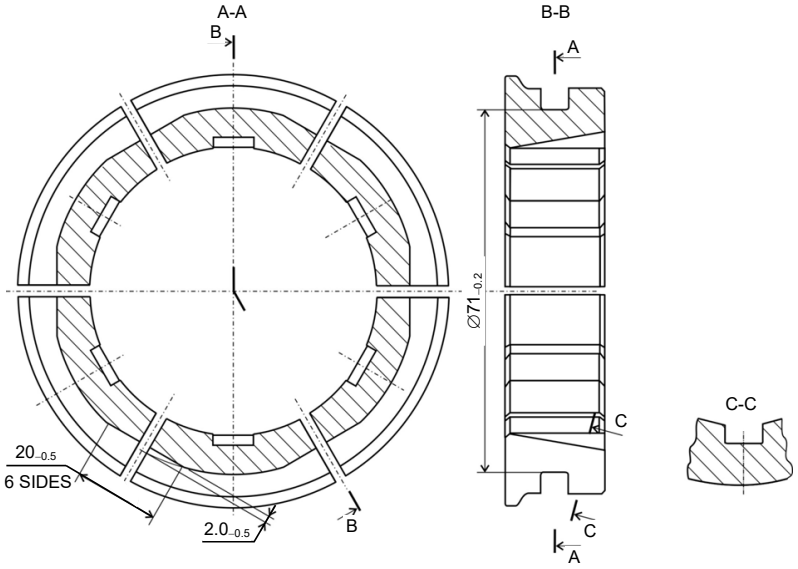

Fig. 9. Sectors of the stamp of the first operation

On the stamp of the second operation with a decrease in the thickness of the tin, two serious problems arose. The first problem was as follows. Since manufacturers use tinplate of increased hardness of the steel base to increase the strength of thin tin covers, it turned out that with an increase in the hardness of the tin, the inner diameter of the lid along the torus-shaped shoulder suddenly began to decrease.

Thus, on the finished workpiece, the diameter of the shoulder d (Fig. 1) decreased from the required 1.80 mm to 1.55...1.60 mm. As a result, the bending torque and maximum stresses in the body of the stops increase, which contributes to their plastic deformation during the closure process.

Subsequently, it was concluded that this behavior of the workpiece is a reaction of thin sheets, associated with a decrease in the plasticity of the tin due to an increase in its hardness. To eliminate this problem, changes were made to the die tool of the second operation, since it is in the second operation that the final preparation of the edge of the workpiece for the formation of a torus-shaped shoulder takes place.

On the tin of hardness degrees TS275 and TH415, during the second operation, the side of the lid passed into the edge bent inside the lid cavity along a radius of $R0.6^{+0.05}$ mm. This radius was determined by the radius on the functional surface of the matrix of the second operation, Fig. 10. On the tin of hardness degree TH435 and strength class TH550, due to a decrease in its ductility, the bending radius of the edge decreased. As a result, the diameter of the ring shoulder on the finished workpiece decreased.

To compensate for the decrease in the bending radius of the edge after the second operation, it was decided to bend the entire end part of the side in the edge bending area towards the axis of the workpiece. To do this, the functional surface of the matrix of the second operation was changed. In the existing matrix (Fig. 10*a*), the diameter of the functional surface $\varnothing 85.2^{+0.02}$ mm passed into a radius R of $0.6^{+0.05}$ mm, and then into a chamfer at an angle of 30° to the inner end surface. In the new matrix, Fig. 10*b*, the cylindrical part of the functional surface with a diameter of $\varnothing 85.2^{+0.02}$ mm at a distance of 4.0 mm from its end surface passes first into the conical part, with an angle of inclination of 15°, and then into a radius R of $0.5^{+0.05}$ mm and a chamfer at an angle of 30° to the inner end surface. As a result, the diameter of the ring shoulder increased to the required 1.8 mm and stabilized, and the cantilever of the threaded stops returned to normal.

The second problem was as follows. During the axial convergence of the matrix 5 (Fig. 7) with the edge of the workpiece, the opposite part of the cylindrical side of the workpiece in the step area began to lose stability.

The loss of stability consisted in the fact that from the action on the edge of the axial force F_1 at the place of the step, a reverse annular depression occurred, Fig. 11*a*. This phenomenon was accompa-

ISSN 2076-2429 (print)
ISSN 2223-3814 (online)

nied by a corresponding loss of high-altitude dimensions of the workpiece, which is unacceptable. To determine the causes of the loss of stability, consider the part of the workpiece that is subjected to axial compression. The cylindrical part of the workpiece from the outside has supports in the form of die parts that support it during compression. Inside, the sidewall of the workpiece has practically no such supports, Fig. 11*b*.

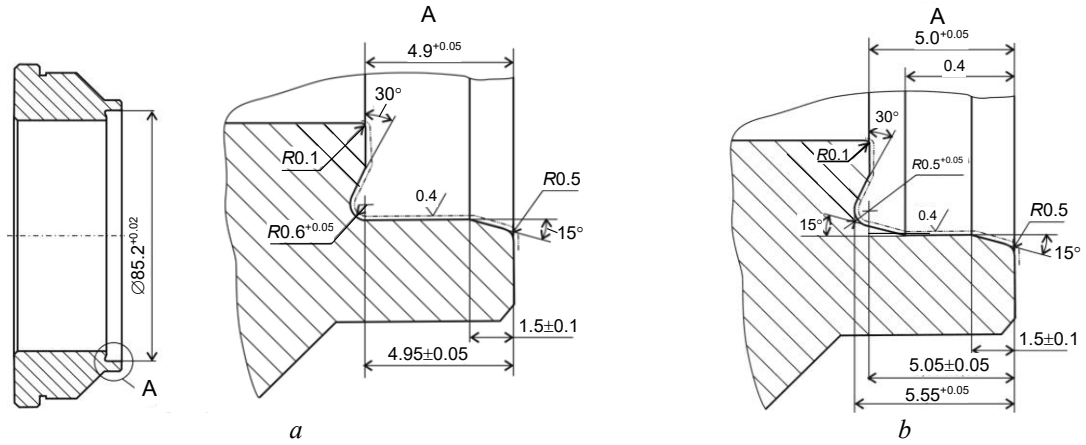

Fig. 10. Die matrix of the second operation: *a* – old matrix; *b* – a new matrix

Let us consider the forces acting on the area where the loss of stability occurs, Fig. 12. The axial force F_1, which acts from the matrix, in the area of the step is transformed into the force F_2 and is directed no longer along the generating cylindrical part of the workpiece, but approximately tangentially to the supporting part, inside which the table moves.

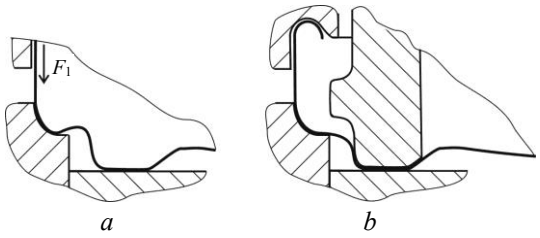

Fig. 11. Loss of stability of the workpiece at the place of the step: *a* – reverse annular recess; *b* – formation blanks of the second operation

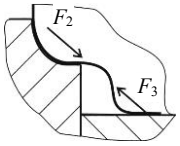

Fig. 12. Forces that cause a loss of stability of the workpiece at the place of the step

At the same time, in the area of the step, at the point of support of the workpiece in the table, an oppositely directed force F_3 acts, caused by the action of the support reaction and a symmetrical force F'_2 from the diametrically opposite side of the workpiece.

These oppositely directed forces compress the step. Structurally, the bend of the step is directed inside the cavity of the workpiece. Therefore, under the influence of two oppositely directed forces, the step bends even more inward, which forms a reverse annular depression.

To prevent loss of stability, it was decided: a support must be introduced at the bend point of the step. For this purpose, the profile of the functional surface of the presser *3* (Fig. 7) was changed. The outer flat annular section of the functional surface was approximated to the end annular section. The distance between them was reduced from 1.5±0.3 mm in the existing design of the clamp, Fig. 13*a*, to $1.0_{-0.1}$ mm in the new, Fig. 13*b*. At the junction of the outer annular section with the outer cylindrical surface of the clamp, instead of a radius of *R*0.8 mm, in the existing design, a chamfer is inserted at an angle of 60° to the axis, in the new one.

Thus, the functional surface of the presser was as close as possible to the inner surface of the bend of the step, creating a support for it. As a result, the loss of stability of the workpiece at the place of the step stopped.

In addition, due to the above-described changes in the design of the edge of the workpiece, associated with an increase in the hardness of the tin of reduced thickness, the width of the inner bend of the edge of the workpiece increased and it began to cling to the clamp when opening the die, so the outer diameter of the clamp was reduced from ∅81.3 mm in the old design (Fig. 13) to ∅81.0 mm in the new one.

Tool mines on the die of the third operation were associated with both the problem of forming covers from tin of reduced thickness, and with a change in the geometric parameters of threaded stops.

In the process of forming threaded stops, the edge of the workpiece is pushed between the forming pads of the matrix *6* and the forming parts of the crackers *5* (Fig. 8), bending inside the cavity of the workpiece. Deformation is carried out in accordance with the configuration of the molding pad of the matrix. However, with a decrease in the thickness of the tin, the cylindrical side of the workpiece in the stop zone began to deform, bending inside the cavity of the workpiece in uncertain places. That is, despite the increase in the hardness of the tin, not only the edge, but also part of the cylindrical side of the lid began to bend.

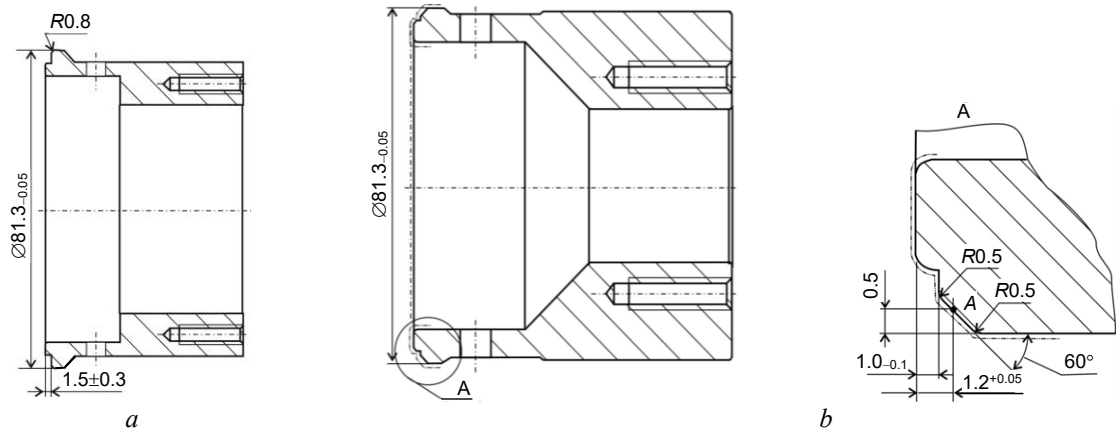

a *b*

Fig. 13. Stamp clamp of the second operation: *a* – old clamp; *b* – a new clamp.

Since the height of the workpiece after the second operation (Fig. 5*b*) is the same throughout the cylinder, then with unregulated bending of the bead inside the workpiece cavity along the stops, the amount of metal that goes to form the latter begins to increase. As a result, the width of individual stops increases along the radius. This size is controlled in the manufacture of lids. Its increase can lead to a serious problem, which is that the lid may not screw onto the neck of the container.

To overcome this problem, the size of the crackers has been changed. The length of the forming part of the crackers was increased from 21.3 mm in the old design to 25.6 mm in the new one, Fig. 14*b*, which brought it as close as possible to the inner surface of the cylindrical side of the workpiece. As a result, the side of the workpiece from the inside received support and its indefinite deformation stopped. To prevent impacts of the upper end edge of the forming part of the crackers through the workpiece into the molding platform of the matrix, the corresponding chamfers were removed on the forming parts of the crackers, with a value of 1.0±0.1 at 45° (Fig. 14*b*). In addition, due to the change in the geometric parameters of the threaded stops, in order to expand the support during their formation, the width of the forming part of the crackers was increased from 12.0 mm in the old design to 13.0 mm in the new one (Fig. 14).

Increasing the length of the threaded stops was achieved by gradually increasing the radii of rounding of the segments forming the annular channel to form the annular shoulder of the workpiece on the matrix *6* of the die of the third operation (Fig. 8). The distance *L* between the points of junction of the radii of rounding the edges of two adjacent segments with fragments of the annular channel, Fig. 15, determines the length of the threaded stop. In the spaces between the segments there are forming pads for forming threaded stops.

Simultaneously with the increase in the radii of rounding of the segments, the thickness of the tin was gradually reduced and its hardness increased. Then the lids were delivered to processing enterprises of the food industry, where their quality was confirmed in the process of production of canned products.

ISSN 2076-2429 (print)
ISSN 2223-3814 (online)

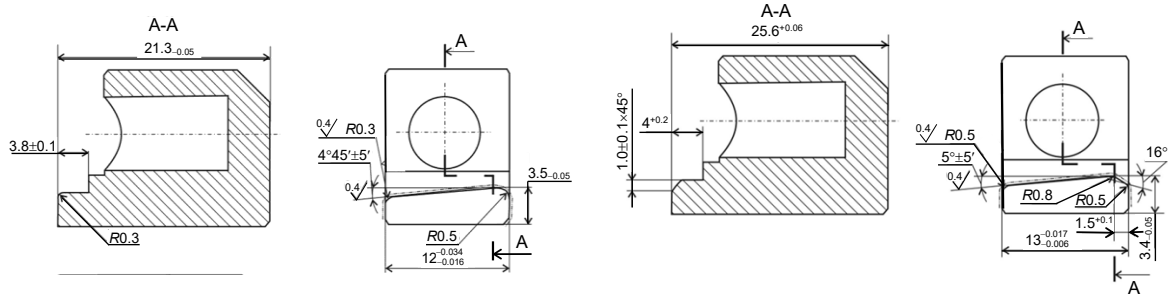

a *b*

Fig. 14. Crackers of the stamp of the third operation: *a* – old; *b* – new

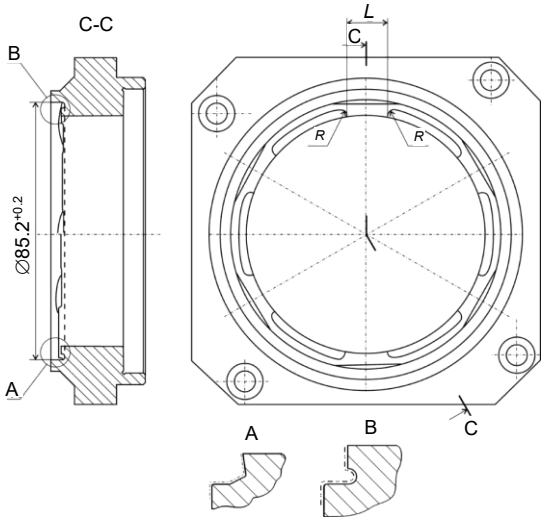

Fig. 15. Die matrix of the third operation

This work turned out to be long-term, in several stages, but it brought a positive result. It has been practically confirmed that the minimum length of the threaded stops of the TO-82 cover with a thickness of 0.20 mm, the degree of hardness of TH415 and TH435 is 18.0 mm. This became the basis for the theoretical design of parametric series of maintenance system covers [10].

The length of the stops from the initial 13.0 mm to the current 18.0 mm was increased by increasing the radii of rounding *R* of the matrix segments, respectively, from *R*0.8 mm, in the existing design, to *R*2.4 mm in the new design (Fig. 15). At the same time, as noted, when making changes to the design of crackers (Fig. 14), the width of the forming parts of the latter was also increased, but in a much smaller proportion – from 12.0 mm to 13.0 mm.

Conclusions

As a result of the development of new technical documentation for the package of dies for the covers of the maintenance system made of tinplate of reduced thickness, the new stamp equipment was manufactured and successfully tested. It has been practically confirmed that the minimum length of the threaded stops of the TO-82 cover made of tin with a thickness of 0.20 mm, the degree of hardness of TH415 and TH435 is 18.0 mm. The length of the stops from the initial 13.0 mm to the current 18.0 mm has been increased by making changes to the dies of each operation. The key changes were the increase in the radii of rounding *R* of the matrix segments, respectively, from R0.8 mm, in the existing design, to *R*2.4 mm in the new one (Fig. 15) and changes to the design of crackers (Fig. 14), the width of the forming parts of the latter was also increased, but in a much smaller proportion – from 12.0 mm to 13.0 mm. A reduction in the weight of the TO-82 lid blank by at least 20% has been achieved, which significantly reduces the cost of lids, saves metal and provides grounds for reducing the weight of lids of other standard sizes.

Література

1. Altan T., Tekkaya A. E. Sheet Metal Forming: Fundamentals. Materials Park, OH : ASM International, 2012. 296 p.
2. Schuler GmbH. Metal Forming Handbook. Berlin : Springer-Verlag, 1998. 720 p.
3. Altan T., Tekkaya A. E. Sheet Metal Forming: Processes and Applications. Materials Park, OH : ASM International, 2012. 365 p.
4. Marciniak Z., Duncan J. L., Hu S. J. Mechanics of Sheet Metal Forming. 2nd ed. Oxford : Butterworth-Heinemann, 2002. 368 p.
5. Hosford W. F., Cadell R. M. Metal Forming: Mechanics and Metallurgy. 4th ed. Boca Raton : CRC Press, 2011. 360 p.
6. Boljanovic V. Sheet Metal Forming Processes and Die Design. New York : Industrial Press Inc., 2004. 350 p.

7. Калюжний В. Л., Калюжний О. В., Піманов В. В. Штамп для виготовлення порожнистих виробів з важкодеформівних матеріалів. *Вестник Национального технического университета «ХПИ»*. Харьков : НТУ «ХПИ», 2009. Вып. 31. С. 45–50.
8. Калюжний В. Л., Запорожченко А. С. Вибір оптимального радіусу заокруглення пуансона для процесу холодного витягування з попередньо спрофільованих листових заготовок. *Вестник Национального технического университета «ХПИ» : сб. науч. тр.* Харків : НТУ «ХПИ», 2011. Вып. 45. С. 135–141.
9. Product Catalog. Packaging Steel. U.S. Steel Košice, s.r.o. URL: https://www.usske.sk/ (дата звернення: 18.10.2025).
10. Ватренко О. В. Зменшення металоємності закупорювальних засобів та безпека харчових продуктів у скляній упаковці. *Пакувальна індустрія (стан та перспективи для харчових продуктів) : матеріали V Наук.-практ. конф. (Алушта, 01–02 черв. 2011 р.)*. 2011. С. 94–106. (Додаток до часопису «Упаковка». 2011. № 3).

References

1. Altan, T., & Tekkaya, A. E. (2012). *Sheet metal forming: Fundamentals*. ASM International.
2. Schuler GmbH. (1998). *Metal forming handbook*. Springer-Verlag.
3. Altan, T., & Tekkaya, A. E. (2012). *Sheet metal forming: Processes and applications*. ASM International.
4. Marciniak, Z., Duncan, J. L., & Hu, S. J. (2002). *Mechanics of sheet metal forming* (2nd ed.). Butterworth-Heinemann.
5. Hosford, W. F., & Cadell, R. M. (2011). *Metal forming: Mechanics and metallurgy* (4th ed.). CRC Press.
6. Boljanovic, V. (2004). *Sheet metal forming processes and die design*. Industrial Press Inc.
7. Kaliuzhnyi, V. L., Kaliuzhnyi, O. V., & Pimanov, V. V. (2009). Die for the production of hollow products from hard-to-deform materials. *Bulletin of the National Technical University "KhPI"*, (31), 45–50.
8. Kaliuzhnyi, V. L., & Zaporozhchenko, A. S. (2011). Selection of the optimal punch fillet radius for the cold drawing process from pre-profiled sheet blanks. *Bulletin of the National Technical University "KhPI": Collection of Scientific Papers*, (45), 135–141.
9. U.S. Steel Košice. (n.d.). *Product catalog: Packaging steel*. https://www.usske.sk.
10. Vatrenko, O. V. (2011). Reducing the metal consumption of closures and food safety in glass packaging. *Packaging Industry (State and Prospects for Food Products): Materials of the V Scientific and Practical Conference*, 94–106.

Ватренко Олександр Віталійович; Oleksandr Vatrenko, ORCID: https://orcid.org/0000-0002-5545-2480
Верхівкер Яков Григорович; Yakov Verkhivker, ORCID https://orcid.org/0000-0002-2563-4419
Прокопович Ігор Валентинович; Ihor Prokopovych, ORCID: https://orcid.org/0000-0002-8059-6507

Received November 02, 2025
Accepted November 29, 2025

ISSN 2076-2429 (print)
ISSN 2223-3814 (online)

ЕНЕРГЕТИКА

ENERGETICS

UDC 658.264

H. Balasanian, DSc, Prof.,
V. Liashenko
Odessa Polytechnic National University, Shevchenko Ave. 1, Odesa, Ukraine, 65044, e-mail: balasanyan@op.edu.ua

PRIORITY REGULATION OF HEAT SUPPLY SYSTEMS TAKING INTO ACCOUNT HYDRAULIC BALANCING

Г. Баласанян, В. Ляшенко. **Пріоритетне регулювання систем теплопостачання з урахуванням гідравлічного балансування.** Сучасні системи централізованого теплопостачання в Україні опинилися в умовах, коли дефіцит енергоресурсів перестав бути теоретичною загрозою і набув статусу постійного обмежувального фактора. Запропоновано інтегровану методику регулювання міських систем теплопостачання, що поєднує гідравлічне балансування та алгоритми пріоритетного розподілу теплової енергії. Практичну апробацію проведено на прикладі центрального теплового пункту (ЦТП-27) у місті Чорноморськ, запропонований алгоритм знижує ризики відключень критичних споживачів, оптимізує роботу котелень і теплових пунктів та формує прозорий механізм розподілу тепла. Виконано побудову п'єзометричних графіків, розрахунок сумарних опорів та визначення коефіцієнтів топології, що дозволило ідентифікувати найбільш уразливих з точки зору гідравліки споживачів. Подальший тепловий розрахунок враховував класи споживачів (A–E), сценарії дефіциту (0…30%) та модератор навантаження, який гарантує захист малих об'єктів від витіснення великими. Даний підхід формує так званий «подвійний баланс»: гідравлічний блок забезпечує технічну подачу теплоносія, тоді як тепловий блок створює справедливий і прозорий розподіл ресурсів відповідно до соціальної значущості об'єктів. Очікуваний ефект полягає у зменшенні ризику відключень критичної інфраструктури, підвищенні ефективності роботи котелень і теплових пунктів та зниженні соціальної напруги в умовах дефіциту газу. Наведена модель базується на припущенні постійних параметрів трубопроводів та стабільного складу споживачів, тому в умовах різких змін навантаження або модернізації мережі потрібне коригування розрахунків. Подальші роботи можуть включати прогнозування добового чи сезонного попиту та розробку методів автоматичного настроювання балансувальних клапанів за даними систем, прогнозних моделей і регуляторів.

Ключові слова: теплопостачання, гідравлічний баланс, дефіцит газу, пріоритетний розподіл тепла, п'єзометричний графік, енергетична безпека

H. Balasanian, V. Liashenko. **Priority regulation of heat supply systems taking into account hydraulic balancing**. Modern centralized heat supply systems in Ukraine find themselves in a situation where energy deficits are no longer a theoretical threat but have become a permanent limiting factor. An integrated methodology for regulating urban heat supply systems is proposed, combining hydraulic balancing and algorithms for the priority distribution of thermal energy. Practical testing was carried out using the example of the central heating station (CHS-27) in the city of Chornomorsk. The proposed algorithm reduces the risk of critical consumers being cut off, optimizes the operation of boiler rooms and heating stations, and creates a transparent heat distribution mechanism. Piezometric graphs were constructed, total resistance was calculated, and topology coefficients were determined, which made it possible to identify the most vulnerable consumers in terms of hydraulics. Further thermal calculations took into account consumer classes (A–E), deficit scenarios (0…30%), and a load moderator that guarantees the protection of small objects from being displaced by large ones. This approach creates a so-called "double balance": the hydraulic block ensures the technical supply of heat carrier, while the thermal block creates a fair and transparent distribution of resources in accordance with the social significance of the facilities. The expected effect is to reduce the risk of critical infrastructure shutdowns, increase the efficiency of boiler rooms and heat distribution points, and reduce social tensions in conditions of gas deficits. The model is based on the assumption of constant pipeline parameters and a stable consumer base, so adjustments to the calculations are needed in the event of sudden changes in load or network modernization. Further work may include forecasting daily or seasonal demand and developing methods for automatically adjusting balancing valves based on system data, forecast models, and regulators.

Keywords: heat supply, hydraulic balance, gas deficit, priority heat distribution, piezometric graph, energy security

Introduction

Modern centralized heat supply systems in Ukraine find themselves in a situation where energy deficits are no longer a theoretical threat but have become a permanent limiting factor [1, 2]. Resolution No. 812 of the Cabinet of Ministers of Ukraine dated July 19, 2022, established a 10% reduction in guaranteed natural gas volumes for heat and power companies compared to previous seasons. This decision was a key signal for the transition from static heat network management to adaptive distribution models focused on the rational use of scarce resources.

Article [3] laid out the conceptual principles of priority regulation of heat supply based on consumer classification, weighting coefficients, and scenario analysis. However, the question of their practical coordination with the actual hydraulic parameters of the networks remained open. It is pre-

DOI: 10.15276/opu.2.72.2025.04

cisely the hydraulic imbalance – pressure losses, differences in height and length of routes – that determines the maximum performance of the system and often makes it impossible to implement even an optimally designed thermal algorithm.

Analysis of literature data and problem statement

The issue of regulating urban heat supply systems is considered in a significant number of works. Researchers emphasize that traditional methods of manual or static network balancing have limited effectiveness in modern conditions: they do not take into account dynamic load fluctuations, daily and seasonal changes in demand, as well as unevenness in supplying different consumer groups [4]. At the same time, regulatory documents, in particular, oblige heat and power companies to reduce guaranteed volumes of natural gas, which requires operators to have more flexible and adaptive resource management schemes.

A separate block of research is devoted to the hydraulic balancing of pipelines. The work of Kulik, Baran, and Kondratyuk proves that hydraulic imbalance is the source of significant energy losses [5, 6]. To eliminate flow unevenness, it is proposed to install automatic balancing valves (for example, Danfoss AFQMP and AME/AMEi actuators) [7, 8]. Properly performed hydraulic balancing not only ensures an even supply of heat carrier to all consumers, but also reduces energy consumption in the system by 15…20% [7]. Some authors introduce topological coefficients that adjust calculations to take into account the length of routes and the height of buildings, but the further integration of these factors into heat distribution procedures remains limited.

Another area of research concerns the priority regulation of thermal loads. A number of studies propose algorithms that take into account the social significance of objects, distributing resources between groups A–E according to their criticality. Such approaches make it possible to protect hospitals, schools, and housing from deficits, but they are most often considered in isolation from the hydraulic properties of the network. Hydraulic constraints (pipes, pressure losses, building height) are not integrated into these algorithms, which complicates their practical application.

Current work on the digitization of heating networks describes the concept of Smart Heat Networks [9]. The authors emphasize the role of SCADA systems, predictive models, and regulators that allow real-time data collection and automatic adjustment of boiler operation. At the same time, in most publications, the digital aspect is reduced to the "thermal" side of the problem – demand forecasting and supply optimization – while hydraulics (network topology, pressure losses) is considered only as a background condition. The lack of synthesis between digital and hydraulic tools limits the effectiveness of such systems.

Thus, there is a "gap" in the literature between the theory of hydraulic balancing and the practice of priority heat distribution. Existing approaches focus either on the physical stabilization of the network or on the social aspect of distribution, but rarely combine these two dimensions. Bridging this gap and forming a "double balance" (hydraulic and thermal) is the basis of this research.

The current state of urban heat supply systems in Ukraine is characterized by a number of critical problems. The most important of these is the high dependence on imported natural gas, which, in conditions of martial law and economic instability, creates real risks of disruption to uninterrupted heat supply [10, 11].

Purpose and objectives of the study

The purpose of the study is to develop and test a methodology for priority regulation of heat supply that takes into account both the hydraulic parameters of the network and the socio-economic significance of different categories of consumers.

To achieve this goal, the following tasks must be solved:

– perform hydraulic calculations and construct a piezometric profile of consumers;

– develop a heat balancing algorithm that takes into account deficit scenarios;

– ensure minimum regulatory levels of heat supply for critical facilities;

– test the effectiveness of the methodology using the example of CHS-27 in the city of Chornomorsk.

Thus, the study aims to create a universal approach that can combine the technical and social aspects of heat network management.

Research materials and methods

Methodology for hydraulic balancing and priority regulation of heat supply. This stage includes the collection of topographical data, pipe characteristics, and consumer heat loads. Using offi-

ISSN 2076-2429 (print)
ISSN 2223-3814 (online)

cial heat network maps and *Google Earth Pro* tools, the lengths of pipelines, geodetic marks, and the height of buildings were determined. A catalog of consumers was compiled, indicating their heat capacities, which was later used to classify objects according to their criticality.

The parameters below (the longest route from CHS-27 to the building at 8A ZAKHYSNYKIV UKRAINY Street, its height, and elevation marks) are an example of such an inventory and illustrate how the initial data is used in further calculations.

Before performing a hydraulic calculation, it is necessary to collect certain input data, namely to determine the lengths of individual sections of the pipeline. For this purpose, official maps of the heating networks of Chornomorsk (Fig. 1) with the relevant information were used. Based on these maps, the longest route from CHS-27 to the residential building at 8A ZAKHYSNYKIV UKRAINY Street was determined, with a total length of 548.5 m. Although this facility is the most remote, the distance parameter alone does not determine the criticality of the consumer in terms of pressure supply. To clarify the geodetic characteristics of the route, *Google Earth Pro* was additionally used. Relief marks were sequentially recorded, and the heights of buildings were determined based on their number of floors. As a result, at the address 8A ZAKHYSNYKIV UKRAINY, the tallest nine-story residential building with an approximate height of about 27 m was identified, in contrast to other five-story consumers with a height of about 15 m. The maximum relief difference along the route does not exceed 5 m, which confirmed the relative flatness of the terrain.

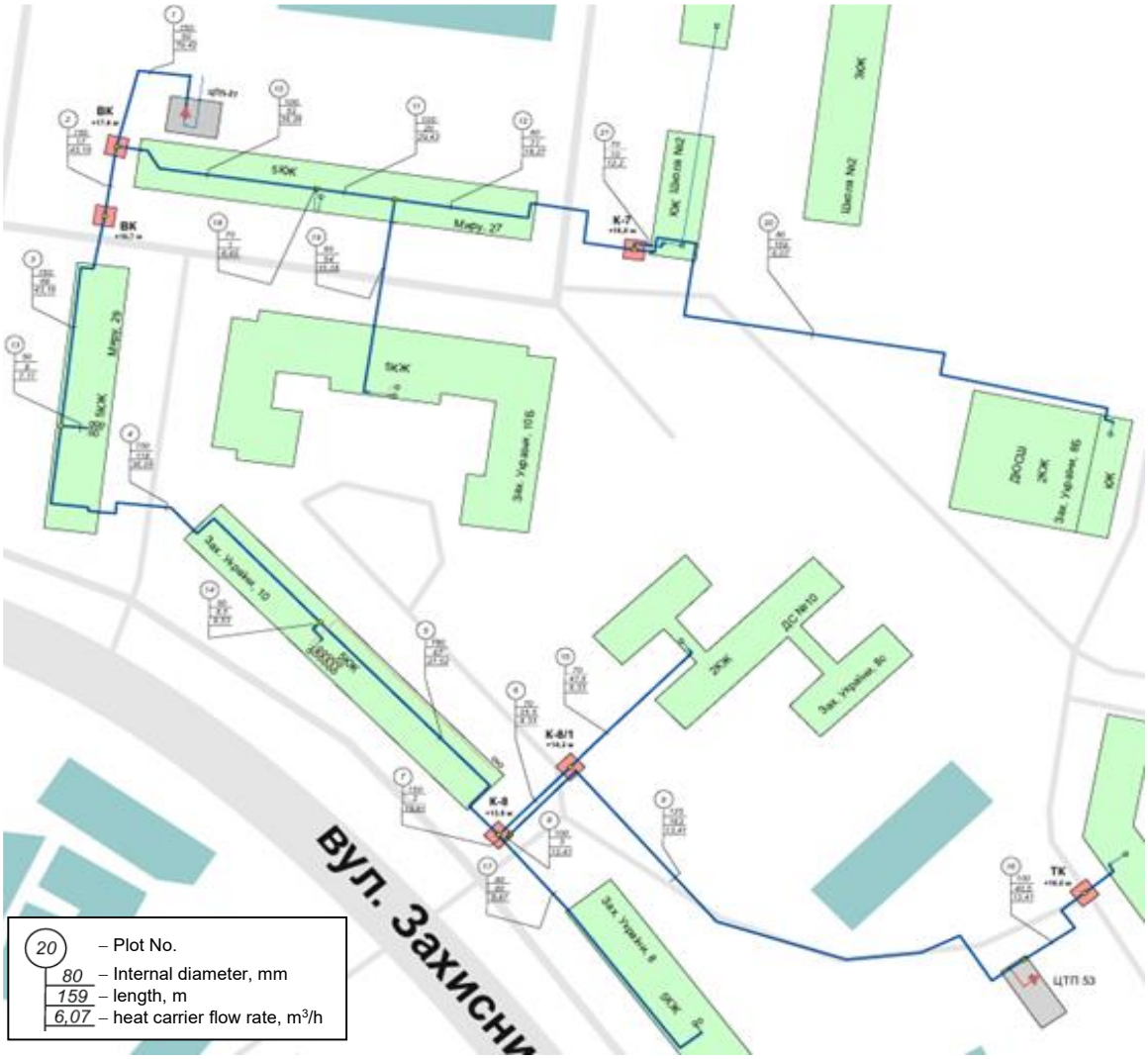

Fig. 1. Map of heating networks from the central heating station 27 m. Chornomorsk

Hydraulic calculation method. The hydraulic calculation was performed in several stages. After determining the lengths of the routes and the heights of the buildings, the volumetric heat carrier flow rate was calculated for each branch. Based on this data, the average flow velocity, Reynolds number,

and friction coefficient were calculated, followed by linear and local head losses. The total resistance of each route takes into account the geodetic mark, the height of the building, and the additional pressure reserve for consumers. Based on the values obtained, the most "difficult" objects in terms of hydraulics were identified and piezometric graphs were constructed.

The highest hydraulic losses were obtained for the building at ZAKHYSNYKIV UKRAINY 8B, where the total resistance was 12.4 m water column. The final selection of the "heaviest" consumer, was made on the basis of hydraulic resistance calculated taking into account all pressure losses. The facility at ZAKHISNYKIV UKRAINY 8A was taken as the basis for constructing a piezometric graph, as it combines real geodetic conditions with maximum head losses, determining the maximum performance of the system.

Standard dependencies were used to perform the hydraulic analysis, which allow determining the speed of the coolant, specific and total head losses for each section. The calculated data are shown in Table 1.

Table 1

Hydraulic calculation of pipeline sections for first Quarter 1

Sections	Inner diameter of the pipeline, mm	Section lengt, m	Coolant flow rate, m^3/h	Coolant velocity, m/s	Roughness coefficient, mm	Specific linear losses, m w.c./m	Linear losses on the section, m w.c.	Number of local hydraulic resistances on the section and their type										Sum of hydraulic resistance coefficients, $\Sigma\xi$	Local losses, m w.c.	Sum of linear and local losses,	Coolant pressure losses at the end of the section starting from the inlet node, m w.c.
								Valve	Narrowing	Widening	Tee for passage	Tee for branch	Crosspiece for passage	Crosspiece for branching	Turn 30°	Turn 60°	Turn 90°				
1	150	50	79.42	1.249	2	0.020	1.984	1	0	0	0	0	0	0	0	0	2	2.5	0.199	2.182	2.182
2	150	17	43.16	0.679	2	0.006	0.199	1	0	0	1	0	0	0	0	0	0	1.5	0.035	0.234	2.417
3	150	68	43.16	0.679	2	0.006	0.797	0	0	0	0	0	0	0	0	0	2	2.0	0.047	0.844	3.261
4	150	118	36.05	0.567	2	0.004	0.964	0	0	0	1	0	0	0	1	0	7	8.5	0.139	1.104	4.364
5	150	87	27.52	0.433	2	0.002	0.414	0	0	0	1	0	0	0	0	0	2	3.0	0.029	0.443	4.807
6	70	25.5	8.33	0.602	2	0.012	0.609	1	2	0	0	1	0	0	0	0	0	2.2	0.041	0.649	5.457
7	150	2	19.18	0.302	2	0.001	0.005	0	0	0	1	0	0	0	0	0	0	1.0	0.005	0.009	4.816
8	100	3	13.41	0.474	2	0.005	0.028	1	2	0	0	1	0	0	0	0	0	2.2	0.025	0.054	4.870
9	125	163	13.41	0.304	2	0.001	0.480	1	0	1	0	0	0	0	3	0	3	5.5	0.026	0.506	5.376
10	100	52	36.26	1.283	2	0.035	3.614	1	2	0	0	1	0	0	2	0	0	3.2	0.269	3.882	6.065
11	100	20	29.43	1.041	2	0.023	0.916	0	0	0	1	0	0	0	0	0	0	1.0	0.055	0.971	7.036
12	80	71	18.27	1.010	2	0.028	4.040	1	1	0	1	0	0	0	0	0	4	5.6	0.291	4.332	11.367
13	50	8	7.11	1.007	2	0.051	0.814	1	3	0	0	1	0	0	0	0	0	2.3	0.119	0.933	4.194
14	50	8.5	8.53	1.207	2	0.073	1.244	2	3	0	0	1	0	0	0	0	2	4.8	0.357	1.601	5.965
15	70	47.5	8.33	0.602	2	0.012	1.134	1	0	0	0	0	0	0	0	0	1	1.5	0.028	1.162	6.618
16	100	40.5	13.41	0.474	2	0.005	0.385	2	1	0	0	0	0	0	0	0	4	5.1	0.058	0.443	5.819
17	80	80	5.78	0.320	2	0.003	0.456	1	2	0	1	0	0	0	0	0	2	3.7	0.019	0.475	5.291
18	70	1	6.83	0.493	2	0.008	0.016	1	1	0	0	1	0	0	0	0	0	2.1	0.026	0.042	6.107
19	80	54	11.16	0.617	2	0.011	1.148	2	1	0	0	1	0	0	0	0	1	3.6	0.070	1.218	8.253
20	80	159	6.07	0.335	2	0.003	0.998	1	1	0	1	0	0	0	0	0	9	10.6	0.061	1.059	12.426
21	70	10	12.20	0.881	2	0.026	0.512	2	1	0	0	1	0	0	0	0	3	5.6	0.222	0.733	12.101

Coolant flow rate:

$$Q_i = \frac{G_i}{\rho}, \tag{1}$$

where:

G_i is the mass flow rate, kg/s;

ρ is the density of water, kg/m³.

In practical calculations in Excel, the volumetric flow rates Q_i in m³/h, shown in Fig. 1, are used directly.

Average speed of coolant flow in the pipe:

$$v = \frac{4Q}{\pi d^2}, \tag{2}$$

where: d is the inner diameter of the pipeline.

Reynolds number for flow regime assessment:

$$\mathrm{Re} = \frac{vd}{\nu}, \tag{3}$$

ISSN 2076-2429 (print)
ISSN 2223-3814 (online)

where: ν is the kinematic viscosity of water, m²/s.

Hydraulic friction coefficient (according to Altshul's formula):

$$\lambda = 0.11\left(\frac{k}{d}+\frac{68}{\mathrm{Re}}\right)^{0.25}, \tag{4}$$

where: k is the equivalent roughness of the pipe wall, m.

Linear resistance of the section:

$$r_{\mathrm{lin}} = \lambda\frac{L}{d}\times\frac{v^2}{2g}, \tag{5}$$

where: L is the length of the section.

Losses at local supports:

$$r_{\mathrm{loc}} = \sum\xi_j \times\frac{v^2}{2g}, \tag{6}$$

where: ξ_j – local resistance coefficients (valves, tees, constrictions/expansions).

Total head losses in the section:

$$R_{\mathrm{seg}} = \sum(r_{\mathrm{lin}} + r_{\mathrm{loc}}). \tag{7}$$

Equivalent head:

$$H_{\mathrm{eq},i} = h_{\mathrm{geo},i} + h_{\mathrm{build},i} + R_{\mathrm{loc},i}, \tag{8}$$

where:

$h_{\mathrm{geo},i}$ is the geodetic elevation, m;

$h_{\mathrm{build},i}$ is the height of the building, m;

$R_{\mathrm{loc},i}$ is the consumer resistance, taking into account the additional pressure of 5 m water column.

Total resistance:

$$R_{\mathrm{path},i} = \sum R_{\mathrm{seg}} + H_{\mathrm{eq},i}, \tag{9}$$

where: $\sum R_{\mathrm{seg}}$ – sum of hydraulic resistances of the entire pipeline to consumer *i*, m water column.

The values obtained allow us to determine the most distant and "heaviest" objects in terms of hydraulics. However, in order to adequately take these differences into account in further balancing, the topology coefficient [5] is introduced:

$$K_{\mathrm{topo},i} = 1+\beta\times\frac{R_{\mathrm{path},i}-R_{\min}}{R_{\max}-R_{\min}}, \tag{10}$$

where:

$R_{\min}, R_{\max}$ – the minimum and maximum values of the total resistance among all consumers;

β – the coefficient of variation of resistance [16]:

$$\beta = \frac{\sigma(R)}{\mu(R)}, \tag{11}$$

where:

$\sigma(R)$ is the root mean square deviation;

$\mu(R)$ is the average value of the total resistance.

This coefficient acts as a corrector that converts hydraulic parameters into a dimensionless form that can be conveniently integrated into further analysis. Its purpose is to emphasize the influence of network topology on the availability of the heat carrier: the greater the resistance of the consumer, the more vulnerable it is to hydraulic deficits. Thus, $K_{\mathrm{topo},i}$ ensures fair consideration of the spatial location of consumers in the system and allows the stages to be divided: first, hydraulic stabilization, and then

thermal regulation according to priorities. As a result, calculated data were obtained with the determination of the coefficient $K_{\text{topo},i}$ for each consumer (Table 2).

Table 2

Hydraulic calculation for each consumer

№	Address	Hydraulic resistance, m w.c	Volume flow rate, m^3/h	Absolute elevation, h_{geo}, m	Number of floors	Building height, h_{build},	Consumer pressure, H, m	Total resistance, R_{path}, m w.c	K_{topo}
1	Zakhysnykiv Ukrainy str., 10	7.97	8.53	16	5	15	16	23.97	1.044
2	Zakhysnykiv Ukrainy str., 10-Б	10.25	11.16	17	5	15	17	27.25	1.077
3	Zakhysnykiv Ukrainy str., 8	7.29	5.78	15	5	15	15	22.29	1.027
4	Zakhysnykiv Ukrainy str., 8-А	7.82	13.41	18	9	27	30	37.82	1.183
5	Zakhysnykiv Ukrainy str., 8-6 (Comprehensive children's and youth sports school)	14.43	6.07	18	3	9	12	26.43	1.069
6	Zakhysnykiv Ukrainy str.8-С (preschool educational institution)	8.62	8.33	20	2	6	11	19.62	1.000
7	Mury Av. (Chornomorskoho kozatstva) 17-А	14.10	12.20	20	3	9	14	28.10	1.085
8	Mury Av. 27 (Chornomorskoho kozatstva)	8.11	6.83	18	5	15	18	26.11	1.065
9	Mury Av.29 (Chornomorskoho kozatstva)	6.19	7.11	18	5	15	18	24.19	1.046

Priority heat supply regulation. The priority regulation algorithm combines the social classification of consumers with mathematical methods of heat load correction. First, all heating network objects are classified into groups A–E according to their criticality (hospitals, schools, housing stock, offices, industry, etc.). For each consumer, the calculated thermal load, the minimum guaranteed level of heat supply, and the weight coefficient are determined. In the event of a resource deficit, a load moderator is applied to the distribution, which increases the supply to small facilities and limits large ones. After normalizing this value, "base" supply coefficients are determined, which are adjusted by a scaling factor so that the total heat supplied corresponds to the given deficit scenario. At the final stage, the supply coefficient is calculated for each consumer, which ensures a balance between supplying critical facilities and saving resources.

Publication [3] presented general principles for constructing an algorithm for the priority distribution of thermal energy in conditions of energy resource deficits. In particular, it considered the classification of consumers into groups A–E, the determination of weighting coefficients, and minimum heat supply levels for each category. Basic provisions for a scenario-based approach (0…30% deficit) were also formulated, allowing the behavior of the system to be described under various resource constraints.

In this work, the methodology is further developed. While the main focus was on the conceptual part – justifying the need for priority regulation and describing its basic mechanisms – this paper considers a detailed heat calculation. It includes the introduction of a load moderator, normalization procedures, and the determination of the final heat supply coefficient for each consumer. Particular emphasis is placed on the relationship between the thermal unit and hydraulic constraints, which allows for the creation of a more realistic and applicable model for practical testing using the example of CHS-27 in the city of Chornomorsk.

To take into account the load characteristics of individual consumers, a load moderator is introduced L_i . Its action is activated only in conditions of heat energy deficit:

ISSN 2076-2429 (print)
ISSN 2223-3814 (online)

$$L_i = \begin{cases} 1; \\ \left(\dfrac{Q_{\text{ref}}}{Q_i} \right)^{\gamma}, \end{cases} \begin{matrix} Def = 0; \\ Def < 1, \end{matrix} \tag{12}$$

where: Q_i – is the calculated thermal load of the consumer, Q_{ref} is the reference thermal load (average for a group of consumers), γ is the sensitivity coefficient.

This expression ensures that in the absence of a deficit ($Def = 0$), the heat supply is equal to the calculated value, while in the case of limited resources, small consumers receive a relative "boost" and large consumers receive a restriction:

$$\gamma = \frac{\sigma(Q)}{\mu(Q)}, \tag{13}$$

where:

$\sigma(Q)$ is the standard deviation of heat loads,

$\mu(Q)$ is the arithmetic mean of heat loads.

Thus, γ reflects the degree of heat load dispersion: in systems with almost identical buildings (Q_i close) – γ is small, the correction is minimal; in systems with a wide range of loads (for example, a kindergarten with 200 kW and a factory with 2000 kW) – γ is higher, the correction is stronger.

Further normalization ensures that moderators are brought to a single scale:

$$N_i = \frac{L_i}{\max(L_j)}, \tag{14}$$

where the maximum value determines the highest priority consumer, and the rest are scaled proportionally.

Next, an intermediate "base" heat supply coefficient is determined for the consumer, taking into account the deficit, normalization, and minimum levels:

$$K_{\text{raw},i} = \max(K_{\text{def},i} \times N_i;\ K_{\min,i}). \tag{15}$$

Calculation of the initial amount:

$$Q_{\text{sum}} = \sum K_{\text{raw},i} \times Q_{\text{design},i}. \tag{16}$$

Determination of the target value:

$$Q_{\text{target}} = (1 - Def) \times \sum Q_{\text{design},i}. \tag{17}$$

Scaling factor:

$$K_{\text{scale}} = \frac{Q_{\text{target}}}{Q_{\text{sum}}}. \tag{18}$$

The final heat supply coefficient is determined as:

$$K_{\text{final},i} = \min(1, \max(K_{\min,i}, K_{\text{raw},i} K_{\text{scale}})). \tag{19}$$

Thus, in normal mode, all consumers receive the design loads, and in conditions of deficit, a priority distribution of resources is formed, taking into account the minimum guaranteed levels.

Adding normalization by sum allowed us to eliminate a systemic error: in case of a high deficit, the total heat decreased more than was specified in the scenario. The new scheme ensures that the total heat distributed is always equal to $(1 - Def) \times \Sigma Q_{\text{design},i}$, while maintaining the priority logic.

The final amount of heat supplied to each consumer is determined by the expression:

$$Q_{\text{deliv},i} = K_{\text{final},i} \times Q_{\text{design},i}. \tag{20}$$

During the development of the methodology, the following decisions were made:

– it is advisable to implement the coefficient (K_{time}) not in calculations, but at the SCADA level for controlling electric drives;

– the coefficient (K_{topo}) was moved to the hydraulic block, as it created a conflict with the heat balance.

This emphasizes the importance of achieving hydraulic stabilization before regulating heat distribution.

A key part of the methodology is the analysis of system behavior under various deficit scenarios. Four scenarios were considered to model the operation of the heating network: no deficit (0% deficit), moderate deficit (10%), medium deficit (20%), and significant deficit (30%). In each scenario, the final supply coefficients $K_{final,i}$ and heat release coefficients $Q_{deliv,i}$ were calculated for all consumer groups. It was shown that the algorithm maintains design loads in normal mode, and in case of a deficit, redistributes the resource so that consumers in classes A–C receive the maximum necessary heat, and restrictions fall mainly on categories D–E. This allows us to quantitatively assess the impact of the deficit on each group and identify the limits beyond which the resource no longer guarantees coverage of minimum needs.

In addition to numerical analysis, the technical implementation of the methodology is an important component. To implement priority regulation in practice, the following are required:

– automatic balancing valves with flow regulators suitable for maintaining hydraulic balance in real time;

– electrically driven actuators to change the position of the valves according to the control system commands;

– a SCADA system or similar monitoring platform that collects data on temperatures, pressures, and flows and generates control actions;

– regular updates of reference information on the condition of pipelines, heat loads, and changes in the composition of consumers.

Synchronization of these components ensures not only an automatic response to deficits, but also the ability to proactively predict situations, particularly during seasonal consumption peaks. This implementation also complies with European energy efficiency requirements and contributes to the fulfillment of national standards.

Research results

Hydraulic calculations for nine consumers connected to CHS-27 in the city of Chornomorsk showed significant differences in the values of total resistance and equivalent pressure. The most "difficult" consumers were the buildings at 8B and 8A Zakhysnykiv Ukrainy Street. For the latter, the critical factors were its greatest distance (~550 m) and the presence of nine floors, which determined it as a critical object from a hydraulic point of view.

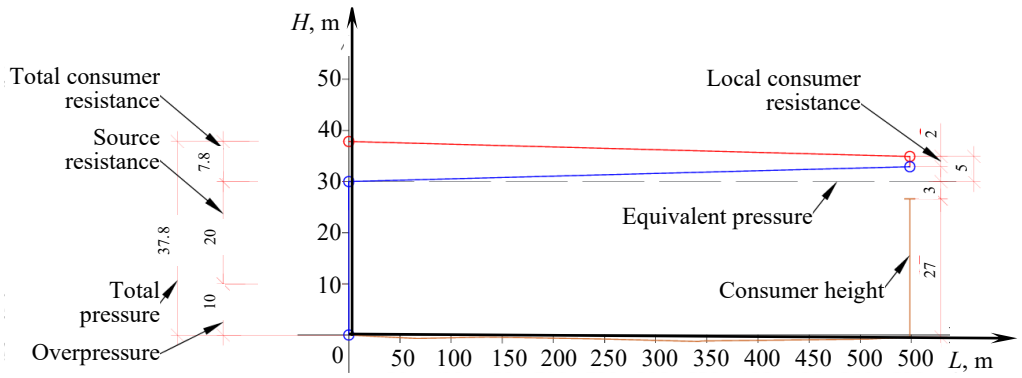

Fig. 2. Piezoelectric graph of the network to the consumer at 8-A Zakhysnykiv Ukrainy Street

Piezometric analysis revealed potential areas of pressure deficiency on the upper floors of this building. This confirms the need to install automatic balancing valves [9] and to take into account the topology coefficient (K_{topo}) in further iterations of regulation (Fig. 2).

With regard to heat regulation, in the base scenario (0%), all consumers receive the design heat loads, which confirms the correctness of the hydraulic and thermal calculations. When the resource is reduced (10…30%), the algorithm forms a priority distribution: critical consumers (classes A–C: hos-

ISSN 2076-2429 (print)
ISSN 2223-3814 (online)

pitals, schools, housing stock) maintain the necessary level of heat supply, while less significant categories (classes D–E: offices, commercial consumers, industry) receive proportionally smaller volumes.

The load moderator played an important role, preventing the dominance of large consumers with low priority and ensuring fair distribution even for small facilities.

Figure 3 shows the distribution of heat supply between actual and theoretical consumers of CHS-27 in scenarios with a deficit of 0%, 10%, and 30%. It can be seen that classes D and E, "Theoretical consumers", have a significantly greater reduction in heat supply-they are the ones that "absorb" the main reductions, thus emphasizing that the algorithm deliberately "protects" priority categories by redistributing the deficit toward less important ones.

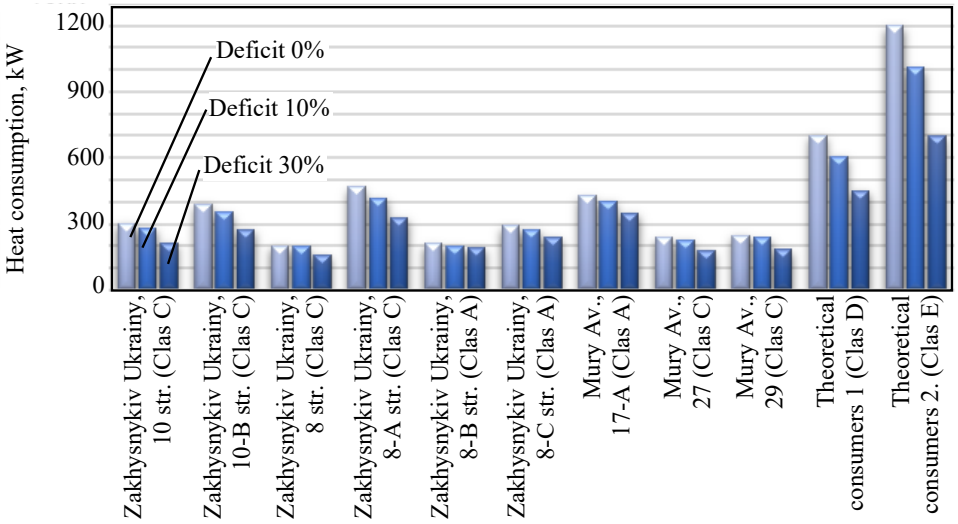

Fig. 3. Diagram of heat supply distribution by priority with theoretical consumers

This model is based on the assumption of constant pipe parameters and a stable consumer composition, so in conditions of sharp changes in load or network modernization, adjustments to the calculations are required. In addition, further work may include forecasting daily or seasonal demand and developing methods for automatically adjusting balancing valves based on SCADA data.

Testing of the methodology on the example of Chornomorsk confirmed its effectiveness. The use of the algorithm allows:

– minimize social risks and shutdowns of critical facilities;

– optimize the operation of boiler rooms and heating stations;

– transparently regulate heat distribution in conditions of deficit.

Wartime conditions and regulatory restrictions necessitate the implementation of such algorithms at the level of heat and power utilities. For practical implementation, it is necessary to use automatic balancing valves and SCADA systems that allow real-time control of the process.

Summarizing the results, it can be noted that hydraulic analysis made it possible to identify the most "heavy" consumers and confirm the need to install balancing valves and use a topological coefficient. The results of heat distribution demonstrate that the integrated algorithm guarantees an adequate level of heat supply for critical groups, which is in line with the principles of energy efficiency and social justice noted in [12, 13]. Comparing the obtained data with previous works, it can be concluded that the combination of hydraulic balance and priority control significantly increases the reliability of the system and allows reducing energy consumption by 15…20% [3, 7]. In addition, the proposed methodology meets regulatory requirements for reducing gas consumption [1] and is consistent with modern Smart Heat Networks concepts [9].

Conclusions

1. An integrated methodology for regulating urban heat supply systems is proposed, which combines hydraulic balancing and priority distribution of thermal energy.

2. The hydraulic unit provides the technical capability to supply heat transfer fluid to all consumers. The construction of piezometric profiles and the calculation of total resistance made it possible to identify the most "difficult" buildings that determine the maximum capacity of the system.

3. The thermal unit implements a priority balancing algorithm that takes into account consumer classes (A–E), deficit scenarios (0…30%), and load moderators. This guarantees that the necessary level of heat supply for critical infrastructure is maintained even in crisis conditions.

4. The proposed “double balance” allows combining the technical stability of the network with social justice in the distribution of heat resources, which is not provided by traditional static methods.

5. Testing of the methodology on the example of CHS-27 in Chornomorsk confirmed its effectiveness: the algorithm reduces the risks of critical consumer disconnections, optimizes the operation of boiler rooms and heat distribution points, and creates a transparent heat distribution mechanism.

6. The implementation of the methodology complies with the regulatory restrictions set out in Resolution No. 812 of the Cabinet of Ministers of Ukraine and can be implemented in practice by heat and power companies through the use of automatic balancing valves and SCADA systems.

Література

1. Міністерство енергетики України. Офіційний сайт. URL: https://www.mev.gov.ua. (дата звернення: 20.08.2025).
2. Про теплопостачання: Закон України від 02.06.2005 № 2633-IV / Відомості Верховної Ради України. 2005. № 28. Ст. 373. URL: https://zakon.rada.gov.ua/laws/show/2633-15#Text. (дата звернення: 20.08.2025).
3. Баласанян Г. А., Ляшенко В. І. Сучасні методи регулювання міських систем теплопостачання в умовах дефіциту енергоресурсів. *Холодильна техніка та технологія*. 2025. Т. 61, № 3. URL: https://journals.ontu.edu.ua/index.php/reftech/article/view/3213/3459. (дата звернення: 20.08.2025).
4. Lund H., Werner S., Wiltshire R., Svendsen S., Thorsen J. E., Hvelplund F., Mathiesen B. V. 4th Generation District Heating (4GDH): Integrating smart thermal grids into future sustainable energy systems. *Energy*. 2014. Vol. 68. P. 1–11. DOI: 10.1016/j.energy.2014.02.089.
5. Kulyk M. M., Zaporozhets A., Babak V., Denysov V. Structure Optimization of Power Systems with Renewable Energy Sources : monograph Cham : Springer, 2025. 146 p. DOI: 10.1007/978 3-031-83697-8.
6. Moustakidis S., Meintanis I., Halikias G., Karcanias N. An Innovative Control Framework for District Heating Systems: Conceptualisation and Preliminary Results. *Resources*. 2019. Vol. 8, No. 1. Art. 27. DOI: 10.3390/resources8010027.
7. Danfoss. Automatic balancing and control valves AFQ, AFQM, AFQMP : technical documentation URL: https://www.danfoss.com. (дата звернення: 20.08.2025).
8. Danfoss. Інтелектуальний електричний привід AMEi 6 iNET : технічний опис. Danfoss, 2025. 10 с. (AI305455457771ua-000203). URL: https://virtus.danfoss.com. (дата звернення: 20.08.2025).
9. Brand L., Calvén A., Englund J., Landersjö H., Lauenburg P. Smart district heating networks – A simulation study of prosumers’ impact on technical parameters in distribution networks. *Applied Energy*. 2014. Vol. 129. P. 39–48. DOI: 10.1016/j.apenergy.2014.04.079.
10. Енергетична стратегія України на період до 2035 року “Безпека, енергоефективність, конкурентоспроможність” : розпорядження КМУ від 18.08.2017 № 605-р. URL: https://zakon.rada.gov.ua/laws/show/605-2017-%D1%80/conv/print. (дата звернення: 20.08.2025).
11. International Energy Agency. Ukraine energy profile. Paris : IEA, 2020. URL: https://www.iea.org/reports/ukraine-energy-profile. (дата звернення: 02.03.2026).
12. Directive 2012/27/EU of the European Parliament and of the Council of 25 October 2012 on energy efficiency… *Official Journal of the European Union*. 14.11.2012. L 315. P. 1–56. URL: https://eur-lex.europa.eu/eli/dir/2012/27/oj/eng. (дата звернення: 20.08.2025).
13. UNDP in Ukraine. EIB and UNDP strengthen cooperation to accelerate Ukraine’s recovery (includes Ukraine District Heating Programme). 2025. URL: https://www.undp.org/ukraine/press-releases/eib-and-undp-strengthen-cooperation-accelerate-ukraines-recovery. (дата звернення: 20.08.2025).

References

1. Ministry of Energy of Ukraine. (n.d.). *Official website*. Retrieved from https://www.mev.gov.ua.
2. *On Heat Supply: Law of Ukraine No. 2633-IV*. (2005, June 2). Vidomosti Verkhovnoi Rady Ukrainy. Retrieved from https://zakon.rada.gov.ua/laws/show/2633-15#Text.
3. Balasanyan, H. A., & Liashenko, V. I. (2025). Modern methods of regulation of urban district heating systems under energy resource deficit conditions. *Refrigeration Engineering and Technology*, *61*(3). Retrieved from https://journals.ontu.edu.ua/index.php/reftech/article/view/3213/3459.

ISSN 2076-2429 (print)
ISSN 2223-3814 (online)

4. Lund, H., Werner, S., Wiltshire, R., Svendsen, S., Thorsen, J. E., Hvelplund, F., & Mathiesen, B. V. (2014). 4th Generation District Heating (4GDH): Integrating smart thermal grids into future sustainable energy systems. *Energy*, *68*, 1–11. DOI: 10.1016/j.energy.2014.02.089.
5. Kulyk, M. M., Zaporozhets, A., Babak, V., & Denysov, V. (2025). *Structure optimization of power systems with renewable energy sources*. Springer. DOI: 10.1007/978 3-031-83697-8.
6. Moustakidis, S., Meintanis, I., Halikias, G., & Karcanias, N. (2019). An innovative control framework for district heating systems: Conceptualisation and preliminary results. *Resources*, *8*(1), Article 27. DOI: 10.3390/resources8010027.
7. Danfoss. (n.d.). *Automatic balancing and control valves AFQ, AFQM, AFQMP: Technical documentation*. Retrieved from https://www.danfoss.com.
8. Danfoss. (2025). *Intelligent electric actuator AMEi 6 iNET: Technical description* (AI305455457771ua 000203). Retrieved from https://virtus.danfoss.com.
9. Brand, L., Calvén, A., Englund, J., Landersjö, H., & Lauenburg, P. (2014). Smart district heating networks – A simulation study of prosumers' impact on technical parameters in distribution networks. *Applied Energy*, *129*, 39–48. DOI: 10.1016/j.apenergy.2014.04.079.
10. Cabinet of Ministers of Ukraine. (2017, August 18). *Energy Strategy of Ukraine until 2035 "Security, Energy Efficiency, Competitiveness"* (Order No. 605-r). Retrieved from https://zakon.rada.gov.ua/laws/show/605-2017-%D1%80/conv/print.
11. International Energy Agency. (2020). *Ukraine energy profile*. IEA. Retrieved from https://www.iea.org/reports/ukraine-energy-profile.
12. *Directive 2012/27/EU of the European Parliament and of the Council of 25 October 2012 on energy efficiency*. (2012, November 14). Official Journal of the European Union, L 315, 1–56. Retrieved from https://eur-lex.europa.eu/eli/dir/2012/27/oj/eng.
13. UNDP in Ukraine. (2025). *EIB and UNDP strengthen cooperation to accelerate Ukraine's recovery*. Retrieved from https://www.undp.org/ukraine/press-releases/eib-and-undp-strengthen-cooperation-accelerate-ukraines-recovery.

Баласанян Геннадій Альбертович; Hennadii Balasanian, ORCID: https://orcid.org/0000-0002-3689-7409
Ляшенко Владислав Ігоревич; Vladyslav Liashenko, ORCID: https://orcid.org/0009-0006-2546-0419

Received September 02, 2025

Accepted October 03, 2025

ISSN 2076-2429 (print)
ISSN 2223-3814 (online)
Proceedings of Odessa Polytechnic University, Issue 2(72), 2025

UDC 658.264

H. Balasanian, DSc, Prof.,
V. Verstak,
A. Ostapenko,
P. Kolesnichenko
Odessa Polytechnic National University, Shevchenko Ave. 1, Odesa, Ukraine, 65044, e-mail: balasanyan@op.edu.ua

HYBRID ENERGY SUPPLY SYSTEM FOR A MULTI-STOREY BUILDING WITH RENEWABLE ENERGY SOURCES

Г. Баласанян, В. Верстак, А. Остапенко., П. Колесниченко. **Гібридна система енергозабезпечення багатоповерхового будинку з відновлювальними джерелами енергії.** Запропоновано конфігурацію гібридної системи енергозабезпечення з відновлювальними джерелами енергії щодо автономного постачання електрики та тепла сучасного багатоповерхового будинку. Поєднання в гібридний системі різних за природою та енергетичним потенціалом джерел енергії сприяє взаємодоповненню їх переваг та, одночасно, взаємокомпенсації їх недоліків. За своєю потужністю гібридної системи енергозабезпечення найбільш придатні для автономного енергозабезпечення невеликих промислових об'єктів, фермерських господарств, житлових, рекреаційних, сільськогосподарських комплексів, тощо. Для кліматичних умов України найбільш розповсюдженими є гібридної системи енергозабезпечення, до яких інтегровано вітроустановки та сонячні фотоелектричні панелі. Конфігурація запропонованої гібридної системи енергозабезпечення складається з вітроустановки, сонячних фотоелектричних панелей, що генерують електрику, когенераційної установки за технологією газової мікротурбіни, що генерує для споживача як електрику так і тепло та електрокотла, як додаткового джерела тепла при пікових навантаженнях. Проведено узагальнення експериментальних даних, щодо швидкості вітру та сонячної інсоляції, що накопичено у базі даних метеостанції національного університету «Одеська політехніка». Опрацьовано методику щодо визначення оптимальних режимів навантаження та параметрів гібридної системи енергозабезпечення запропонованої конфігурації за критерієм мінімізації небалансу між генерацією та споживанням електрики в системі. Параметрами, що оптимізуються, є площа фотоелектричних панелей та площа лопатей вітроустановки, які сумісно генерують додаткову електрику, та разом з когенераційної установкої забезпечують повне покриття потреб споживачів. Отримано оптимальні режими електричного та теплового навантаження гібридної системи та її складових частин за місяцями року. Підтверджено, що сезонна нерівномірність вітрових та сонячних енергоресурсів може бути повністю компенсована шляхом інтеграції до гібридної системи різних за енергетичним потенціалом та природою джерел енергії, оптимізації їх генеруючої потужності та режимів навантаження.

Ключові слова: відновлювальні джерела енергії**,** гібридна система енергозабезпечення, когенераційна установка, вітроустановка, фотоелектричні сонячні панелі, режими навантаження оптимізація параметрів

H. Balasanian, V. Verstak, A. Ostapenko, P. Kolesnichenko. **Hybrid energy supply system for a multi-storey building with renewable energy sources.** A configuration of a hybrid energy supply system (HES) with renewable energy sources for the autonomous supply of electricity and heat to a modern multi-storey building is proposed. The combination of energy sources that are different in nature and energy potential in a hybrid system contributes to the mutual complementarity of their advantages and, at the same time, mutual compensation for their disadvantages. In terms of power, a hybrid energy supply system are most suitable for the autonomous energy supply of small industrial facilities, farms, residential, recreational and agricultural complexes, etc. For the climatic conditions of Ukraine, the most common are a hybrid energy supply system that integrate wind turbines and solar photovoltaic panels. The configuration of the proposed hybrid energy supply system consists of a wind turbine, solar photovoltaic panels that generate electricity, a cogeneration unit based on gas microturbine technology that generates both electricity and heat for the consumer, and an electric boiler as an additional source of heat during peak loads. A summary of experimental data on wind speed and solar insolation accumulated in the database of the meteorological station of the Odessa Polytechnic National University has been carried out. A methodology was developed to determine the optimal load modes and parameters of the proposed configuration based on the criterion of minimizing the imbalance between electricity generation and consumption in the system. The parameters to be optimized are the area of photovoltaic panels and the area of wind turbine blades, which jointly generate additional electricity and, together with the control unit, ensure full coverage of consumer needs. The optimal electrical and thermal load modes of the hybrid system and its components for each month of the year have been obtained. It has been confirmed that the seasonal unevenness of wind and solar energy resources can be fully compensated for by integrating energy sources with different energy potentials and natures into the hybrid system, optimizing their generating capacity and load modes.

Keywords: renewable energy sources**,** hybrid energy supply system, cogeneration plant, wind turbine, photovoltaic solar panels, load modes, parameter optimization

Introduction

The use of hybrid energy supply systems is becoming increasingly widespread in Ukraine and around the world [1]. This is due to the high energy efficiency of hybrid energy systems, which combine traditional energy technologies and renewable energy sources (RES) in a single system [2]. The combination of energy sources that differ in nature and energy potential in a single system contributes to the

DOI: 10.15276/opu.2.72.2025.05

ISSN 2076-2429 (print)
ISSN 2223-3814 (online)

mutual complementarity of their advantages and, at the same time, the mutual compensation of their disadvantages [3]. The widespread use of HES is also linked to the steady rise in prices for fossil fuels, heat and electricity, as well as increased environmental requirements for energy facilities and energy supply reliability. The energy capacity of HES is lower than that of traditional power generation systems. This is due to limitations in the energy potential of RES and their high specific cost, but systems with a capacity of several kW to several MW are quite widespread.

Analysis of literature data and problem statement

The use of HES is most effective in the autonomous supply of electricity and heat to consumers. In terms of their capacity, RES are most suitable for the autonomous energy supply of small industrial facilities, farms, residential, recreational and agricultural complexes, etc. [4]. For the climatic conditions of Ukraine, the most common are HES that integrate wind turbines (WT) and solar photovoltaic panels (SPP) [5, 6]. Depending on the operating mode, HES can be either completely autonomous or connected to electricity and gas networks. Autonomous operation also requires the system to have storage devices to compensate for the variability of wind and solar energy resources.

HES for electricity generation only have become more widespread, but for certain categories of consumers HES systems are used to meet their heating and hot water supply (HWS) needs. Such systems have a more complex configuration, as they additionally integrate heat generators – gas or electric boilers, heat pumps, etc. For such HES systems, electricity consumption will increase significantly during the heating season, leading to a corresponding increase in RES generation capacity and reducing the economic efficiency of the system. Recently, cogeneration plants based on gas turbines or internal combustion engines have been used for combined electricity and heat production in various industries. Integrating a cogeneration plant into a HES can significantly increase the efficiency of the system during the heating season, while in the summer months, efficient generation will be carried out mainly by RES [7].

A configuration of a HES system with a cogeneration unit – a gas microturbine, a heat recovery unit and a photovoltaic solar power plant – is proposed for consideration (Fig. 1). The proposed HES only needs to be connected to the gas network and is completely autonomous in terms of electricity generation. CU based on gas microturbines have found wide application for autonomous supply of electricity and heat to consumers [8] with high energy efficiency. The efficiency indicator of CU, the fuel utilisation factor (FUF), reaches up to 90%. During the non-heating period, consumer demand for heat is significantly reduced and, accordingly, the CU FUF can drop to 30%. The presence of a wind turbine and a solar photovoltaic system in the proposed HES configuration will largely compensate for the low efficiency of the CU during the non-heating period. The energy efficiency of the wind turbine is significantly higher in the winter months, while the solar photovoltaic system reaches its maximum in the summer months, so the proposed hybrid energy system is quite relevant for supplying consumers with significant heat consumption during the heating period with full electricity supply throughout the year.

For the proposed HES, the question of the optimal capacity of each energy source in the system becomes relevant [9, 10].

Purpose and objectives of the study

The purpose of the study is to investigate load modes and optimise the parameters of the HES for combined energy supply to consumers, taking into account the climatic conditions of the Odessa region.

To achieve the aim of the study, the following tasks must be solved:

– summarise experimental data on wind speed and solar insolation accumulated in the database of the meteorological station of the Odessa Polytechnic National University;

– develop a methodology for optimising the load modes and parameters of the proposed configuration of the solar energy system, taking into account the wind and solar radiation potential for the Odessa region;

– conduct research on the HES system to determine the optimal energy parameters of the system and load modes of the system components.

Research materials and methods

Fig. 1 shows the functional diagram of the proposed HES system. The object of energy supply is a modern 150-apartment multi-storey residential building.

The configuration of the proposed HES consists of a wind turbine, solar photovoltaic panels that generate electricity, a gas microturbine control unit that generates both electricity and heat for the consumer, and an electric boiler as an additional source of heat during peak loads. The electrical power

ISSN 2076-2429 (print)
ISSN 2223-3814 (online)
Proceedings of Odessa Polytechnic University, Issue 2(72), 2025

generated by the wind turbine and solar panels is usually supplied as direct current, which is quite convenient for charging batteries. The controller's function is to protect the battery from deep discharge and overcharging. Next, the inverter converts direct current into alternating current with a standard frequency of 50 Hz and a voltage of 220 or 380 V. Due to the utilized heat from the cogeneration unit, the main share of heat supply in the system is provided, additional peak heat loads are compensated by the electric boiler.

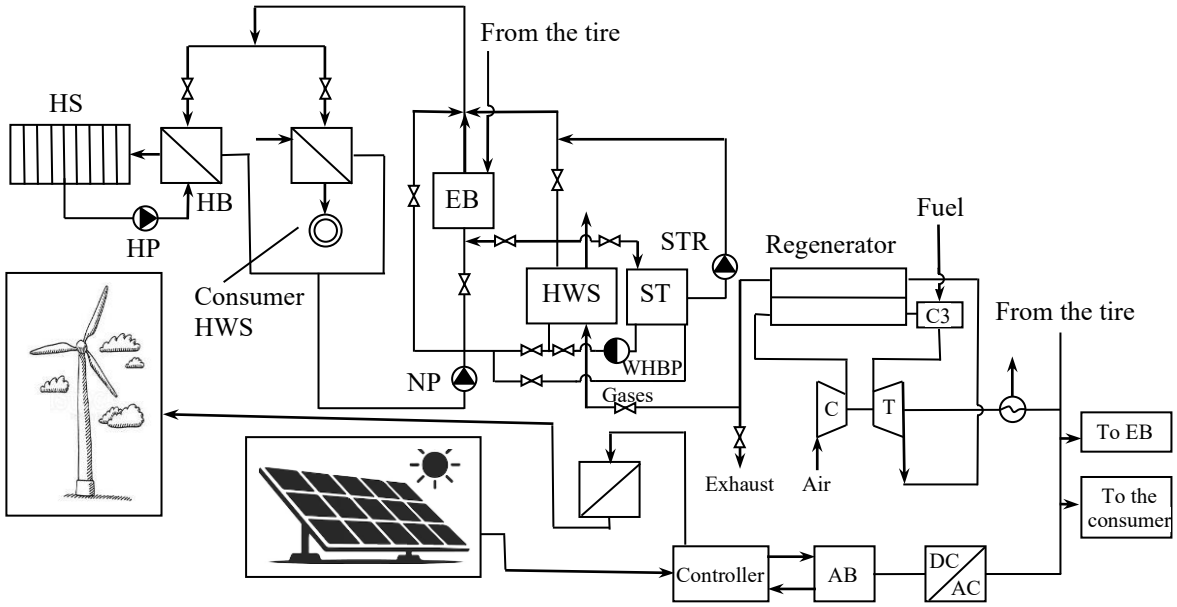

Fig. 1. Functional diagram of a HES system: T – gas turbine; C – compressor; ST – storage tank; EB – electric boiler; WHB – waste heat boiler; HS – heating system; HB – heating boiler; NP – network pump; HP – heating pump; STR – storage tank pump; WHBP – waste heat boiler pump

Methods for determining the capacity and performance of HES systems integrated with heat recovery boilers and solar panels are based on generalised climate data from long-term observations of wind speed and solar insolation for a given region. The parameters and structure of the SHE can be optimised in various ways: for example, according to technical indicators that characterise the reliability and efficiency of energy supply, or according to economic indicators such as the cost of energy products or capital investment in system components [11].

To optimise load modes and HES parameters, a target function (TF) is proposed that minimises the imbalance between electricity generation and consumption in the system: $F = E_{\text{gen}} - E_{\text{con}} \to 0$. The parameters to be optimized are the area of photovoltaic panels F_{PV} and the area of wind turbine blades F_{WT}, which jointly generate additional electricity and, together with the CU, ensure full coverage of consumer needs.

In addition to the TF, the task of optimising load modes and HES parameters also includes a system of balance equations (BE) and corresponding constraints (CC) on the generation and consumption of electricity and heat in the system.

The balance between heat consumption and production is described by the equation:

$$Q^i_{\text{hs}} + Q^i_{\text{HWS}} = Q^i_{\text{CU}} + Q^i_{\text{EB}}, \tag{1}$$

where:

$Q^i_{\text{hs}}, Q^i_{\text{HWS}}$ are the average monthly values of the thermal power of the heating system and HWS, respectively;

$Q^i_{\text{CU}}, Q^i_{\text{EB}}$ are the average monthly values of the utilised thermal power of the heating system and hot water supply, respectively;

i is the ordinal number of the month of the year.

The balance of electricity consumption and production is described by the equation:

ISSN 2076-2429 (print)
ISSN 2223-3814 (online)

$$E^i_{\text{con}} + E^i_{\text{EB}} = E^i_{\text{CU}} + E^i_{\text{PV}} + E^i_{\text{WT}}, \quad (2)$$

where:

E^i_{con}, E^i_{EB} – average monthly values of electricity consumer capacity and EC capacity, respectively;

E^i_{CU}, E^i_{PV}, E^i_{WT} – the average monthly values of the electrical power of the CU, SPP and WT, respectively.

Additional conditions may also be included in the system of equations, for example, the ratio between the nominal capacities of the wind turbine and photovoltaic panels $E^{\text{nom}}_{\text{PV}} / E^{\text{nom}}_{\text{WT}}$, which for this SPP is accepted as $E^{\text{nom}}_{\text{PV}} / E^{\text{nom}}_{\text{WT}} = 1$. The ratio between the nominal capacities of the heat source and photovoltaic panels can also be specified, for example, provided that the capital investments in the heat source ($K_{\text{heat source}}$) and photovoltaic panels (K_{PV}) are equal: $K_{\text{heat source}} / K_{\text{PV}} = 1$.

System of restrictions on electricity and heat generation in the HES:

$$Q^i_{\text{CU}} \le Q^{\text{nom}}_{\text{CU}} E^i_{\text{CU}} \le E^{\text{nom}}_{\text{CU}}; \; E^i_{\text{PV}} \le E^{\text{nom}}_{\text{PV}}; \; E^i_{\text{WT}} \le E^{\text{nom}}_{\text{WT}},$$

where: $Q^{\text{nom}}_{\text{CU}}$, $E^{\text{nom}}_{\text{CU}}$, $E^{\text{nom}}_{\text{PV}}$, $E^{\text{nom}}_{\text{WT}}$ are the nominal values of the thermal and electrical power of the CU, the electrical power of the SPP and the WT, respectively.

Finally, the task of optimising the load modes and parameters of the HES of the proposed configuration is as follows:

$$\begin{cases} F = E_{\text{gen}} - E_{\text{con}} \to \min \text{ (TF)}; \\ Q^i_{\text{hs}} + Q^i_{\text{HWS}} = Q^i_{\text{CU}} + Q^i_{\text{EB}} \text{ (BE)}; \\ E^i_{\text{con}} + E^i_{\text{EB}} = E^i_{\text{CU}} + E^i_{\text{PV}} + E^i_{\text{WT}} \text{ (BE)}; \\ Q^i_{\text{CU}} \le Q^{\text{nom}}_{\text{CU}}; \; E^i_{\text{CU}} \le E^{\text{nom}}_{\text{CU}}; \; E^i_{\text{PV}} \le E^{\text{nom}}_{\text{PV}}; \; E^i_{\text{WT}} \le E^{\text{nom}}_{\text{WT}} \text{ (CC)}; \\ E^{\text{nom}}_{\text{PV}} / E^{\text{nom}}_{\text{WT}} = 1 \text{ or } \dfrac{K_{\text{WT}}}{K_{\text{PV}}} = 1; \\ i = \overline{1.12.} \end{cases} \quad (3)$$

The "Find Solution" option in Excel spreadsheets was selected as the tool for solving the task of optimising the parameters of the HES. The result of solving the problem is the optimal values of the wind turbine blade area $F_{\text{ВУ}}$, the area of photovoltaic panels – F_{PV}, the average monthly values of utilised heat and electrical power of the CU – Q^i_{CU}, E^i_{CU}, the average monthly value of the electrical power of the EC, WT and SPP – $E^i_{\text{WT}}, E^i_{\text{EB}}, E^i_{\text{PV}}$, which satisfy the conditions of the problem.

Research results

The energy supply facility considered in this work is a modern 150-apartment multi-storey residential building with the following calculated technical characteristics:

– total heated area – 11.250 m²;
– number of residents – 370;
– specific heating characteristic – q_0 =1.4 W/(m²°C);
– hot water consumption – 100 litres per person per day;

The parameters for heat consumption for hot water supply and heating are determined according to the methodology [13].

Table 1 shows the total electricity and heat consumption at the facility during the calendar year.

The average monthly heat load of the facility for heating and hot water supply throughout the year is shown in Fig. 2. The facility's heat demand in winter and summer differs significantly and, accordingly, has a ratio of about 7:1, due to the fact that heat in summer is consumed only for hot water supply.

A cogeneration unit is installed at the facility – a Capstone-200 gas microturbine (manufactured in the USA) with the following nominal technical characteristics:

– turbine electrical power, kW – 200;
– utilised thermal power, kW – 393;
– natural gas consumption, nm³/hour – 65;
– turbine rotation speed, rpm – 65,000;
– exhaust gas temperature, °C – 280;

ISSN 2076-2429 (print)
ISSN 2223-3814 (online)
Proceedings of Odessa Polytechnic University, Issue 2(72), 2025

– turbine electrical efficiency, % – 33;
– fuel utilisation factor (FUF), % – 90.

Table 1

Generalised electricity and heat consumption volumes

Electricity consumption, kWh	97500	89700	89700	82500	65625	84375	93750	93750	65625	78000	97500	97500
Average monthly electricity load, kW	135	133	125	115	88	117	126	126	91	105	135	135
Average monthly heating load, kW	331	331	236	142	0	0	0	0	0	158	221	284
Heat consumption for hot water supply, kW	82	82	82	48	45	64	64	64	45	48	50	82
Total thermal load, kW	413	413	318	190	45	64	64	64	45	206	271	366

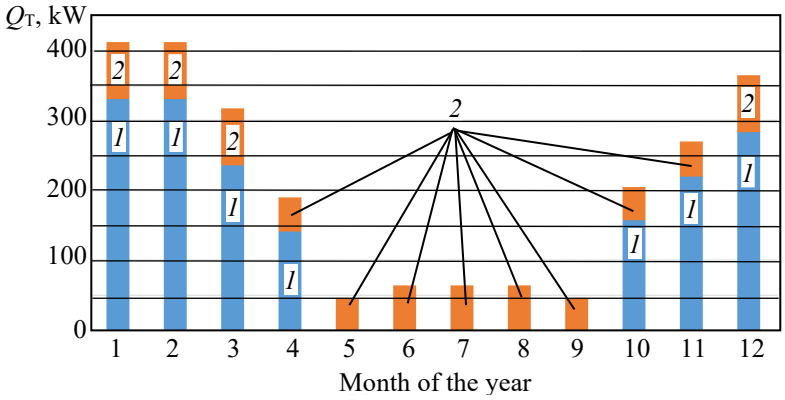

Fig. 2. Thermal load of the facility by month of the year: *1* – Heating; *2* – HWS

Analysis of the data in Table 2 shows that the electrical power of photovoltaic panels in the summer months is 6…8 times higher than in winter, which, accordingly, will contribute to their effective use with limited power of the CU in summer (Fig. 3). On the contrary, the electrical power of heat engines is 4…5 times higher in the autumn and winter months than in the summer, which contributes to natural gas savings for heat engines.

Table 2

Electricity generation by wind turbines and photovoltaic panels by month of the year

Month	1	2	3	4	5	6	7	8	9	10	11	12
Insolation, kWh/m^2	28	47	115	161	177	211	200	184	130	70	32	27
Specific electricity generation of solar power plants, W/m^2	7.6	14.2	31	45.4	46.7	57.5	52.5	48.2	36.7	19.4	8.5	7.4
Average monthly electrical capacity of solar power plants, kW	14	26	59	85	88	109	99	91	68	36	16	14
Average monthly wind speed, m/s	4.8	5	4.8	4.8	3.7	2.9	2.9	2.7	2.9	3.2	4.4	4.7
Average monthly electrical power of the WT, kW	15.6	17.7	15.6	15.6	7.2	3.4	3.4	2.8	3.4	4.6	12	14.7

The results of solving the problem of optimising load modes and HES parameters under the condition of equal nominal capacities of wind turbines and photovoltaic panels $E_{PV}^{nom} / E_{WT}^{nom} = 1$ are as follows:

– total SPP – 1638 m^2;
– the area of the rotor blades is 995 m^2, which corresponds to a wind turbine diameter of 62 m.

Fig. 4 shows the optimal modes for utilised heat from the CU and heat from the EC by month of the year.

Analysis of Fig. 4 shows that during the heating season (October to April), heat utilised from the CU provides the majority of heat for the consumer. The EC is used to coordinate the thermal and electrical load schedules in the system and to cover peak loads, so the share of heat from the EC is significantly lower. The heat recovered from the CU is used only for HWS in the summer, so the CU operates periodically only to accumulate hot water, and the EC is switched on to coordinate the thermal and electrical loads of the system.

ISSN 2076-2429 (print)
ISSN 2223-3814 (online)

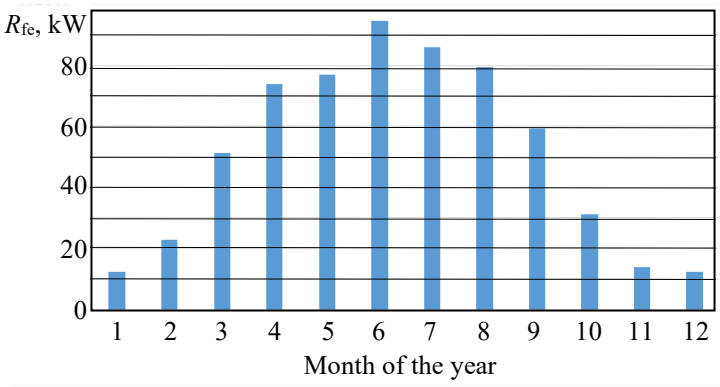

Fig. 3. Power of photovoltaic panels by month of the year

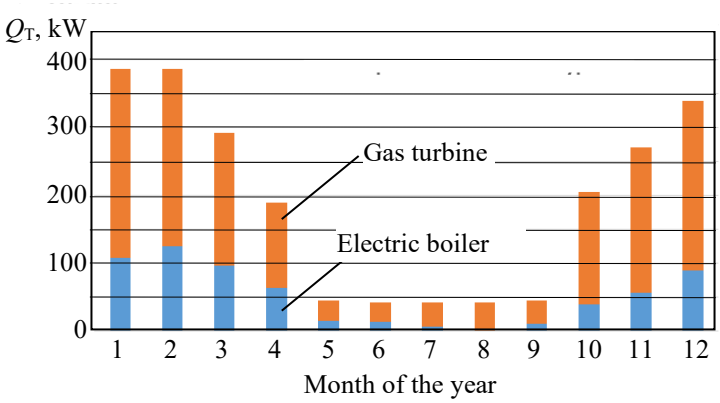

Fig. 4. Optimal modes of heat generation from the CU and EC by month of the year

Fig. 5 shows the optimal modes of electricity generation by the CU, WT and SPP by month of the year. Analysis of Fig. 5 shows that the main share of electricity during the heating period in the HES is provided by a gas microturbine. Although the share of electricity from the heat pump is smaller than that from the heat exchanger, it is several times greater than the share of electricity from the heat pump. Electricity supply to consumers in the summer months is mainly provided by the heat pump. The share of electricity from the microturbine is small and is due to the supply of utilised heat to the DHW. In the summer months, the WT generates several times less electricity than the SPP.

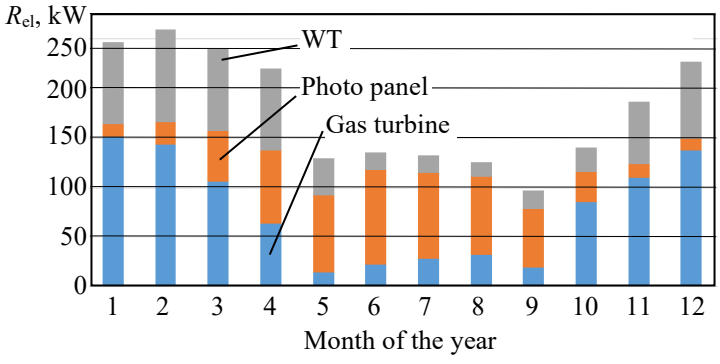

Fig. 5. Optimal electricity generation modes in the HES by month of the year, assuming equal nominal capacities of WT and photovoltaic panels

If the task of optimising the parameters and load modes of the HES is solved under the condition of equal capital investments in accordance with the WT(K_{WT}) and photovoltaic panels (K_{PV}):

$$K_{WT} / K_{PV} = 1,$$

then the optimisation results change significantly (Fig. 6). The share of electricity from CU and SPP increases significantly, while electricity from WT, on the contrary, does not have a significant impact on the energy balance of the SGE.

ISSN 2076-2429 (print)
ISSN 2223-3814 (online)
Proceedings of Odessa Polytechnic University, Issue 2(72), 2025

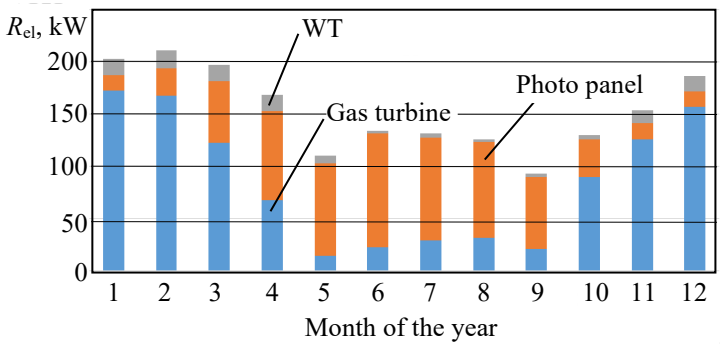

Fig. 6. Optimal electricity generation modes in the HES by month of the year, assuming equal capital investments in thermal power plants and photovoltaic panels

Conclusions

1. A HES system for autonomous electricity and heat supply of a modern multi-storey residential building has been proposed, taking into account the energy potential of wind and solar energy for the Odessa region.

2. A methodology has been developed for determining the optimal load modes and parameters of the proposed HES configuration based on the criterion of minimising the imbalance between electricity generation and consumption in the system.

3. The optimal modes of electrical and thermal load of the hybrid system and its components by month of the year have been obtained.

4. It has been confirmed that the seasonal unevenness of wind and solar energy resources can be fully compensated by integrating energy sources with different energy potentials and natures into the hybrid system, optimising their generating capacity and load modes.

Література

1. Global and Regional Externalities of the Ukrainian Energy Sector / O. Sabishchenko et al. *International Journal of Energy Sector Management*. 2023. Vol. 17, No. 1. P. 145–166. DOI: https://doi.org/10.1108/IJESM-05-2021-0005.
2. Okinda V. O., Odero N. A. A Review of Techniques In Optimal Sizing of Hybrid Renewable Energy Systems. *IJRET: International Journal of Research in Engineering and Technology*. 2015. Vol. 4, No. 11. P. 153–163. URL: https://www.researchgate.net/publication/319165346_A_REVIEW_OF_TECHNIQUES_IN_OPTIMAL_SIZING_OF_HYBRID_RENEWABLE_ENERGY_SYSTEMS.
3. Hybrid renewable energy microgrid for a residential community: a techno-economic and environmental perspective in the context of SDG7 / N. M. Kumar et al. *Sustainability*. 2020. Vol. 12, Is. 10. Art. 3944. DOI: https://doi.org/10.3390/su12103944.
4. Popadchenko S. A. Hybrid electrical networks – necessity and prospects for development in Ukraine. *Bulletin of the Petro Vasylenko Kharkiv National Technical University of Agriculture*. 2017. Issue 186. P. 39–43.
5. Jihane K., Cherkaoui M. Study of the different structures of hybrid systems in renewable energies: A review. *Energy Procedia*. 2019. Vol. 157. P. 323–330. URL: https://www.researchgate.net/publication/330664793_Study_of_the_different_structures_of_hybrid_systems_in_renewable_energies_A_review/fulltext/5e5d9dbb92851cefa1d69f33/Study-of-the-different-structures-of-hybrid-systems-in-renewable-energies-A-review.pdf.
6. Shvedchikova I. O., Pisotsky A. V. Preliminary assessment of the efficiency of a hybrid wind-solar system for meeting the needs of a local consumer. *Technologies and Engineering*. 2023. No. 4 (15). P. 53–64. DOI: https://doi.org/10.30857/2786-5371.2023.4.5.
7. Cogeneration technologies in small-scale energy : monograph / V. A. Malyarenko et al. ; Kharkiv National University of Municipal Economy named after O. M. Beketov, Institute of Mechanical Engineering Problems named after A. M. Pidgorny. Kharkiv : KNUCE named after O. M. Beketov, 2018. 454 p.
8. Potential for integrating cogeneration systems into Ukraine's small-scale energy sector / V. A. Malyarenko et al. *Integrated Technologies and Energy Saving*. 2012. No. 4. P. 11–17.
9. Balasanian H., Semenyii A., Ostapenko A. Research on a hybrid energy supply system with renewable energy sources. *Proceedings of Odessa Polytechnic University*. 2024. Vol. 2 (70). P. 31–38. DOI: 10.15276/opu.2.70.2024.04.
10. Hybrid energy supply system for a multi-storey residential building / V. Verstak et al. *Refrigeration Engineering and Technology*. 2025. Vol. 61, No. 2. P. 178–185.

ISSN 2076-2429 (print)
ISSN 2223-3814 (online)

11. Kuznetsov M., Lysenko O., Melnik O. Optimisation tasks for combined energy systems based on economic criteria. *Renewable Energy*. 2019. No. 4. P. 6–14. DOI: https://doi.org/10.36296/1819-8058.2019.4(59).6-14.
12. ДСТУ А.2.2-12:2015. Енергоефективність будівель. Метод розрахунку енергоспоживання при опаленні, охолодженні, вентиляції, освітленні та гарячому водопостачанні. [Чинний від 2015-07-01]. Вид. офіц. Київ : Держспоживстандарт України, 2015. 162 с. (Національний стандарт України).
13. Balasanian H., Semenyii A. Research on a combined heat supply system with alternative energy sources. *Proceedings of Odessa Polytechnic University*. 2023. Vol. 2 (68). P. 25–32. DOI: 10.15276/opu.2.68.2023.03.

References

1. Sabishchenko, O., Skrypnyk, A., Klymenko, N., Voloshyn, S., & Holiachuk, O. (2023). Global and regional externalities of the Ukrainian energy sector. *International Journal of Energy Sector Management, 17*(1), 145–166. DOI: https://doi.org/10.1108/IJESM-05-2021-0005.
2. Okinda, V. O., & Odero, N. A. (2015). A review of techniques in optimal sizing of hybrid renewable energy systems. *International Journal of Research in Engineering and Technology, 4*(11), 153–163. Available at https://www.researchgate.net/publication/319165346_A_REVIEW_OF_TECHNIQUES_IN_OPTIMAL_SIZING_OF_HYBRID_RENEWABLE_ENERGY_SYSTEMS.
3. Kumar, N. M., Chopra, S. S., Chand, A. A., Elavarasan, R. M., & Shafiullah, G. M. (2020). Hybrid renewable energy microgrid for a residential community: A techno-economic and environmental perspective in the context of SDG7. *Sustainability, 12*(10), Article 3944. DOI: https://doi.org/10.3390/su12103944.
4. Popadchenko, S. A. (2017). Hybrid electrical networks – necessity and prospects for development in Ukraine. *Bulletin of the Petro Vasylenko Kharkiv National Technical University of Agriculture, 186*, 39–43.
5. Jihane, K., & Cherkaoui, M. (2019). Study of the different structures of hybrid systems in renewable energies: A review. *Energy Procedia, 157*, 323–330. Available at https://www.researchgate.net/publication/330664793_Study_of_the_different_structures_of_hybrid_systems_in_renewable_energies_A_review/fulltext/5e5d9dbb92851cefa1d69f33/Study-of-the-different-structures-of-hybrid-systems-in-renewable-energies-A-review.pdf.
6. Shvedchikova, I. O., & Pisotsky, A. V. (2023). Preliminary assessment of the efficiency of a hybrid wind-solar system for meeting the needs of a local consumer. *Technologies and Engineering, 4*(15), 53–64. DOI: https://doi.org/10.30857/2786-5371.2023.4.5.
7. Malyarenko, V. A., Shubenko, O. L., Andreyev, S. Yu., Babak, M. Yu., & Senetsky, O. V. (2018). *Cogeneration technologies in small-scale energy: Monograph*. KNUCE named after O. M. Beketov.
8. Malyarenko, V. A., Shubenko, A. L., Senetsky, A. V., & Temnokhud, I. A. (2012). Potential for integrating cogeneration systems into Ukraine's small-scale energy sector. *Integrated Technologies and Energy Saving, 4*, 11–17.
9. Balasanian, H., Semenyii, A., & Ostapenko, A. (2024). Research on a hybrid energy supply system with renewable energy sources. *Proceedings of Odessa Polytechnic University, 2*(70), 31–38. DOI: 10.15276/opu.2.70.2024.04.
10. Verstak, V., Palamarchuk, O., Bessatyan, Yu., Shilov, P., & Tarasyuk, O. (2025). Hybrid energy supply system for a multi-storey residential building. *Refrigeration Engineering and Technology, 61*(2), 178–185.
11. Kuznetsov, M., Lysenko, O., & Melnik, O. (2019). Optimisation tasks for combined energy systems based on economic criteria. *Renewable Energy, 4*, 6–14. DOI: https://doi.org/10.36296/1819-8058.2019.4(59).6-14.
12. National Standard of Ukraine. (2015). *Energy efficiency of buildings. Method for calculating energy consumption for heating, cooling, ventilation, lighting and hot water supply* (DSTU A.2.2-12:2015). Official publication.
13. Balasanian, H., & Semenyii, A. (2023). Research on a combined heat supply system with alternative energy sources. *Proceedings of Odessa Polytechnic University, 2*(68), 25–32. DOI: 10.15276/opu.2.68.2023.03.

Баласанян Геннадій Альбертович; Hennadii Balasanian, ORCID: https://orcid.org/0000-0002-3689-7409
Верстак Віталій Олександрович; Vitalii Verstak, ORCID: https://orcid.org/0009-0001-6842-7006
Остапенко Артем Сергійович; Artem Ostapenko
Колесниченко Павло Вадимович; Pavel Kolesnichenko

Received September, 24, 2025
Accepted October 27, 2025

UDC 658-264

A. Mazurenko, DSc, Prof.,
A. Pustovit,
Zh. Doroshenko, PhD, Assoc. Prof.,
S. Gryshchenko
Odessa Polytechnic National University, Shevchenko Ave. 1, Odesa, Ukraine, 65044, E-mail: mazurenko@op.edu.ua

POSSIBILITIES FOR IMPROVING THE RELIABILITY OF HEAT AND ELECTRICITY GENERATING FACILITIES IN HEAT SUPPLY SYSTEMS, TAKING INTO ACCOUNT THE INSTALLATION OF RESERVE CAPACITIES

А. Мазуренко, А. Пустовіт, Ж. Дорошенко, С. Гріщенко. **Можливості підвищення надійності роботи тепло та електро генеруючих установок систем теплопостачання з урахуванням встановлення резервних потужностей.** Зниження надійності теплозабезпечення споживачів можливе через підвищену аварійність устаткування, як через зовнішній вплив в екстремальних умовах, так і в умовах відпрацювання розрахункового ресурсу частиною встановленого генеруючого обладнання. Характерним для енергетичних установок є циклічний режим роботи. Забезпечення високої надійності енергосистем можливе за рахунок високих показників надійності використовуваного обладнання та за рахунок належної структури та резервування систем генерації. В роботі розглянути методи визначення величини резерву генеруючої потужності системи теплопостачання. Величина необхідного резерву тісно пов'язана з визначенням параметрів аварійності обладнання, що використовується, а також від резерву залежить вирішенням задачі планування ремонтів. Після завершення опалювального сезону система теплопостачання, як правило, переходить в режим заниженої потужності, необхідної для гарячого водопостачання. Проте, в деяких регіонах значна кількість систем теплопостачання працює лише в період опалювального сезону, а це спрощує вирішення питань планування капітального ремонту устаткування системи та її резервування. Виконані необхідні розрахунки для побудови графіка визначення резерву системи теплопостачання. Розглянуто планування капітальних ремонтів та їх періодичність. Для практичного використання в більшості випадків, розв'язання задачі резервування потужності виконано за більш простою і більш точною при невеликій кількості елементів системи методикою, побудованій на розподілі Бернуллі. При цьому був використано математичний пакет Maple. Результати отримані у вигляді графіків. При більшій загальній кількості елементів відповідно зменшується відносна доля впливу відмови окремого елемента (котла) на працездатність всієї системи (котельні) при прийнятому значені мінімального резерву. Середня аварійність приймається досить часто постійною для однотипного енергетичного обладнання, проте необхідно мати на увазі, що навіть таке устаткування може мати показники, які значно відрізняються по надійності. Це робить доцільним проведення систематичного індивідуального обліку, збору та відповідної обробки статистичних даних по всіх елементах системи, особливо для енергетичного устаткування, яке відпрацювало значну частину свого ресурсу.

Ключові слова: система теплопостачання, надійність енергосистем, аварійність обладнання, резервування потужностей

A. Mazurenko, A. Pustovit, Zh. Doroshenko, S. Gryshchenko. **Possibilities for improving the reliability of heat and electricity generating facilities in heat supply systems, taking into account the installation of reserve capacities.** The reliability of heat supply to consumers may decrease due to increased equipment failure rates, both due to external influences in extreme conditions and due to the depletion of the design life of some of the installed generating equipment. Cyclical operation is characteristic of power plants. High reliability of power systems can be ensured by high reliability indicators of the equipment used and by the proper structure and redundancy of generation systems. The paper considers methods for determining the reserve capacity of the heat supply system. The amount of the required reserve is closely related to the determination of the failure rate parameters of the equipment used, and the reserve also depends on the solution of the repair planning problem. After the end of the heating season, the heat supply system usually switches to a reduced power mode required for hot water supply. However, in some regions, a significant number of heat supply systems operate only during the heating season, which simplifies the planning of major repairs to the system's equipment and its reserve capacity. The necessary calculations have been made to construct a schedule for determining the reserve capacity of the heat supply system. The planning of major repairs and their frequency are considered. For practical use in most cases, the problem of power reserve is solved using a simpler and more accurate method for a small number of system elements, based on the Bernoulli distribution. The Maple mathematical package was used for this purpose. The results are presented in the form of graphs. With a larger total number of elements, the relative share of the impact of the failure of a single element (boiler) on the performance of the entire system (boiler room) decreases accordingly, given the accepted minimum reserve value. The average failure rate is often assumed to be constant for energy equipment of the same type, but it should be borne in mind that even such equipment may have significantly different reliability indicators. This makes it advisable to systematically record, collect and process statistical data on all elements of the system, especially for power equipment that has worked out a significant part of its resource.

Keywords: heat supply system, reliability of power systems, equipment failure rate, power reserve

Introduction

A characteristic difference between thermal power equipment, thermal and electrical power plants and manufacturing enterprises in other industries is the requirement to ensure a continuous balance between “heat and electrical energy production and consumption”. This condition must be met

DOI: 10.15276/opu.2.72.2025.06

ISSN 2076-2429 (print)
ISSN 2223-3814 (online)

regardless of the time of day, day of the week, seasonal fluctuations in demand for the products manufactured, instability in the quality of the fuel supplied, etc.

A decrease in the reliability of heat supply to consumers is possible due to increased equipment failure rates, both due to external influences in extreme conditions [1, 2] and due to the depletion of the design life of some of the installed generating equipment.

Analysis of literature data and problem statement

The main task of power systems is to ensure uninterrupted power supply to consumers. This task can only be solved if the equipment is in good working order and operates reliably.

The reliability of heat and power generating equipment is its ability to maintain the capacity to produce electrical and thermal energy of certain parameters according to the required load schedule with a given system of maintenance and repair of equipment.

A characteristic feature of power plants is their cyclical mode of operation, shown in Fig. 1 in the form of a graph. After a certain period of operation, the plant is shut down for planned preventive maintenance (PPM), and in the event of failures during operation, unplanned repairs (UR) are carried out. In some cases, the period of plant downtime may be related to the modernisation and reconstruction of its individual elements or to external factors not related to the technical condition of the plant, for example, its decommissioning due to a reduction in electricity or heat consumption, a lack of funds to purchase fuel, or an accident in the power system.

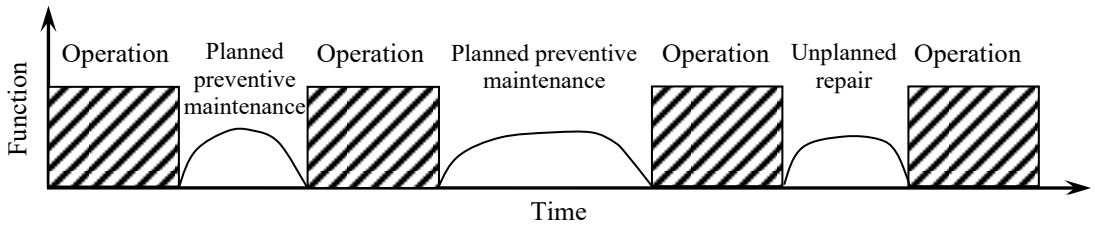

Fig. 1. Heating system operation schedule

Thus, the reliability of a power plant consists of several components: fault tolerance, durability, maintainability, and preservation.

To increase the reliability of heat and power generation systems, redundancy is used – a method of increasing the reliability of an object by introducing additional elements and functional capabilities beyond the minimum necessary for the normal performance of the object's specified functions. In this case, failure occurs only after the failure of the main element and all backup elements.

The level of reliability of energy supply to consumers in most countries is set at a fairly high level of 0.999, which corresponds to a single emergency power outage lasting one day every 2.74 years [3 – 7]. The main reasons for the extreme operating conditions of heat supply systems in Eastern Europe may be extremely low winter temperatures, strong winds, precipitation and other climatic features [8]. In the current conditions in Ukraine, additional aspects include wartime problems, including damage to infrastructure as a result of hostilities, interruptions in the supply of fuel, water and electricity, difficulties in accessing repair work in affected areas, etc. [9].

The necessary level of energy supply reliability can be achieved through passive protection, the creation of a structure of generating sources with an appropriate level of reliability [10], or, taking into account the technical characteristics of existing equipment, through an appropriate reserve of installed capacity.

In addition, high reliability of power systems can be ensured through high reliability indicators of the equipment used and through the appropriate structure and redundancy of generation systems [1].

Centralised heat supply systems are complex, spatially distributed engineering structures with a fundamental lack of statistical information about component failures and the laws governing the distribution of random variables.

The aim of this work is to determine the possibility of improving the reliability of heat and power generating units in heat supply systems, taking into account the installation of reserve capacities.

To achieve this goal, the following tasks must be solved:

– analysis of methods for determining the reserve capacity of heat supply systems;

– calculation of the power reserve of the energy system;
– construction of a graph for determining the reserve capacity of the heat supply system;
– construction of graphs showing the probability of failure of energy equipment.

Materials and methods

Let us consider methods for determining the amount of generating capacity reserve required to compensate for losses due to emergency repairs (N_{ar}), scheduled (major) repairs (N_{kr}), and possible exceedances of forecast load values (N_h) at consumers. The amount of the required reserve is closely related to the determination of the failure rate parameters of the equipment used, and the reserve also depends on the solution of the repair planning problem.

For example, let us consider a heat supply energy system consisting of n generating units with available capacity N_i, emergency shutdown intensity λ_i, and period between major repairs T_i^{kr} before the start of the heating season (e.g., in October – T_{10}).

After the end of the heating season (in this case, in April), the system usually switches to a reduced power mode, which is necessary for hot water supply. However, in some regions, a significant number of heating systems operate only during the heating season, which simplifies the planning of major repairs and maintenance of the system equipment.

The graph in Fig. 2 is presented in coordinates – power $N(t_j)$ and annual operating time T_y with monthly – ΔT_j breakdown of performance indicators, which shows the main indicators: $N^p(t_j)$ – total power that can be carried by the installed generating equipment in the j-th period of operation, J – heating system load, corresponding power reserve in the system N_j^r, and N_m^r – calculated reserve of the heating system during the period of maximum load in the current year of operation.

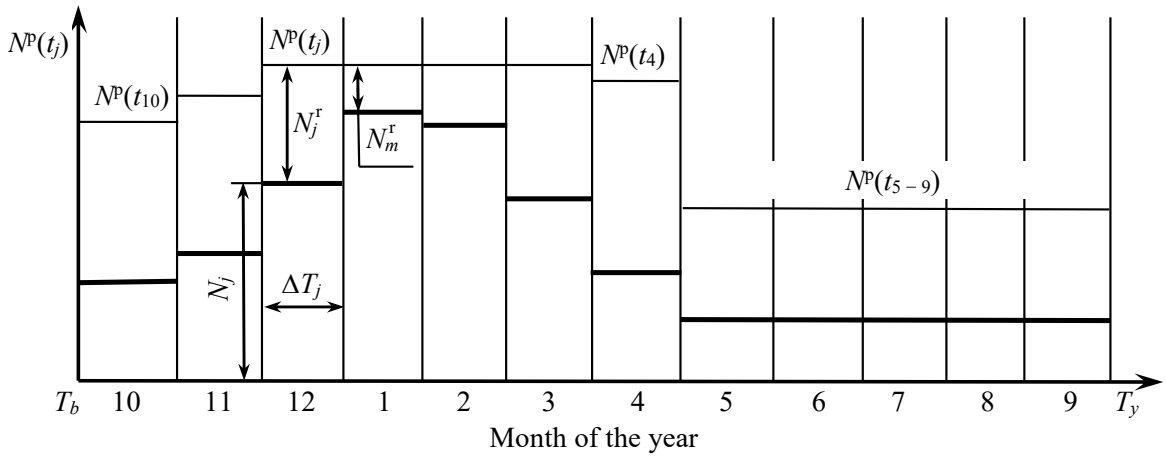

Fig. 2. Graph showing the determination of the heat supply system reserve

For a concentrated power system, its power at the beginning of period T_b is equal to:

$$N^p(t_{10}) = \sum_{i=1}^{n} N_i^p(t_{10}), \quad (1)$$

where: n – the number of types of generating equipment with different parameters used in the system.

It is important to note that an energy system can be considered concentrated if the throughput capacity of its energy networks (including during scheduled and emergency repairs of both main equipment and network elements) does not limit the use of the capacity of energy supply facilities at any point of consumption at all load values, i.e. the generating capacities and consumers in the calculation scheme that combines its elements through a branched system of ring or radial redundancy can be conditionally concentrated in a common node. The closest to concentrated are electrical systems with powerful electrical networks. Existing heat supply systems correspond to the concept of concentrated systems to a lesser extent. However, the existing trend of combining individual boiler rooms and their power-generating elements is a real direction for the transition to their concentration in the future. The energy load schedule N_y for the entire planned operating period T_y (as a rule, this period is the entire year for continuous operation of the heat and power supply system, or the heating season for operation exclusively for heat supply) must be specified as a piecewise constant function N_j at equal intervals

ISSN 2076-2429 (print)
ISSN 2223-3814 (online)

ΔT_j, period T_y, where the number of intervals j is usually equal to 12 monthly intervals for year-round operation, or 6 – 8 (depending on the characteristics of the region) for system operation only during the heating period. In this case, the monthly maximums can be considered as interval load values. It should be noted that the graph in Fig. 1 reflects a situation where, during the calculation period T_y, there is a possible change in the installed capacity in the power system with a simultaneous increase (relative to the previous calculation period) in the maximum load due to the growth in consumption, for example, when the outside temperature drops in winter for heating systems. There may be situations in which there is no increase in installed capacity, or even a decrease due to the decommissioning of emergency or obsolete equipment. In addition, the predicted change in peak loads is ambiguous and sometimes controllable. Calculating the power reserve of the power system to ensure its stability and the operation of vital consumers for such conditions is no less relevant and can be performed if there is sufficiently complete information about the technical condition of the generating equipment.

When planning major repairs, their frequency can be accepted:

$$T_i^{\text{kr}} = n_i \cdot T_y, \tag{2}$$

where: n_i – a number that characterises the frequency of major repairs in years, usually no more than three.

As a result of planning, the start and end times of major repairs of m units with a capacity of N_i^{p} (i=1, m), that are to be carried out during the period T_y (obviously, $m<n$) must be determined. The task of determining the reserve generating capacity is to determine for each interval ΔT_i^y of the period T_y such available capacity $N^{\text{p}}(t_j)$ that the probability of a deficit-free state of the power system q_j in any of the intervals ΔT_i^y is not lower than the required q^{o}, i.e. $q_j \geq q^{\text{o}}$, j = 1, 12. Theoretically, it is necessary to strive for equality in the above ratio, since excessive reliability requires additional costs, but taking into account unpredictable situations and changes in equipment reliability indicators, a positive reserve value should be planned. The value of the power reserve $N^{\text{r}}(t_j)$ at a given moment is determined as the difference between the available installed capacity of the system and its load:

$$N^{\text{r}}(t_j) = N^{\text{p}}(t_j) - N_j. \tag{3}$$

The calculated reserve value for the period T_y is taken as the value corresponding to the annual maximum load. In our case, this refers to January, the coldest period of the heating season.

Therefore, in our case:

$$N_m^{\text{r}} = N^{\text{p}}(t_1) - N_1. \tag{4}$$

it must exceed the maximum power that can be lost in the event of an emergency shutdown of at least one generating unit in the system. The probability of system reliability q_m in the interval m, i.e. at maximum load, can be determined by the formula:

$$q_m = 1 - p_m(A \mid B) = 1 - \frac{p_m(A \cap B)}{p_m(B)}, \tag{5}$$

where:

$p_m(A \cap B)$ – the probability of both events A and B occurring simultaneously. An event means that the failure of k units causes the system to fail;

$p_m(B)$ – probability of event B occurring, i.e. failure of k units in the m-th interval;

$p_m(A)$ – probability of failure of the entire power system to function properly, in our example during the most stressful January period ΔT_1.

The probability of k failures of units in the j-th interval P_j^k can be found using the formula for Poisson distribution, which describes the probability of events occurring within a set time interval ΔT_j that are independent of each other. In each test, the probability is assumed to be constant, and if the general condition is satisfied, i.e. the number of elements in the system n multiplied by the probability of failure p-n-p<10, then the probability that failure will occur exactly k times in n tests is approximately equal to:

$$P_j^k = \frac{(\lambda_j)^k}{k!} \cdot \exp(-\lambda_j), \tag{6}$$

where:

λ_j – total failure rate in the *j*-th interval;

$p(N_m^r \mid k)$ – conditional probability that, if *k* units fail in the *j*-th interval, the system will fail when the total capacity of the power units taken out of service due to failures exceeds the capacity of the operational reserve; its value can be determined by the Bernoulli or Laplace distribution.

The Laplace distribution is a continuous probability distribution used to model data with "heavy tails" (a higher probability of extreme values) compared to the normal distribution. This means that it has a higher probability for values far from the mean, making it suitable for modelling phenomena where extreme events occur more frequently. The Laplace integral function is as follows:

$$\Phi_i = \frac{1}{\sqrt{2 \cdot \pi}} \cdot \int_0^x e^{-\frac{s^2}{2}} \cdot dx \,, \tag{7}$$

where: $s=x_1..x_2$, and *x* in turn:

$$x_i = \frac{k_i - n \cdot p}{\sqrt{n \cdot p \cdot (1-p)}} \,. \tag{8}$$

In general, x_1 and x_2 are determined, respectively, at the minimum number of elements that can fail in the system – k_1, and at the maximum number – k_2. If the option of a possible failure from 0 to *k* is considered, then $k_1 = 0$.

After obtaining the values of the tabular functions Φ_1 and Φ_2, the probability of failure of *k* elements is determined as the difference between these functions:

$$P = \Phi_2 - \Phi_1. \tag{9}$$

The value of the reserve N_m^r in the formula for determining the conditional probability $p(N_m^r \mid k)$ is the difference between the total capacity of the installed and ready-to-operate generating elements of the system and the total capacity of n operating units N_i during the period of maximum system load ($j=m$):

$$N_m^r = \sum_{i=1}^{\overline{n_j}} N_i^p - \sum_{i=1}^{n_m} N_i \,. \tag{10}$$

Thus, taking into account the assumptions made, the values necessary for establishing the probability of failure-free operation of the heat supply system q_j and the value of the power reserve of the power system N_m^r are determined for known general parameters of the power system and reliability indicators of its generating equipment. It should be noted that the presented method of using the tabulated Laplace distribution requires tables of local and integral functions, which somewhat complicates its practical implementation.

Research results

For practical use in most cases, the problem of power reservation can be solved using a simpler and more accurate method for a small number of system elements, based on the Bernoulli distribution, which we will use for in-depth analysis.

According to this method, the probability P_j^k of *k* failures of units in the *j*-th time interval:

$$P_j^k = \frac{n! \cdot p^k \cdot (1-p)^{(n-k)}}{k! \cdot (n-k)!} \,, \tag{11}$$

where:

n – total number of installed generation facilities;

k – number of refusals considered;

p – probability of failure of a single system component.

Let us analyse the following options for reserving a boiler room with n= 6, 8 and 12 boilers of the same type with possible failure probabilities p = 0.05; 0.1 and 0.2. Based on this initial data, we will determine the probability of emergency shutdown of one, two, three and four boilers.

To simplify the calculations, especially when there are a large number of system elements, one of the

ISSN 2076-2429 (print)
ISSN 2223-3814 (online)

well-known mathematical packages such as MatCad, Maple or Matlab can be used. Thus, in Maple, the program (left) and the calculation results (right) look as shown in Figure 3.

RESTART	
$q := (p, n, k) \to \frac{n! p^k (1-p)^{(n-k)}}{k!(n-k)!}$	$q := (p, n, k) \to \frac{n! p^k (1-p)^{(n-k)}}{k!(n-k)!}$
$q_1 := sion(q(0.1, 6, s), s = 0...1)$	$q_1 := 0.8857350000$
$q_2 := sion(q(0.1, 6, s), s = 0...2)$	$q_2 := 0.9841500000$
$q_3 := sion(q(0.1, 6, s), s = 0...3)$	$q_3 := 0.9987300000$
$q_4 := sion(q(0.1, 6, s), s = 0...4)$	$q_4 := 0.9999450000$

Fig. 3. Calculation using Maple

In this particular case, the calculation of the probability of failure of one, or simultaneously 2, 3, 4 boilers of the system (here s is the number of failures from 0 to k) is shown, with the probability of failure of each element p=0.1 and the total number of elements in the system n=6.

In this case, the opposite result – the probability of failure of elements in the given situation – is determined as $p_k = 1 - q_k$, and these values for all options are given in Table 1.

Table 1

Probability of failure of power supply system components

k	n=6			n=8			n=12		
	p=0.05	p=0.1	p=0.2	p=0.05	p= 0.1	p=0.2	p=0.05	p=0.1	p=0.2
1	0.032774	0.186895	0.34464	0.057245	0.186895	0.496684	0.11836	0.186895	0.725122
2	0.00223	0.038092	0.09888	0.005788	0.038092	0.203082	0.019568	0.038092	0.441654
3	8.64E-05	0.005024	0.01696	0.000372	0.005024	0.056282	0.002236	0.005024	0.205431
4	1.8E-06	0.000432	0.0016	1.54E-05	0.000432	0.010406	0.000184	0.000432	0.072555

It is advisable to present the results obtained in a more visual form using appropriate graphs. It should be noted that in probabilistic calculations, qualitative assessment and identification of trends in the influence of various factors on the probability of certain events occurring are often more important than “dry” numerical values.

Analysis of the graph in Fig. 4 shows that with a small total number of generating elements in the system, the probability of failure of individual elements is quite high. Moreover, the probability of failure of one element is the highest, the probability of failure of two elements at the sa

me time is significantly lower, and the probability of failure of three and four elements is very low.

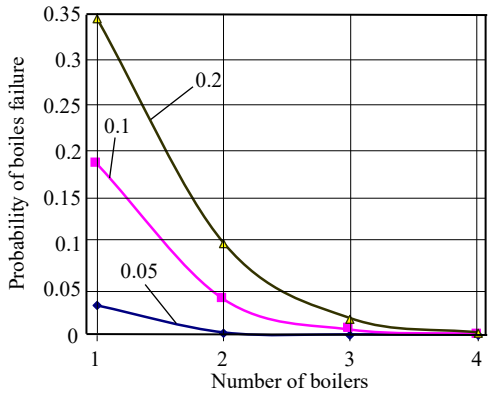

Fig. 4. Probability of failure of individual system elements when their total number is n=6

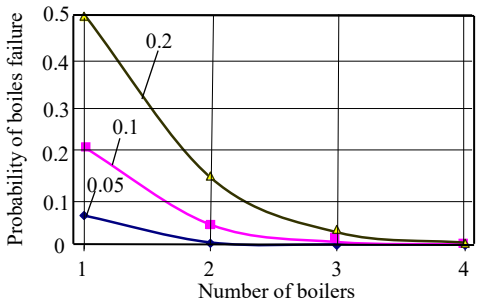

Fig. 5. Probability of failure of individual system components when their total number is n=8

Of course, in all cases with higher reliability indicators of elements, the probability of failure for different numbers of them is significantly lower.

When the total number of system elements is increased to n=8 and n=12 (Fig. 5, 6), there is an increase in the probability of failure of different numbers of elements k due to the increase in the sample size. However, with a larger total number of elements, the relative share of the impact of the failure of a single element (boiler) on the performance of the entire system (boiler room) decreases accordingly, given the accepted minimum reserve value.

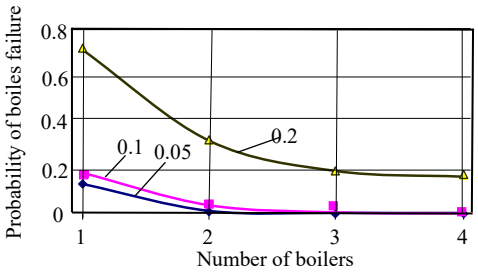

Fig. 6. Probability of failure of individual system elements when their total number is n=12

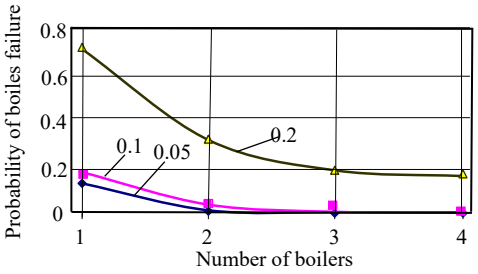

Fig. 7. Nature of change in probability of failure of individual elements with individual probability of failure p=0.05 when the total number of elements n changes from 6 to 12

The result of the analysis of the impact of the total number of elements, or generating boilers in the heat supply system, including concentrated with a large number of elements, can also be made on the basis of the graphs shown in Figures 7 and 8. And if, with high reliability of individual elements with p=0.05, the situation is obvious, then with low reliability of individual elements with p=0.2, a completely different nature of dependencies $p=f(k)$ is observed when one element of the system fails and four elements fail simultaneously. Additional calculations with an increase in the value of n to 16 confirmed this feature.

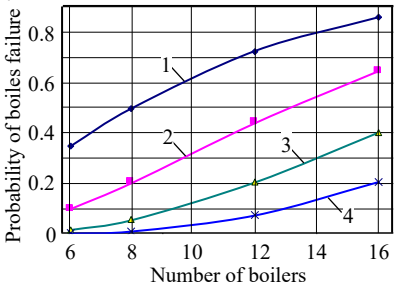

Fig. 8. Nature of change in probability of failure of individual elements with individual probability of failure p=0.2 when the total number of elements n changes from 6 to 16

Obviously, this peculiarity of the influence of the total number of system elements on the probability of failure of $k_{1\text{-}4}$ elements can be explained by the fact that when n is very large – several hundred (for example, in microelectronic elements, chips), the difference in the probability of failure of one or four elements will be insignificant.

As noted, the total reserve of the power system is determined by the sum of the load reserve – N_{h}, the repair reserve – N_{pr}, and the emergency reserve – N_{ar}:

$$N_y^{\text{r}} = N_{\text{h}} + N_{\text{pr}} + N_{\text{ar}} . \tag{12}$$

During periods of maximum load, the minimum value of the required reserve N_m^{r} is determined as the corresponding value N_{ar}, since the reliability of power supply is mainly determined by the level of emergency reserve, as the rest of the components can be fixed.

In the case of a system reserve consisting of equipment of different capacities and reliability indicators, the emergency reserve of the power system is determined as the sum of the reserves of individual types of equipment:

$$N_{\text{ar}} = \sum_{i=1}^{k} N_i^{\text{r}} , \tag{13}$$

where:

N_i^{r} – reserve of equipment of this type;

k – the amount of backup generating equipment of the appropriate type.

ISSN 2076-2429 (print)
ISSN 2223-3814 (online)

The value of N_i^r can be determined using the formula:

$$N_i^r = N_i \cdot n_i \cdot \overline{r}_i \,, \tag{14}$$

where:

N_i – power of a power plant of a certain type;

n_i – number of elements in the system (in our case, boilers or autonomous electric generators) of the same type;

$\overline{r}_i$ – specific reserve, determined by specific power:

$$\bar{N}_i = N_i / N^{pi}(t_m), \tag{15}$$

where:

p_i – average failure rate of units of type i;

$N^p(t_m)$ – total capacity that can be carried by the installed generating equipment during periods of maximum load on the heat supply power system.

The accident rate for a specific heat supply installation can be estimated using the following formula:

$$p_i = \frac{\tau_{av}}{\tau_y - \tau_{av}}, \tag{16}$$

where:

τ_y – the time during which the unit is in operation, i.e. annual or seasonal operating hours;

τ_{av} – equipment downtime due to its failure during the relevant period.

The average failure rate p_i is often assumed to be constant for energy equipment of the same type, but it should be borne in mind that even such equipment may have significantly different reliability indicators. This makes it advisable to systematically record, collect and process statistical data on all elements of the system, especially for power equipment that has worked out a significant part of its resource.

Conclusions

The paper examines the possibilities of improving the reliability of the heat supply system when installing reserve capacities. The following conclusions were made:

1. The calculated reserve value is taken to be the value corresponding to the annual maximum load; it must be greater than the maximum capacity that can be lost in the event of an emergency shutdown of at least one generating unit of the system;

2. In the course of the analysis of existing methods for calculating the reserve capacity of thermal equipment, the method based on Bernoulli distribution is simpler and more accurate for a small number of system elements;

3. The probability of failure in the heat supply system is quite high when there are a small number of generating elements of individual elements; moreover, the probability of failure of one element is significantly higher than the probability of failure of two elements at the same time, and the probability of failure of three or four elements is very low;

4. With high reliability indicators for elements, the probability of failure for different numbers of elements is significantly lower;

5. With a larger total number of elements, the relative impact of the failure of a single element (boiler) on the performance of the entire system (boiler room) decreases accordingly, given the accepted minimum reserve value.

Therefore, it is necessary to conduct appropriate systematic individual accounting, collection and appropriate processing of statistical data on all elements of the heat supply system, paying particular attention to energy equipment that has worked out a significant part of its resource.

Література

1. Проблеми забезпечення надійного теплопостачання в умовах негарантованого електропостачання теплогенеруючим підприємствам / A. Mazurenko, O. Klymchuk, G. Pozdniakova et al. *Праці Одеського політехнічного університету*. 2024. Вип. 1(69). С. 23–31. DOI: https://doi.org/10.15276/opu.1.69.2024.03.

2. Klymchuk O., Pozdniakova G. Підвищення надійності роботи систем теплопостачання в умовах відключення електроенергії. *Праці Одеського політехнічного університету*. 2024. Вип. 2(70). С. 48–54. DOI: https://doi.org/10.15276/opu.2.70.2024.06.
3. Енергетична ефективність України. Кращі проектні ідеї: Проект «Професіоналізація та стабілізація енергетичного менеджменту в Україні» / уклад.: С. П. Денисюк, О. В. Коцар, Ю. В. Чернецька. Київ : КПІ ім. Ігоря Сікорського, 2016. 79 с.
4. Денисюк С. П., Таргоньский В. А. Енергоефективність України: проблеми та шляхи її зростання. *Енергетика: економіка, технології, екологія*. 2017. № 4. С. 7–28. DOI: https://doi.org/10.20535/1813-5420.4.2017.130871.
5. Про схвалення Енергетичної стратегії України на період до 2050 року : Розпорядження Кабінету Міністрів України від 21 квіт. 2023 р. № 373-р. URL: https://zakon.rada.gov.ua/laws/show/373-2023-%D1%80#Text (дата звернення: 06.11.2025).
6. Борисов М. А. Реабілітація ТЕС. Забезпечення сталої роботи об'єднаної енергосистеми України. *Енергетика и електрифікація*. 2004. № 3. С. 2–3.
7. Про теплопостачання : Закон України від 02.06.2005 № 2633-IV. URL: http://zakon.rada.gov.ua/laws/show/2633-15. (дата звернення: 06.11.2025).
8. European Energy Security Strategy : Strategy of 28.05.2014 no. 52014DC0330 / European Commission. URL: https://eur-lex.europa.eu/legal-content/EN/TXT/?uri=celex:52014DC0330. (дата звернення: 06.11.2025).
9. Визначення ймовірності відмов в роботі елементів систем міського теплопостачання в екстремальних умовах експлуатації / A. Mazurenko, A. Pustovit, P. Shylov et al. // *Праці Одеського політехнічного університету*. 2025. Вип. 1(71). С. 98–103. DOI: https://doi.org/10.15276/opu.1.71.2025.11.
10. Забезпечення підвищення надійності та ефективності систем теплопостачання за рахунок використання мікротурбін в умовах нестабільного енергоживлення / A. Mazurenko, O. Klymchuk, G. Luzhanska et al. *Праці Одеського політехнічного університету*. 2022. Вип. 2(66). С. 58–63. DOI: https://doi.org/10.15276/opu.2.66.2022.07.

References

1. Mazurenko, A., Klymchuk, O., Pozdniakova, G., Pustovit, A., & Shavrov, V. (2024). Problems of reliable heat supply providing in the conditions of non-guaranteed electricity supply to heat-generating enterprises. *Proceedings of Odessa Polytechnic University*, *1*(69), 23–31. DOI: https://doi.org/10.15276/opu.1.69.2024.03.
2. Klymchuk, O., & Pozdniakova, G. (2024). Improving the reliability of heat supply systems in the conditions of power outage. *Proceedings of Odessa Polytechnic University*, *2*(70), 48–54. DOI: https://doi.org/10.15276/opu.2.70.2024.06.
3. Denysyuk, S. P., Kotsar, O. V., & Chernetska, Y. V. (Eds.). (2016). Energy efficiency of Ukraine. Best project ideas: Project "Professionalization and stabilization of energy management in Ukraine". Igor Sikorsky Kyiv Polytechnic Institute.
4. Denysyuk, S. P., & Tarhonksyy, V. A. (2017). Energy efficiency of Ukraine: Problems and ways of its growth. *Energetika: Ekonomika, Tekhnologii, Ekologiya*, (4), 7–28. DOI: https://doi.org/10.20535/1813-5420.4.2017.130871.
5. Cabinet of Ministers of Ukraine. (2023, April 21). *On the approval of the Energy Strategy of Ukraine for the period up to 2050* (Decree No. 373-r). Retrieved from https://zakon.rada.gov.ua/laws/show/373-2023-%D1%80#Text.
6. Borysov, M. A. (2004). Rehabilitation of TPPs. Ensuring stable operation of the integrated power system of Ukraine. *Energetika i Elektrifikatsiya*, (3), 2–3.
7. On heat supply, Law of Ukraine No. 2633-IV (2005). http://zakon.rada.gov.ua/laws/show/2633-15.
8. European Commission. (2014). *European energy security strategy* (COM/2014/0330). Retrieved from https://eur-lex.europa.eu/legal-content/EN/TXT/?uri=celex:52014DC0330.
9. Mazurenko, A., Pustovit, A., Shylov, P., Shylov, D., & Stanislavov, V. (2025). Determination of the probability of failures in the operation of elements of urban heat supply systems in extreme operating conditions. *Proceedings of Odessa Polytechnic University*, *1*(71), 98–103. DOI: https://doi.org/10.15276/opu.1.71.2025.11.

ISSN 2076-2429 (print)
ISSN 2223-3814 (online)

10. Mazurenko, A., Klymchuk, O., Luzhanska, G., Ivanov, P., & Sergeiev, I. (2022). Ensuring increased reliability and efficiency of heat supply systems due to the use of microturbines in conditions of unstable power supply. *Proceedings of Odessa Polytechnic University*, *2*(66), 58–63. DOI: https://doi.org/10.15276/opu.2.66.2022.07.

Мазуренко Антон Станіславович; Anton Mazurenko, ORCID: https://orcid.org/0000-0002-0165-3826
Пустовіт Анатолій Васильович; Anatoliy Pustovit, ORCID: https://orcid.org/0009-0008-4320-953X
Дорошенко Жанна Федорівна; Zhanna Doroshenko, ORCID: https://orcid.org/0000-0002-8019-7864
Грищенко Сергій Ігорович; Sergii Gryshchenko, ORCID: http://orcid.org/0000-0002-0686-1149

Received November 18, 2025
Accepted December 16, 2025

UDC 629.031

V. Skalozubov, DSc, Prof.,
H. Derbenov,
Iu. Katsarskyi,
Ye. Mazur,
V. Kochneva
Odessa Polytechnic National University, Shevchenko Ave. 1, Odesa, Ukraine, 65044, e-mail: valer_nov13@ukr.net

METHODOLOGY FOR DETERMINING THE CONDITIONS FOR THE OCCURRENCE OF STEAM EXPLOSIONS DURING ACCIDENTS WITH COMPLETE POWER OUTAGES AND INTER-CIRCUIT LEAKS AT NUCLEAR POWER PLANTS WITH VVER

В. Скалозубов, Г. Дербеньов, Ю. Кацарський, Є. Мазур, В. Кочнєва. **Методика визначення умов виникнення парових вибухів під час аварій з повним знеструмленням та міжконтурними течами на ядерних енергоустановках з ВВЕР.** Розроблено детерміністський метод визначення умов і наслідків парових вибухів у процесі аварій з повним знеструмленням та міжконтурними течами ядерних енергоустановок з реакторами типу WWER/PWR. Необхідні умови парових вибухів визначаються на базі принципу термодинамічної нестійкості систем – одночасне збільшення тиску і маси в парових об'ємах реактора та/або парогенератора відповідає умовам парових вибухів. Визначальні параметри умов парових вибухів – швидкості збільшення тиску і парового об'єму. Наслідки парових вибухів визначаються енергетичною потужністю парових вибухів, яка залежить від швидкості збільшення тиску і парового об'єму. На основі розробленого методу встановлено найбільш критичні ситуації щодо умов і наслідків парових вибухів під час аварії з повним знеструмленням та між контурними течами ядерних енергоустановок з реакторами типу WWER/PWR. Установлено необхідні умови успішної кваліфікації на відкриття в умовах парових вибухів запобіжних клапанів реактора та парогенератора, а також паро-скидальних пристроїв парогенератора. Установлено необхідність модернізації системи аварійного підживлення об'ємів парогенератора для ефективного управління аваріями з повним знеструмленням та між-контурними течами ядерних енергоустановок з реакторами типу WWER/PWR та запобігання умовам і наслідкам парових вибухів. Розроблені методи визначення умов парових вибухів на ядерних енергоустановках можуть бути включені до складу детерміністських кодів моделювання аварій зі «щільним» реакторним контуром/між-контурними течами в об'ємі парогенераторів, а також до експлуатаційної документації (керівництва/інструкції з управління аваріями) для удосконалення/модернізації стратегій управління аваріями на ядерних енергоустановках з реакторами типу WWER/ PWR.
Ключові слова: аварія, знеструмлення, міжконтурна теча, паровий вибух, ядерна енергоустановка

V. Skalozubov, H. Derbenov, Iu. Katsarskyi, Ye. Mazur, V. Kochnieva. **Methodology for determining the conditions for the occurrence of steam explosions during accidents with complete power outages and inter-circuit leaks at nuclear power plants with VVER.** A deterministic method has been developed to determine the conditions and consequences of steam explosions during complete power outages accidents with inter circuit leaks at nuclear power plants with WWER/PWR reactors. The required conditions for steam explosions are determined based on the principle of thermodynamic instability of systems – a simultaneous increase in pressure and mass in the steam volumes of the reactor and/or steam generator corresponds to the conditions for steam explosions. The determining parameters of the conditions for steam explosions are the rates of increase in pressure and steam volume. The consequences of steam explosions are determined by the energy capacity of steam explosions, which depends on the rate of increase in pressure and steam volume. Based on the developed method, the most critical situations regarding the conditions and consequences of steam explosions of complete power outages accidents with intercircuit leaks have been found for nuclear power plants with WWER/PWR reactors. The required conditions for successful qualification for opening the safety valves of the reactor and steam generator, as well as the steam dump devices of the steam generator under steam explosion conditions, have been found. The need to modernize the emergency feed system of the steam generator volumes has been recognized for the effective management of out with intercircuit leaks of nuclear power plants with WWER/PWR reactors and the prevention of the conditions and consequences of steam explosions. The developed methods to determine the conditions for steam explosions at nuclear power plants can be included in the deterministic codes for modelling accidents with a "tight" reactor circuit/intercircuit leaks in the volume of steam generators, as well as in the operational documentation (manuals/instructions for accident management) for the improvement/ modernization of accident management strategies at nuclear power plants with WWER/PWR reactors.
Keywords: accident, compete power outages, intercircuit leak, steam explosion, nuclear power plant

Introduction

In the traditional safety analysis of nuclear power plants with VVER/PWR reactors, the possibility of a steam explosion was excluded based on the results of design and operational tests of the reactor safety valves and steam generator, which were carried out at a quasi-static ("slow") increase in

DOI: 10.15276/opu.2.72.2025.07

ISSN 2076-2429 (print)
ISSN 2223-3814 (online)

pressure to the level of maximum permissible values.

However, the conditions of design and operational tests of safety valves by a "slow" increase in pressure can differ significantly from the conditions of a steam explosion, which are characterized by a pulsed ("rapid") increase in pressure. Therefore, in the conditions of a steam explosion, the safety valves may not have time to react to a "rapid" increase in pressure.

In addition, it should be noted that the failures of the reactor safety valves became the main cause of a serious accident at the TMI-2 NPP (USA, 1979) and an emergency incident at the Rivne NPP (2009).

During accidents with a sufficiently large intercircuit leak, steam explosion conditions may occur in the volume of the steam generator isolated from the 2nd circuit (requirements of accident management instructions). Under such emergency conditions, the "hot" coolant of the 1st circuit, which enters the volume of the steam generator, boils, which leads to an increase in steam pressure in the volume of the steam generator. At certain sizes of the intercircuit leak, the increase in steam pressure in the volume of the steam generator can be of a pulsed ("high-speed") nature, when the steam boiler safety systems of the steam generator do not "have time" to work, which determines the conditions of a steam explosion in the volume of the steam generator in the process of accidents with intercircuit leaks.

With sufficiently small flow sizes, steam explosion conditions can occur in the 1st circuit in the case of a fairly rapid (impulse) increase in pressure in the reactor.

Thus, in the general case, when modeling and analyzing accidents in nuclear power plants, it is necessary to take into account the possibility of occurrence and consequences of a steam explosion.

For nuclear power plants with VVER/PWR, the conditions of a steam explosion can be realized in accidents with compete power outages of power units (an analogue of one of the causes of the Fukushima accident) and intercircuit leaks in steam generators (the dominant group of accidents in nuclear power plants with VVER/PWR), which determines the relevance of the presented work.

Analysis of known developments on the topic and problem statement

In the paper [1], based on the analysis of the experience of overcoming and learning from the Chornobyl accident, it was found that it was a powerful destructive steam explosion that became the main cause of catastrophic environmental consequences – the total emission of highly radioactive nuclides cesium and iodine into the environment amounted to more than $5.0 \cdot 10^{18}$ Bq.

Based on the analysis of the causes and consequences of the accidents at the Fukushima nuclear power plant (Japan, 2011), the IAEA mission of experts [2] established the causes of the steam explosion at the 2nd power unit. A devastating steam explosion at Unit 3 triggered the next hydrogen explosion and catastrophic environmental consequences in the environment. According to various experts, the total emission of highly radioactive nuclides cesium and iodine amounted to (0.3…1.4)·1018 Bq [3, 4]. At the same time, "Fukushima" highly radioactive nuclides were also recorded in the Kyiv region [5].

The paper [6] analyzes the results of operational tests of safety valves of reactors and steam generators in the process of scheduled repairs of power units with VVER. It was established that all tests were carried out in the mode of "slow" pressure increase to the maximum permissible value, corresponding to the opening of the reactor/steam generator safety valves.

In the paper [7], an analysis of the known results of simulation of accidents at nuclear power plants with VVER/PWR/SMR was carried out. It was established that the issue of determining the conditions and consequences of a steam explosion in the course of accidents was not considered. The main reasons for this situation are related to the fact that a priori the "absolute" reliability of the safety valves of reactors/steam generators was assumed, as well as the lack of sufficiently substantiated methods for determining the conditions and consequences of a steam explosion in nuclear power plants with VVER/PWR reactors.

The analysis of the known results allows you to formulate the purpose and objectives of the presented work.

The purpose of the study is to develop a method for determining the conditions and consequences of steam explosions during accidents with compete power outages of power units and intercircuit leaks in nuclear power plants with VVER/PWR reactors.

Main objectives of the study

1. To develop a method for determining the conditions and consequences of steam explosions during accidents with compete power outages of power units and intercircuit leaks (CPO-ICL).

2. To analyze the impact of the emergency state of the nuclear power plant on the conditions and consequences of a steam explosion during accidents with MB-IL.

Model of a steam explosion during accidents with compete power outages of power units and intercircuit leaks

Basic provisions and assumptions

1. A generalized scheme of the model of the nuclear installation with VVER/PWR in the process of an accident with CPO-ICL is shown in Fig. 1.

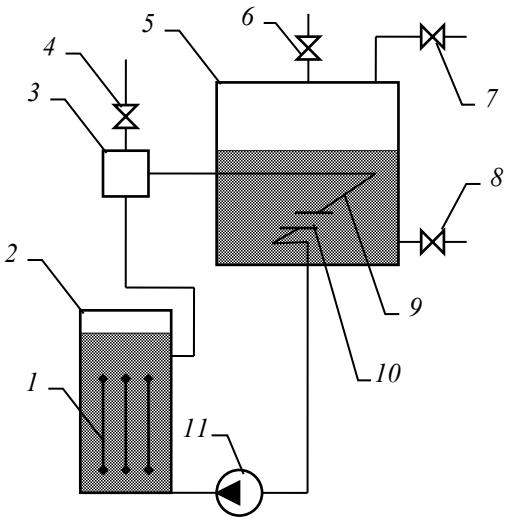

Fig. 1. Generalized diagram of the model of nuclear power plants with VVER/PWR: *1* – active zone; *2* – reactor vessel; *3* – pressure compensator; *4* – pressure compensator safety valve; *5* – steam generator; *6* – steam generator safety valve; *7*, *8* – insulation fittings of the 2nd circuit during an accident; *9* – heat exchange tubes of the steam generator; *10* – intercarrier leak; *11* – main circulation pump

2. The following chronology of the initial stages of the accident is accepted:

– registration of signals/symptoms of an accident with the CPO-ICL;

– emergency shutdown of the reactor;

– emergency stop of the circulation pump;

– insulation of the 2nd circuit with shut-off valves of the steam pipeline and the supply water pipeline of the steam generator, as well as shutdown of the turbine plant.

3. As a result of a complete de-energization of the power unit, the failure of all active safety systems (with electric pumps) for the accident control of the reactor core cooling and emergency power supply of the steam generator is expected.

4. A refusal to open the safety valves of the pressure compensator, safety valves and steam discharge devices of the steam generator in the conditions of a steam explosion with a pulsed ("fast") pressure change in the reactor/steam generator is conservatively provided. The basis for such an assumption is the lack of design and operational tests of experimental qualification of pressure compensator safety valves, safety valves and steam generator spray devices under steam explosion conditions [6, 7].

5. The necessary conditions of a steam explosion can be determined according to the principle of thermodynamic instability (TDI) [5] – a simultaneous increase in the system (in this case, it is the steam volume of the reactor circuit/steam generator) P and mass (volume) V determines the conditions of the TDI.

6. According to the requirements of the accident management instructions in the accident process, the SG is isolated from the 2nd circuit for steam and feed water.

In this case, the conditions of steam pressure and explosion due to TDI in the steam volume of the reactor circuit/steam generator are required:

$$v_P = \frac{dP}{dt} > 0 \text{ and } v_V = \frac{dV_V}{dt} > 0. \quad (1)$$

Sufficient conditions for the occurrence of a steam explosion due to pulsed TDI:

$$v_P \geq (v_P)_{\text{cr}}, \quad (2)$$

where $(v_P)_{\text{cr}}$ – critical for steam explosion conditions pressure increase rate.

According to known experimental data on the parameters of the steam explosion obtained on model installations [5], the conservative estimate of $(v_P)_{\text{cr}} \approx 1.0$ MPa/s.

7. Energy power of a steam explosion (which determines the consequences of a steam explosion) [5]:

$$N_e = \frac{d(PV_{\text{V}})}{dt} = V_V v_P + P v_V, \quad (3)$$

where V_v – vapor phase volume.

Taking into account the accepted provisions and assumptions, the equation of heat and mass balance in the reactor and steam generator during the accident with the CPO-ICL:

ISSN 2076-2429 (print)
ISSN 2223-3814 (online)

$$\frac{d(\rho_{VR}V_{VR})}{dt} = \Delta G_{VR}, \tag{4}$$

$$\frac{d(\rho_{VR}V_{VR}i_{VR})}{dt} = \Delta G_{VR}i_{VR}, \tag{5}$$

$$\frac{d(\rho_{LR}V_{LR})}{dt} = \Delta G_{VR} - G_T, \tag{6}$$

$$\frac{d(\rho_{LR}V_{LR}i_{LR})}{dt} = N_R - Q - \Delta G_{VR}(i_{VR} - i'_{LR} - i_{LR}), \tag{7}$$

$$\frac{d(\rho_{VG}V_{VG})}{dt} = \Delta G_{VG}, \tag{8}$$

$$\frac{d(\rho_{VG}V_{VG}i_{VG})}{dt} = Q + G_T i_R + \Delta G_{VG}(i_{VG} - i'_{LG} - i_{LG}), \tag{9}$$

$$\frac{d(\rho_{LG}V_{LG})}{dt} = -\Delta G_{VG} + G_T, \tag{10}$$

$$\frac{d(\rho_{LG}V_{LG}i_{LG})}{dt} = Q - \Delta G_{VG}(i_{VG} - i'_{LG} - i_{LG}) + G_T(i_{LR} - i_{LG}), \tag{11}$$

where:

ρ_{VR}, ρ_{VG} – Steam density in the reactor and steam generator;
V_{VR}, V_{VG} – Steam volume in the reactor and steam generator;
i_{VR}, i_{VG} – Specific enthalpy of steam in a reactor and steam generator;
ρ_{LR}, ρ_{LG} – Density of the liquid phase in the reactor and steam generator;
V_{LR}, V_{LG} – Volume of liquid phase in reactor and steam generator;
i_{LR}, i_{LG} – Specific enthalpy of the liquid phase in the reactor and steam generator;
G_{VR}, G_{VG} – Mass flow rate of vaporization in the reactor and steam generator;
N_R, Q – reactor power and heat removal in the volume of the steam generator;
G_T – mass flow rate of coolant in an intercircuit leak

$$G_T = \mu_T F_T \sqrt{\rho_{LR}(P_R - P_G)}, \tag{12}$$

where:

μ_T – cost coefficient in ICL;
F_T – ICL Cross-sectional area;
P_R, P_G – Pressure in the reactor and steam generator;
i'_{LR}, i'_{LG} – Specific enthalpy of liquid phase saturation in a reactor and steam generator.
Given:

$$V_{0R} = V_{LR} + V_{VR};$$

$$V_{0G} = V_{LG} + V_{VG};$$

$$\frac{d\rho}{dt} = \frac{d\rho}{dP}\frac{dP}{dt} = \frac{dP}{dt}a^{-2};$$

$$\frac{di}{dt} = \frac{di}{dP}\frac{dP}{dt} = \frac{dP}{dt}C_T.$$

After transformations of equations (4) – (12), we get a system of nonlinear equations:

$$\frac{dP_R}{dt} = v_{PR}(N_R, Q, P_R, P_G, i_{LR}, i_{LG}, F_T), \tag{13}$$

$$\frac{dV_{VR}}{dt} = v_{VR}(N_R, Q, P_R, P_G, i_{LR}, i_{LG}, F_T), \tag{14}$$

$$\frac{dP_G}{dt} = v_{PG}(N_R, Q, P_R, P_G, i_{LR}, i_{LG}, F_T), \tag{15}$$

$$\frac{dV_{VG}}{dt} = v_{VG}(N_R, Q, P_R, P_G, i_{LR}, i_{LG}, F_T), \quad (16)$$

$$\frac{di_{LR}}{dt} = v_{iR}(N_R, Q, P_R, P_G, i_{LR}, i_{LG}, F_T), \quad (17)$$

where:

V_{0R}, V_{0G} – "free" from structures internal volume of the reactor circuit and steam generator;

a – Speed of sound;

C_T – Isothermal heat capacity;

P_R, P_G – average pressure in the reactor circuit and the volume of the steam generator.

Thus, the necessary conditions for a steam explosion (1) in the reactor and in the volume of the steam generator:

$$v_{PR} > 0 \text{ and } v_{VR} > 0, \quad (19)$$

$$v_{PG} > 0 \text{ and } v_{VG} > 0. \quad (20)$$

Sufficient conditions for a steam explosion due to pulsed TDI:

$$v_{PR} \geq (v_P)_{cr}, \quad (21)$$

$$v_{PG} \geq (v_P)_{cr}. \quad (22)$$

Analysis of the obtained results

The analysis of the obtained dependencies (13) – (18) of determining the conditions of the steam explosion (19) – (22) of the CPO-ICL accident in the reactor/steam generator of the nuclear power plant with VVER/PWR established the following.

1. The most critical situation regarding a steam explosion in the reactor circuit under the following conditions:

$$N_R >> Q, \quad (23)$$

$$F_T \leq (F_T)_{cr} = \frac{N_R / \sqrt{\rho_{LR}(P_R - P_G)}}{\mu(i_{VR} - i'_{LR} - i_{LR})}. \quad (24)$$

At $F_T > (F_T)_{cr}$ the ICL actually "performs" the safety function of preventing the destruction of the reactor vessel.

2. The necessary conditions for a steam explosion in the volume of a steam generator (20) can be realized in the entire range of ICL sizes, and sufficient conditions for a steam explosion as a result of a pulsed TDI (22) can be realized at $F_T > (F_T)_{cr}$.

3. Prevention of steam explosion conditions during an accident with CPO-ICL, VVER/PWR nuclear power plants can be based on additional qualification/modernization of the safety systems of the emergency feeding of the steam generator and the safety valves of the pressure compensator/safety valves of the steam generator/steam dispensing devices.

The qualification of pressure compensator/steam generator safety valves/steam discharge devices under steam explosion conditions can be based on a comparison of the time of inertial delay of opening the valve t_i and the propagation time of the steam explosion pulse t_d:

$$t_d \approx \frac{\max P - P_0}{(v_P)_{cr}}, \quad (25)$$

where:

P – Maximum permissible pressure of the start of reactor/steam generator destruction;

P_0 – operating pressure in the reactor/steam generator in normal operation.

Condition for successful qualification of pressure compensator safety valves/steam generator safety valves/steam discharge devices:

$$t_i < \frac{\max P - P_0}{(v_P)_{cr}}. \quad (26)$$

ISSN 2076-2429 (print)
ISSN 2223-3814 (online)

At present, based on the lessons of the Fukushima accident, the following upgrades of the emergency system of the steam generator on NPP with VVER in the conditions of the accident with CPO have been introduced/are being implemented:

– mobile pumping units installed at the NPP industrial site;

– emergency feeding of the steam generator with natural circulation from the deaerator units of the turbine compartment (D-7).

Main limitations of the effectiveness of said systems for accident management with CPO:

– both systems are low-pressure and can feed the steam generator at a fairly low-pressure level in the steam generator volume. Therefore, in the conditions of an accident with CPO-ICL, these systems may not be effective enough for the entire duration of emergency processes;

– according to the lessons of the Fukushima accident, under extreme external conditions (flooding of an industrial site, fall of large/explosive objects, etc.), mobile pumping units may also be insufficiently efficient [5].

Therefore, approaches to modernizing the emergency feeding system of the steam generator, carried out by pumps with a steam drive from a steam generator, seem more promising [3, 4].

Conclusions

1. A deterministic method for determining the conditions and consequences of steam explosions in the process of accidents with complete de-energization and intercircuit leaks of nuclear power plants with WWER/PWR reactors has been developed.

2. The necessary conditions for steam explosions are determined on the basis of the principle of thermodynamic instability of systems – a simultaneous increase in pressure and mass in the steam volumes of the reactor and/or steam generator corresponds to the conditions of steam explosions. Determining parameters of the conditions of steam explosions – the rate of increase in pressure and vapor volume.

3. The consequences of steam explosions are determined by the energy power of steam explosions, which depends on the rate of increase in pressure and vapor volume.

4. On the basis of the developed method, the most critical situations regarding the conditions and consequences of steam explosions during an accident with complete de-energization and intercircuit leaks of nuclear power plants with WWER/PWR reactors were established.

The necessary and sufficient conditions for steam explosions in the reactor/SG have been established. In general terms, the expressions (21) and (22) correspond to the conditions under which the rate of pressure increase in the reactor/SG (depending on the current reactor power, current thermodynamic parameters in the 1st and 2nd circuits, the size of the intercircuit leak) exceeds the critical rate of inertial actuation of the reactor/SG safety valves, which are established by the technical documentation of the safety valves.

5. The necessary conditions for successful qualification for the opening of the reactor safety valves and steam generator, as well as the steam generator vaporizer devices in the conditions of steam explosions, have been established, namely, the flow rate of the coolant through the safety valves must exceed the mass rate of vaporization in the reactor core.

6. It is established that it is necessary to modernize the system of emergency replenishment of steam generator volumes for effective management of accidents with complete de-energization and intercircuit leaks of nuclear power plants with WWER/PWR reactors and prevention of conditions and consequences of steam explosions.

Література

1. A set of methods for reviewing the safety of nuclear energy in Ukraine, taking into account the lessons of environmental disasters in Chernobyl and Fukushima / Ed. G. A. Oborskyi. Odessa : Astroprint, 2013. 244 p.
2. Mazur Ye. Passive systems safety of nuclear power plants. LAP LAMBERT Academic Publishing, 2024. 227p. ISBN 978-620-8-41532-7.
3. Підвищення безпеки ядерної енергетики з урахуванням уроків важких аварій / Кондратюк В. А., Письменний Є. М., Вєрінов О. М., Філатов В. І., Остапенко А. І. *Ядерна та радіаційна безпека*. 2022. № 3. С. 76–81. DOI: https://doi.org/10.32918/nrs.2022.3(95).08.

4. Комаров Ю. О. Результати досліджень деяких питань безпеки та ефективності експлуатації АЕС ризик-орієнтованими методами. *Ядерна фізика та енергетика*. 2013. Т. 14, № 4. С. 356–362. DOI: https://doi.org/10.15407/jnpae2013.04.
5. Kondratyk V., Komarov Ju., Kosenko S., Fedorov D. Prevention of hydrodynamic instability conditions in safety systems with pumps of nuclear power plants. *Proceeding of Odessa Polytechnic University*. 2022. Vol. 1(65). pp. 70–75. DOI 10.15276/opu.1.65.2022.08.
6. Дербеньов Г. Стратегії контролю концентрації борного розчину теплоносія ядерних енергоустановок. LAP LAMBERT Academic Publishing, 2024. 86 с. ISBN 978-620-0-3247-6.
7. Makarenko A., Chaikovskyi M., Mazurok O., Zuyok V., Mykhaylenko O. Calculation Analysis of VVER-1000 RCCA Elements to Justify Lifetime Extension. *Nuclear and Radiation Safety*. 2024. № 3. С. 26–35. DOI: https://doi.org/10.32918/nrs.2024.3(103).03.
8. Вимоги до технічного обслуговування і ремонту обладнання систем, важливих для безпеки атомних станцій / Кухоцький О. В., Гуменюк Д. В., Лігоцький О. І., Потоскуєв В. С., Шишута А. М., Остаповець А. О. *Ядерна та радіаційна безпека*. 2024. № 3. С. 52–59. DOI: https://doi.org/10.32918/nrs.2024.3(103).06.
9. Грибанов В. Кваліфікація міцності мостового крана ядерних енергоустановок. LAP LAMBERT Academic Publishing, 2025. 43 с. ISBN 978-613-58350-8.
10. Risk-informed methods and applications in nuclear and energy engineering: modelling, experimentation, and validation / Ed. by C. L. Smith, K. Le Blanc, and D. Mandelli. Elsevier Inc., Academic Press, 2023. 386 p. DOI: https://doi.org/10.1016/C2020-0-04468-3.

References

1. Oborskyi, H.O. (Ed.) (2013) *A set of methods for reviewing the safety of nuclear energy in Ukraine, taking into account the lessons of environmental disasters in Chernobyl and Fukushima*. Odesa: Astroprint.
2. Mazur, Ye. (2024) *Passive systems safety of nuclear power plants*. LAP LAMBERT Academic Publishing. ISBN 978-620-8-41532-7.
3. Kondratyuk, V., Pysmennyy, Y., Verinov, O., Filatov, V., & Ostapenko, I. (2022) Improvement of nuclear safety taking into account the lessons learned from severe accidents. *Nuclear and Radiation Safety*, 3, 76–81. DOI 10.32918/nrs.2022.3(95).08.
4. Komarov, Yu. (2013) Some research results by risk-inform approaches for NPP safety and operational efficiency. *Nuclear Physics and Atomic Energy*, 4(14), 356–362. DOI 10.15407/jnpae2013.04.
5. Kondratyk, V., Komarov, Ju., Kosenko, S., & Fedorov, D. (2022) Prevention of hydrodynamic instability conditions in safety systems with pumps of nuclear power plants. *Proceeding of Odessa Polytechnic University*, 1(65), 70–75. DOI 10.15276/opu.1.65.2022.08.
6. Derbenov, H. (2024) *Strategies for controlling the concentration of boron solution in the coolant of nuclear power plants*. LAP LAMBERT Academic Publishing. ISBN 978-620-0-3247-6.
7. Makarenko, A., Chaikovskyi, M., Mazurok, O., Zuyok, V., & Mykhaylenko, O. (2024) Calculation Analysis of VVER-1000 RCCA Elements to Justify Lifetime Extension. *Nuclear and Radiation Safety*, 3, 26–35. DOI 10.32918/nrs.2024.3(103).03.
8. Kukhotskyi, O., Gumeniuk, D., Ligotskyy, O., Potoskuiev, O., Shyshuta, A., & Ostapovets, A. (2024) Requirements for Maintenance of Equipment in Systems Important to Safety of Nuclear Power Plants. *Nuclear and Radiation Safety*, 3, 52–59. DOI 10.32918/nrs.2024.3(103).06.
9. Hrybanov, V. (2025) *Strength qualification of bridge crane of nuclear power plants*. LAP LAMBERT Academic Publishing. ISBN 978-613-58350-8.
10. Smith, C.L., Le Blanc, K., & Mandelli, D. (Ed.) (2023) *Risk-informed methods and applications in nuclear and energy engineering: modelling, experimentation, and validation*. Elsevier Inc., Academic Press. DOI 10.1016/C2020-0-04468-3

Скалозубов Володимир Іванович; Volodymyr Skalozubov, ORCID: https://orcid.org/0000-0003-2361-223X
Дербеньов Гліб Сергійович; Hlib Derbenov**,** ORCID: https://orcid.org/0009-0005-1881-2853
Кацарський Юрій Сергійович; Iurii Katsarskyi,Номер ORCID: https://orcid.org/0009-0001-9932-2880
Мазур Євгеній Вікторович; Yevhenii Mazur, ORCID: https://orcid.org/0009-0005-0936-4411
Кочнєва Валерія Юріївна; Valeriia Kochnieva, ORCID: https://orcid.org/0000-0001-7397-3573

Received November 01, 2025

Accepted November 29, 2025

ISSN 2076-2429 (print)
ISSN 2223-3814 (online)

UDC 629.031

V. Skalozubov, DSc, Prof.,
Iu. Katsarskyi,
H. Derbenov,
Ye. Mazur,
V. Kochnieva
Odessa Polytechnic National University, Shevchenko Ave. 1, Odesa, Ukraine, 65044, e-mail: valer_nov13@ukr.net

METHODS FOR QUALIFYING THE THERMODYNAMIC STABILITY OF SAFETY VALVES AND STEAM DUMP DEVICES OF NUCLEAR POWER PLANTS

В. Скалозубов, Ю. Кацарський, Г. Дербеньов, Є. Мазур, В. Кочнєва. **Методи кваліфікації термодинамічної стійкості запобіжних клапанів та пароскидальних пристроїв ядерних енергоустановок.** Аналіз відомих розробок у напрямках аналізу надійності запобіжних клапанів і пароскидальних пристроїв реактора та парогенераторів ядерних енергоустановок з ВВЕР встановив необхідність розрахункової кваліфікації запобіжних клапанів і пароскидальних пристроїв в умовах аварійних режимів, які не передбачені експлуатаційними випробуваннями ядерних енергоустановок. Одним з таких питань є визначення умов імпульсної та коливальної термодинамічної нестійкості запобіжних клапанів і пароскидальних пристроїв у аварійних режимах. Наслідками термодинамічної нестійкості може бути порушення виконання критичних функцій безпеки в умовах управління аваріями. Експериментальна кваліфікація запобіжних клапанів і пароскидальних пристроїв в аварійних умовах не є можливою, тому потрібна розрахункова кваліфікація. Необхідність розрахункової кваліфікації також актуальна у зв'язку з перспективними програмами експлуатації реакторів в умовах підвищеної тривалості паливних кампаній, в яких зменшується кількість випробувань пасивних систем безпеки у планові ремонти енергоблоків. Розроблено метод кваліфікації пропускної спроможності запобіжних клапанів і пароскидальних пристроїв пасивних систем безпеки ядерних енергоустановок в умовах імпульсної та коливальної термодинамічної нестійкості. Встановлено необхідну умову імпульсної термодинамічної нестійкості – формування трансзвукового режиму потоку робочого середовища в конфузорній зоні запобіжних клапанів/пароскидальних пристроїв. Наслідки імпульсної термодинамічної нестійкості – гідродинамічний «удар» внаслідок перетворення кінетичної енергії потоку у внутрішню енергію гідродинамічного «удару» та гальмування потоку. Визначено максимальну амплітуду тиску гідродинамічного «удару» внаслідок імпульсної термодинамічної нестійкості при повному гальмуванні потоку. Встановлено умови і наслідки коливальної термодинамічної нестійкості в дозвукових режимах потоку в проточних зонах запобіжних клапанів/пароскидальних пристроїв на основі фундаментального принципу термодинамічної нестійкості рівноважних систем. На базі розробленого метода кваліфікації пропускної спроможності запобіжних клапанів/пароскидальних пристроїв визначено умови і підходи забезпечення термодинамічної стійкості потоку в проточних зонах запобіжних клапанів/ пароскидальних пристроїв та запобігання гідродинамічним «ударам».

Ключові слова: кваліфікація, пасивна система безпеки, арматура, реактор, парогенератор, термодинамічна стійкість, ядерна енергоустановка

V. Skalozubov, Iu. Katsarskyi, H. Derbenov, Ye. Mazur, V. Kochnieva. **Methods for qualifying the thermodynamic stability of safety valves and steam dump devices of nuclear power plants.** Analysis of known developments in reliability analysis of safety valves and steam dump devices of reactors and steam generators of nuclear power plants with VVER has recognized the need for calculation qualification of safety valves and steam dump devices under emergency conditions that are not provided for operational tests of nuclear power plants. One of such problems is determining the conditions for pulse and oscillatory thermodynamic instability of safety valves and steam dump devices under emergency conditions. The consequences of thermodynamic instability may be a violation of the performance of critical safety functions under accident management conditions. Experimental qualification of safety valves and steam dump devices under emergency conditions is not possible, therefore calculation qualification is required. The need for calculation qualification is also relevant for prospective programs for reactor operation in conditions of extended fuel campaign time, when the number of tests of passive safety systems during scheduled repairs of power units is reduced. A method for qualifying the throughflow capacity of safety valves and steam dump devices of passive safety systems of nuclear power plants under conditions of pulsed and oscillatory thermodynamic instability has been developed. A necessary condition for pulsed thermodynamic instability has been established. It is the formation of a transonic flow regime of the operating medium in the confusion zone of safety valves/steam dump devices. The consequences of pulsed thermodynamic instability are water "hummer" due to the conversion of kinetic energy of the flow into the internal energy of the water "hummer" and flow stagnation. The maximum pressure amplitude of the water "hummer" due to pulsed thermodynamic instability with complete flow stagnation has been determined. The conditions and consequences of oscillatory thermodynamic instability in subsonic flow regimes in the flow zones of safety valves/steam dump devices have been found based on the fundamental principle of thermodynamic instability of equilibrium systems. Based on the developed method for qualifying the throughflow capacity of safety valves/steam dump devices, the conditions and approaches for ensuring thermodynamic flow stability in the flow zones of safety valves/steam dump devices and preventing water "hummers" have been determined.

Keywords: qualification, passive safety system, armature, reactor, steam generator, thermodynamic stability, nuclear power plant

Introduction

Safety valves and spray devices of safety systems of nuclear power plants (NPP) are designed to prevent the destruction of equipment enclosures and pipelines of systems important for safety, as well as, if necessary, for accident management [1 – 5].

The safety valves of the pulse-safety device of the pressure compensator ensure the integrity of the reactor vessel and internal vessel devices at a pressure in the reactor circuit greater than the maxi-

DOI: 10.15276/opu.2.72.2025.08

mum permissible value.

Safety valves of steam generators ensure the integrity of the body and internal devices of the steam generator at a pressure in the volume of the steam generator greater than the maximum permissible value.

Steam boilers of steam generators (high-speed reduction units for discharging steam from the steam generator to the environment/turbine condenser) regulate the pressure in the volume of the steam generator during emergency modes.

The main mode of operation of safety valves/vaporizers of safety systems is the "standby" mode of performing the necessary safety functions. Therefore, the technological regulations for the safe operation of nuclear power plants with VVER [2] provide for experimental qualification (justification) of operability and reliability of safety valves/vapor discharge devices of safety systems when performing the necessary safety functions by periodic operational tests during the periods of planned preventive maintenance (PM) of NPP power units.

The need to conduct operational tests of safety valves/vapor discharge devices of safety systems only during PM is due to the fact that the operation of safety valves/vapor discharge devices during operational tests actually corresponds to "artificial" emergencies with leaks in the reactor circuit and in the volume of the steam generator in the operating modes of the nuclear power plant.

The conditions for conducting operational tests by opening safety valves/vapor dumping devices during the PM may generally not correspond to the real conditions of emergency modes. For example, operational tests for opening safety valves/steam discharge devices of a steam generator during the PM are carried out on a steam-air environment. In the event of an accident with intercircuit leaks of the coolant into the volume of the steam generator, it may be necessary to qualify the reliable throughput of the safety valves/vapor discharge devices of the steam generator in the conditions of liquid phase or two-phase flow entering the working bodies of the safety valves/vapor discharge devices. Another typical example is related to the consequences of the accident at the Rivne NPP in 2009 during operational tests of the safety valves of the pulse-fuse device of the pressure compensator during the PM in the reactor hot shutdown mode. In the process of operational tests, after opening the safety valves of the pulse-fuse device of the pressure compensator, there was a failure to close the safety valves, which led to the release of the coolant under the nominal pressure into the pressurized volume of the nuclear power plant.

Thus, it is relevant to develop analytical (calculated) methods for qualifying the operability and reliability of safety valves/steam dumping devices of safety systems in conditions as close as possible to emergency modes of nuclear power plants.

The prospects for the nuclear power industry of Ukraine to switch to an 18-month fuel campaign of nuclear power plants with VVER also determine both the need to modernize the strategy of operational tests of safety valves/vapor discharge devices during the PM, and the development of analytical methods for the qualification of safety valves/vapor discharge devices of safety systems.

In the presented paper, a new deterministic method for qualifying the throughput capacity of safety valves/steam discharge devices of safety systems of nuclear power plants under conditions of thermodynamic instability has been developed.

Analysis of known literature data and problem statement

Most of the works on the study of the influence of hydrodynamic "shocks" on the throughput of valves (analytical reviews of these works are given, for example, in [1 – 4] are based on the well-known formula of M.E. Zhukovsky for determining the maximum amplitude of water hammer ΔP_g at complete flow braking:

$$\Delta P_{\text{g}} \le \rho_{\text{l}} a_{\text{l}} v_{\text{l}}, \tag{1}$$

where ρ_{l} – Fluid density; a_{l} – Speed of sound; v_{l} – flow rate to water hammer.

Analysis of the validity of formula (1) for the conditions of safety valves/vapor dispensing devices allows us to make the following basic comments.

1. Formula (1) takes into account only the effect of fluid compressibility (parameter a_l) on ΔP_{g}. However, the dominant effect during a water hammer may be the conversion of the kinetic energy of the flow into the internal energy of the water hammer impulse [5].

2. Formula (1) does not generally determine the causes and conditions of water hammer [7].

In works [6, 7, 8], water hammer in the channels of active safety systems of nuclear power plants was modelled as a result of hydrodynamic oscillatory instability of flow in transitional modes of pump

ISSN 2076-2429 (print)
ISSN 2223-3814 (online)

start-up. These works established that the occurrence of water hammer due to hydrodynamic flow instability is determined by the inertia of the "delayed" response of the pressure-flow characteristics of pumps to sufficiently "rapid" changes in flow rates in transient modes.

However, the causes and conditions of water hammer due to hydrodynamic instability of flows in the flow zones of safety valves/vapor dispensers of passive safety systems may differ significantly from the corresponding conditions in the channels of active safety systems (with pumps).

In the papers [9,10], the issues of conditions and consequences of high-frequency thermodynamic instability of the coolant (thermoacoustic instability) in the reactor core were studied. It has been established that the conditions for the occurrence of thermoacoustic instability are the inertia of heat-mass exchange processes of vapor phase condensation in acoustic disturbances (waves) of the coolant. Under conditions of thermoacoustic instability in the core of the VVER reactor, the maximum amplitudes of pressure fluctuations can reach 50% of the average value, and the fundamental frequency of oscillations (1st harmonic) is several hundred Hertz. At such parameters of thermoacoustic instability, high-frequency and high-amplitude hydrodynamic actions (water hammers) occur on the reactor in-vessel devices (including fuel rods).

However, the causes and conditions of thermodynamic instability in the reactor core can differ significantly from the conditions for the occurrence of thermodynamic instability in the flow zones of safety valves/steaming devices.

Thus, it is relevant to develop deterministic methods for analyzing the conditions and consequences of water hammer due to various types of thermodynamic instability in the systems of safety valves/vapor dumping devices.

The aim of the study is to develop a method for assessing the reliability of safety valves and steam release devices in VVER nuclear power plant safety systems under conditions of thermodynamic instability.

Main tasks

1. Analysis of known approaches/methods for qualifying the reliability of systems important for nuclear reactor safety.

2. Development of the main provisions of an alternative method for qualifying the reliability of safety valves and steam release devices under conditions of thermodynamic instability.

3. Analysis of the results obtained and practical recommendations.

Method for qualifying the flow capacity of safety valves/steam traps

Key assumptions and assumptions:

1. The flow zone model of safety valves/steam traps is conditionally divided into a confuser zone (*K*), a working body zone (*O*) and a diffuser zone (*D*) (Fig. 1*a*).

2. Conditions of thermodynamic instability are modelled in two modes of working medium flow in the flow zones of safety valves/steam traps:

– transonic flow mode in the confluence zone (Fig. 1*b*);

– subsonic flow mode (Fig. 1*c*).

3. In the confluence zone, the average flow velocity v increases due to a decrease in the cross-sectional area $F(z)$ and reaches its maximum value in the working body zone (*O*). Pressure P decreases due to an increase in flow velocity and reaches its minimum value in the working body zone.

4. When the flow velocity v is reached in zone *O*, the sound velocity v_a (the speed of propagation of acoustic disturbances in the flow) creates conditions for transonic flow of the working medium in safety valves/steam traps (see Fig. 1*b*) [1, 2, 3]:

$$M(z = L_{\text{K}}) = \frac{v(z = L_{\text{K}})}{v_a(z = L_{\text{K}})} \geq 1, \tag{2}$$

where M – Mach criterion, L_{K} – confusion zone length.

When the transonic regime condition (2) is reached, impulse flow deceleration occurs and conditions for a water hammer with an impulse pressure increase arise, and the kinetic energy of flow deceleration is converted into the energy of the water hammer impulse [10]. Consequences of transonic flow regime – conditions of water hammer due to impulsive thermodynamic instability and corresponding impulsive reduction in the throughput capacity of safety valves/steam traps.

5. At subsonic flow regimes of the working medium (M<1), conditions of oscillatory thermodynamic instability may arise in the flow zones of safety valves/steam blowdown devices (see Fig. 1*c*).

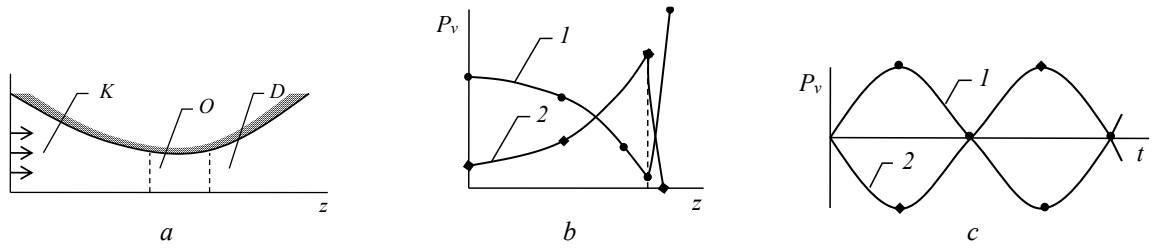

Fig. 1. Models of impulse thermodynamic and oscillatory thermodynamic instability in safety valves/steam traps: safety valve/steam trap model (*a*): *K* – confuser zone, *O* – working body zone, *D* – diffuser zone; model of impulse thermodynamic instability (*b*) and oscillatory thermodynamic instability (*c*): *1* – pressure *P*, *2* – velocity *v*

The conditions for the occurrence of oscillatory thermodynamic instability in the flow zones of safety valves/steam blowdown devices are determined based on the fundamental principle of thermodynamic instability of systems in equilibrium [1 – 6]:

$$\frac{\delta P}{\delta v} > 0\,, \tag{3}$$

where δP, δv – simultaneous deviation from the equilibrium state of pressure and flow velocity in the system.

Pressure and velocity fluctuations occur in antiphase (see Fig. 1*b*), and the frequency of fluctuations ω [1, 2, 3]:

$$\omega \sim v / L_0\,, \tag{4}$$

where L_0 – total length of the flow zone of the safety valve/steam trap.

The occurrence of oscillatory thermodynamic instability violates the conditions of normal throughput capacity of safety valves/steam release devices, and in extreme cases can lead to pulsating thermodynamic instability with complete flow inhibition.

Based on the presented provisions, the conditions for thermodynamic stability of the throughput capacity of safety valves/steam release devices:

$$M(z = L_{\text{K}}) < 1\,, \tag{5}$$

$$\frac{\delta P}{\delta v} < 0\,. \tag{6}$$

Under conservative assumptions of no irreversible thermal and hydraulic losses in the confuser zone, the equations of conservation of mass, momentum, and energy in the format of parameters distributed along the length of the K-zone in a steady-state homogeneous condition [1, 2, 3]:

$$\frac{d(\rho\, v\, F)}{dz} = 0\,, \tag{7}$$

$$\frac{d(\rho\, v^2\, F)}{dz} = \frac{d(PF)}{dz}\,, \tag{8}$$

$$\frac{d(\rho\, i\, F)}{dz} = \frac{d(PF)}{dz}\,, \tag{9}$$

where $\rho = \rho_{\text{l}} - (\rho_{\text{l}} - \rho_v)\varphi$, ρ_{l}, ρ_v – density of liquid and vapour phases, $\varphi = i - i_{\text{l}}/(i_{\text{v}} - i_{\text{l}})$ – vapour content parameter, i, i_{l}, i_{v} – specific enthalpy of flow, liquid and vapour phases, P – pressure, v – average flow rate, $F(z)$ – area of the confluent zone's passage cross-section, z – longitudinal coordinate.

After transformations (6) – (8), we obtain:

$$a_1 \frac{dv}{dz} + a_2 \frac{dP}{dz} + a_3 \frac{di}{dz} + a_4 \frac{dF}{dz} = 0\,, \tag{10}$$

$$b_1 \frac{dv}{dz} + b_2 \frac{dP}{dz} + b_3 \frac{di}{dz} + b_4 \frac{dF}{dz} = 0\,, \tag{11}$$

ISSN 2076-2429 (print)
ISSN 2223-3814 (online)

$$c_1 \frac{di}{dz} + c_2 \frac{dP}{dz} + c_3 \frac{dF}{dz} = 0, \tag{12}$$

where $a_1 = \rho F$, $a_2 = vF/v_a^2$, $a_3 = vF\partial\rho/\partial i$, $a_4 = \rho v$, $b_1 = 2v\rho F$, $b_2 = (M^2 - 1)F$, $b_3 = v^2 F\partial_\rho/\partial_i$, $b_4 = \rho v^2 - P$, $c_1 = \rho F + iF\partial\rho/\partial_i$, $c_2 = iF/v_a^2 - F$, $c_3 = b_4$, $v_a^2 = dP/d\rho$ [1].

After transforming equations (10) – (12), the system of nonlinear differential equations in dimensionless format:

$$\frac{dv}{dz} = \mathbf{K}_v[\mathbf{v}(z), \mathbf{P}(z), \mathbf{i}(z), \mathbf{F}(z)], \tag{13}$$

$$\frac{dP}{dz} = \mathbf{K}_P[\mathbf{v}(z), \mathbf{P}(z), \mathbf{i}(z), \mathbf{F}(z)], \tag{14}$$

$$\frac{di}{dz} = \mathbf{K}_v[\mathbf{v}(z), \mathbf{P}(z), \mathbf{i}(z), \mathbf{F}(z)], \tag{15}$$

$$\mathbf{v}(z=0)=1, \tag{16}$$

$$\mathbf{P}(z=0)=1, \tag{17}$$

$$\mathbf{i}(z=0)=1, \tag{18}$$

where $\mathbf{v} = v / v_0$, $\mathbf{P} = P / P_0$, $\mathbf{i} = i / i_0(\varphi_0)$, $\mathbf{z} = z / L_\text{K}$, v_0, P_0, i_0, φ_0 – working medium flow parameters at the inlet to the flow zone of safety valves/steam traps.

Solutions to equations (13)–(18) in general form:

$$\mathbf{v}(L_\text{K}) = 1 + \int_0^{L_\text{K}} \mathbf{K}_v dz, \tag{19}$$

$$\mathbf{P}(L_\text{K}) = 1 + \int_0^{L_\text{K}} \mathbf{K}_P dz, \tag{20}$$

$$\mathbf{i}(L_\text{K}) = 1 + \int_0^{L_\text{K}} \mathbf{K}_i dz. \tag{21}$$

Then the conditions for impulsive thermodynamic instability (2):

$$\int_0^{L_\text{K}} \mathbf{K}_v dz \geq \mathbf{v}_a - 1, \tag{22}$$

where $\mathbf{v}_a = v_a L_\text{K} / v_0$.

In general, solutions (19) – (22) can be obtained by numerical methods of integrating nonlinear differential equations (13)–(18).

The maximum pressure pulse of the water hammer ΔP_g due to the condition of impulse thermodynamic instability (22) is determined by the conversion of the kinetic energy of flow deceleration rv_a^2 into the energy of the water hammer pulse $\Delta\rho_{ig}$.

In the extreme case (complete flow stoppage):

$$\boldsymbol{\rho}\mathbf{v}_a^2 = \Delta(\boldsymbol{\rho}_1\mathbf{i}_\text{g}) = \frac{d(\boldsymbol{\rho}_1\mathbf{i}_1)}{\mathrm{d}\mathbf{P}}\Delta\mathbf{P}_\text{g}. \tag{23}$$

From (23) follows the maximum pressure pulse of the water hammer:

$$\Delta\mathbf{P}_\text{g} = \left[\frac{d(\boldsymbol{\rho}_1\mathbf{i}_1)}{\mathrm{d}\mathbf{P}}\right]^{-1} \boldsymbol{\rho}\mathbf{v}_a^2. \tag{24}$$

Formula (24) for determining the maximum pressure pulse of a water hammer due to impulsive thermodynamic instability in safety valves/steam traps differs significantly from the corresponding Zhukovsky formula (1).

The conditions for impulse thermodynamic stability in safety valves/steam release devices follow from (22):

$$\int_0^{L_K} \mathbf{K}_v d\mathbf{z} < \mathbf{v}_a - 1. \tag{25}$$

The conditions for oscillatory thermodynamic instability in the flow zone of safety valves/steam traps are determined for subsonic conditions.

Equations of motion and energy conservation in the flow zones of safety valves/steam traps in equilibrium [1, 2, 3]:

$$P_0 - P_A = \xi \frac{G^2}{\rho F_{\min}^2} = 0\,, \tag{26}$$

$$G(i_0 - i_A) = \xi \rho^{-1} L_0 G^2, \tag{27}$$

where $G = \rho v F_{\min}$ – mass flow rate of the working medium, $F_{\min}$ – minimum cross-sectional area in the flow section of safety valves/steam traps, ξ – parameter (hydraulic resistance coefficient), L_0– total length of the flow section of safety valves/steam traps, P_A, i_A – pressure and specific enthalpy of the working medium at the outlet of safety valves/steam traps.

When assuming $\partial(P_0 - P_A)/\partial G = \partial(P_0 - P_A)/\partial P = 0$ equations (26) and (27) in the format of simultaneous fluctuation-independent deviations $\delta G << G$ and $\delta P << P$:

$$A_1 \delta P = A_2 \delta G, \tag{28}$$

$$B_1 \delta P = B_2 \delta G, \tag{29}$$

where:

$$A_1 = G \frac{d(\rho^{-1})}{dP}, \tag{30}$$

$$A_2 = -2G\rho^{-1}, \tag{31}$$

$$B_1 = G(i_0 - i_A) - \xi L_0 G^2 \frac{d(\rho^{-1})}{dP}, \tag{32}$$

$$B_2 = 2\xi \rho^{-1} L_0 G - (i_0 - i_A). \tag{33}$$

Equations (28) and (29) give rise to the conditions for the oscillatory thermodynamic stability of safety valves/steam traps [1 – 6].

$$\frac{\partial P}{\partial G} = \frac{A_2}{A_1} < 0\,, \tag{34}$$

$$\frac{\partial P}{\partial G} = \frac{B_2}{B_1} < 0\,. \tag{35}$$

Analysis of the results obtained

1. The obtained conditions for thermodynamic stability of the working medium in the passage zone (25), (34), (35), which ensure the necessary throughput capacity of safety valves/steam blowdown devices, can be determined in general by numerical integration using the Runge–Kutta method for given initial conditions (16)–(18) and design and technical parameters (L_K,L_0,$F(z)$,ξ).

2. Regulation of thermodynamic stability conditions can be ensured by modernising/reconstructing the structural and technical parameters of safety valves/steam traps.

3. The maximum pressure pulse of a water hammer with complete flow braking (lack of throughput capacity of safety valves/steam traps) due to pulsed thermodynamic instability is determined by the conversion of the kinetic energy of the flow into the energy of the water hammer pulse (24). Unlike the well-known Zhukovsky formula (1), the solution obtained takes into account the causes and conditions of water hammer occurrence, as well as the combined effect of energy effects and liquid phase compressibility on the maximum amplitude of water hammer back pressure.

4. Analysis of equations (13) – (15) for forming conditions of water hammer due to impulse thermodynamic instability in the confluence zone of safety valves/steam traps established the following.

ISSN 2076-2429 (print)
ISSN 2223-3814 (online)

The velocity gradient along the length of the confluence zone increases in proportion to the gradient of the cross-sectional area change:

$$\frac{dv}{dz} \sim - \frac{dF}{dz} > 0 . \quad (36)$$

The flow velocity reaches its maximum value in the area with the minimum cross-sectional area $F_{\min}$.

In extreme cases, under certain conditions, the flow velocity reaches the speed of sound at this intersection (see Fig. 1*b*):

$$M = v / v_a = 1 . \quad (37)$$

Pressure gradient along the length of the confluence zone:

$$\frac{dP}{dz} \sim \frac{-(dv/dz)}{(1 - M^2)} < 0 , \quad (38)$$

when transonic mode is reached (37) according to (38), there is a sudden increase in back pressure in the $F_{\min}$ cross-section (water hammer condition) and a corresponding deceleration of the flow (see Fig. 1*b*).

In the extreme case of complete flow deceleration, the maximum amplitude of the counterpressure pulse can be determined using formula (24).

5. The conditions of oscillatory thermodynamic instability in subsonic flow regimes are determined by the effects of simultaneous independent fluctuation deviations (disturbances) in pressure δP and flow rate δG on the thermodynamic state of the system.

Let us consider a specific case of simultaneous fluctuation increase in pressure $\uparrow\delta P$ and flow rate $\uparrow\delta G$.

The consequence of $\uparrow\delta P$ in a thermodynamic equilibrium state should be a corresponding decrease in flow rate $\downarrow\delta Gp$. However, in the case of $\uparrow\delta G > |\downarrow\delta Gp|$, the total relative flow rate will increase with a relative increase in pressure – the system is in an unstable thermodynamic equilibrium state (3) and conditions of oscillatory thermodynamic instability arise with an oscillation frequency (4) (see Fig. 1*c*).

In the case of $\uparrow\delta G<|\downarrow\delta Gp|$, the system is in a stable equilibrium thermodynamic state (34), (35) and the amplitudes of the initial fluctuation deviations of the thermodynamic parameters decrease.

In the case of $\uparrow\delta G=|\downarrow\delta Gp|$, the system is at the boundary of the region of oscillatory thermodynamic instability.

Thus, the conditions of thermodynamic stability in subsonic modes are determined by the actual thermodynamic state of the system, which is reflected in the values of parameters A_1, A_2, B_1, B_2 in formulas (34), (35).

Conclusions

1. A method has been developed for qualifying the throughput capacity of safety valves and steam release devices in passive safety systems of nuclear power plants under conditions of pulsating and oscillatory thermodynamic instability.

2. The necessary condition for impulse thermodynamic instability has been established – the formation of a transonic flow regime of the working medium in the confluence zone of safety valves/steam ejectors.

The consequences of pulsed thermodynamic instability are a hydrodynamic "shock" due to the conversion of the kinetic energy of the flow into the internal energy of the hydrodynamic "shock" and the deceleration of the flow. The maximum pressure amplitude of the hydrodynamic "shock" due to pulsational thermodynamic instability at full flow deceleration has been determined.

3. The conditions and consequences of oscillatory thermodynamic instability in subsonic flow regimes in the flow zones of safety valves/steam blowdown devices have been established based on the fundamental principle of thermodynamic instability of equilibrium systems.

4. Based on the developed method for qualifying the throughput capacity of safety valves/steam traps, conditions and approaches have been determined to ensure thermodynamic stability of flow in the flow zones of safety valves/steam traps and to prevent hydrodynamic “shocks”.

Література

1. Mazur Ye. Passive systems safety of nuclear power plants. LAP LAMBERT Academic Publishing, 2024. 227p. ISBN 978-620-8-41532-7.
2. . Підвищення безпеки ядерної енергетики з урахуванням уроків важких аварій / Кондратюк В. А., Письменний Є. М., Вєрінов О. М., Філатов В. І., Остапенко А. І. *Ядерна та радіаційна безпека*. 2022. № 3. С. 76–81. DOI: https://doi.org/10.32918/nrs.2022.3(95).08.
3. Комаров Ю. О. Результати досліджень деяких питань безпеки та ефективності експлуатації АЕС ризик-орієнтованими методами. *Ядерна фізика та енергетика*. 2013. Т. 14, № 4. С. 356–362. DOI: https://doi.org/10.15407/jnpae2013.04.
4. Комплекс методов переоценки безопасности атомной энергетики Украины с учетом уроков экологических катастроф в Чернобыле и Фукусиме / Под ред. Г. А. Оборского. Одесса : Астропринт, 2013. 244 с.
5. The method of express analysis of nuclear and ecological safety during the modernization of nuclear fuel / Skalozubov V. I., Melnik S. I., Vashchenko V. M., Korduba I. B., Hrib V. Yu. *Journal of Geology, Geography and Geoecology*. 2023. V. 32, No. 2. P. 388–395. DOI: https://doi.org/10.15421/112335.
6. Дербеньов Г. Стратегії контролю концентрації борного розчину теплоносія ядерних енергоустановок. LAP LAMBERT Academic Publishing, 2024.86 с. ISBN 978-620-0-3247-6.
7. Calculation Analysis of VVER-1000 RCCA Elements to Justify Lifetime Extension / Makarenko A., Chaikovskyi M., Mazurok O., Zuyok V., Mykhaylenko O. *Nuclear and Radiation Safety*. 2024. № 3. С. 26–35. DOI: https://doi.org/10.32918/nrs.2024.3(103).03.
8. Вимоги до технічного обслуговування і ремонту обладнання систем, важливих для безпеки атомних станцій / Кухоцький О. В., Гуменюк Д. В., Лігоцький О. І., Потоскуєв В. С., Шишута А. М., Остаповець А. О. *Ядерна та радіаційна безпека*. 2024. № 3. С. 52–59. DOI: https://doi.org/10.32918/nrs.2024.3(103).06.
9. Грибанов В. Кваліфікація міцності мостового крана ядерних енергоустановок. LAP LAMBERT Academic Publishing, 2025. 43 с. ISBN 978-613-58350-8.
10. Risk-informed methods and applications in nuclear and energy engineering: modelling, experimentation, and validation / Ed. by C. L. Smith, K. Le Blanc, and D. Mandelli. Elsevier Inc., Academic Press, 2023. 386 p. DOI: https://doi.org/10.1016/C2020-0-04468-3.

References

1. Mazur, Ye. (2024). *Passive systems safety of nuclear power plants*. LAP LAMBERT Academic Publishing. ISBN 978-620-8-41532-7.
2. Kondratyuk, V., Pysmennyy, Y., Verinov, O., Filatov, V., & Ostapenko, I. (2022). Improvement of nuclear safety taking into account the lessons learned from severe accidents. *Nuclear and Radiation Safety*, 3, 76–81. DOI: 10.32918/nrs.2022.3(95).08.
3. Komarov, Yu. (2013). Some research results by risk-inform approaches for NPP safety and operational efficiency. *Nuclear Physics and Atomic Energy*, 4(14), 356–362. DOI: 10.15407/jnpae2013.04.
4. Oborskyi, H.O. (Ed.) (2013). *A set of methods for reviewing the safety of nuclear energy in Ukraine, taking into account the lessons of environmental disasters in Chernobyl and Fukushima*. Odessa: Astroprint.
5. Skalozubov, V.I., Melnik, S.I., Vashchenko, V.M., Korduba, I.B., & Hrib, V. Yu. (2023). The method of express analysis of nuclear and ecological safety during the modernization of nuclear fuel. *Journal of Geology, Geography and Geoecology*, 2(32), 388–395. DOI: 10.15421/112335.
6. Derbenov, H. (2024). *Strategies for controlling the concentration of boron solution in the coolant of nuclear power plants*. LAP LAMBERT Academic Publishing. ISBN 978-620-0-3247-6.
7. Makarenko, A., Chaikovskyi, M., Mazurok, O., Zuyok, V., & Mykhaylenko, O. (2024). Calculation Analysis of VVER-1000 RCCA Elements to Justify Lifetime Extension. *Nuclear and Radiation Safety*, 3, 26–35. DOI: 10.32918/nrs.2024.3(103).03.

ISSN 2076-2429 (print)
ISSN 2223-3814 (online)

8. Kukhotskyi, O., Gumeniuk, D., Ligotskyy, O., Potoskuiev, O., Shyshuta, A., & Ostapovets, A. (2024). Requirements for Maintenance of Equipment in Systems Important to Safety of Nuclear Power Plants. *Nuclear and Radiation Safety*, 3, 52–59. DOI: 10.32918/nrs.2024.3(103).06.
9. Hrybanov, V. (2025). *Strength qualification of bridge crane of nuclear power plants*. LAP LAMBERT Academic Publishing. ISBN 978-613-58350-8.
10. Smith, C.L., Le Blanc, K., & Mandelli, D. (Ed.) (2023). *Risk-informed methods and applications in nuclear and energy engineering: modelling, experimentation, and validation*. Elsevier Inc., Academic Press. DOI: 10.1016/C2020-0-04468-3.

Скалозубов Володимир Іванович; Volodymyr Skalozubov, ORCID: https://orcid.org/0000-0003-2361-223X
Кацарський Юрій Сергійович; Iurii Katsarskyi, ORCID: https://orcid.org/0009-0001-9932-2880
Дербеньов Гліб Сергійович; Hlib Derbenov, ORCID: https://orcid.org/0009-0005-1881-2853
Мазур Євгеній Вікторович; Yevhenii Mazur, ORCID: https://orcid.org/0009-0005-0936-4411
Кочнєва Валерія Юріївна; Valeriia Kochnieva, ORCID: https://orcid.org/0000-0001-7397-3573

Received November 10, 2025
Accepted December 12, 2025

UDC 621.43.068:006.83:339.138(477)

N. Orekhovskaya,
Yu. Shikhireva, PhD
Separate structural subdivision Odessa Automobile and Road Professional College National University "Odessa Polytechnic", Tiraspolska Str. 6, Odesa, Ukraine, 65045, e-mail: juliashikhirrva@gmail.com

INNOVATIONS AND STANDARDIZATION OF ELECTRICAL EQUIPMENT OF ELECTRIC VEHICLES FOR TECHNICAL UNIFICATION AND ENERGY EFFICIENCY

Н. Ореховська, Ю. Шихірева. **Інновації та стандартизація електрообладнання електромобілів для технічної уніфікації та енергоефективності.** Стаття присвячена аналізу проблем і перспектив стандартизації електрообладнання електромобілів, що забезпечує технічну сумісність, енергоефективність і зниження собівартості виробництва. Досліджено міжнародні стандарти, які регулюють системи живлення, зарядну інфраструктуру, протоколи зв'язку та захист від кібератак. Основними викликами є регіональні відмінності в стандартах, різноманітність протоколів зв'язку, вразливості до кіберзагроз і фрагментація технологій бездротової зарядки. У контексті України обмежена інфраструктура зарядних станцій, воєнні ризики та пільги на імпорт компонентів створюють унікальні можливості для розвитку локального виробництва. Запропоновано підходи до гармонізації стандартів, зокрема впровадження єдиних технічних вимог і технологій взаємодії транспортних засобів із електромережею, що сприяють інтеграції штучного інтелекту для оптимізації зарядки. Уніфікація стандартів може знизити собівартість виробництва електрообладнання на 15–20%, підвищити енергоефективність і розширити доступність зарядної інфраструктури. В Україні гармонізація стандартів сприятиме залученню інвестицій, розвитку сталого ринку електромобілів і покращенню споживчого сприйняття. Перспективи включають створення єдиної мережі зарядних станцій, сумісної з міжнародними стандартами, що стимулюватиме зростання електромобільної галузі та інтеграцію з європейськими ринками. Стаття підкреслює необхідність співпраці між виробниками, урядом і міжнародними організаціями для подолання технічних і ринкових бар'єрів, що є ключовим для масштабування електромобільності в Україні та світі.

Ключові слова: електромобільність, стандартизація, уніфікація, електрообладнання, зарядна інфраструктура, енергоефективність, кібербезпека, локальне виробництво, ринок електромобілів, гармонізація стандартів

N. Orekhovska, Y. Shikhireva. **Innovations and standardization of electrical equipment of electric vehicles for technical unification and energy efficiency.** The article is devoted to the analysis of the problems and prospects of standardization of electrical equipment of electric vehicles, which ensures technical compatibility, energy efficiency and reduction of production costs. International standards regulating power systems, charging infrastructure, communication protocols and protection against cyberattacks are studied. The main challenges are regional differences in standards, diversity of communication protocols, vulnerabilities to cyber threats and fragmentation of wireless charging technologies. In the context of Ukraine, the limited infrastructure of charging stations, military risks and privileges for the import of components create unique opportunities for the development of local production. Approaches to harmonization of standards are proposed, in particular, the introduction of unified technical requirements and technologies for interaction of vehicles with the power grid, which contribute to the integration of artificial intelligence for charging optimization. Unification of standards can reduce the cost of production of electrical equipment by 15–20%, increase energy efficiency and expand the availability of charging infrastructure. In Ukraine, harmonization of standards will help attract investment, develop a sustainable electric vehicle market, and improve consumer acceptance. Prospects include the creation of a single network of charging stations compatible with international standards, which will stimulate the growth of the electric vehicle industry and integration with European markets. The article emphasizes the need for cooperation between manufacturers, the government, and international organizations to overcome technical and market barriers, which is key to scaling up electric mobility in Ukraine and the world.

Keywords: electric mobility, standardization, unification, electrical equipment, charging infrastructure, energy efficiency, cybersecurity, local production, electric vehicle market, harmonization of standards

Introduction

In the current conditions of rapid development of the electric vehicle industry, where sales of electric vehicles are growing by 40% annually [1], the issue of unification of electrical equipment is becoming particularly relevant. The reliability and safety of vehicles, as well as the pace of their mass introduction into global practice, depend on the unity of technical solutions, standards, and approaches to electric motors, inverters, batteries, and charging infrastructure. Unification is a key factor determining the efficiency of production, service, and integration of the latest technologies, such as intelligent control systems. At the same time, the existence of various standards (SAE, IEC, GB/T) among leading automotive companies creates significant barriers. Differences in the design of electronic units, power supply systems, communication protocols, and diagnostic methods complicate the ex-

DOI: 10.15276/opu.2.72.2025.09

ISSN 2076-2429 (print)
ISSN 2223-3814 (online)

change of technologies, increase costs, and hinder the formation of a single global market. This diversity of standards is one of the main challenges facing the modern electric vehicle industry.

Analysis of literature data and problem statement

The main idea of the article is that the standardization of electric vehicle equipment, including batteries, electric motors, inverters, control systems, and charging infrastructure, is a critical factor in ensuring energy efficiency, reducing production costs by 15…20%, [1], and accelerating the global adoption of electric vehicles.

The unification of standards such as SAE J3400 (NACS), IEC 62196, and ISO 15118 allows regional barriers to be overcome, ensures the compatibility of electromechanical components, and optimizes the integration of innovative technologies such as V2G (Vehicle-to-Grid – two-way energy exchange between an electric vehicle and the power grid) and AI-based diagnostic systems (Artificial Intelligence) [2, 3].

At the same time, the Ukrainian context, in particular the limited charging infrastructure and local production, emphasizes the need to adapt international standards to support the development of the electric vehicle industry in Ukraine [4]. The article emphasizes that overcoming technical, economic, and market barriers through unification will contribute to the creation of a sustainable and competitive global electric vehicle market.

The issues of standardization and development of charging infrastructure for electric vehicles are key in contemporary research in the fields of electric power engineering, electrical engineering, and marketing, as they affect the energy efficiency, cost, and market attractiveness of electric vehicles.

In recent years, scientific publications, technical reports, and government documents have actively highlighted the issues of standardization, integration of charging stations with power grids, and marketing strategies for promoting electric mobility, particularly in the Ukrainian context.

Wajdi W. and Chakir A. [2] analyze charging standards (IEC 61851, IEC 62196) and their impact on integration with power grids, emphasizing that the unification of connectors and communication protocols (OCPP, ISO 15118) reduces infrastructure costs by 10…15% and increases its accessibility.

Kakkar R. et al. [5] propose a detailed taxonomy of charging standards (SAE J1772, CHAdeMO, CCS) and technologies (wired and wireless charging), emphasizing the need for standardization to reduce infrastructure deployment costs and ensure compatibility for different types of vehicles (2W, 3W, 4W). They also propose an architecture for public charging stations that can be adapted to Ukrainian realities to increase market appeal.

Funke S.Á. et al. [6] emphasize that the incompatibility between CCS and CHAdeMO complicates the marketing of electric vehicles due to infrastructure fragmentation, increasing costs by 10…20% and causing confusion among consumers.

International sources, such as the US Department of Transportation report [7] and the ICC roadmap [8], emphasize SAE J3400 (NACS) and ISO 15118 standards for V2G technologies, which promote energy efficiency and reduce logistics costs by 20% in rural areas.

Lieven T. [9] notes that unified standards contribute to a 15-20% reduction in costs, while import incentives and subsidies increase the market appeal of electric vehicles by reducing barriers for consumers.

Ukrainian scientists Davydov V.O. and Stafidov E.B. [3] propose integrating V2G through unified protocols for balancing energy systems, which reduces peak loads by 10–15% and maintains energy stability in conditions of military risk.

O.V. Stetsyuk et al. [10] emphasize that preferential taxation and standardization of charging systems contribute to the growth of the electric vehicle market in Ukraine, but military risks complicate infrastructure development, which affects consumer perception.

Zakharchenko Yu.V. et al. [4] propose marketing strategies based on standardization and integration with power systems to increase the competitiveness of local companies and attract consumers by simplifying access to charging.

Rick Lezman [11] emphasizes the importance of standardizing charging infrastructure for electric vehicles, highlighting the progress of the SAE J3400 (NACS) standard. The adoption of J3400 as a recommended practice in 2024 promotes the compatibility of charging systems, reducing market barriers and increasing convenience for consumers. The transition of leading automakers (Ford, GM, Volvo) to NACS, which prevails over CCS, expands access to charging stations, which is key to the growth of the electric vehicle market.

This echoes the work of Stetsyuk O.V. et al. and Zakharchenko Y.V. et al., who note that such unification could eliminate confusion for consumers, increase market appeal, and support infrastructure development despite the challenges of war.

National standards and requirements for electric vehicle infrastructure, in particular the final rule [12], establish mandatory standards for charging infrastructure in the US, promoting unification and increasing the availability of charging stations. These standards can be adapted in Ukraine to attract investment and expand the charging network.

Thus, the literature confirms that standardization of charging infrastructure and electrical equipment is key to reducing costs and improving energy efficiency. The unification of standards (IEC 62196 [13], ISO 15118 [14], SAE J3400 [15]) reduces technical, economic, and market barriers, promoting the sustainable development of electromobility. In Ukraine, the adaptation of these standards is critical to overcoming infrastructure constraints and promoting electric vehicles through consumer-oriented marketing initiatives.

Purpose and objectives of the study

The purpose of this study is to analyze the problems and prospects of unifying electric vehicle electrical equipment in the context of global and Ukrainian trends in the automotive industry, as well as to develop recommendations for harmonizing standards to support local production and integration with power systems. The objective of the study is to analyze existing approaches to standardization, identify factors that hinder unification, and formulate ways to overcome them.

Research materials and methods

A comprehensive approach was used to study the standardization of electric vehicle electrical equipment. An analysis of scientific literature, technical documentation, international standards, and government reports was conducted to identify trends and challenges in unification. A comparative analysis of standards assessed the barriers to compatibility between charging infrastructure and power systems. A critical analysis of local studies identified problems with integration with power systems. Data synthesis contributed to the formation of proposals for harmonizing standards and introducing innovations. Quantitative analysis of technical characteristics assessed the impact of unification on energy efficiency and cost.

Scientific novelty

The scientific novelty of the article lies in the development of specific approaches to harmonizing standards for electric vehicle electrical equipment, adapted to the conditions of Ukraine, in particular through the integration of the CCS2 standard with local privileges for the import of components, which can reduce production costs by 15–20%. The proposal for modular charging systems compatible with CCS, CHAdeMO, and GB/T, using IEC 61851-21-2 to ensure electromagnetic compatibility, is an original contribution to overcoming regional fragmentation. A quantitative assessment of the effect of implementing ISO 15118 for V2G technologies, which can reduce peak loads on Ukraine's power systems by 10…15%, adds practical value. In addition, the integration of AI for adaptive battery temperature control with unified protocols, in particular ISO 19363 for wireless charging, represents an innovative approach that takes into account military risks and limited infrastructure, creating a basis for the further development of local electric vehicle production.

Research results

Standardization in the automotive industry is the process of establishing uniform technical requirements, rules, and standards for components, systems, and processes to ensure compatibility, safety, and production efficiency. Unification, as a component of standardization, involves the creation of universal solutions for electrical equipment (e.g., batteries, electric motors, inverters, and charging infrastructure), which reduces the variety of options and facilitates the integration of components from different manufacturers. In the context of electric vehicles, standardization and unification are aimed at

ISSN 2076-2429 (print)
ISSN 2223-3814 (online)

overcoming regional barriers, improving energy efficiency, and reducing costs, thereby contributing to the global development of the industry [2, 8].

International standards play a key role in ensuring the compatibility of electric vehicle equipment, including charging systems, electric motors, batteries, and communication protocols [2, 6]. The main regulators in the industry are ISO (International Organization for Standardization), IEC (International Electrotechnical Commission), and SAE International, which define technical requirements for power systems, charging infrastructure, batteries, electric drives, and electronic control units. In particular:

– ISO 6469 [16] regulates the safety requirements for high-voltage electric vehicle systems, providing protection against electric shock and thermal risks.

– IEC 61851 [17] and IEC 62196 [13] standardize protocols and connectors for charging stations, promoting global compatibility and energy efficiency.

– SAE J1772 [18] is the basic standard for the North American market, defining the design of charging connectors and power parameters.

– ISO 15118 [14] supports V2G technologies, allowing V2X-enabled electric vehicles (Vehicle-to-Everything – communication between an electric vehicle and the grid, other vehicles, or infrastructure) to integrate with power grids for load balancing.

– ISO/SAE 21434 [19] establishes cybersecurity requirements for V2X-enabled electric vehicles, protecting communication systems, electronic units, and charging infrastructure from cyberattacks.

– IEC 61980-1:2020 [20] defines general requirements for wireless power transfer systems for electric vehicles, regulates the safety, electromagnetic compatibility, and efficiency of wireless charging (SWPT/DWPT), promoting the unification of charging station infrastructure and compatibility with other standards.

– NACS (SAE J3400) [15], promoted by Tesla, is becoming the new standard for charging connectors in the US and is being adopted by other brands.

– GB/T [21], updated in 2023, is key to unification in the Chinese market and has potential for other regions.

– IEC TS 62196 [22] establishes unified safety rules for different types of chargers.

Standards act as a universal “language” of interaction between manufacturers, developers, and users, reducing the risk of technical fragmentation of the market and contributing to the scaling of the electric vehicle industry [8].

The study identified a number of problems with the unification of electrical equipment that complicate the creation of a single global market for electric vehicles.

1. Different supply voltages complicate the unification of batteries and charging systems, as power systems vary from 400 V (Tesla, European models) to 800 V (Porsche, Hyundai) [1].

2. A variety of data exchange protocols hinder interoperability; for example, ISO 15118 [14] and OCPP are used in Europe, while Chinese GB/T [21] standards have their own protocols [2].

3. Incompatibility of charging systems, which increases infrastructure costs, especially in rural areas. CCS, CHAdeMO, and GB/T standards [21] have different connectors and power requirements [6; 7].

4. Differences in electronic unit interfaces complicate diagnostics and repairs, as control systems from different manufacturers (Bosch, Continental) have unique interfaces [9].

5. Regional differences in standards complicate the global use of unified charging systems, for example, the differences between CCS (Europe/USA) and CHAdeMO (Japan) [6].

6. Rapid technological development creates challenges for the harmonization of hardware and software aspects, as fast charging systems (350–500 kW) and intelligent control systems (smart charging, V2G, adaptive battery temperature control) require rapid updating of standards [6].

7. Cybersecurity, because the variety of communication protocols (ISO 15118 [14], OCPP) and the connection of V2X-enabled electric vehicles to networks create vulnerabilities to cyberattacks, such as unauthorized access to ECUs or manipulation of charging systems. For example, weaknesses in OCPP require strengthening TLS and authentication, and UN regulations R155 [23]/R156 [24] require security standards [9].

8. Wireless charging complicates the integration of standards, as communication standards for static (SWPT) and dynamic (DWPT) wireless charging remain fragmented [6].

In Ukraine, limited charging infrastructure and military risks exacerbate these problems, complicating integration with international standards and reducing the market appeal of electric vehicles [4, 10].

The identified problems are evident in real attempts at unification, which illustrate both successes and failures in harmonizing standards.

Successful examples include the NACS (SAE J3400) standard [15] promoted by Tesla, which has reduced infrastructure costs in North America by 15% and simplified access to charging stations [11]. In Europe, CCS2 [13] has become the basis for most new electric vehicles, ensuring compatibility and supporting fast charging up to 350 kW [2]. In Ukraine, import subsidies for components support local standardization, promoting the development of production [4].

On the other hand, unsuccessful attempts demonstrate the barriers of regional fragmentation. Funke S.Á. et al. [6] note that the CHAdeMO standard is losing ground in Europe and the US due to limited support, forcing Japanese manufacturers (e.g., Nissan) to adapt models such as the Leaf to CCS, which increases the cost by 10…20%. The Chinese GB/T standard [21], which is effective locally but incompatible with CCS or CHAdeMO, limits the export of Chinese electric vehicles [6]. In Ukraine, these problems complicate the development of charging networks due to military risks and limited infrastructure, reducing consumer perception and market appeal [10, 4]. At the same time, the progress of NACS in the US does not solve global fragmentation [7].

To overcome the identified problems, the following is proposed:

1. Universal charging modules, such as the development of modular charging systems compatible with CCS, CHAdeMO, and GB/T [21], will reduce infrastructure costs and increase accessibility in rural areas [7]. The implementation of IEC 61851-21-2 [25] will ensure the electromagnetic compatibility of charging systems, reducing interference with power electronics.

2. Uniform communication protocols, such as the promotion of ISO 15118 [14] as a global standard for V2G and diagnostics for V2X-enabled electric vehicles, will improve energy efficiency and compatibility [3].

3. Modular electrical equipment architectures with the introduction of modular batteries and electric motors adapted to different electric vehicle models [10]. ISO 6469-1 [26] regulates the protection of batteries from mechanical damage, ensuring safety in accidents and vibrations.

4.Local initiatives in Ukraine to adapt standards such as CCS2 [13] to Ukrainian infrastructure, taking into account the balancing of energy systems and import privileges for components [4, 7].

5. Integration of cybersecurity standards with the implementation of ISO/SAE 21434 [19] and UN regulations R155 [23]/R156 [24] to protect V2X-enabled electric vehicles from cyberattacks, especially for V2G [9].

6. Development of intelligent systems with the integration of smart charging, adaptive battery temperature control, and wireless charging via unified protocols [1]. ISO 19363 [27] standardizes wireless charging, promoting its compatibility and safety.

Unification of electrical equipment, including cybersecurity, can reduce the cost of electric vehicle production by 15…20% through component standardization. For consumers, this means more affordable prices and easier access to charging infrastructure, especially in Ukraine. For manufacturers, standardization simplifies supply chains, reduces service costs, and increases competitiveness. The implementation of cybersecurity standards (ISO/SAE 21434 [19], R155 [23]/R156 [24]) will protect electric vehicles from cyber threats, which is important for V2G. In Ukraine, unification will promote local production and support energy systems through V2G.

Conclusions and recommendations

Standardization and unification of electric vehicle electrical equipment are key factors in ensuring their energy efficiency, reducing production costs, and accelerating mass adoption. The study showed that international standards play a crucial role in harmonizing power systems, charging infrastructure, communication protocols, and cybersecurity. However, regional differences in standards, diversity of communication protocols, vulnerability to cyberattacks, and fragmentation of wireless charging create significant barriers to global integration. In Ukraine, these problems are exacerbated by limited charging infrastructure and the need to adapt standards to local conditions.

The practical significance of unification lies in reducing the cost of electric vehicle production by 15…20% through the standardization of components such as batteries, electric motors, and inverters,

ISSN 2076-2429 (print)
ISSN 2223-3814 (online)

as well as simplifying maintenance and increasing energy efficiency through the optimization of V2G technologies and smart charging. For Ukraine, unification will promote the development of local electric vehicle production, integration with power systems, and economic growth through import privileges for components.

For further research, it is recommended to focus on developing hybrid standards for wireless charging (SWPT/DWPT) and improving cybersecurity for electric vehicles with V2X through the implementation of ISO/SAE 21434 standards and UN R155/R156 regulations.

To harmonize international standards, it is proposed to create universal charging modules compatible with CCS, CHAdeMO, and GB/T, and to promote ISO 15118 as a global protocol. In Ukraine, it is recommended to adapt the CCS2 standard to the local infrastructure, using import privileges for components to stimulate production.

Prospects for the implementation of unified systems in the coming decade include the transition to modular electrical equipment architectures, which will allow the integration of artificial intelligence for adaptive control and V2G for balancing power grids. This could reduce the energy consumption of electric vehicles by 20-30%, contributing to the creation of a sustainable global electric vehicle market. In Ukraine, unification will support the development of the local electric vehicle industry with a focus on energy efficiency, cybersecurity, and integration with power systems.

Література

1. Alanazi F. Electric Vehicles: Benefits, Challenges, and Potential Solutions for Widespread Adoption. *Applied Sciences*. 2023. Vol. 13, No. 10. Article 6016. DOI: https://doi.org/10.3390/app13106016.
2. Wajdi W., Chakir A. Electric vehicles standards, charging infrastructure, and impact on grid integration: A technological review. *Renewable and Sustainable Energy Reviews*. 2019. Vol. 120. Article 109618. DOI: https://doi.org/10.1016/j.rser.2019.109618.
3. Давидов В. О., Стафідов Є. Б. Використання зарядних станцій для електромобілів як спосіб балансування електричного навантаження енергетичних систем. *ISG-Journal*. 2023. № 12. С. 45–52. URL: https://isg-journal.com/isjea/article/download/563/315/570.
4. Маркетинг в електроенергетиці України: проблеми та перспективи ринку зарядних станцій для електромобілів / Ю. В. Захарченко та ін. *Економічний вісник Дніпровської політехніки*. 2025. № 2. С. 79–91. URL: https://doi.org/10.33271/ebdut/90.079.
5. A Review on Standardizing Electric Vehicles Community Charging Infrastructures / R. Kakkar et al. *Applied Sciences*. 2022. Vol. 12, No. 23. Article 12096. DOI: https://doi.org/10.3390/app122312096.
6. How much charging infrastructure do electric vehicles need? A review of the evidence and international comparison / S. Á. Funke et al. *Transportation Research Part D: Transport and Environment*. 2018. Vol. 59. P. 224–242. DOI: https://doi.org/10.1016/j.trd.2018.03.004.
7. Implementation Challenges and Evolving Solutions for Rural Electrification of Electric Vehicle Chargers / U.S. Department of Transportation, Federal Highway Administration. Washington, DC, 2025. 45 p. URL: https://www.transportation.gov/rural/ev/toolkit/ev-benefits-and-challenges/challenges-and-evolving-solutions.
8. Standardization Roadmap for Electric Vehicles / International Code Council. 2023. 68 p. URL: https://share.ansi.org/evsp/ANSI_EVSP_Roadmap_June_2023.pdf.
9. Lieven T. Policy measures to promote electric mobility – A global perspective [Electronic resource]. *Transportation Research Part A: Policy and Practice*. 2015. Vol. 82. P. 165–178. URL: https://doi.org/10.1016/j.tra.2015.09.008.
10. Електромобільність в Україні: реалії розвитку, європейський контекст і вплив воєнного стану / О. В. Стецюк та ін. *Наукові інновації та передові технології*. 2024. № 9(37). С. 770–795. DOI: https://doi.org/10.52058/2786-5274-2024-9(37)-770-795.
11. Lezman R. EV Chargers: Navigating the Road to Standardization. *Electrical Contractor Magazine*. 2024. URL: https://www.ecmag.com/magazine/articles/article-detail/ev-chargers-navigating-the-road-to-standardization.
12. National Electric Vehicle Infrastructure Standards and Requirements: Final Rule / Federal Highway Administration, U.S. Department of Transportation. *Federal Register*. 2023. 28 Feb. URL: https://www.federalregister.gov/documents/2023/02/28/2023-03500/national-electric-vehicle-infrastructure-standards-and-requirements.
13. IEC 62196-2:2016. Plugs, socket-outlets, vehicle connectors and vehicle inlets – Conductive charging of electric vehicles – Part 2: Dimensional compatibility and interchangeability requirements for a.c. pin

and contact-tube accessories / International Electrotechnical Commission. Geneva, 2016. URL: https://webstore.iec.ch/en/publication/24204.
14. ISO 15118-1:2019. Road vehicles – Vehicle to grid communication interface – Part 1: General information and use-case definition / International Organization for Standardization. Geneva, 2019. URL: https://www.iso.org/standard/69113.html.
15. SAE J3400:2023. North American Charging Standard (NACS) / SAE International. Warrendale, PA, 2023. URL: https://www.sae.org/standards/content/j3400_202312.
16. ISO 6469-3:2021. Electrically propelled road vehicles – Safety specifications – Part 3: Protection of persons against electric shock / International Organization for Standardization. Geneva, 2021. URL: https://www.iso.org/obp/ui/#iso:std:iso:6469:-3:ed-4:v1:en.
17. IEC 61851-1:2017. Electric vehicle conductive charging system – Part 1: General requirements / International Electrotechnical Commission. Geneva, 2017. URL: https://webstore.iec.ch/publication/33644.
18. SAE J1772:2017. Electric Vehicle and Plug in Hybrid Electric Vehicle Conductive Charge Coupler / SAE International. Warrendale, PA, 2017. URL: https://www.sae.org/standards/content/j1772_201710.
19. ISO/SAE 21434:2021. Road vehicles – Cybersecurity engineering / International Organization for Standardization. Geneva, 2021. URL: https://www.iso.org/standard/70918.html.
20. IEC 61980-1:2020. Electric vehicle wireless power transfer (WPT) systems – Part 1: General requirements / International Electrotechnical Commission. Geneva, 2020. URL: https://webstore.iec.ch/publication/67729.
21. GB/T 27930-2023. Communication protocols between off-board conductive charger and battery management system for electric vehicle [Standard] / Standardization Administration of China. Beijing, 2023. URL: https://www.chinesestandard.net/PDF.aspx/GBT27930-2023.
22. IEC TS 62196-4:2022. Plugs, socket-outlets, vehicle connectors and vehicle inlets – Conductive charging of electric vehicles – Part 4: Dimensional compatibility and interchangeability requirements for DC pin and contact-tube accessories / International Electrotechnical Commission. Geneva, 2022. URL: https://standards.iteh.ai/catalog/standards/sist/b94f4603-aceb-4777-9eb0-4018ae1b00c8/iec-ts-62196-4-2022.
23. UN Regulation No. 155 – Cybersecurity and cybersecurity management system / United Nations Economic Commission for Europe. Geneva, 2021. URL: https://unece.org/sites/default/files/2021-03/R155e.pdf.
24. UN Regulation No. 156 – Uniform provisions concerning the approval of vehicles with regards to software update and software updates management system [Regulation 2021/388] / United Nations Economic Commission for Europe. Luxembourg, 2021. URL: https://op.europa.eu/en/publication-detail/-/publication/ec74fcfc-8079-11eb-9ac9-01aa75ed71a1.
25. IEC 61851-21-2:2018. Electric vehicle conductive charging system – Part 21-2: EMC requirements for off-board electric vehicle charging systems / International Electrotechnical Commission. Geneva, 2018. URL: https://webstore.iec.ch/en/publication/31282.
26. ISO 6469-1:2019. Electrically propelled road vehicles – Safety specifications – Part 1: Rechargeable energy storage system (RESS) / International Organization for Standardization. Geneva, 2019. URL: https://www.iso.org/standard/68665.html.
27. ISO 5474-4:2025. Electrically propelled road vehicles – Functional and safety requirements for power transfer between vehicle and external electric circuit – Part 4: Magnetic field wireless power transfer / International Organization for Standardization. Geneva, 2025. URL: https://www.iso.org/standard/81300.html.

References

1. Alanazi, F. (2023). Electric vehicles: Benefits, challenges, and potential solutions for widespread adoption. *Applied Sciences, 13*(10), Article 6016. DOI: https://doi.org/10.3390/app13106016.
2. Wajdi, W., & Chakir, A. (2019). Electric vehicles standards, charging infrastructure, and impact on grid integration: A technological review. *Renewable and Sustainable Energy Reviews, 120*, Article 109618. DOI: https://doi.org/10.1016/j.rser.2019.109618.
3. Davydov, V. O., & Stafidov, Ye. B. (2023). Use of charging stations for electric vehicles as a way of balancing the electrical load of energy systems. *ISG-Journal, (12)*, 45–52. Available at https://isg-journal.com/isjea/article/download/563/315/570.
4. Zakharchenko, Yu. V., et al. (2025). Marketing in the electric power industry of Ukraine: Problems and prospects of the market of charging stations for electric vehicles. *Economic Bulletin of Dnipro Polytechnic, (2)*, 79–91. DOI: https://doi.org/10.33271/ebdut/90.079.

ISSN 2076-2429 (print)
ISSN 2223-3814 (online)

5. Kakkar, R., et al. (2022). A review on standardizing electric vehicles community charging infrastructures. *Applied Sciences, 12*(23), Article 12096. DOI: https://doi.org/10.3390/app122312096.
6. Funke, S. Á., et al. (2018). How much charging infrastructure do electric vehicles need? A review of the evidence and international comparison. *Transportation Research Part D: Transport and Environment, 59*, 224–242. DOI: https://doi.org/10.1016/j.trd.2018.03.004.
7. U.S. Department of Transportation, Federal Highway Administration. (2025). *Implementation challenges and evolving solutions for rural electrification of electric vehicle chargers*. Available at https://www.transportation.gov/rural/ev/toolkit/ev-benefits-and-challenges/challenges-and-evolving-solutions.
8. International Code Council. (2023). *Standardization roadmap for electric vehicles*. https://share.ansi.org/evsp/ANSI_EVSP_Roadmap_June_2023.pdf.
9. Lieven, T. (2015). Policy measures to promote electric mobility – A global perspective. *Transportation Research Part A: Policy and Practice, 82*, 165–178. DOI: https://doi.org/10.1016/j.tra.2015.09.008.
10. Stetsiuk, O. V., et al. (2024). Electromobility in Ukraine: Realities of development, European context and the impact of martial law. *Scientific Innovations and Progressive Technologies, 9*(37), 770–795. DOI: https://doi.org/10.52058/2786-5274-2024-9(37)-770-795.
11. Lezman, R. (2024). EV chargers: Navigating the road to standardization. *Electrical Contractor Magazine*. Available at https://www.ecmag.com/magazine/articles/article-detail/ev-chargers-navigating-the-road-to-standardization.
12. Federal Highway Administration, U.S. Department of Transportation. (2023, February 28). National electric vehicle infrastructure standards and requirements: Final rule. *Federal Register*. Available at https://www.federalregister.gov/documents/2023/02/28/2023-03500/national-electric-vehicle-infrastructure-standards-and-requirements.
13. International Electrotechnical Commission. (2016). *Plugs, socket-outlets, vehicle connectors and vehicle inlets – Conductive charging of electric vehicles – Part 2: Dimensional compatibility and interchangeability requirements for a.c. pin and contact-tube accessories* (IEC Standard No. 62196-2:2016). Available at https://webstore.iec.ch/en/publication/24204.
14. International Organization for Standardization. (2019). *Road vehicles – Vehicle to grid communication interface – Part 1: General information and use-case definition* (ISO Standard No. 15118-1:2019). Available at https://www.iso.org/standard/69113.html.
15. SAE International. (2023). *North American Charging Standard (NACS)* (SAE Standard No. J3400:2023). Available at https://www.sae.org/standards/content/j3400_202312.
16. International Organization for Standardization. (2021). *Electrically propelled road vehicles – Safety specifications – Part 3: Protection of persons against electric shock* (ISO Standard No. 6469-3:2021). Available at https://www.iso.org/obp/ui/#iso:std:iso:6469:-3:ed-4:v1:en.
17. International Electrotechnical Commission. (2017). *Electric vehicle conductive charging system – Part 1: General requirements* (IEC Standard No. 61851-1:2017). Available at https://webstore.iec.ch/publication/33644.
18. SAE International. (2017). *Electric vehicle and plug in hybrid electric vehicle conductive charge coupler* (SAE Standard No. J1772:2017). Available at https://www.sae.org/standards/content/j1772_201710.
19. International Organization for Standardization. (2021). *Road vehicles – Cybersecurity engineering* (ISO/SAE Standard No. 21434:2021). Available at https://www.sae.org/standards/content/j1772_201710.
20. International Electrotechnical Commission. (2020). *Electric vehicle wireless power transfer (WPT) systems – Part 1: General requirements* (IEC Standard No. 61980-1:2020). Available at https://webstore.iec.ch/publication/67729.
21. Standardization Administration of China. (2023). *Communication protocols between off-board conductive charger and battery management system for electric vehicle* (Standard No. GB/T 27930-2023). Available at https://www.chinesestandard.net/PDF.aspx/GBT27930-2023.
22. International Electrotechnical Commission. (2022). *Plugs, socket-outlets, vehicle connectors and vehicle inlets – Conductive charging of electric vehicles – Part 4: Dimensional compatibility and interchangeability requirements for DC pin and contact-tube accessories* (IEC Standard No. TS 62196-4:2022). Available at https://standards.iteh.ai/catalog/standards/sist/b94f4603-aceb-4777-9eb0-4018ae1b00c8/iec-ts-62196-4-2022.
23. United Nations Economic Commission for Europe. (2021). *UN Regulation No. 155 – Cybersecurity and cybersecurity management system*. Available at https://unece.org/sites/default/files/2021-03/R155e.pdf.
24. United Nations Economic Commission for Europe. (2021). *UN Regulation No. 156 – Uniform provisions concerning the approval of vehicles with regards to software update and software updates*

management system. Available at https://op.europa.eu/en/publication-detail/-/publication/ec74fcfc-8079-11eb-9ac9-01aa75ed71a1.

25. International Electrotechnical Commission. (2018). *Electric vehicle conductive charging system – Part 21-2: EMC requirements for off-board electric vehicle charging systems* (IEC Standard No. 61851-21-2:2018). Available at https://webstore.iec.ch/en/publication/31282.
26. International Organization for Standardization. (2019). *Electrically propelled road vehicles – Safety specifications – Part 1: Rechargeable energy storage system (RESS)* (ISO Standard No. 6469-1:2019). Available at https://www.iso.org/standard/68665.html.
27. International Organization for Standardization. (2025). *Electrically propelled road vehicles – Functional and safety requirements for power transfer between vehicle and external electric circuit – Part 4: Magnetic field wireless power transfer* (ISO Standard No. 5474-4:2025). Available at https://www.iso.org/standard/81300.html.

Ореховська Наталія Олексіївна; Natalia Orekhovskaya, ORCID: http://orcid.org/0009-0003-0724-8295
Шихірева Юлія Володимирівна; Yulia Shikhireva, ORCID: https://orcid.org/0009-0006-9950-1551

Received September 12, 2025
Accepted October 03, 2025

Праці Одеського політехнічного університету, 2025. Вип. 2(72)
ISSN 2076-2429 (print)
ISSN 2223-3814 (online)

ІНФОРМАЦІЙНІ ТЕХНОЛОГІЇ

INFORMACION TECHNOLOGY

UDC 004.1

O. Arsirii, DSc, Prof.,
D. Ivanov
Odessa Polytechnic National University, Shevchenko Ave. 1, Odesa, Ukraine, 65044, e-mail: e.arsiriy@gmail.com

AFFINITY ANALYSIS MODELS OF TRANSACTIONAL AND BEHAVIORALCUSTOMER DATA FOR PERSONALIZED CONTENT GENERATION IN B2B E-COMMERCE SYSTEMS

О. Арсірій, Д. Іванов. **Моделі афінітивного аналізу транзакційних і поведінкових даних клієнтів систем B2B електронної комерції для створення персоналізованого контенту.** Зростання фінансової значущості та структурної складності сегмента ринку систем B2B електронної комерції, а також необхідність підвищення його ефективності зумовило актуальність проведення системного аналізу існуючих моделей афінітивного аналізу транзакційних і поведінкових даних для обгрунтування шляхів їх адаптації з метою підвищення персоналізації товарного, інформаційного та рекомендаційного контенту системи B2B електронної комерції. На основі порівняння E-commerce System B2B та B2C за основними показниками встановлено специфіку B2B E-commerce System для пояснення концепції транзакцій «Бізнес-для-бізнесу» та зроблено висновок щодо орієнтації товарного, інформаційного та рекомендаційного контенту на раціональні рішення, великі обсяги закупівель та довгострокові партнерські відносини. Проаналізовано моделі афінітивного аналізу які базуються на алгоритмах та структурах даних Apriori, FP-Growth, а також Eclat та визначено їх недоліки щодо аналізу транзакційних і поведінкових даних B2B-клієнтів. Проаналізовано шляхи підвищення персоналізації товарного, інформаційного та рекомендаційного контенту системи B2B електронної комерції за рахунок використання моделей афінітивного аналізу транзакційних і поведінкових даних. Розроблено елементи концептуальної моделі комерційної активності B2B для персоналізації контенту на базі понять афінітивного аналізу із врахуванням великих обсягів, індивідуальних цін та поведінкових сценаріїв оптових покупок. Розроблено структуру концептуальної моделі для аналізу комерційної активності B2B. Визначено складові групи показників для комплексної оцінки ефективності персоналізації контенту B2B, яка базується на розробленій концептуальній моделі комерційної активності B2B.

Ключові слова: електронна комерція, системи B2B, транзакційні та поведінкові данні, афінітивний аналіз, асоціативні правила, Apriori, FP-Growth, Eclat, метрики якості

O. Arsirii, D. Ivanov. **Affinity Analysis Models of Transactional and Behavioral Customer Data for Personalized Content Generation in B2B E-commerce Systems.** The growing financial significance and structural complexity of the B2B e-commerce market segment, coupled with the necessity to enhance its efficiency, have necessitated a systematic analysis of existing affinity analysis models for transactional and behavioral data. This study aims to justify the adaptation of these models to improve the personalization of product, information, and recommendation content within B2B e-commerce systems. Based on a comparative analysis of B2B and B2C e-commerce systems across key indicators, the specific characteristics of B2B systems are established to define the "Business-to-Business" transaction concept. The study concludes that product, information, and recommendation content must prioritize rational decision-making, large-scale procurement volumes, and long-term partnerships. The paper analyzes affinity analysis models based on Apriori, FP-Growth, and Eclat algorithms and data structures, identifying their limitations regarding the analysis of B2B customer transactional and behavioral data. Furthermore, it explores pathways for enhancing content personalization by leveraging these models. A key contribution of this research is the development of conceptual model elements for B2B commercial activity. This model for content personalization is built upon affinity analysis concepts while accounting for wholesale purchase characteristics, such as large volumes, individual pricing, and specific behavioral scenarios. The structure of the conceptual model for B2B commercial activity analysis is established. Finally, the study defines a comprehensive set of metrics to evaluate the effectiveness of B2B content personalization, based on the proposed conceptual model.

Keywords: B2B e-commerce, personalization, affinity analysis, transactional data, behavioral data, sequential patterns, conceptual modeling, Apriori, FP-Growth, Eclat, quality metrics

Introduction

The relevance of conducting affinity analysis, also known as association rule mining, of transactional and behavioral data of customers of B2B e-commerce systems to create personalized content in B2B e-commerce systems is due to the financial significance and structural complexity of this market segment, as well as the need to improve its efficiency.

The relevance of conducting affinity analysis, also known as association rule mining, of transactional and behavioral data of customers of B2B e-commerce systems to create personalized content in

DOI: 10.15276/opu.2.72.2025.10

ISSN 2076-2429 (print)
ISSN 2223-3814 (online)
Proceedings of Odessa Polytechnic University, Issue 2(72), 2025

B2B e-commerce systems is due to the financial significance and structural complexity of this market segment, as well as the need to improve its efficiency.

The relevance of conducting affinity analysis, also known as association rule mining, of transactional and behavioral data of customers of B2B e-commerce systems to create personalized content in B2B e-commerce systems is due to the financial significance and structural complexity of this market segment, as well as the need to improve its efficiency.

The relevance of conducting affinity analysis, also known as association rule mining, of transactional B2B e-commerce systems is due to the financial significance and structural complexity of this market segment, as well as the need to improve its efficiency. The critical importance of effective B2B personalization is confirmed by the enormous financial volumes of this segment. The global B2B e-commerce market, estimated at $11.54 trillion in 2024, significantly exceeds the B2C market ($6.55 trillion). Its projected growth to $60.62 trillion by 2034 indicates that even a slight increase in the effectiveness of customer interactions through personalization will have a multi-trillion-dollar economic impact [1]. At the same time, it has been established that traditional affinity analysis models are focused on data mining, aimed at identifying hidden relationships and patterns between different elements (goods, events, actions) in large data sets, particularly in transaction databases developed for the B2C segment of e-commerce. They are focused on emotions, impulse purchases, and a simple user experience, which is not effective enough for B2B [2]. Since B2B purchases are rational, high-value, and driven by the need for ROI (return on investment), there is an urgent need to analyze and adapt existing models to address B2B challenges such as: the complexity of the buying center (Buying Center), where the decision to purchase a product or service is made not by one person, but by a group of people or departments within the purchasing organization, individual pricing conditions, data sparsity (rare but large orders) and the need for long-term partnerships [3]. This creates a need to adapt and modernize affinity analysis models that can work effectively in a B2B environment to create truly relevant and rationally justified content (product, informational, recommendatory).

Therefore, conducting a systematic analysis of existing models that use transactional data to identify affinity rules and typical purchasing patterns and behavioral data to understand purchasing scenarios and the needs of different roles in the client company of a B2B e-commerce system is a pressing task.

Literature review and problem statement

In [3], a B2B e-commerce system is defined as a comprehensive online platform or set of interrelated technological solutions designed to carry out commercial transactions, exchange information, and automate business processes between two or more legal entities (enterprises) To explain the concept of “Business-to-Business” (B2B) transactions, let’s use Figure 1.

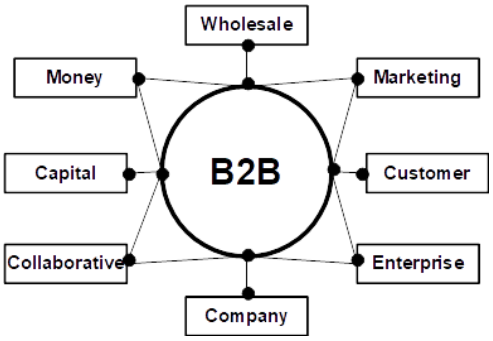

Fig. 1. B2B Transaction Conceptual Scheme

It is known that B2B transactions are the exchange of goods, services, or information between two or more companies [1]. According to the concept of transactions (Fig.1), the first aspect is wholesale trade. This business model allows retailers to purchase products at a lower price and resell them to consumers at a markup. Another important concept is marketing. B2B marketing strategies focus on building relationships with other businesses rather than individual consumers. This often involves a longer sales cycle and more complex decision-making processes.

In a B2B context, the customer is another business rather than an individual. These business customers have different needs and purchasing behaviors compared to individual consumers. B2B companies must understand the specific needs and challenges of their business customers in order to provide valuable solutions. The main customers in B2B transactions are enterprises or corporations. These enterprises require reliable solutions to support their complex operations, making them a key target market for B2B companies. A company represents enterprises involved in B2B transactions, ranging in size from small startups to large corporations.

Their interaction forms the basis of the B2B ecosystem. Collaboration is a key element of B2B relationships. Enterprises often work closely together to achieve common goals. This collaborative

ISSN 2076-2429 (print)
ISSN 2223-3814 (online)

approach promotes long-term partnerships and innovation. In B2B, capital refers to various objectives, such as investing in new technologies, expanding operations, or acquiring other companies. Access to capital is crucial for B2B companies to remain competitive. Finally, the Money block represents financial transactions that occur between businesses. In B2B, these transactions can be large and complex, involving different payment methods and terms. Effective cash flow management is important for the financial health of B2B companies [1, 2, 3].

Thus, a B2B e-commerce system (B2B E-commerce System) is a comprehensive online platform or set of interconnected technological solutions designed to carry outcommercial transactions, exchange information, and automate business processes between two or more legal entities (enterprises) [3]. This system is a digital environment that enables seller organizations to present their product, information, and recommendation content (catalogues, price lists, terms of cooperation) to other buyer organizations for their production, commercial, or resale needs. Table 1 shows the results of a comparative analysis of B2B and B2C e-commerce systems based on key indicators. Thus, modern B2B e-commerce systems operate in a highly competitive Internet environment, where the quality of content determines the speed and accuracy of meeting the needs of wholesale customers. For the B2B model, the content of the online platform is created with a focus on rational decisions, large purchase volumes, and long-term partnerships [4].

Table 1

Comparison of E-commerce System B2B and B2C by key indicators

B2B (Business-to-Business)	B2C (Business-to-Consumer)
Target audience	
The number of buyers is smaller. They include other companies, startups, enterprises, large corporations, government agencies, and non-profit organizations.	A large number of buyers are individual consumers
Transaction value	
High cost, higher volumes, lower frequency.	Low cost, lower volumes, higher frequency.
Purchase motivation	
Rational: focused on business efficiency, cost reduction, profit increase, long-term goals.	Emotional/Impulsive: focused on satisfying personal needs, desires, based on price, brand, trends.
Duration of the decision-making process	
Longer and more complex: involves multiple stakeholders, negotiations, possible testing, contracts.	Shorter and simpler: often a single solution, a quick purchase.
Sales cycle	
Long (from 1 to 6 months).	Short (from 1 to 6 days).
Features of customer relations	
Long-term partnerships: emphasis on building trust, support, tailor-made solutions.	Short-term, transactional.
Features of marketing	
Focus on logic, values, ROI, personalized offers, direct sales, content marketing.	Focus on emotions, image, advertising, social networks, promotions, convenience.
Payment Methods	
Sophisticated methods (lines of credit, invoices, bank transfers, deferred payments). Higher security priority.	Fast and convenient methods (credit/debit cards, mobile wallets, electronic payments).
Product/Service Customization	
High degree of customization, specialized solutions.	Standardized “ready-made” products.

However, in [5, 6], attention is focused on the situation where the vast majority of e-commerce platforms use static methods of content formation based on fixed rules or universal recommendations for individual customers. This approach does not take into account purchasing patterns, the specifics of the wholesale customer’s business, seasonality, or dependencies between products. This limits the effectiveness of the service and reduces the likelihood of repeat purchases [7, 8]. Resolving such issues requires a systematic analysis of existing models, methods, and technologies for affinity analysis of customer transaction and behavioral data in order to modify them to improve the personalization of product, information, and recommendation content in B2B e-commerce systems.

ISSN 2076-2429 (print)
ISSN 2223-3814 (online)
Proceedings of Odessa Polytechnic University, Issue 2(72), 2025

It is known that modern algorithms for data analysis to create associative rules (Association Rule Mining) are aimed at finding frequently repeated combinations of goods or events in customer transactions. That is, such algorithms are based on the concept of frequent itemsets, which occur in multiples and are related to the concept of frequency. The method of searching for association rules (AR) using frequent itemsets consists of two steps: finding the most frequent itemsets and using them to generate ARs that meet the conditions of minimum support and confidence, and then using the resulting purchase and behavioral data to create personalized content in the B2B e-commerce system.

It is known that to search for frequent sets of elements, the following algorithms are used: the Apriori algorithm [9], which performs a search of candidates with subsequent rejection of unpopular sets, the FP-Growth algorithm, which builds an FP-Tree for further search without generating candidates [10], and the Eclat algorithm, which searches for popular sets by intersecting pre-built TID lists [11].

Based on information from literary sources, let us consider the advantages and disadvantages of popular affinity analysis algorithms in more detail.

The model for searching for frequent sets of items (Frequent Itemsets) in transactional databases through iterative generation of candidates and their testing is based on the Apriori algorithm.

The main idea of the algorithm is based on the a priori property of Apriori Property— that is, any subset of a frequent set of items must also be frequent.

The algorithm works from the bottom up (from shorter sets to longer ones), using frequent sets found in the previous step to generate candidates for the next one. At the same time, those candidate sets that are guaranteed not to be frequent are pruned [9].

According to the FP-Growth (Frequent Pattern Growth) model, a compact data structure called an FP tree (Frequent Pattern Tree) is constructed, and based on this, a recursive search for frequent patterns is performed [10]. In this case, the generation of candidates and exhaustive search, unlike Apriori, are replaced by a search for possible combinations of goods or behavioral patterns in the FP tree.

According to the Eclat (Equivalence CLAss Transformation) model, the search for frequent item sets in transactional and behavioral data uses intersections of transaction identifier lists (TID lists), as opposed to enumerating candidates in Apriori or constructing trees in FP-Growth. [11]. The main idea behind Eclat is to store a list of transaction identifiers.

(TID lists) for each item where that item occurs and to find frequent itemsets by intersecting these lists.

The results of comparisons of the considered associative rule search algorithms are shown in Table 2.

Table 2

Advantages and disadvantages according to the principle of operation of algorithms for searching associative rules

Principle of operation	Advantages	Disadvantages
Apriori		
Candidate generation	Simple, classic	Slow on large sets
FP-Growth		
FP Tree	Fast, no candidates	More difficult to implement
Eclat		
Crossing TID lists	Simple, fast on small data	Requires a lot of memory on big data

A study of B2B e-commerce systems and existing affinity analysis algorithms (Apriori, FP-Growth, Eclat) revealed a significant gap between theoretical methods for identifying patterns and their practical effectiveness in a B2B environment. That is, the algorithms are effective for searching for associations in large transactional databases of B2C systems where transactions are homogeneous. At the same time, they are not adapted to the specifics of B2B because they do not take into account the sparsity and structural complexity of data in B2B transactions and, as a result, do not provide a rational justification for recommendation decisions to B2B managers.

Thus, to improve the effectiveness of B2B systems, it is necessary to adapt and expand affinity analysis models. This should be done by integrating transactional (financial) and behavioral (scenario) data with subsequent classification of customers, which determines the purpose and objectives of this study.

The aim and objectives of the research

The purpose of this study is to conduct a systematic analysis of existing models of affinity analysis of transactional and behavioral data to substantiate ways to adapt them to increase the personalization

ISSN 2076-2429 (print)
ISSN 2223-3814 (online)

of product, informational and recommendation content of the B2B e-commerce system. The objectives of the study include:

– analysis of ways to increase the personalization of product, informational and recommendation content of the B2B e-commerce system through the use of models of affinity analysis of transactional and behavioral data;

– development of elements of a conceptual model of B2B commercial activity for personalization of content based on the concepts of affinity analysis, taking into account large volumes, individual prices, and behavioral scenarios of wholesale purchases;

– development of a conceptual model structure for analyzing B2B commercial activity in content personalization systems;

– identification of components for a comprehensive assessment of the effectiveness of B2B content personalization, which is based on the developed conceptual model of B2B commercial activity.

The research materials and methods

Analysis of ways to increase personalization of B2B content. Increasing the personalization of content in B2B e-commerce systems requires a shift from emotionally-oriented B2C methods to rationally informed decisions that directly affect the efficiency, profitability, and operating costs of the client. Affinity analysis is a key tool for achieving this goal, as it allows you to identify not only the fact of the purchase, but also the logic and sequence of purchasing decisions.

Let's consider the possibilities of affinity analysis models for transactional data creation for *creating B2B commodity content* [12].

Classical affinity analysis, applied to transactional data (invoices, bulk orders), traditionally focuses on finding frequent sets (Apriori, FP-Growth, and Eclat). In a B2B system, this model should be adapted to form product content in the form *of complex offers* by integrating financial and quantitative metrics [12]. For example*, the formation of "Wholesale* Bundles", when transactional analysis reveals associative rules, where instead of frequency (Support), the *total cost* or *margin of the* set dominates:

If {Item A, Item B}, then {Item C}→

This allows the system to offer not just related products, but complex purchasing solutions that, from the customer's point of view, optimize logistics and reduce overall costs (for example, offer of specialized fasteners and tools when ordering a large batch of building materials).

Another example of product content creation is the *personalization of the price offer* when associative rules can be applied to define individual conditions, i.e.:

If {The customer belongs to the "Premium" class,

Orders Product A monthly},

then {10% discount on Product B}→

The system generates not just a general promotion, but a personalized investment plan for the client, showing how the inclusion of associated products will allow them to obtain more favorable wholesale prices.

Consider using consistent templates to create *B2B recommendation content*. Sequential Pattern Mining (SPM) works with behavioral and temporal data, identifying cycles and sequences of events, which allows you to predict the next logical step of a B2B client, which will be the basis for creating recommendation content [13]. For example, forecasting replenishment of stocks (Restock Prediction). SPM detects the typical time interval between orders for certain sets of products.

If {Order Winter Shoe Collection}, then {Order Skincare Products (After 6 Weeks)} →

At the same time, the system will generate a recommendation notification a week before the predicted date, reminding the client of the need to replenish the stock. This increases loyalty because the system acts as an assistant in managing the customer's inventory.

Another example of recommendations is possible scenarios for the behavior of the Buying Center. Sequential analysis is applied to the actions of different employees of the buying company.

If {View specifications by Engineer}, then {Request final price by Financier}→

That is, when the engineer has reviewed the characteristics, a recommendation notification is automatically generated to the financier in the form of an ROI calculation or a special price list for this product, speeding up the sales cycle.

ISSN 2076-2429 (print)
ISSN 2223-3814 (online)
Proceedings of Odessa Polytechnic University, Issue 2(72), 2025

Consider the use of transactional and behavioral data to create *information content in a* B2B system. Informational content in B2B includes not only technical characteristics, but also conditions, reports, and analytics [14]. Thus, affinity analysis of transactional data is used to provide personalized analytics. For example, the system compares the customer's buying behavior with typical patterns of their industry or segment.

If {Customer does not buy Product B, but his competitors buy Product B together with A},

then {Send Analytical Report on Product B and its benefits}→

Automatically generated informational content is rationally reasonable, as it appeals to lost profits or competitors' best practices.

Analysis of sequential patterns can detect behavioral anomalies preceding churn of customers (Churn), which is essential for risk management:

If {Drastic Volume Reduction, Old Invoice Loading},

then {Search for New Suppliers (Outlook)}→

These triggers personalized communication aimed at retaining customers, such as offering special, customized terms of cooperation.

Thus, affinity analysis adapted to B2B metrics such as cost, volume, time, behavioral scenario is necessary to transform a B2B E-commerce system from a simple catalog into an intelligent assistant that provides rationally reasoned, proactive, and personalized content.

Development of elements of a conceptual model of B2B commercial activity. Taking into account the fundamental concepts of affinity analysis, such as transaction, sequence, sequential pattern, and associative rule, as well as metrics for assessing the quality of their construction, we will determine the elements of the B2B model of commercial activity. For B2B, this is one wholesale order placed by a buyer company, which includes several commodity items (Stock Keeping Unit SKU) and financial conditions. The SKU has a unique alphanumeric code used by the business (seller, distributor, retailer) for internal identification, tracking, and inventory management [12].

Then, formally*, the commodity item* (element) is defined as:

$$I = \{i_1, i_2, \dots i_n\}, \tag{1}$$

where I is the set of all commodity items i_k (SKU), available for order in the B2B system. *The transaction T* is *a logical unit of work* that occurs at a single point in time t, is a subset of I, that is, $T \subseteq I$ is defined by the set of tuples of the total number m:

$$T = \{t_1, t_2, \dots t_m\}. \tag{2}$$

Each element of the transaction t_j is a tuple, which describes the purchased or executed element, taking into account its quantity (Quantity) q_k and cost p_k:

$$t_j = \langle i_k, q_k, p_k \rangle, \tag{3}$$

where i_k – Commodity item identifier (SKU), $i_k \in I$; p_k – individual price (Price) per unit applied for this client (takes into account his discounts and purchase volume).

A sequence s_j in B2B is a time-ordered activity log of a single customer (or Buying Center), consisting of a set of *T transactions* that occurred at different points in time:

$$s_j = \langle T_{t_1}, T_{t_2}, \dots, T_{t_k} \rangle, \tag{4}$$

where T_{t_i} – it is a B2B transaction (1) that occurred at a point in time t_i. At the same time, we have time ordering $t_1 < \dots < t_k$.

Association Rule (AP) in B2B reflects the simultaneous presence of goods, services, or actions within the same transaction T (1) Let I be the set of all elements (SKU/services/actions), and A and B be two sets of elements, such that $B=A \subset I$, $B \subset I$, $A \cap \varnothing$. The associative rule is formulated in the form

$$AR = A \rightarrow B, \tag{5}$$

i.e. – *if a* set of elements A is present in a wholesale order (Transaction), *then* there is a high probability that a set of elements B is present in the same order.

ISSN 2076-2429 (print)
ISSN 2223-3814 (online)

The *Sequential Pattern* (SP*)* in B2B reflects the time-ordered occurrence of transactions or behavioral events (3) that form the chain of customer activity. Let *S* be the set of all B2B sequences of customers s_j (3), α and β – two sequences of transactions or events $\alpha = \langle T_{t_a} \rangle, \beta = \langle T_{t_b} \rangle$.

A consistent pattern is formulated as follows:

$$SP{=}\alpha \Rightarrow \beta. \tag{6}$$

That is, if at a given moment in time t_a the client performed event or set of transactions α, then there is a high probability that at the next moment in time t_b, $t_a<t_b$ the will perform event or set of transactions β. The symbol "⇒" is used to emphasize the temporal sequence.

Let us define quality metrics that characterise the relationship between sets of goods established using APs constructed during affinity analysis.

Support for AP shows how often the set $\{AB\}$ appears in the general database of B2B transactions D. Then, for AP $A \to B$, *support* $S_{AR}(A \to B)$ looks like:

$$S_{AR}(A \to B) = S_{AR}(AB) = \frac{\left|\{TD \mid ABT\}\right|}{\left|D\right|}, \tag{7}$$

where $\left|\{TD \mid ABT\}\right|$ – total number of transactions containing *A* and *B,* $\left|D\right|$ – total number of transactions in the B2B database.

Confidence AP $A \to B$ shows the probability that if a customer bought *A*, they will also buy *B* in the same transaction. This is a direct measure of the predictive value of set *A* for the sale of *B* within a single wholesale order. *D*. Then for AP *A→B confidence* $C_{AR}(A \to B)$ looks like:

$$C_{AR}(A \to B) = \frac{S_{AR}(AB)}{S_{AR}(A)}. \tag{8}$$

For B2B systems, the quality assessment (Support, Confidence) AP should take into account not only the number of transactions $\left|D\right|$, but also the total financial value or volume of elements *A* and *B* in these transactions, i.e. it should be *Weighted* according to definition (3).

Lift shows how often the set $\{A \cup B\}$ appears more frequently than expected if *A* and *B* were independent. Then, for $A \to B$, *Lift* $L_{AR}(A \to B)$ looks like this:

$$L_{AR}(A \to B) = \frac{C_{AR}(A \to B)}{S_{AR}(A)} = \frac{S_{AR}(AB)}{S_{AR}(A)S_{AR}(B)}. \tag{9}$$

If $L_{AR}>1$, then there is a positive correlation (rational sense) in joint purchasing; if $L_{AR}<1$, then there is a negative correlation (substitute goods). This is a key metric for B2B, as it excludes trivial rules that are common simply because of the high overall popularity of one of the goods.

Leverage measures the difference between the actual frequency of joint occurrence of sets *A* and *B* and the frequency that would be expected if *A* and *B* were completely independent of each other. Then for $A \to B$ *Leverage* $Le_{AR}(A \to B)$ looks like this:

$$Le_{AR}(A \to B) = S_{AR}(AB) - S_{AR}(A)S_{AR}(B). \tag{10}$$

If $Le_{AR} = 0$, then elements *A* and *B* are independent. Their joint appearance in orders is purely coincidental. If $Le_{AR} > 0$, there is a strong logical connection between the elements, i.e. they appear together more often than expected. This indicates a strong logical connection. In B2B, this is a signal for creating bundles or joint logistics. If $Le_{AR} < 0$, then the items appear together less frequently than expected. This may indicate that the products are competitors or substitutes.

Conviction shows how often AP (5) gives incorrect predictions. It measures the dependence of set *A* on set *B*. Then, for $A \to B$, Conviction $V_{AR}(A \to B)$ looks like this:

$$V_{AR}(A \to B) = \frac{1 - S_{AR}(B)}{1 - C_{AR}(A \to B)}. \tag{11}$$

A high V_{AR} value indicates that the rule is very strong, and set *A* really "forces" *B* to appear. This is useful for filtering rules when A is very popular.

ISSN 2076-2429 (print)
ISSN 2223-3814 (online)
Proceedings of Odessa Polytechnic University, Issue 2(72), 2025

Without going into too much detail, let us define the quality metrics that characterise the relationship between sequential *SP* patterns (6). They apply to the sequence base *S* when event β occurs after event α:

Support for SP

$$S_{SP}(\alpha \Rightarrow \beta) = \frac{\left|\{s \in S \mid \textit{precedes } \beta \text{ in sequence s}\}\right|}{|S|}. \quad (12)$$

Confidence SP

$$C_{SP}(\alpha \Rightarrow \beta) = \frac{S_{SP}(\alpha \Rightarrow \beta)}{S_{SP}(\alpha)}. \quad (13)$$

Lift for SP

$$L_{SP}(\alpha \Rightarrow \beta) = \frac{S_{SP}(\alpha \Rightarrow \beta)}{S_{SP}(\alpha) S_{SP}(\beta)}. \quad (14)$$

Leverage for SP

$$Le_{SP}(\alpha \Rightarrow \beta) = S_{SP}(\alpha \Rightarrow \beta) - S_{SP}(\alpha) S_{SP}(\beta). \quad (15)$$

Conviction for SP

$$V_{SP}(\alpha \Rightarrow \beta) = \frac{1 - S_{SP}(\beta)}{1 - C_{SP}(\alpha \Rightarrow \beta)}. \quad (16)$$

As a practical example, we will provide the form of associative rules and sequential patterns built for *Wholesale B2B Portal* [7].

Associative rule (Product):

{Women's trainers Art. 403, Men's trainers Art. 510}→{Comfort insoles set}.

Associative rule (Product + Service):

{Order over 1000 pairs} → {60-day credit line provided}.

Sequential pattern (Seasonality):

<Order for winter boots> → <Order for salt protection products (in 2 months)>.

Sequential pattern (Forecasting):

<Request for individual price for new collection, Receipt of technical documentation>→<Placing main wholesale order (within 14 days)>/

Development of a conceptual model structure for analysing B2B commercial activity Let us present the structure of the conceptual model of B2B commercial activity in the form of a three-level hierarchy – "Entities, Relationships, Metrics".

The first level of entities contains data objects. It is the foundation of the conceptual model, which transforms "raw" data into structured information. The entity level consists of:

– Sets of commodity items *I* (1), where i_k (*SKU)* is an atomic unit of analysis;

– Transactions *T* (2), which are a logical grouping of goods taking into account volume and personal price (rational context);

– Client sequences S (3), which are a chronological chain of transactions that reflects the customer life cycle.

The second level of logical connections contains the so-called analytical vectors. Due to the establishment of such ties, data is converted into knowledge about behavior. The second level is based on:

– vectors of associative rules *AR* (5), which describe the presence of horizontal relationships, i.e. commodity items t_j (3), which are purchased together. This is the basis for "commodity personalization" and the formation of bundles;

– vectors of sequential SP patterns (6), which describe vertical (temporal) relationships s_j (4), i.e. what follows what. This is the basis for "predictive personalization", recommendation content, and management of replenishment cycles.

ISSN 2076-2429 (print)
ISSN 2223-3814 (online)

The third level of evaluation and validation contains quality metrics, the values of which are tools for selecting the most significant rules or patterns that make economic sense, namely:

– *Support S* (7) and (12) characterizes the scale of the rule or pattern;

– *Confidence C (*8) and (13) characterizes the reliability of the prediction against a rule or pattern;

– *Lift L* (9) and (14) elevator characterizes the degree of connection between transactions or patterns, taking into account its non-triviality and intellectual novelty;

– *Leverage Le* (10) and (15) characterizes the value of absolute benefit/weight of a rule or pattern for a business;

– *Conviction V* (11) and (16) characterizes the resistance of a rule or pattern to random fluctuations.

Thus, the proposed conceptual model of B2B commercial activity allows formalizing complex multifactorial processes of interaction between the supplier and the client. It combines static associative relationship analysis to optimize product content and dynamic sequential pattern analysis for proactive demand forecasting. Its development provides a mathematical basis for the automated personalization of product, recommendation, and informational content of the B2B platform.

Identifying the components for a comprehensive assessment of the effectiveness of B2B content personalization

Taking into account the identified ways to increase the personalization of product, informational and recommendation content of the B2B e-commerce system, the elements and structure of the conceptual model for analyzing B2B commercial activity have been developed, a comprehensive assessment of the effectiveness of content personalization in B2B e-commerce systems has been proposed, which combines four groups of indicators.

Group 1 contains indicators for determining the quality of analytics (*Model Performance*) of Q_{analyt} and is based on previously developed metrics for *AR* and *SP,* namely:

– Average *Lift* (L_{avg}), determines how non-trivial and useful connections the system finds. Time accuracy ($T_{accuracy}$) determines for sequential patterns how accurately the system predicted the date of the next order (deviation Δt);

– Inventory Coverage determines what percentage (%) of all SKUs participate in the generated personalized offers.

Group 2 contains indicators for determining technological efficiency (Engine Performance) Q_{tech} to assess the system's ability to work with large amounts of data in real time, namely:

– Generation speed (latency) – the time it takes to form a recommendation block when loading a page (should not exceed 100…200 m/s);

– Freshness – the time it takes for a new customer transaction to be reflected in the update of their affinity profile;

– Scalability – the ability of affinity analysis algorithms (Apriori, FP-Growth, and Eclat) to process a growing number of transactions without an exponential increase in memory consumption.

Group 3 contains indicators for determining commercial effectiveness (Business Impact) Q_{comm}, such as key indicators for the business of the B2B platform owner, namely:

– Conversion Rate (CVR) – The indicator of the effectiveness of converting information content into actual purchases is defined as the ratio of the number of successful orders to the number of personalised sessions on the B2B platform;

– Average Order Value (AOV) – an indicator of the quality of commercial content, characterising the ability of a B2B platform to encourage customers to purchase comprehensive solutions and defined as the increase in the average customer spend (Δq Δp) thanks to AR bundles;

– Churn Rate Reduction (CRR) – An indicator of the quality of recommendation content, characterising the ability of a B2B platform to retain customers through a sense of "partner support" and defined as a reduction in customer churn thanks to proactive SP recommendations;

Group 4 contains indicators for determining customer value (Q_{cust}). These indicators measure:

– Time-to-Purchase (TTP) – reduction in the time spent by the purchasing manager on creating a basket thanks to recommendations;

– Stock-out Prevention Rate (SPR) – percentage of cases when the system reminded the customer to replenish stocks in time, preventing the customer's business from stopping.

Taking into account the indicators from the four groups, we will define a comprehensive assessment of the effectiveness of content personalisation in B2B e-commerce systems as:

ISSN 2076-2429 (print)
ISSN 2223-3814 (online)
Proceedings of Odessa Polytechnic University, Issue 2(72), 2025

$$E_{pers} = \omega_1 Q_{analyt} + \omega_2 Q_{tech} + \omega_3 Q_{comm} + \omega_4 Q_{cust},$$

where: E_{pers} –integral personalisation effectiveness index; Q – normalised values for each group of metrics; $\omega_{1..4}$ – weighting coefficients (whose sum = 1).

It should be noted that for B2B systems at the implementation stage, higher priority is usually given to the values of ω_4 (value for the customer) and $_1$ (quality of analytics), as these are the factors that build long-term loyalty.

Conclusions

Based on the system analysis and development of conceptual elements of the model, the following conclusions can be formulated:

It is shown that the growth of financial significance and structural complexity of the market segment of B2B e-commerce systems caused the need to increase its efficiency, which determined the relevance of conducting a systematic analysis of existing models of affinity analysis of transactional and behavioral data to substantiate ways of their adaptation in order to increase the personalization of product, informational and recommendation content of the B2B e-commerce system.

The conceptual scheme of B2B transactions and the comparison of the B2B and B2C E-commerce System in terms of the main indicators are defined. The specifics of personalization in B2B systems of electronic commerce are determined. It has been established that unlike B2C, where emotional factors dominate, in B2B, personalization should be based on rational calculations, ROI, and maintaining long-term partnerships.

A study of existing algorithms of affinity analysis has been carried out and a significant gap between theoretical methods of pattern detection and their practical effectiveness in the B2B environment has been identified. That is, the algorithms Apriori, FP-Growth, Eclat are effective for finding associations in large transaction databases of B2C systems where transactions are homogeneous and not adapted to the specifics of B2B because they do not take into account the sparsity and structural complexity of data in B2B transactions and, as a result, do not provide a rational justification for recommending decisions to B2B managers.

The ways to increase the personalization of product, recommendation and informational content of the B2B system are analyzed and it is shown that conducting affinity analysis adapted to B2B metrics such as cost, volume, time, behavioral scenario is necessary to transform the B2B E-commerce system from a simple catalog into an intelligent assistant that provides rationally reasoned, proactive and personalized content.

A conceptual model of commercial activity has been formed. The model integrates time-ordered sequences of transactions and behavioral events, which makes it possible to formalize the work of the “Buying Center” of the client company.

Affinity analysis metrics have been adapted. The use of weighted indicators of support and reliability, taking into account the financial value of orders, is proposed. Differentiation of metrics for associative AR rules and sequential SP patterns allows you to clearly separate static relationships between goods and the dynamics of purchasing cycles.

Ways of practical implementation are proposed. It is determined that the use of affinity analysis models allows automating the generation of personalized price proposals, bundles for logistics optimization and proactive notifications about the need to replenish the client’s warehouse stocks.

The foundations for creating a comprehensive assessment have been developed. Groups of indicators (analytical, technological, commercial and client) have been established, which together allow measuring the effectiveness of the implemented personalization system through an integral index.

Thus, the study creates the necessary theoretical basis for transforming B2B e-commerce systems from passive catalogs to intelligent decision support systems, which increases customer loyalty and the cost-effectiveness of the platform.

Література

1. Global Ecommerce Statistics: Trends to Guide Your Store in 2025. *Shopify*. URL: https://www.shopify.com/enterprise/blog/global-ecommerce-statistics (дата звернення: 01.11.2025).

ISSN 2076-2429 (print)
ISSN 2223-3814 (online)

2. Mobile commerce shopping trends and stats. *Insider Intelligence*. URL: www.emarketer.com (дата звернення: 01.11.2025).
3. Панасюк Т. С., Зубенко І. Р. Перспективи розвитку b2c електронної комерції в світі. 2024. DOI: https://doi.org/10.5281/zenodo.14603373.
4. Арсірій О. О., Іванов Д. В., Бабілунга О. Ю. Аналіз моделей, методів та технологій створення персоналізованого контенту в системам B2B електронної комерції. *Інформатика. Культура. Техніка*. 2025. Том 2. С. 273–278. URL: https://ict.op.edu.ua/index.php/journal/uk/issue/view/3.
5. Шведа Н. М., Краузе О. І. Електронна комерція: сучасний стан та стратегії розвитку. *Міжнародний науковий журнал «Інтернаука». Серія: Економічні науки*. 2024. Вип. 2 (82). DOI: https://doi.org/10.25313/2520-2294-2024-2-9639.
6. Hu Y. H., Chen Y. L., Tang K. Mining sequential patterns in the B2B environment. *Journal of Information Science*. 2009. Vol. 35, No. 6. P. 677–694. DOI: https://doi.org/10.1177/0165551509103600.
7. Система електронної комерції B2B «База взуття» : сайт. URL: https://bazaobuvi.com.ua/ua/ (дата звернення: 01.11.2025).
8. Cramer-Flood E. Global Ecommerce Forecast & Growth Projections. *Insider Intelligence*. URL: https://www.insiderintelligence.com/content/globalecommerce-forecast-2022 (дата звернення: 01.11.2025).
9. Agrawal R., Imieliński T., Swami A. Mining association rules between sets of items in large databases. *Proceedings of the 1993 ACM SIGMOD international conference on Management of data (SIGMOD '93)*. New York : ACM, 1993. P. 207–216. DOI: https://doi.org/10.1145/170035.170072.
10. Han J., Pei J., Yin Y. et al. Mining Frequent Patterns without Candidate Generation: A Frequent-Pattern Tree Approach. *Data Mining and Knowledge Discovery*. 2004. Vol. 8. P. 53–87. DOI: https://doi.org/10.1023/B:DAMI.0000005258.31418.83.
11. Zaki M. J. Scalable algorithms for association mining. *IEEE Transactions on Knowledge and Data Engineering*. 2000. Vol. 12, No. 3. P. 372–390. DOI: 10.1109/69.
12. Grow your B2B sales with 6 smart B2B product bundling strategies. *Turis*. URL: https://turis.app/b2b-ecommerce/grow-b2b-sales-6-b2b-product-bundle-strategies/ (дата звернення: 01.11.2025).
13. Bloomenthal A. SKU: What It Is and How It Works. *Investopedia*. URL: https://www.investopedia.com/terms/s/stock-keeping-unit-sku.asp (дата звернення: 15.06.2025).
14. Арсірій О. О., Любомська О. М., Руденко О. В., Іванов Д. В. Гібридна рекомендаційна система для підтримки UI/UX дизайнерів. *Одеська політехніка*. 2024. С. 29–35. DOI: https://doi.org/10.15276/ict.01.2024.30.
15. Koh Y. S., Rountree N. Rare Association Rule Mining and Knowledge Discovery: Technologies for Infrequent and Critical Event Detection. *IGI Global*, 2009. DOI: 10.4018/978-1-60566-754-6.
16. Larose D. T., Larose C. D. Discovering Knowledge in Data: An Introduction to Data Mining. Hoboken : John Wiley & Sons, Inc., 2014. DOI: 10.1002/9781118874059.
17. Sengupta D. et al. Association rule mining based study for identification of clinical parameters akin to occurrence of brain tumor. *Bioinformation*. 2013. Vol. 9 (11). P. 555–559. DOI: 10.6026/97320630009555.
18. Lakshmi K. S., Vadivu G. Extracting Association Rules from Medical Health Records Using Multi-Criteria Decision Analysis. *Procedia Computer Science*. 2017. Vol. 115. P. 290–295. DOI: https://doi.org/10.1016/j.procs.2017.09.137.
19. Zimek A., Assent I., Vreeken J. Frequent Pattern Mining Algorithms for Data Clustering. *Frequent Pattern Mining* / ed. by C. Aggarwal, J. Han. Springer, Cham, 2014. DOI: https://doi.org/10.1007/978-3-319-07821-2_16.
20. Heaton J. Comparing Dataset Characteristics that Favor the Apriori, Eclat or FP-Growth Frequent Itemset Mining Algorithms. *arXiv:1701.09042 [cs.DB]*. 2017. DOI: https://doi.org/10.48550/arXiv.1701.09042.

References

1. Shopify. (2025). *Global ecommerce statistics: Trends to guide your store in 2025*. https://www.shopify.com/enterprise/blog/global-ecommerce-statistics.
2. Insider Intelligence. (2025). *Mobile commerce shopping trends and stats*. Emarketer. www.emarketer.com.
3. Panasiuk, T. S., & Zubenko, I. R. (2024). Prospects for the development of b2c e-commerce in the world. https://doi.org/10.5281/zenodo.14603373.
4. Arsirii, O. O., Ivanov, D. V., & Babilunha, O. Y. (2025). Analysis of models, methods and technologies for creating personalized content in B2B e-commerce systems. *Informatyka. Kultura. Tekhnika*, *2*, 273–278. https://ict.op.edu.ua/index.php/journal/uk/issue/view/3.

ISSN 2076-2429 (print)
ISSN 2223-3814 (online)
Proceedings of Odessa Polytechnic University, Issue 2(72), 2025

5. Shveda, N. M., & Krauze, O. I. (2024). E-commerce: current state and development strategies. *Internauka. Series: Economic Sciences*, *2*(82). https://doi.org/10.25313/2520-2294-2024-2-9639.
6. Hu, Y. H., Chen, Y. L., & Tang, K. (2009). Mining sequential patterns in the B2B environment. *Journal of Information Science*, *35*(6), 677–694. https://doi.org/10.1177/0165551509103600.
7. Baza Obuvi. (n.d.). *B2B e-commerce system "Shoe Base"*. Retrieved November 2025, Retrieved from https://bazaobuvi.com.ua/ua/.
8. Cramer-Flood, E. (2022). *Global ecommerce forecast & growth projections*. Insider Intelligence. Retrieved from https://www.insiderintelligence.com/content/globalecommerce-forecast-2022.
9. Agrawal, R., Imieliński, T., & Swami, A. (1993). Mining association rules between sets of items in large databases. *Proceedings of the 1993 ACM SIGMOD International Conference on Management of Data*, 207–216. https://doi.org/10.1145/170035.170072.
10. Han, J., Pei, J., & Yin, Y. (2004). Mining frequent patterns without candidate generation: A frequent-pattern tree approach. *Data Mining and Knowledge Discovery*, *8*, 53–87. https://doi.org/10.1023/B:DAMI.0000005258.31418.83.
11. Zaki, M. J. (2000). Scalable algorithms for association mining. *IEEE Transactions on Knowledge and Data Engineering*, *12*(3), 372–390. DOI: 10.1109/69.
12. Turis. (n.d.). *Grow your B2B sales with 6 smart B2B product bundling strategies*. Retrieved from https://turis.app/b2b-ecommerce/grow-b2b-sales-6-b2b-product-bundle-strategies/.
13. Bloomenthal, A. (2025, June 15). *SKU: What it is and how it works*. Investopedia. https://www.investopedia.com/terms/s/stock-keeping-unit-sku.asp.
14. Arsirii, O. O., Liubomska, O. M., Rudenko, O. V., & Ivanov, D. V. (2024). Hybrid recommendation system to support UI/UX designers. *Odeska Politekhnika*, 29–35. https://doi.org/10.15276/ict.01.2024.30.
15. Koh, Y. S., & Rountree, N. (2009). *Rare association rule mining and knowledge discovery: Technologies for infrequent and critical event detection*. IGI Global. DOI 10.4018/978-1-60566-754-6.
16. Larose, D. T., & Larose, C. D. (2014). *Discovering knowledge in data: An introduction to data mining*. John Wiley & Sons, Inc. DOI 10.4018/978-1-60566-754-6.
17. Sengupta, D., Sood, M., Vijayvargia, P., Hota, S., & Naik, P. K. (2013). Association rule mining based study for identification of clinical parameters akin to occurrence of brain tumor. *Bioinformation*, *9*(11), 555–559. DOI 10.6026/97320630009555.
18. Lakshmi, K. S., & Vadivu, G. (2017). Extracting association rules from medical health records using multi-criteria decision analysis. *Procedia Computer Science*, *115*, 290–295. https://doi.org/10.1016/j.procs.2017.09.137.
19. Zimek, A., Assent, I., & Vreeken, J. (2014). Frequent pattern mining algorithms for data clustering. In C. Aggarwal & J. Han (Eds.), *Frequent pattern mining* (pp. 403–423). Springer, Cham. https://doi.org/10.1007/978-3-319-07821-2_16.
20. Heaton, J. (2017). *Comparing dataset characteristics that favor the Apriori, Eclat or FP-growth frequent itemset mining algorithms*. arXiv. https://doi.org/10.48550/arXiv.1701.09042.

Арсірій Олена Олександрівна; Olena Arsirii, ORCID: https://orcid.org/0000-0001-8130-9613
Іванов Дмитро Вячеславович; Dmitriy Ivanov, ORCID: https://orcid.org/0009-0009-3958-5310

Received November 03, 2025
Accepted November 29, 2025

ISSN 2076-2429 (print)
ISSN 2223-3814 (online)

UDC 004.896:629.735.05

O Babilunga, PhD, Assoc. Prof.,
D. Dmytrenko,
O. Andriianov, PhD, Assoc. Prof.
Odessa Polytechnic National University, Shevchenko Ave. 1, Odesa, Ukraine, 65044, e-mail: 4068167@stud.op.edu.ua

A METHOD FOR RATIONAL ROLE ALLOCATION IN A COMPUTER-VISION-ENABLED SWARM OF UNMANNED AERIAL VEHICLES UNDER RESOURCE CONSTRAINTS

О. Бабілунга, Д. Дмитренко, О. Андріянов. **Метод раціонального розподілу ролей у рої безпілотних літальних апаратів із комп'ютерним зором з урахуванням обмежених ресурсів.** Розподіл ролей у рої БПЛА з бортовим комп'ютерним зором ускладнюється тим, що «важкі» алгоритми сприйняття споживають енергію, займають обчислювальний ресурс і підвищують вимоги до радіоканалу. Для малорозмірних платформ це напряму пов'язано з обмеженнями розміру, маси та потужності (SWaP) і, як наслідок, зі скороченням часу польоту. Більшість практичних евристик вибирає виконавців ролей за геометрією або поточним зарядом і тому не враховує взаємозв'язок між енергетикою, обчисленнями та зв'язністю. У роботі запропоновано децентралізовану процедуру призначення ролей (Scout, Mapper, Relay, Worker), у якій кожен апарат формує ставку з урахуванням прогнозованих витрат на пропульсію, обчислення, сенсори та передачу даних, а також ризику зростання багатострибкової відстані до базової станції. Призначення виконується аукціонною процедурою з локальним узгодженням переможців між сусідніми агентами. Запроваджено правила допустимості, що відсікають призначення ролей при недостатньому запасі батареї або дефіциті обчислювального бюджету, і штраф за перемикання ролей для зменшення осциляцій. Метод перевірено у відтворюваній симуляції на ПК для роїв із 20 і 50 апаратів у межах області 1000×1000 м за обмеженого радіуса зв'язку та гетерогенних обчислювальних можливостей; оцінювалися SR, Time, CR, Conn і Sw. У складнішому сценарії (N=20) запропонований підхід забезпечує завершення місії (SR=1.00), тоді як геометрична евристика та статичний розподіл не досягають порогу (SR=0). Порівняно з SoC-евристикою метод зменшує Sw приблизно у 7–8 разів за збереження 100% успішності та прийнятної зв'язності з базою. Запропонована модель вартості може бути використана в системах керування роєм і надалі розширена на сценарії колективного сприйняття, коли частина апаратів виконує обчислювально важку обробку зору.

Ключові слова: ройова робототехніка, розподіл ролей, безпілотні літальні апарати, комп'ютерний зір, енергоменеджмент, обчислювальні обмеження, зв'язність мережі, децентралізована координація, моделювання, симуляційний експеримент

O. Babilunga, D. Dmytrenko, O. Andriianov. **A Method for Rational Role Allocation in a Computer-Vision-Enabled Swarm of Unmanned Aerial Vehicles Under Resource Constraints.** Role allocation in unmanned aerial vehicle swarms equipped with onboard vision is constrained not only by geometry but also by size, weight and power limits typical for small platforms. Vision pipelines increase energy draw, occupy the onboard compute budget and raise the demand on the wireless link. Heuristics that assign roles solely from distance or state of charge often overlook this coupling and may trigger unnecessary re-assignments. We propose a decentralized auction-based role allocation scheme (Scout, Mapper, Relay, Worker) where each vehicle computes a bid from (*i*) predicted energy cost for propulsion, sensing, computation and radio, and (*ii*) the risk of increasing the multi-hop distance to a base station. Feasibility checks prevent assigning vision-heavy roles to agents with insufficient battery reserve or compute capacity, and a switching penalty reduces oscillations. The approach is evaluated in a reproducible PC simulation (1000×1000 m area, limited communication range and heterogeneous computing capabilities) with swarms of 20 and 50 UAVs. We report mission success rate, completion time, mission progress, average base connectivity and the number of role switches. In the more challenging N=20 case the proposed method completes the mission (SR=1.00) while the distance-based and static baselines fail (SR=0). Compared with the battery-only heuristic, it preserves the same success rate but reduces role switching by about 7–8 while maintaining acceptable connectivity. For N=50 all methods succeed, yet the proposed approach keeps the number of switches at 310±52 versus 2386±320 for the battery-only baseline. The cost model can be integrated into swarm management systems and extended to collaborative perception, where a subset of vehicles performs vision-heavy processing and shares compact results under progressive battery depletion.

Keywords: swarm robotics, role allocation, unmanned aerial vehicles, computer vision, energy management, computational constraints, network connectivity, decentralized coordination, simulation, mission planning

1. Introduction

Unmanned aerial vehicles (UAVs) equipped with onboard computing modules (single-board computers, embedded GPUs, etc.) are increasingly used for computer-vision tasks: object detection and tracking, mapping, VIO/SLAM-based localization, and elements of collaborative perception. Integrating such algorithms increases energy consumption and the load on the onboard computer, and also raises the requirements for the wireless link. For small platforms this directly manifests as size, weight and power (SWaP) constraints: additional mass and power draw reduce endurance and decrease the available control authority margin.

In swarm systems these constraints interact with formation control, network connectivity mainte-

DOI: 10.15276/opu.2.72.2025.11

nance, and the distribution of functions among agents. Surveys in swarm robotics and formation control emphasize that scaling a swarm is not possible without decentralized coordination and information-exchange protocols [1, 2]. Role allocation enables specialization of subsets of vehicles: some perform scouting and data collection, others relay traffic and maintain the network, while others execute compute-intensive vision tasks. Common approaches include contract-net mechanisms, auction-based methods, and consensus algorithms such as CBBA [3, 4].

This paper proposes a decentralized role allocation approach for a UAV swarm with onboard vision that simultaneously accounts for predicted energy costs, available computing resources, and the risk of degrading multi-hop connectivity to a base station. In practical terms, an agent's bid is not reduced to "closer/farther" or "higher/lower SoC"; instead, it includes the expected costs of propulsion, data processing, sensing, and communication, as well as a penalty for frequent role switching. The novelty of the approach lies in combining these components within a single auction procedure together with feasibility rules that prevent assigning resource-intensive roles to energy- or compute-limited platforms. The workflow of the method is shown in Fig. 1.

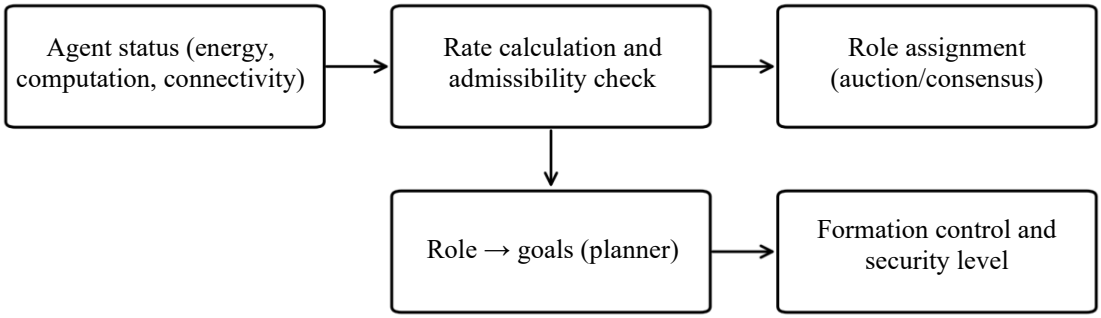

Fig. 1. Workflow of role allocation considering energy, computation, and connectivity

2. Literature review and problem statement

Designing UAVs with onboard computers requires reconciling size-weight and energy constraints with the demands of vision algorithms. Energy consumption and power-supply selection for UAVs are actively discussed in the literature, particularly in the context of mission endurance and flight profiles [5]. At the same time, modern camera-based navigation and mapping systems (VIO/SLAM), such as VINS-Mono and ORB-SLAM2, demonstrate high accuracy but require stable computing performance and, in collective settings, efficient mechanisms for data exchange [6, 7]. A related direction is energy-efficient sensing and computing (e.g., event cameras), which can potentially reduce power demand [8].

For UAV swarms, key challenges include formation control, cooperative trajectory planning, and maintaining network connectivity during maneuvering. Survey works [1, 2] summarize distributed control and coordination approaches and highlight the role of communication topology. Role and task allocation in multi-robot systems is often implemented via market-based mechanisms and auctions, which ensure scalability but require a well-defined cost function [3, 4]. However, in many publications the role/task cost is dominated by geometric or temporal factors (distance, time-to-arrival), while the energy price of onboard computation and the risk of losing connectivity to the base station are accounted for only indirectly or ignored. This gap defines the focus of the present study.

Classical works on Multi-Robot Task Allocation (MRTA) provide formal taxonomies and criteria for comparing task-allocation algorithms, which is useful for a correct problem formulation in UAV swarms [9, 10]. For scenarios with dynamic communication constraints, extensions of CBBA have been proposed that consider time windows, resource costs, and changing network topology [11], as well as approaches that reduce inter-agent communication to accelerate convergence [12] and methods that explicitly account for limited bandwidth and collisions in a shared channel [13]. A review of task allocation methods specifically for UAV systems is given in [14]. Despite substantial progress, most works still lack an integrated treatment of three groups of constraints: (*i*) energy (SoC and cost prediction), (*ii*) onboard computing (load from computer-vision pipelines), and (*iii*) connectivity requirements for delivering data to a base station. The proposed approach focuses on this integrated setting.

Problem statement. Let the swarm consist of N agents. For the i-th agent, the state $s_i(t)$ includes, in particular, the remaining battery charge $\mathrm{SoC}_i(t)$, the effective performance of the onboard computer

ISSN 2076-2429 (print)
ISSN 2223-3814 (online)

C_i, and local information about neighbors in the network. The goal is to assign roles $r_i(t) \in$ {Scout, Mapper, Relay, Worker} so as to maximize mission progress under the following constraints:

1) $SoC_i(t)$ does not drop below SoC_{min} given predicted expenditures;

2) roles with vision load do not exceed the available compute budget;

3) multi-hop connectivity to the base station is maintained to deliver data.

The problem is complicated by the fact that energy cost and compute demand depend on the role, while communication topology changes as agents move. For quantitative evaluation, we use PC-based simulation; examples of UAV simulation environments include AirSim and RotorS [15, 16].

3. Aim and objectives

The aim of this study is to develop a role allocation method for a UAV swarm with onboard vision computing that enables rational use of energy, computing, and communication resources.

To achieve this aim, the following tasks are addressed:

– define role profiles in terms of computing demand, traffic, and typical energy (SoC) consumption;

– build a resource-aware role cost model (energy + computation + connectivity) and feasibility rules;

– develop an auction-based role assignment procedure with a switching penalty;

– define a simulation evaluation protocol and compare the proposed method with baseline heuristics.

4. Materials and methods

The proposed method treats role assignment as a local decision made by each agent based on its own state and messages from neighbors. Every Δt seconds, an agent checks role feasibility with respect to battery reserve and compute budget, computes bids, and exchanges them with neighbors within communication range. After local agreement on winners (given role quotas), assignments are activated for the next control interval, while a switching penalty reduces oscillations in role composition.

4.1. Roles and resource profiles. Four roles are defined in the swarm: Scout, Mapper, Relay, and Worker. Each role is described by a profile of compute requirements, traffic demand, and typical relative state-of-charge consumption. The profiles used in this paper are listed in Table 1 (all values are given in relative units).

Table 1

Role profiles and resource requirements

Role	Main tasks	Compute demand (rel.)	Traffic (rel.)	SoC drain, 1/s
Scout	object search/detection, video data collection	1.5	1.0	0.0019
Mapper	SLAM/mapping, local map alignment	1.2	1.2	0.0016
Relay	packet relaying, connectivity maintenance	0.8	1.5	0.0012
Worker	tracking/coverage, auxiliary tasks	0.5	0.3	0.0010

4.2. Connectivity and local network model. The communication structure is modeled as an undirected graph $G(t) = (V, E(t))$, where vertices V correspond to agents and an edge $(i, j) \in E(t)$ exists if the distance between agents does not exceed the communication range R. The base station B is connected to agent i if $d(i, B) \le R$. An agent is considered connected to the base if there exists a path from i to B in the graph (multi-hop). The fraction of agents connected to the base is defined as $C_B(t) = N_B(t)/N$, where $N\_B(t)$ is the number of connected agents at time t. To assess network risk, we use the hop distance $h_i(t)$, i.e., the length of the shortest path from agent i to the base in $G(t)$ (if no path exists, we set $h_i(t) = \infty$). We deliberately use hop distance as a simple local metric: it can be obtained from neighbor messages without computationally expensive global network estimates.

4.3. Energy model and cost prediction. The agent's energy expenditure is decomposed into components associated with flight (propulsion), computation, communication, and sensing. At the level of instantaneous power:

$$P_i(t) = P_{i,\text{prop}}(t) + P_{i,\text{comp}}(r_i,t) + P_{i,\text{comm}}(r_i,t) + P_{i,\text{sens}}(r_i,t)\,. \quad (1)$$

To check feasibility and compute bids, we estimate the energy "price" of a role over a horizon H. In the simplest case, we use a prediction of the average power for role r and obtain:

$$E_{i,\text{pred}}(r,t) = P_i(r,t)\cdot H\,. \tag{2}$$

4.4. Computing constraints and load. Because some roles (Scout, Mapper) execute vision algorithms, we introduce the effective compute capability C_i of agent i and a relative role load $C(r)$. The normalized compute utilization is defined as:

$$u_i(r,t) = C(r)\,/\,C_i\,. \tag{3}$$

4.5. Role feasibility rules. Before participating in the auction, an agent discards roles that cannot be executed given the minimum battery reserve and the available compute resources. For role r, the feasibility conditions are:

$$\text{SoC}_i(t) - E_{i,\text{pred}}(r,t)\,/\,E_{i,\text{bat}} \geq \text{SoC}_{\min},\; u_i(r,t) \leq 1\,. \tag{4}$$

4.6. Bid function and switching penalty. For each feasible role, the agent forms a bid $b_i(r,t)$, which is maximized in the auction procedure (5). In (5), $U_i(r,t)$ is the role utility, $\bar{E}_i(r,t)$ is the normalized estimate of energy expenditure over horizon H, $\acute{L}_i(r,t)$ is the normalized estimate of the risk of degrading connectivity to the base station, and $J_{i,\text{sw}}$ is the penalty for changing roles (to reduce assignment oscillations). Normalization is introduced so that no term dominates solely due to its scale: $\bar{E}_i(r,t)=E_{i,\text{pred}}(r,t)/(\text{SoC}_i(t)-\text{SoC}_{\min}+\varepsilon)$, $\acute{L}_i(r,t)=\min(1,\; h_i\text{^pred}(r,t)/h_{\max})$, where h_i^pred is the predicted shortest-path length (in hops) from agent i to the base after one motion step in role r, h_max is a threshold (in our experiments $h_{\max}=6$), and $\varepsilon=10\text{^}-3$. For brevity, the arguments (r,t) in the right-hand side of (5) are omitted.

$$b_i(r,t) = U_i - \alpha\cdot\bar{E}_i - \beta\cdot u_i - \gamma\cdot\acute{L}_i - J_{i,sw}\,. \tag{5}$$

4.7. Auction-based role assignment. At each replanning step t, the agent computes bids for all feasible roles and sends to its neighbors messages of the form ⟨role, bid, agent identifier, timestamp⟩. Agreement is implemented as an iterative max-consensus procedure: for each role and its quota K_r, agents exchange the best known candidates over L_c communication rounds, after which a consistent winner list is formed. Conflicts are resolved by priority (higher bid; if equal, lower identifier). In our experiments we use L_c=5 (Table 2), which provides stable agreement within the local communication range.

Table 2

Simulation parameters

Parameter	Symbol	Value
Mission area size	L	1000×1000 m
Speed (simplified)	v	5 m/s
Energy prediction horizon	H	20 s
Consensus iterations	L_c	5
Agent compute resources (rel.)	C_i	40%: 1.5; 60%: 1.0
Simulation time	T	600 s
Replanning step	Δt	5 s
Initial state of charge	$\text{SoC}_i(0)$	1.0
Mission progress threshold	M_{th}	1000 a.u.
Communication range	R	180 m
Minimum battery reserve	$\text{SoC}_{\min}$	0.10
Number of agents	N	20 and 50
Role quotas (N=20)	K	Scout=2, Mapper=2, Relay=3
Role quotas (N=50)	K	Scout=5, Mapper=5, Relay=7

The penalty $J_{i,\text{sw}}$ reduces frequent re-assignments and the associated overhead (communication/replanning) and decreases the risk of control instability. The overall role-consensus procedure is given as pseudocode in Algorithm 1 – Decentralized SWaP-aware role allocation (CBBA-like):

Input: roles R with quotas K_r; weights $w=(\alpha,\beta,\gamma,\eta)$; prediction horizon H; threshold $\text{SoC}_{\min}$; communication graph $G(t)$.

Output: role assignment $r_i(t)$ for each agent i.

ISSN 2076-2429 (print)
ISSN 2223-3814 (online)

For each replanning epoch t:

1. (Evaluation) each agent i forms the set of feasible roles $F_i(t)$ and bids $b_i(r,t)$ according to (5).
2. (Initial bid) agent i ranks roles in descending order of b_i and chooses the current proposal $r_i \leftarrow \text{argmax}\_r\ b_i(r,t)$.
3. Repeat until convergence or maxiter:
   3.1. (Exchange) send neighbors a message $m\_i=(i, r_i, b_i(r_i), t)$.
   3.2. (Local ranking) based on received $\{m\_j\}$, build for each role r a candidate list and locally select winners W_r – the K_r best bids (ties are resolved by ID).
   3.3. (Max-consensus) agree on Wr with neighbors; if Wr changes, continue iterations.
   3.4. (Try alternatives) if agent i is not in W_{ri}, remove ri from the local list and choose the next best role; if $F_i(t)$ is empty, set $ri \leftarrow$ Worker.
4. After convergence, each agent adopts role $ri(t)$ according to the agreed winner sets Wr.

Simulation protocol and baselines. The evaluation is performed in an agent-based PC simulation over a time interval T=600 s with replanning every Δt=5 s. The motion and network models are described in Sections 4.2…4.4, while the vision workload is parameterized (without running real inference) through the compute and bandwidth requirements in Table 1. For a fair comparison, all methods use the same feasibility rules (4) with respect to battery reserve and compute budget; the methods differ in the bidding/selection criterion and in the re-assignment mechanism. The mission completion threshold is set to M_{th}=1000 arbitrary units. The experiment parameters are given in Table 2.

Mission progress model. Let $n_S(t)$ and $n_M(t)$ denote the number of agents with roles Scout and Mapper, respectively, that have a path to the base station (i.e., $h_i(t) \le h_{\max}$). The accumulated mission progress $M(t)$ (arbitrary units) is updated discretely with step Δt according to:

$$M(t+\Delta t) = M(t) + \Delta t \cdot (w_S \cdot n_S(t) + w_M \cdot n_M(t)). \quad (6)$$

Initially, $M(0)$=0, and the mission is considered completed if $M(t) \ge M_{th}$.

The proposed approach is compared with three baseline methods: (1) “Distance” – role assignment using a geometric heuristic with quotas (Scout – farthest from the base; Mapper – closest; Relay – intermediate distances); (2) “Battery level” – role assignment based solely on maximum SoC, without explicit connectivity consideration and without a switching penalty; (3) “Static roles” – a fixed role distribution at the start, without replanning. The proposed method is denoted as “SWaP-aware”.

5. Results and discussion

5.1. Evaluation metrics. We use the following metrics: SR – share of successful runs (reaching the threshold M_th within time T); Time – mean completion time (s); CR – relative mission progress at the end of the simulation ($M(T)/M$_th); Conn – mean fraction of agents connected to the base ($c\_B(t)$); Sw – total number of role switches in the swarm. Additionally, to characterize resource use we report: ΔSoC_avg – mean battery charge consumed per agent per run; SoC_min,end – minimum SoC among agents at completion; Viol – number of violations of feasibility rules (4); VisionHigh – share of Scout/Mapper assignments to agents with sufficient compute resources. Summary results are given in Tables 3 and 4, and an ablation study is reported in Table 5.

Table 3

Comparison of methods by main metrics (mean ± std over 12 runs)

Method	N	SR	Time, s	CR	Conn	Sw
SWaP-aware	20	1.00	443.8±22.4	1.00	0.92±0.03	115±18
Distance	20	0.00	600.0	0.84	0.78±0.05	344±41
Battery level	20	1.00	395.0±19.1	1.00	1.00±0.00	953±175
Static roles	20	0.00	600.0	0.77	0.82±0.04	0
SWaP-aware	50	1.00	182.1±14.7	1.00	0.87±0.04	310±52
Distance	50	1.00	276.7±18.9	1.00	0.79±0.05	365±49
Battery level	50	1.00	160.0±12.4	1.00	1.00±0.00	2386±320
Static roles	50	1.00	275.8±16.4	1.00	0.83±0.04	0

5.2. Quantitative comparison. Table 3 shows that for the N=20 swarm the static distribution and the “Distance” heuristic do not reach the threshold within time T (SR=0.00), whereas SWaP-aware and “Battery level” achieve SR=1.00. At the same time, SWaP-aware substantially reduces assignment oscillations: Sw=115±18 versus 953±175 for the SoC-only heuristic (about 8.3× fewer switches), while maintaining high mean connectivity (Conn=0.92±0.03). Table 4 shows that all methods satisfy the feasibility rules (Viol=0) and assign Scout/Mapper only to agents with sufficient compute resources (VisionHigh=100%). From an energy perspective, the SoC-only heuristic predictably main-

tains a higher minimum charge (SoC_min,end≈0.28), but at the cost of a much larger number of re-assignments.

Table 4

Energy and computing metrics (mean ± std over 12 runs)

Method	N	ΔSoC_{avg}	$SoC_{min,end}$	Viol	VisionHigh, %
SWaP-aware	20	0.52±0.04	0.16±0.03	0	100
Distance	20	0.71±0.05	0.10±0.00	0	100
Battery level	20	0.47±0.06	0.28±0.04	0	100
Static roles	20	0.70±0.04	0.10±0.00	0	100
SWaP-aware	50	0.22±0.02	0.65±0.04	0	100
Distance	50	0.33±0.03	0.48±0.06	0	100
Battery level	50	0.19±0.03	0.72±0.03	0	100
Static roles	50	0.33±0.03	0.47±0.05	0	100

Table 5

Ablation study of SWaP-aware (N=20; mean ± std over 12 runs)

Variant	SR	Time, s	CR	Conn	Sw
Full (α,β,γ,η)	1.00	443.8±22.4	1.00	0.92±0.03	115±18
No network term (γ=0)	0.75	548.0±34.6	0.93±0.05	0.80±0.06	138±25
No switching penalty (η=0)	1.00	412.5±20.1	1.00	0.91±0.04	740±120

For N=50 all methods reach the threshold (SR=1.00), yet differences appear in assignment stability and network quality. The SoC-only heuristic achieves Conn≈1.00, but at the cost of a very large number of switches (Sw=2386±320). SWaP-aware reduces Sw to 310±52 (about 7.7× fewer switches) while preserving high connectivity (0.87±0.04). The ablation study (Table 5) shows that removing the network term (γ=0) degrades connectivity and success rate, while removing the switching penalty (η=0) causes a sharp increase in Sw. To illustrate the mission progress dynamics for N=20, Fig. 2 shows a representative single run.

Figure 2 shows a typical example (one run) of the mission progress dynamics for N=20. In this run, the adaptive methods “SWaP-aware” and “Battery level” reach the completion threshold M_{th}, while the “Distance” and “Static roles” baselines exhibit long plateaus due to episodes of degraded network connectivity. Aggregate (mean ± std over 12 runs) values of CR and Time are reported in Table 3. Base-station connectivity for the same run is shown in Fig. 3.

Figure 3 illustrates the influence of role assignment on maintaining connectivity to the base station. In the shown run, “SWaP-aware” provides more stable connectivity compared to the “Distance” baseline, for which deeper and longer intervals of reduced connectivity are observed. This degrades data delivery to the base and slows down mission progress in Fig. 2. The number of role switches (Sw) is reported in Table 3.

5.3. Discussion and limitations. The results indicate that for swarms with onboard computers it is important to jointly consider energy, computing load, and connectivity. The ablation study (Table 5) shows that the network term $\gamma \acute{L}_i$ is critical for sparse-topology scenarios (N=20), while the switching penalty η limits oscillations without a noticeable loss in SR. Nevertheless, the study has several limitations: (1) the vision profiles are parameterized and do not include real neural-network inference; (2) the communication and motion models are simplified and do not account for obstacles, varying throughput, or delays; (3) the evaluation is simulation-only, without hardware validation. Future work includes integration with AirSim/RotorS and experiments with real onboard computers and cameras. It is also worth noting that in the current configuration computing constraints do not become a bottleneck (Table 4: Viol=0; VisionHigh=100%), therefore their impact should be further evaluated in scenarios with stronger compute heterogeneity and possible throttling.

ISSN 2076-2429 (print)
ISSN 2223-3814 (online)

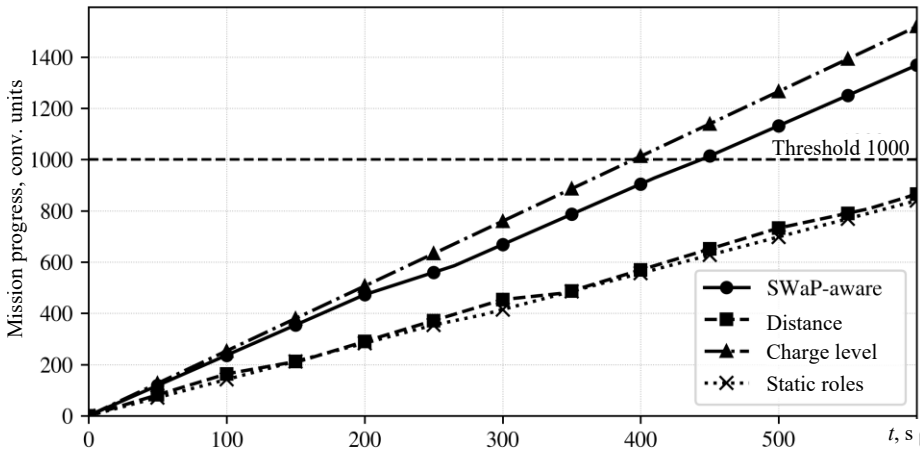

Fig. 2. Mission progress over time for N=20 (single run; threshold d = 1000)

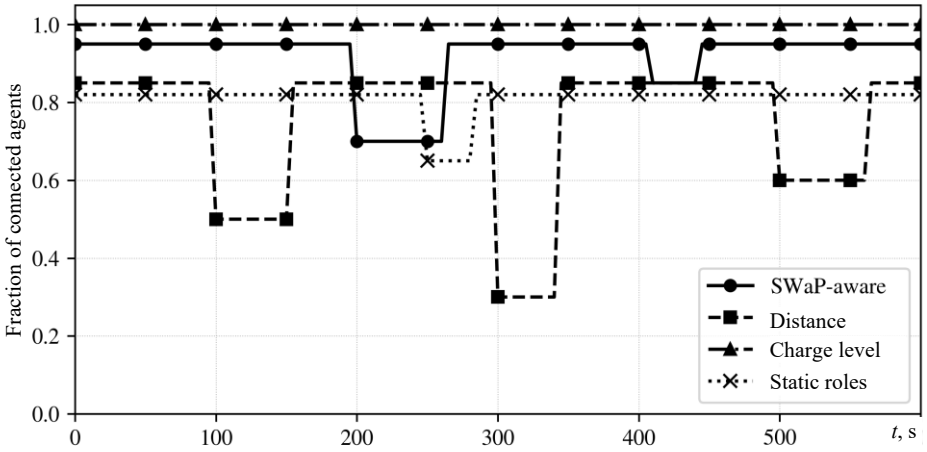

Fig. 3. Base-station connectivity over time for N=20 (fraction of connected agents; same run as in Fig. 2)

6. Conclusions

In summary, this paper proposes a decentralized role allocation method for a computer-vision-enabled UAV swarm that combines energy, computing, and network factors within a single assignment procedure. The main results can be summarized as follows:

– role profiles and a resource cost model covering propulsion, computation, sensing, and data transmission are formulated;

– feasibility rules and a bid function with normalized penalties for energy, network risk, and role switching are proposed;

– in simulation, the method achieves SR=1.00 for N=20 and N=50; in the more challenging N=20 scenario it outperforms the geometric heuristic and the static distribution (SR=0), and compared with the SoC-only heuristic it substantially reduces role switching (115±18 vs. 953±175 for N=20 and 310±52 vs. 2386±320 for N=50) while maintaining acceptable connectivity;

– future steps are outlined: more realistic channel and delay models, integration with AirSim/RotorS, and hardware experiments on onboard platforms.

Література

1. A Survey on Aerial Swarm Robotics / S.-J. Chung, A. A. Paranjape, P. Dames et al. *IEEE Transactions on Robotics*. 2018. Vol. 34, no. 4. P. 837–855. DOI: 10.1109/TRO.2018.2857475.
2. Oh K.-K., Park M.-C., Ahn H.-S. A Survey of Multi-Agent Formation Control. *Automatica*. 2015. Vol. 53. P. 424–440. DOI: 10.1016/j.automatica.2014.10.022.

3. Choi H.-L., Brunet L., How J. P. Consensus-Based Decentralized Auctions for Robust Task Allocation. *IEEE Transactions on Robotics*. 2009. Vol. 25, no. 4. P. 912–926. DOI: 10.1109/TRO.2009.2022423.
4. Market-Based Multirobot Coordination: A Survey and Analysis / M. B. Dias, R. Zlot, N. Kalra, A. Stentz. *Proceedings of the IEEE*. 2006. Vol. 94, no. 7. P. 1257–1270. DOI: 10.1109/JPROC.2006.876939.
5. Boukoberine M. N., Zhou Z., Benbouzid M. E. H. A Critical Review on Unmanned Aerial Vehicle Power Supply and Energy Management: Solutions, Strategies, and Prospects. *Applied Energy*. 2019. Vol. 255. 113823. DOI: 10.1016/j.apenergy.2019.113823.
6. Qin T., Li P., Shen S. VINS-Mono: A Robust and Versatile Monocular Visual-Inertial State Estimator. *IEEE Transactions on Robotics*. 2018. Vol. 34, no. 4. P. 1004–1020. DOI: 10.1109/TRO.2018.2853729.
7. Mur-Artal R., Tardós J. D. ORB-SLAM2: An Open-Source SLAM System for Monocular, Stereo, and RGB-D Cameras. *IEEE Transactions on Robotics*. 2017. Vol. 33, no. 5. P. 1255–1262. DOI: 10.1109/TRO.2017.2705103.
8. Fully neuromorphic vision and control for autonomous drone flight / F. Paredes-Vallés, J. J. Hagenaars, J. Dupeyroux et al. *Science Robotics*. 2024. Vol. 9. eadi0591. DOI: 10.1126/scirobotics.adi0591.
9. Gerkey B. P., Matarić M. J. A Formal Analysis and Taxonomy of Task Allocation in Multi-Robot Systems. *The International Journal of Robotics Research*. 2004. Vol. 23, no. 9. P. 939–954. DOI: 10.1177/0278364904045564.
10. Korsah G. A., Stentz A., Dias M. B. A Comprehensive Taxonomy for Multi-Robot Task Allocation. *The International Journal of Robotics Research*. 2013. Vol. 32, no. 12. P. 1495–1512. DOI: 10.1177/0278364913496484.
11. Decentralized Planning for Complex Missions with Dynamic Communication Constraints / S. Ponda, J. Redding, H.-L. Choi et al. *Proc. of the 2010 American Control Conference (ACC)*. 2010. P. 3998–4003. DOI: 10.1109/ACC.2010.5531232.
12. Kim K.-S., Kim H.-Y., Choi H.-L. Minimizing Communications in Decentralized Greedy Task Allocation. *Journal of Aerospace Information Systems*. 2019. Vol. 16, no. 8. P. 340–345. DOI: 10.2514/1.I010624.
13. Raja S., Habibi G., How J. P. Communication-Aware Consensus-Based Decentralized Task Allocation in Communication Constrained Environments. *IEEE Access*. 2022. Vol. 10. P. 19753–19767. DOI: 10.1109/ACCESS.2021.3138857.
14. Skaltsis G. M., Shin H.-S., Tsourdos A. A Review of Task Allocation Methods for UAVs. *Journal of Intelligent & Robotic Systems*. 2023. Vol. 109. Article 76. DOI: 10.1007/s10846-023-02011-0.
15. Shah S., Dey D., Lovett C., Kapoor A. AirSim: High-Fidelity Visual and Physical Simulation for Autonomous Vehicles. *Field and Service Robotics*. Springer, 2017. P. 621–635. DOI: 10.1007/978-3-319-67361-5_40.
16. Furrer F., Burri M., Achtelik M., Siegwart R. RotorS — A Modular Gazebo MAV Simulator Framework. *Simulation, Modeling, and Programming for Autonomous Robots*. Springer, 2016. P. 595–625. DOI: 10.1007/978-3-319-26054-9_23.

References

1. Chung, S.-J., Paranjape, A. A., Dames, P., Shen, S., & Kumar, V. (2018). A survey on aerial swarm robotics. *IEEE Transactions on Robotics*, *34*(4), 837–855. https://doi.org/10.1109/TRO.2018.2857475.
2. Oh, K.-K., Park, M.-C., & Ahn, H.-S. (2015). A survey of multi-agent formation control. *Automatica*, *53*, 424–440. https://doi.org/10.1016/j.automatica.2014.10.022.
3. Choi, H.-L., Brunet, L., & How, J. P. (2009). Consensus-based decentralized auctions for robust task allocation. *IEEE Transactions on Robotics*, *25*(4), 912–926. https://doi.org/10.1109/TRO.2009.2022423.
4. Dias, M. B., Zlot, R., Kalra, N., & Stentz, A. (2006). Market-based multirobot coordination: A survey and analysis. *Proceedings of the IEEE*, *94*(7), 1257–1270. https://doi.org/10.1109/JPROC.2006.876939.
5. Boukoberine, M. N., Zhou, Z., & Benbouzid, M. E. H. (2019). A critical review on unmanned aerial vehicle power supply and energy management: Solutions, strategies, and prospects. *Applied Energy*, *255*, Article 113823. https://doi.org/10.1016/j.apenergy.2019.113823.
6. Qin, T., Li, P., & Shen, S. (2018). VINS-Mono: A robust and versatile monocular visual-inertial state estimator. *IEEE Transactions on Robotics*, *34*(4), 1004–1020. https://doi.org/10.1109/TRO.2018.2853729.

ISSN 2076-2429 (print)
ISSN 2223-3814 (online)

7. Mur-Artal, R., & Tardós, J. D. (2017). ORB-SLAM2: An open-source SLAM system for monocular, stereo, and RGB-D cameras. *IEEE Transactions on Robotics*, *33*(5), 1255–1262. https://doi.org/10.1109/TRO.2017.2705103.
8. Paredes-Vallés, F., Hagenaars, J. J., Dupeyroux, J., Stroobants, S., Xu, Y., & de Croon, G. C. H. E. (2024). Fully neuromorphic vision and control for autonomous drone flight. *Science Robotics*, *9*(86), Article eadi0591. https://doi.org/10.1126/scirobotics.adi0591.
9. Gerkey, B. P., & Matarić, M. J. (2004). A formal analysis and taxonomy of task allocation in multi-robot systems. *The International Journal of Robotics Research*, *23*(9), 939–954. https://doi.org/10.1177/0278364904045564.
10. Korsah, G. A., Stentz, A., & Dias, M. B. (2013). A comprehensive taxonomy for multi-robot task allocation. *The International Journal of Robotics Research*, *32*(12), 1495–1512. https://doi.org/10.1177/0278364913496484.
11. Ponda, S., Redding, J., Choi, H.-L., How, J. P., Vavrina, M., & Vian, J. (2010). Decentralized planning for complex missions with dynamic communication constraints. In *Proceedings of the 2010 American Control Conference (ACC)* (pp. 3998–4003). IEEE. https://doi.org/10.1109/ACC.2010.5531232.
12. Kim, K.-S., Kim, H.-Y., & Choi, H.-L. (2019). Minimizing communications in decentralized greedy task allocation. *Journal of Aerospace Information Systems*, *16*(8), 340–345. https://doi.org/10.2514/1.I010624.
13. Raja, S., Habibi, G., & How, J. P. (2022). Communication-aware consensus-based decentralized task allocation in communication constrained environments. *IEEE Access*, *10*, 19753–19767. https://doi.org/10.1109/ACCESS.2021.3138857.
14. Skaltsis, G. M., Shin, H.-S., & Tsourdos, A. (2023). A review of task allocation methods for UAVs. *Journal of Intelligent & Robotic Systems*, *109*, Article 76. https://doi.org/10.1007/s10846-023-02011-0.
15. Shah, S., Dey, D., Lovett, C., & Kapoor, A. (2017). AirSim: High-fidelity visual and physical simulation for autonomous vehicles. In *Field and Service Robotics* (pp. 621–635). Springer.
16. Furrer, F., Burri, M., Achtelik, M., & Siegwart, R. (2016). RotorS—A modular Gazebo MAV simulator framework. In *Simulation, Modeling, and Programming for Autonomous Robots* (pp. 595–625). Springer. https://doi.org/10.1007/978-3-319-26054-9_23.

Бабілунга Оксана Юріївна; Oksana Babilunga, ORCID: https://orcid.org/0000-0001-6431-3557
Дмитренко Дмитро Олександрович; Dmytro Dmytrenko, ORCID: https://orcid.org/0009-0004-9948-9682
Андріянов Олександр Вікторович; Oleksandr Andriianov, ORCID: https://orcid.org/0000-0001-7037-0523

Received November 05, 2025

Accepted December 01, 2025

UDC 621.39:004.62

S. Nesterenko, DSc, Prof.,
O. Naumov
Odessa Polytechnic National University, Shevchenko Ave. 1, Odesa, Ukraine, 65044, e-mail: sa.nesterenko@ukr.net

MODBUS TCP BACKBONE THROUGHPUT ANALYSIS FOR NOISY IEEE 802.11 WIRELESS CHANNEL

С. Нестеренко, О. Наумов. **Аналіз пропускної здатності магістральної мережі "Modbus TCP" для шумного бездротового каналу IEEE 802.11.** Застосування високошвидкісних безпровідних каналів IEEE 802.11 (802.11n/ac/ax) для магістралі Modbus TCP в автоматизованих системах управління промисловими підприємствами (АСУТП) потребує оцінки продуктивності магістралі в умовах роботи каналів зв'язку з урахуванням особливостей функціонування АСУТП, де присутній високий рівень бітових помилок у каналах зв'язку. На основі аналізу алгоритмічної структури магістралі та часових діаграм передавання в безпровідному каналі отримано аналітичні залежності для розрахунку часу транзакції та пропускної здатності магістралі для реального безпровідного каналу. Проведено аналіз пропускної здатності магістралі для типових операцій з урахуванням різного рівня бітових помилок – Bit error rate (BER) у безпровідному каналі зв'язку. Виділено класи операцій магістралі Modbus TCP (прості та складені). Показано, що складені операції формуються як композиція певної кількості простих операцій. На відміну від моделей з ідеальними каналами зв'язку, у моделях для реальних каналів враховано механізми повторної передавання кадрів і додаткові затримки, пов'язані з бітовими помилками під час передавання інформації. Отримані вирази для часу виконання операцій і пропускної здатності дають змогу оцінити реальну продуктивність магістралі Modbus TCP для безпровідних каналів з помилками. Проведений розрахунок пропускної здатності демонструє суттєвий вплив бітових помилок на пропускну здатність магістралі для одноканальних і мультиканальних реалізацій магістралі Modbus TCP на базі безпровідних каналів сімейства IEEE 802.11. Отримані аналітичні залежності часу виконання типових операцій і пропускної здатності магістралі є інструментом для вибору оптимальних конфігурацій під час проєктування та модернізації промислових мереж на базі безпровідних реалізацій магістралі Modbus TCP у межах концепції «Індустрія 4.0».

Ключові слова: Modbus TCP, стандарт IEEE 802.11, АСУТП, алгоритмічна структура, час транзакції, пропускна здатність, прості та складені операції, бітові помилки, повторна передача

S. Nesterenko, O. Naumov. **Modbus TCP backbone throughput analysis for noisy IEEE 802.11 wireless channel.** The use of high-speed wireless IEEE 802.11 channels (802.11n/ac/ax) for the Modbus TCP backbone in automated control systems of industrial enterprises (APCS) requires an assessment of backbone performance under communication channel operating conditions, taking into account the specific features of APCS operation, where a high level of bit errors is present in the communication channels. Based on an analysis of the algorithmic structure of the backbone and transmission timing diagrams in a wireless channel, analytical relationships were obtained for calculating transaction time and backbone throughput for a real wireless channel. An analysis of the backbone throughput for typical operations was carried out, taking into account different levels of bit error rate (BER) in the wireless communication channel. Classes of Modbus TCP backbone operations (simple and composite) are identified. It is shown that composite operations are formed as a composition of a certain number of simple operations. Unlike models with ideal communication channels, models for real channels take into account frame retransmission mechanisms and additional delays associated with bit errors during information transmission. The obtained expressions for operation execution time and throughput make it possible to assess the real performance of the Modbus TCP backbone for wireless channels with errors. The performed throughput calculation demonstrates a significant impact of bit errors on the backbone throughput for single-channel and multi-channel implementations of the Modbus TCP backbone based on wireless channels of the IEEE 802.11 family. The obtained analytical relationships for the execution time of typical operations and backbone throughput represent a tool for selecting optimal configurations in the design and modernization of industrial networks based on wireless implementations of the Modbus TCP backbone within the framework of the "Industry 4.0" concept.

Keywords: Modbus TCP, IEEE 802.11 standard, APCS, algorithmic structure, transaction time, throughput, simple and composite operations, bit errors, retransmission

1. Introduction

The implementation of the "Industry 4.0" concept requires ensuring reliable data transmission with deterministic temporal characteristics at all levels of automated control systems of industrial enterprises (APCS). In accordance with the IEC/ISO 62264 classification, the APCS architecture represents a hierarchical structure of five levels, where the lower levels include SCADA systems and local subsystems with controllers, sensors, and actuators. In modern industrial networks, there is a predominance of high-speed H2-class backbones, among which solutions based on the Modbus TCP protocol occupy a dominant position. In parallel with this, there is active adoption of wireless technologies compliant with the IEEE 802.11 standards.

The application of IEEE 802.11 family wireless channels for implementing industrial communication backbones is driven by a combination of technical and economic factors: reduction of capital expenditures on cable infrastructure deployment, increased network topology flexibility, and simpli-

DOI: 10.15276/opu.2.72.2025.12

ISSN 2076-2429 (print)
ISSN 2223-3814 (online)

fied reconfiguration procedures during production system modernization. However, the specifics of the industrial operating environment are characterized by the presence of significant levels of electromagnetic interference from power equipment, multipath propagation of radio signals due to reflections from metal structures, as well as temporal instability of channel parameters. The combination of these factors leads to a substantial increase in the bit error rate (BER), the values of which in industrial conditions can reach the range of $10^{-4}…10^{-6}$, which is several orders of magnitude higher than the indicators for office and residential applications of Wi-Fi technology.

Existing analytical models for the performance of IEEE 802.11 wireless networks are based on the assumption of stochastic multiple access of stations to a shared transmission medium and account for probabilistic characteristics of collisions during contention-based access via the CSMA/CA mechanism. The architecture of Modbus TCP networks fundamentally differs in its strictly deterministic "master station – slave devices" interaction scheme, in which all transactions are initiated exclusively by the master station, eliminating the possibility of collisions between requests. This fundamental difference renders classical random multiple access models inapplicable for accurate evaluation of the performance of Modbus TCP backbones implemented over wireless channels, creating a methodological gap between the theoretical apparatus for analyzing wireless networks and the practical tasks of designing industrial automation systems.

2. Literature Review and Problem Statement

There is a significant number of works devoted to modeling the temporal characteristics and throughput of wireless channels of the IEEE 802.11 standard.

In paper [1], an analytical model is presented for calculating the maximum theoretical throughput of IEEE 802.11 under ideal conditions. The model takes into account the size of transmitted data, overhead associated with physical- and MAC-layer headers, interframe intervals, and transmission deferral time. It is shown that for IEEE 802.11a with a nominal data rate of 54 Mbit/s, the actual throughput does not exceed 25 Mbit/s, which is only 46% of the physical layer transmission rate.

Study [2] extends the analytical model by considering different medium access mechanisms (CSMA/CA and RTS/CTS). It is shown that the use of the RTS/CTS mechanism further reduces throughput by 20…25% due to the transmission of additional control frames.

In paper [3], a stochastic Markov model is proposed for analyzing the throughput of IEEE 802.11 DCF under conditions of station contention for medium access, taking collisions into account. The model makes it possible to calculate the transmission probability and collision probability as functions of the number of competing stations. It is established that when the number of stations increases from 5 to 50, throughput with the basic access method decreases by 15…20%, whereas the RTS/CTS mechanism provides more stable performance. The prediction accuracy of the model reaches up to 10…12% under various traffic load scenarios.

All the considered models describe scenarios with multiple random access of stations to the wireless channel, where throughput strongly depends on the number of competing stations and the probability of collisions. The Modbus TCP network architecture fundamentally differs due to its centralized "master station – slave devices" topology, in which all transactions are initiated exclusively by the master station. This eliminates collisions between requests and makes classical multiple-access models inapplicable for accurate evaluation of the throughput of a Modbus backbone over a Wi-Fi channel.

The relevance of studying the temporal characteristics and throughput of the Modbus TCP backbone when using wireless channels of the IEEE 802.11 family is determined by the need to account for real industrial environment conditions with a high level of bit errors. Of particular importance is the development of mathematical models for real wireless channels of automated control systems of industrial enterprises and the analysis of the impact of the bit error rate (BER) on the temporal parameters of backbone operation, including the study of the dependence of backbone throughput on the bit error intensity in the transmission channel.

The obtained results make it possible to select the required configuration of wireless channels to ensure specified temporal characteristics while taking into account the existing level of bit errors in the transmission medium during the design and modernization of industrial networks based on wireless implementations of the Modbus TCP backbone in accordance with the principles of the "Industry 4.0" concept.

3. The purpose and objectives of the research

The aim of this work is to develop and study mathematical models of the throughput of the Modbus TCP backbone when using wireless channels of the IEEE 802.11 standard, taking into account the

impact of bit errors in the communication channel on transaction time. The model development considers the operational features of the backbone, which operates according to a master-slave scheme, eliminating collisions in the channel and ensuring a deterministic method of access to slave devices. The developed mathematical models allow evaluating the performance of the backbone under various levels of bit errors in the communication channel for both single-channel and multi-channel configurations of wireless channels within the IEEE 802.11 family. The obtained models enable the design of automated control system subsystems with the required performance based on the Modbus TCP backbone using wireless channels of the IEEE 802.11 standard.

4. Materials and methods of the research

Modbus TCP is an industrial data exchange protocol that implements a client-server architecture in automated systems based on the TCP/IP protocol stack [4]. This protocol is an extension of the Modbus RTU protocol for operation in a TCP/IP environment and provides reliable high-speed information transfer between control devices and actuator modules in industrial automation systems.

When using IEEE 802.11 wireless technologies as the physical and data link layer protocols, Modbus TCP enables data transmission without the need for wired connections, significantly increasing the mobility and flexibility of industrial systems. Wireless communication channels of the IEEE 802.11 family retain all functional advantages of the Modbus TCP protocol, including ease of implementation, compatibility with Ethernet networks, and low deployment cost, making them a promising solution for industrial automation within the framework of the Industry 4.0 concept [5, 6].

The Modbus TCP protocol supports the transmission of control commands, data collection and processing, as well as diagnostic functions to improve the reliability of automated systems. Within the OSI model [7], the protocol uses five layers: application, transport, network, data link, and physical, where each layer contributes to the overall throughput and transaction time characteristics of the backbone. The structure of the application layer packet is shown in Fig. 1.

The application layer header H1 (Header 1) contains control information, including the transaction identifier, device address, and operation code. The data field D has a size ranging from 1 to *N* bytes, depending on the type of operation code in the H1 field.

The structure of the transport layer packet is shown in Fig. 2.

The transport layer header H2 (Header 2) is 20 bytes in size and contains control information, including fields such as the sender and receiver port numbers, packet sequence number, acknowledgment window size, header checksum, and data urgency pointer.

The structure of the network layer packet is shown in Fig. 3.

H1 (8 bytes)	D (*N* bytes)

Fig. 1. Application layer packet structure

H2 (20 bytes)	H1 (8 bytes)	D (*N* bytes)

Fig. 2. Transport layer packet structure

H3 (20 bytes)	H2 (20 bytes)	H1 (8 bytes)	D (*N* bytes)

Fig. 3. Network layer packet structure

The network layer header H3 (Header 3) is 20 bytes in size and contains control information, including the protocol version, header length, header checksum, sender IP address, and receiver IP address.

The structure of the data link layer packet is shown in Fig. 4 [8].

H4 (30 bytes)	H3 (20 bytes)	H2 (20 bytes)	H1 (8 bytes)	D (*N* bytes)	FSC (4 bytes)

Fig. 4. Data link layer packet structure

The data link layer header H4 (Header 4) contains the receiver and sender addresses, frame type, wireless channel occupancy time, and sequence number of the transmission. The frame checksum field (FSC) is used to detect errors at the data link layer [9].

The structure of the physical layer packet is shown in Fig. 5.

Preamble	PHeader	H4 (30 bytes)	H3 (20 bytes)	H2 (20 bytes)	H1 (8 bytes)	D (*N* bytes)	FSC (4 bytes)

Fig. 5. Physical layer packet structure

ISSN 2076-2429 (print)
ISSN 2223-3814 (online)

The Preamble and PHeader fields do not have a fixed size in bytes, they are measured in time and are defined individually for each specific standard within the 802.11 family [9].

For calculating temporal parameters, the wireless channel operation mode BTC (Base Transmission Cycle) was used, since the operation principle of the Modbus TCP backbone in the master-slave scheme specifically employs this wireless channel mode.

In BTC mode, there is no procedure for establishing a connection between the transmitter and receiver; the first frame immediately transmits the payload data. The operation diagram of the BTC mode in an ideal channel is shown in Fig. 6 [10].

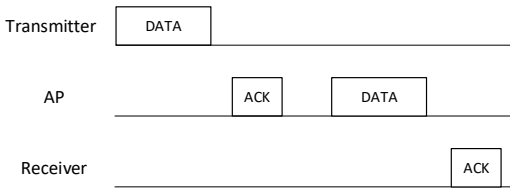

Fig. 6. BTC mode operation diagram in an ideal channel

Timing diagram of a single data frame transmission through a wireless access point (AP) in BTC mode in an ideal channel is shown in Fig. 7.

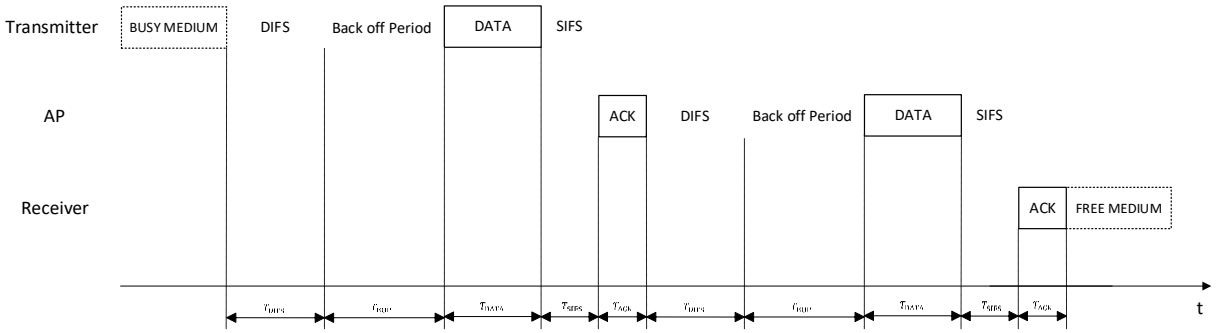

Fig. 7. Timing diagram of frame transmission in BTC mode in an ideal channel

In the event of errors during the transmission of a data packet or an ACK packet in wireless communication channels of the IEEE 802.11 family standards, a retransmission process of the corrupted frame is carried out. The transmitting side waits for a time interval called ACK Timeout, the value of which is regulated by the relevant wireless communication standards, after which it initiates the retransmission procedure of the corrupted data packet. This retransmission process can be repeated multiple times until the maximum number of transmission attempts specified by the corresponding IEEE 802.11 standard is reached.

The timing diagram of a packet transmission through a wireless AP in the event of transmission errors is shown in Fig. 8.

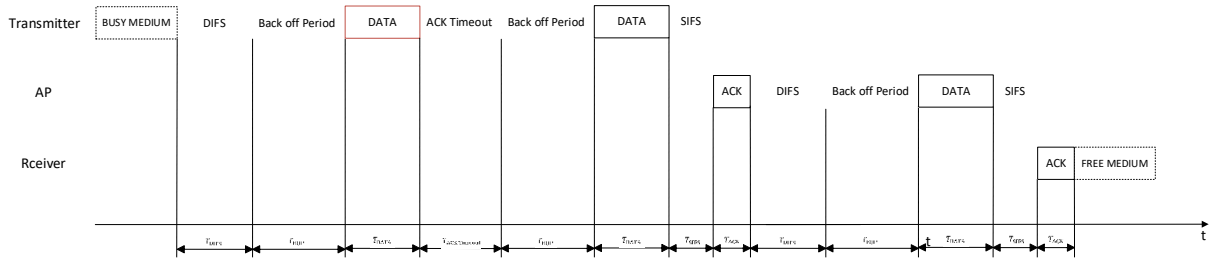

Fig. 8. Timing diagram of frame transmission in BTC mode in the event of transmission errors

The formula for calculating the transaction time over the physical channel of the Modbus TCP backbone when using BTC mode is as follows:

$$T_{\mathrm{TR}}^{\mathrm{BTC}} = 2(T_{\mathrm{DIFS}} + T_{\mathrm{BOP}} + T_{\mathrm{DATA}} + T_{\mathrm{SIFS}} + T_{\mathrm{ACK}}), \quad (1)$$

where: T_{DATA} – data frame transmission time; T_{ACK} – acknowledgment frame transmission time; T_{DIFS} – fixed interframe spacing; T_{BOP} – transmission delay; T_{SIFS} – short interframe spacing.

According to the 802.11ac standard, the data frame transmission time is calculated using the following formula:

$$T_{\text{DATA}} = T_{\text{Preamble}} + T_{\text{PHeader}} + \left\lceil \frac{8L_{\text{DATA}}}{DR} \right\rceil, \tag{2}$$

where: T_{Preamble} – preamble transmission time; T_{PHeader} – physical layer header transmission time; L_{DATA} – size of the data frame. These parameters are defined by the specific standard within the 802.11 family, and DR – data transmission rate.

The size of the data frame transmitted over the physical channel, according to the standard, is determined by the following formula:

$$L_{\text{DATA}} = \text{H4+H3+H2+H1+D} + \text{FCS}. \tag{3}$$

The backbone throughput in an ideal channel is determined by the following formula:

$$V = \frac{L}{T_{\text{TR}}^{\text{BTC}}}, \tag{4}$$

where: V – backbone throughput in an ideal channel; L – size of the payload; $T_{\text{TR}}^{\text{BTC}}$ – transaction time in an ideal channel.

The transaction time for transmission in a real channel is determined by the following formula:

$$T_{\text{TR. R.}}^{\text{BTC}} = T_{\text{TR}}^{\text{BTC}} + (T_{\text{TR}}^{\text{BTC}})P_{\text{RT}}, \tag{5}$$

where: $T_{\text{TR}}^{\text{BTC}}$ – transaction time in an ideal channel; P_{RT} – probability of frame retransmission.

In the event of a corrupted data frame, it is retransmitted. The probability of retransmission is calculated using the following formula:

$$P_{\text{RT}} = \frac{P_{\text{FC}}}{1 - P_{\text{FC}}}, \tag{6}$$

where: P_{FC} – probability of frame corruption.

The probability of frame corruption is calculated by multiplying the probability of a single bit error by the total number of bits transmitted in one transaction:

$$P_{\text{FC}} = N \cdot \text{BER}, \tag{7}$$

where: N – total number of bits transmitted in one transaction; BER – probability of a single bit error.

The total number of transmitted bits (N) is the sum of the bits in the data frame and the acknowledgment (ACK) frame:

$$N = N_1 + N_2, \tag{8}$$

where: N_1 – number of bits in the data frame; N_2 – number of bits in the acknowledgment frame.

The throughput during transmission in a real channel is determined by the following formula:

$$V^P = \frac{L}{T_{\text{TR. R.}}^{\text{BTC}}}, \tag{9}$$

where: $T_{\text{TR. R.}}^{\text{BTC}}$ – transaction time in a real channel; L – size of the payload.

In the analysis, elementary read (T_{RD}) and write (T_{WR}) operations are considered, where each operation includes not only the execution of commands (T_{CRD}) and receiving a response (T_{CRE}) but also mechanisms for error handling and retransmission of corrupted frames.

The execution time of a read operation in a real channel is calculated using the following formula:

$$T_{\text{RD}}^{\text{R}} = T_{\text{CRD}}^{\text{R}} + T_{\text{CRE}}^{\text{R}}, \tag{10}$$

ISSN 2076-2429 (print)
ISSN 2223-3814 (online)

where: T_{CRD}^{P} – transaction time of the read command in a real channel; T_{CRE}^{P} – transaction time of the response command in a real channel.

The backbone throughput during the execution of a read operation in a real channel is evaluated using the following formula:

$$V_{\text{RD}}^{\text{R}} = \frac{L}{T_{\text{RD}}^{\text{R}}}, \tag{11}$$

where: L – size of the payload; T_{RD}^{R} – transaction time of the read operation in a real channel.

The write operation (T_{WR}) includes the sequential execution of the write command followed by receiving a response from the actuator.

The execution time of a write operation in a real channel is calculated using the following formula:

$$T_{\text{WR}}^{\text{R}} = T_{\text{CWR}}^{\text{R}} + T_{\text{CRE}}^{\text{R}}, \tag{12}$$

where: $T_{\text{CWR}}^{\text{R}}$ – transaction time of the write command in a real channel; $T_{\text{CRE}}^{\text{R}}$ – transaction time of the response command in a real channel.

The backbone throughput during the execution of a write operation is determined based on the amount of transmitted data and the time spent on sequential execution of the write command and receiving the response. The formula for estimating the throughput is as follows:

$$V_{\text{WR}}^{\text{R}} = \frac{L}{T_{\text{WR}}^{\text{R}}}, \tag{13}$$

where: L – size of the payload; T_{WR}^{R} – transaction time of the write operation in a real channel.

A composite operation, in general, represents a sequence of an arbitrary number of elementary operations, such as write and read operations.

The execution time of a composite operation, in general, is calculated using the following formula:

$$T_{\text{CO}}^{\text{R}} = \sum_{i}^{N} T_{\text{RD}_i}^{\text{R}} + \sum_{j}^{M} T_{\text{WR}_j}^{\text{R}}, \tag{14}$$

where: $T_{\text{RD}_i}^{\text{R}}$ – execution time of the i-th read operation in a real channel; $T_{\text{WR}_j}^{\text{R}}$ – execution time of the j-th write operation in a real channel.

The backbone throughput during the execution of a composite operation, in general, is evaluated using the following formula:

$$V_{\text{CO}}^{\text{R}} = \frac{L}{T_{\text{CO}}^{\text{R}}}, \tag{15}$$

where: L – size of the payload; T_{CO}^{R} – transaction time of an arbitrary composite operation in a real channel.

Expressions (1) – (15) describe the mathematical model of a real wireless Modbus TCP backbone channel with errors for the IEEE 802.11 standard.

Research results

To assess the impact of bit error rates (10^{-4}, 10^{-5}, 10^{-6}), the throughput of the backbone is calculated when using the IEEE 802.11ac standard as the wireless channel.

Graphs showing the dependence of Modbus TCP backbone throughput on different bit error rates when using an IEEE 802.11ac wireless channel, for both multi-channel and single-channel backbone implementations and for various payload sizes, are presented in Figures 9 – 14.

The conducted analysis of the wireless Modbus TCP backbone throughput demonstrates the impact of bit errors on backbone performance. Throughput decreases by 0.04% at a bit error rate of 10^{-6} for the minimum frame size and by 0.14% for the maximum frame size; by 0.8% at a bit error rate of 10^{-5} for the minimum frame size and by 1.8% for the maximum frame size; and by 10% at a bit error rate of 10^{-4} for the minimum frame size and by 25% for the maximum frame size.

Conclusions

Analytical relationships have been obtained for calculating the transaction time and throughput of the Modbus TCP backbone when transmitted over IEEE 802.11 wireless channels, taking into account bit errors for both simple and composite backbone operations. The developed mathematical model al-

lows evaluating the impact of noise levels on system performance for various wireless channel configurations, including single-channel and multi-channel implementations.

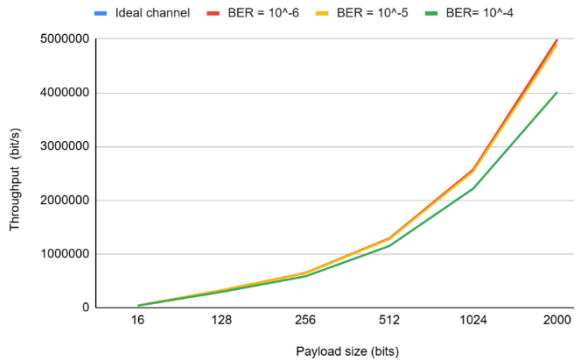

Fig. 9. Backbone throughput for a read operation in a single-channel backbone configuration

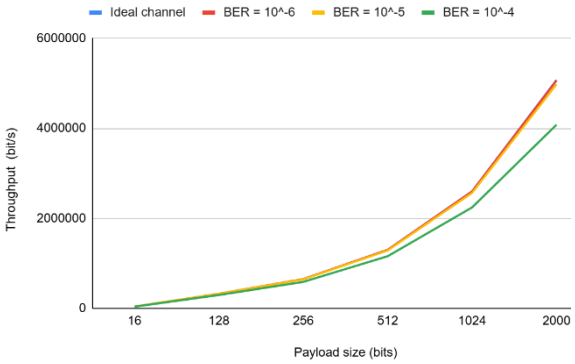

Fig. 10. Backbone throughput for a read operation in a multi-channel (4 channels) backbone configuration

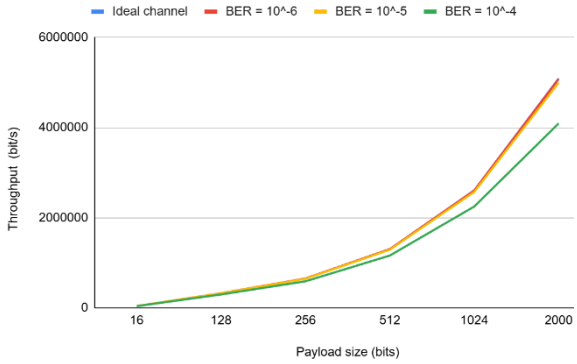

Fig. 11. Backbone throughput for a read operation in a multi-channel (8 channels) backbone configuration

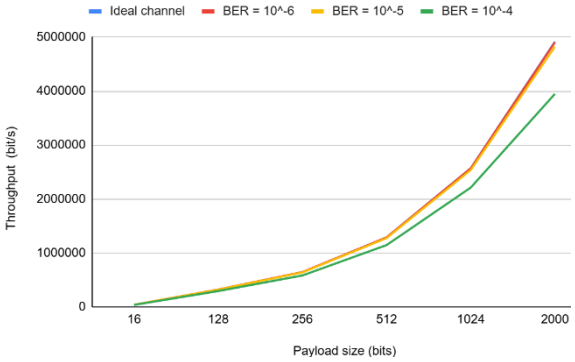

Fig. 12. Backbone throughput for a write operation in a single-channel backbone configuration

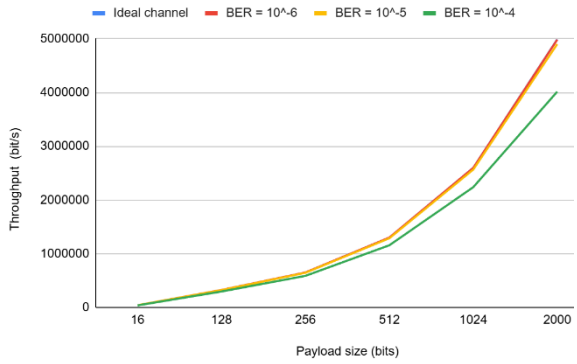

Fig. 13. Backbone throughput for a write operation in a multi-channel (4 channels) backbone configuration

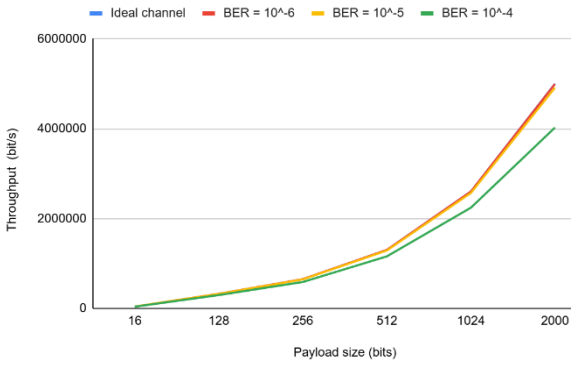

Fig. 14. Backbone throughput for a write operation in a multi-channel (8 channels) backbone configuration

Throughput calculations were performed for read and write operations at different bit error rates and frame sizes. Analysis of the results shows an increase in transmission time and a decrease in throughput with increasing packet size and bit error rate, which is associated with a higher number of frame retransmissions. Significant throughput reduction occurs only at a high bit error rate of 10^{-4}, reaching up to 25% compared to an ideal transmission channel. Bit error rates of 10^{-6} and 10^{-5} do not cause significant changes in the throughput of the Modbus TCP backbone based on IEEE 802.11ac.

The obtained analytical models provide a tool for selecting the optimal configuration of a wireless Modbus TCP backbone during the design and modernization of industrial automated control systems within the framework of the “Industry 4.0” concept.

ISSN 2076-2429 (print)
ISSN 2223-3814 (online)

Література

1. Islam G. Z. Throughput Analysis of Wireless Local Area Network. *International Journal of Engineering and Technical Research*. 2016. V. 6, Is. 4. P. 53–60. URL: https://www.erpublication.org/published_paper/IJETR042733.pdf.
2. Throughput Limits of IEEE 802.11 and IEEE 802.15.3 / S. Ullah, Y. Zhong, S. M. R. Islam et al. //Wireless Communications, Networking and Mobile Computing (WiCOM '08) : 4th International Conference (Dalian, 2008). URL: www.researchgate.net (дата звернення: 20.10.2025).
3. Chatzimisios P. Throughput and delay analysis of IEEE 802.11 protocol / Networked Appliances : Proceedings. 2002 IEEE 5th International Workshop (Liverpool, 2002). URL: https://www.researchgate.net/publication/4041174_Throughput_and_delay_analysis_of_IEEE_80211_protocol (дата звернення: 20.10.2025).
4. MODBUS Messaging on TCP/IP Implementation Guide. URL: https://www.modbus.org/docs/Modbus_Messaging_Implementation_Guide_V1_0b.pdf. (дата звернення: 20.10.2025).
5. Hozdic E. Smart factory for industry 4.0: A review. *Journal of Modern Manufacturing Systems*. 2015. URL: https://www.acatech.de/wp-content/uploads/2018/03/Final_report__Industrie_4.0_dec_2013.pdf (дата звернення: 20.10.2025).
6. IEC 62264-1 Edition 2.0 2013 Enterprise-control system integration – Part 1: Models and terminology. 2013. URL: https://webstore.iec.ch/en/publication/6675 (дата звернення: 20.10.2025).
7. Monostori L. Cyber-physical production systems: Roots, expectations and R&D challenges. *Procedia CIRP*. 2014. V. 17. P. 9–13. DOI: https://doi.org/10.1016/j.procir.2014.03.115. (дата звернення: 20.10.2025).
8. RFC 791 Internet Protocol (IP). 1981. URL: https://tools.ietf.org/html/rfc791 (дата звернення: 20.10.2025).
9. IEEE 802.3-2018 – Ethernet Technology. 2018. URL: https://standards.ieee.org/standard/802_3-2018.html. (дата звернення: 20.10.2025).
10. Naumov O., Nesterenko S. Analysis of cycle time in a Modbus RTU channel with errors. *Наука і техніка сьогодні*. 2025. 10(51). URL: https://perspectives.pp.ua/index.php/nts/issue/view/410/513. (дата звернення: 20.10.2025).

References

1. Islam, G. Z. (2016). Throughput analysis of wireless local area network. *International Journal of Engineering and Technical Research, 6*(4), 53–60. Available at https://www.erpublication.org/published_paper/IJETR042733.pdf.
2. Ullah, S., Zhong, Y., Islam, S. M. R., et al. (2008, October 12–14). *Throughput limits of IEEE 802.11 and IEEE 802.15.3*. 4th International Conference on Wireless Communications, Networking and Mobile Computing (WiCOM '08), Dalian, China. Retrieved October 20, 2025. Available at https://www.researchgate.net.
3. Chatzimisios, P. (2002, October 8–9). *Throughput and delay analysis of IEEE 802.11 protocol.* 2002 IEEE 5th International Workshop on Networked Appliances, Liverpool, UK. Retrieved October 20, 2025. Available at https://www.researchgate.net/publication/4041174_Throughput_and_delay_analysis_of_IEEE_80211_protocol.
4. Modbus Organization. (n.d.). *MODBUS messaging on TCP/IP implementation guide*. Available at https://www.modbus.org/docs/Modbus_Messaging_Implementation_Guide_V1_0b.pdf.
5. Hozdic, E. (2015). Smart factory for industry 4.0: A review. *Journal of Modern Manufacturing Systems*. Available at https://www.acatech.de/wp-content/uploads/2018/03/Final_report__Industrie_4.0_dec_2013.pdf.
6. International Electrotechnical Commission. (2013). *Enterprise-control system integration – Part 1: Models and terminology* (IEC 62264-1:2013). Available at https://webstore.iec.ch/en/publication/6675.
7. Monostori, L. (2014). Cyber-physical production systems: Roots, expectations and R&D challenges. *Procedia CIRP, 17*, 9–13. DOI: https://doi.org/10.1016/j.procir.2014.03.115.
8. Postel, J. (1981). *Internet Protocol* (RFC No. 791). Internet Engineering Task Force. Available at https://tools.ietf.org/html/rfc791.
9. IEEE. (2018). *IEEE 802.3-2018 – Ethernet technology*. Available at https://standards.ieee.org/standard/802_3-2018.html.
10. Naumov, O., & Nesterenko, S. (n.d.). Analysis of cycle time in a Modbus RTU channel with errors. *Scientific Works of ONAT*. 10(51). Available at https://perspectives.pp.ua/index.php/nts/issue/view/410/513.

Нестеренко Сергій Анатолійович; Serhii Nesterenko, ORCID: http://orcid.org/0000-0002-3757-6594
Наумов Олексій Денисович; Oleksii Naumov, ORCID: https://orcid.org/0009-0003-0232-0841

Received November 21, 2025
Accepted December 19, 2025

UDC 004.94 : 005.8

I. Putii
P. Teslenko, PhD, Assoc. Prof.
Odessa Polytechnic National University, Shevchenko Ave. 1, Odesa, Ukraine, 65044, E-mail: teslenko@op.edu.ua

COMPLEX IT PROJECT MANAGEMENT INFORMATION SYSTEM

І. Путій, П. Тесленко. **Інформаційна система управління складними ІТ-проєктами.** Статтю присвячено розробці концепції та архітектури інформаційної системи управління складними ІТ-проєктами, що забезпечує автоматизоване виявлення, аналіз і зниження невизначеності в умовах високої складності реалізації проєктів. Показано, що сучасні ІТ-проєкти характеризуються високим рівнем динаміки, технологічної новизни, мультидисциплінарністю та великою кількістю взаємопов'язаних елементів. В таких проєктах складність проявляється не лише у масштабі чи кількості компонентів, а насамперед у взаємозалежності технічних, організаційних і поведінкових факторів. Це ускладнює передбачення результатів і знижує ефективність класичних методів управління. Сформульовано проблему — відсутність системного підходу до управління невизначеністю, яка виникає внаслідок складності реалізації ІТ-проєктів та безпосередньо впливає на їх успішність. Показано, що складність доцільно розглядати як складність реалізації, яка охоплює технологічні, організаційні, комунікаційні, часові та поведінкові аспекти проєкту. Саме вони формують джерело невизначеності, що унеможливлює стабільне прогнозування результатів і створює ризики зриву термінів або невідповідності очікуванням замовника. Для системного подолання цієї проблеми запропоновано метод управління складними ІТ-проєктами, що базується на ідеї послідовного зниження невизначеності. Метод реалізовано у вигляді етапів: виявлення зон невизначеності, формування гіпотез, перевірка їх ефективності через Spike, PoC або R&D-експерименти, подальший рефакторинг процесів управління та оновлення плану проєкту. Розроблено структуру інформаційної системи управління складними ІТ-проєктами, яка включає дев'ять модулів і забезпечує повну автоматизацію циклу управління. Система використовує інструменти обробки природної мови, багатокритеріального аналізу, машинного навчання та предиктивної аналітики для формування управлінських рішень на основі даних. Реалізовано логічну архітектуру з замкненим адаптивним контуром, що забезпечує безперервне вдосконалення управлінських дій і стабілізацію стану проєкту. Впровадження запропонованої системи дозволить мінімізувати вплив людського фактору, підвищити прогнозованість і забезпечити кероване зниження невизначеності, що є критично важливим для успішного завершення складних ІТ-проєктів.

Ключові слова: складний ІТ-проєкт, невизначеність, предиктивна аналітика, Spike, Proof of Concept, рефакторинг управління, метод управління складними ІТ-проєктами, інформаційна система управління складними ІТ-проєктами

I. Putii, P. Teslenko. **Complex IT project management information system.** The article is devoted to the development of the concept and architecture of an information system for managing complex IT projects, which provides automated detection, analysis and reduction of uncertainty in conditions of high complexity of project implementation. It is shown that modern IT projects are characterized by a high level of dynamics, technological novelty, multidisciplinary nature and a large number of interconnected elements. In such projects, complexity is manifested not only in the scale or number of components, but primarily in the interdependence of technical, organizational and behavioral factors. This complicates the prediction of results and reduces the effectiveness of classical management methods. The problem is formulated – the lack of a systematic approach to managing uncertainty, which arises as a result of the complexity of implementing IT projects and directly affects their success. It is shown that complexity should be considered as the complexity of implementation, which covers technological, organizational, communication, time and behavioral aspects of the project. They form a source of uncertainty, which makes it impossible to predict results stably and creates risks of missing deadlines or not meeting customer expectations. To systematically overcome this problem, a method for managing complex IT projects has been proposed, based on the idea of sequentially reducing uncertainty. The method is implemented in the form of stages: identifying areas of uncertainty, forming hypotheses, testing their effectiveness through Spike, PoC or R&D experiments, further refactoring of management processes and updating the project plan. The structure of an information system for managing complex IT projects has been developed, which includes nine modules and provides full automation of the management cycle. The system uses natural language processing tools, multi-criteria analysis, machine learning and predictive analytics to form management decisions based on data. A logical architecture with a closed adaptive loop has been implemented, which ensures continuous improvement of management actions and stabilization of the project state. The implementation of the proposed system will minimize the impact of the human factor, increase predictability and ensure a controlled reduction in uncertainty, which is critically important for the successful completion of complex IT projects.

Keywords: complex IT project, uncertainty, predictive analytics, Spike, Proof of Concept, management refactoring, complex IT project management method, complex IT project management information system

1. Introduction

Modern IT projects are characterized by high dynamics of development, multidisciplinarity and a significant number of interrelated elements. Complex IT projects are understood to be those that simultaneously combine technological innovation, integration of heterogeneous systems, changing requirements and interdependence of teams, i.e. complexity of implementation including the need for scientific research [1]. In such projects, it is impossible to fully predict the behaviour of the system or the consequences of decisions made, since each change at one level can create chain effects at others. The complexity here is not limited to the number of components or scale; it is systemic in nature –

DOI: 10.15276/opu.2.72.2025.13

ISSN 2076-2429 (print)
ISSN 2223-3814 (online)

technical, organisational, communicational, temporal, and behavioural.

Technological complexity arises when a project is based on new or unstable technologies for which there are no established development or testing practices yet. Organisational complexity is related to the distribution of responsibilities between departments, developers and stakeholders, who often have different priorities and visions of the outcome. Communication complexity manifests itself in a large number of information exchange channels, which complicates the control of requirements integrity and team synchronisation. Time complexity arises from the multi-level dependencies between tasks and the high variability of plans, where the results of one stage significantly affect the feasibility of the next. Finally, behavioural complexity arises from the human factor: different experiences of team members, differing understandings of goals, or resistance to change.

The combination of these types of complexity creates significant uncertainty, which is the main threat to the successful completion of complex IT projects. Uncertainty in requirements, time estimates, code quality, or technical limitations directly increases the risks of missed deadlines, reduced quality, or failure to meet customer expectations [2]. It cannot be completely eliminated, but it can be systematically managed to reduce its impact on critical project elements.

To this end, the software development industry uses tools such as Spike, Proof of Concept (PoC), and research and development experiments (R&D experiments) [1].

Spike is used for short-term research into an unknown technological problem – it is a quick experiment that answers a narrow technical question without creating a complete product. Proof of Concept is broader in nature and aims to test the viability of an idea or architectural solution in a controlled environment, demonstrating that the concept can be implemented in practice. Research and development work differs in scale and depth – it is a stage at which a hypothesis is tested in conditions close to real life, involving a full cycle of development, testing, and evaluation of results [3]. The main difference between them lies in the depth of analysis and the degree of influence on the further architecture of the project: Spike answers the question “is it possible”, PoC – “how exactly to do it”, and R&D work – “how to integrate it into the system without risk”.

However, in most organisations, such actions are performed sporadically and without integration into the overall management system, which leads to a loss of connection between research and the actual state of the project. For systematic, rather than random, uncertainty management, a conceptual model for managing complex IT projects [4] and a method for forming hypotheses for complex IT projects [5] have been developed.

This model is based on the principle of cyclicality: identifying areas of uncertainty, forming hypotheses for action, testing their effectiveness, refactoring management processes, and adapting the project plan. Refactoring here acts as a separate management procedure – changing internal processes, roles, communications, or plans based on confirmed experimental results, which allows you to maintain flexibility without losing controllability. That is why it is advisable to integrate it as a separate module in the structure of the information system for managing complex IT projects – instead of the “classic” plan adaptation module, which now performs the functions of management refactoring.

Based on this conceptual model and method, it is envisaged to create an information system (IS) for managing complex IT projects that automates all stages of this cycle – from data collection to evaluation of refactoring results. Using analytical models, natural language processing algorithms, and machine learning elements, such a system eliminates the influence of the human factor, minimises the risks of additional errors in decision-making, and ensures a controlled, predictable reduction in uncertainty. Its implementation should ensure control over the execution of complex IT projects and increase the likelihood of successful completion even in unstable project conditions.

2. Analysis of literature data and problem statement

Article [6] examines the evolution of approaches to managing complex projects from classical to modern integrated methodologies. The author interprets a complex project as a multi-level system with numerous interdependencies, where a change in one element affects the entire structure. The main problem highlighted by the researcher is the lack of a single methodological standard capable of taking into account the different conditions of project implementation, which leads to ineffective management and wrong decisions. The proposed solution is to use hybrid management models that combine the advantages of network planning, CPM and PERT, as well as the use of information technology to simulate project implementation scenarios.

In article [7], a complex project is described as part of a program portfolio operating in a highly turbulent external and internal environment. The authors point to a key management problem: the mismatch between methodologies and the level of project complexity. When a company uses the same approaches for different types of projects, a "manual control effect" arises, which reduces efficiency and manageability. The solution proposed is a dual adaptive control system that simultaneously controls the object and learns based on accumulated information, i.e., combines the principles of adaptive control and self-organisation.

The authors [8] define a complex IT project as a multifunctional process with a high level of risk, rapid changes in requirements, and the need for constant adaptation. The main management problem lies in budget, resource, and time constraints, while at the same time ensuring flexibility. The authors propose a hybrid methodology that integrates Agile and Waterfall, supplemented by mathematical modelling and simulation to optimise resource allocation and increase the adaptability of the management system.

In the monograph "Project Management: Theory, Practice, Information Technology" (O. Zatchko, A. Ivanusa, D. Kobilkin, 2019) [9], complex projects are considered through the prism of information support. The authors emphasise that the complexity of modern projects requires instrumental support – the use of software tools such as MS Project to coordinate resources, deadlines and risks. The lack of a unified information environment for coordinating technical and management processes is identified as a problem. The proposed solution is to integrate the classic PMBOK and P2M methodologies with digital management platforms that ensure transparency and systematic control.

In the study "Succeeding Against the Odds: Project Management in Complex IT Scenarios" [10], a complex project is viewed as a system with a large number of nonlinear relationships, where each management decision creates a reverse effect. The author emphasises that the main problem lies in the loss of controllability due to information overload and inconsistency between teams. This leads to missed deadlines, incorrect prioritisation of tasks, and duplication of work. The proposed solution is to implement a digital knowledge management system that accumulates information from all project subsystems (Jira, GitLab, Confluence) and provides cognitive support for managerial decisions.

In article [11], complex projects are described as innovative ecosystems that combine research (R&D) and production phases. The authors point to the problem of the gap between innovation management and project management: in R&D projects, complexity arises due to the unpredictability of results and constantly changing parameters. This complicates resource and schedule planning. The proposed solution is to integrate innovation management models with Agile methods and create digital twins to simulate possible project development scenarios. The information system described in the article supports risk forecasting and automatic assessment of the technological maturity of solutions.

In contrast, the authors [12] emphasise that complex projects in the digital environment are characterised by a high level of dynamism and unpredictability. The main problem is the lack of connection between digital tools and management decision-making processes. As a result, digital systems record data but do not generate instructions for action. The authors propose the concept of "data-driven management", i.e., the creation of a management system that not only aggregates data but also uses analytics to predict problem areas and suggest courses of action. The system involves the use of predictive analytics and artificial intelligence algorithms to assess the progress of IT projects.

In the 2020 article "Definitions, Characteristics and Measures of IT Project Complexity – Systematic Review" [13], project complexity is defined by five groups of factors: structural, technological, organisational, project uncertainty and dynamic. The authors analysed more than 100 literature sources and point out that the main problem of management lies in the subjective perception of complexity — the lack of uniform criteria for measuring it. This leads to even experienced managers underestimating the level of risk. As a solution, they propose creating a Project Complexity Index metric and integrating it into management information systems for automated monitoring of project complexity.

Next, we note the journal Research-Technology Management [14], which contains numerous publications where complex projects are defined as interdisciplinary R&D initiatives with high uncertainty of technological results. The main problem is the lack of connection between research and commercialisation of results, which leads to a loss of innovative potential. The authors emphasise the need to create knowledge management systems that combine managerial and technical processes, ensuring the tracking of hypotheses, experiments and decisions within a single digital environment.

ISSN 2076-2429 (print)
ISSN 2223-3814 (online)

The article “A Hybrid Agent-Based and System Dynamics Framework for Modelling Project Execution and Technology Maturity in Early-Stage R&D” [15] is devoted to modelling complex R&D projects. The authors define complexity as the result of the interaction of people, technologies and management processes. The main problem is the inability to predict the trajectory of technology development in the early stages. A hybrid agent-system model is proposed, which combines the behavioural patterns of agents (developers, managers, customers) with the dynamics of technological maturity development. The model is implemented as an information system for forecasting time, costs and risk of failure.

It should be noted that the ISO 21500 – Guidance on Project Management [16] standard does not contain a separate definition of a complex project. It uses the general term ”project”, described as “a unique process consisting of controlled tasks with a defined beginning and end”. However, in the context of the document, it is noted that “some projects may be more complex due to their scale, number of stakeholders, or technical novelty”. Thus, the standard only points to the existence of complexity as a factor that complicates management, but does not offer a specific tool for assessing or overcoming it.

The authors of all the articles reviewed agree that the main problem in managing complex projects is not only technical multi-levelness, but also methodological inconsistency. They propose a transition to hybrid, adaptive, or information-supported management systems capable of responding dynamically to changes and reducing the level of uncertainty, which is a prerequisite for the success of modern complex IT projects. Based on the review and analysis of the literature, we note that there is a need to develop an IS that automates human-dependent processes of identifying project uncertainty, analysing it, and forming measures to reduce this uncertainty in order to ensure the successful completion of a complex IT project.

3. Purpose and objectives of the study

The purpose of the study is to develop a method for managing complex IT projects, which is the basis for creating a logical representation of the corresponding information system, the implementation of which ensures a constant reduction in the level of uncertainty and increased manageability of IT project implementation.

To achieve this goal, tasks are solved that are related to the identification of project uncertainties, their analysis, and the formulation of project decisions that should lead to a reduction in these uncertainties.

4. Justification of the method for managing complex IT projects

The proposed method for managing complex IT projects is based on a conceptual model for managing complex IT projects involving research and development, supplemented by three key tools: a hypothesis formation canvas, a two-stage hypothesis filtering method, and a refactoring method for managing IT projects.

Classic project management stages, such as initiation, requirements and team formation, feasibility verification, and role distribution, are not included in the method [17]. This article provides a detailed sequence of stages, starting with the identification of areas of project uncertainty and ending with the refactoring of the management structure.

The first stage is the identification of areas of uncertainty. Based on natural language processing (NLP) technology, content units are automatically extracted: problems, risks, contradictions, and gaps in experience, skills, etc. Next, a problem base is formed, i.e., where there is uncertainty or where risks of complexity are observed.

Problem signals are extracted from backlog, Jira, Confluence, Service Desk, etc. The NLP module forms the Problem Base and classifies records by category (functional, UX, security, architecture, etc.).

The second stage is the formation of hypotheses based on the hypothesis formation method canvas [5]. Each area of uncertainty is described in the structure: problem – hypothesis – expected result – verification criteria – resources. This standardises the general representation of the problem and formalises assumptions for further verification. Hypotheses structured in this way are stored in the Hypothesis Management System (HMS) knowledge base, where they are grouped by semantic connections or technological directions.

Each problem is converted into a hypothesis using the “If... then... because...” template, and a database of hypotheses (HMS Knowledge Base) is created.

The third stage is a two-stage filtering of hypotheses. This ensures that only those that are of high value to the project and can be implemented in practice are selected. The first filter assesses the impact of the problem on strategic goals using the MCDA (Multi-Criteria Decision Analysis) model, which calculates an integral importance index. It takes into account the impact, risk, scale, and number of stakeholders. The second filter evaluates feasibility through an index that includes time, financial, and resource constraints. Hypotheses with low index values are automatically filtered out as redundant or irrational.

The MCDA calculates the Feasibility_Index as a measure of feasibility, resulting in only relevant hypotheses being retained.

The fourth stage is hypothesis testing, during which either Spikes, Proof of Concept, or research and development work is carried out. This allows hypotheses to be confirmed or refuted in practice and also allows the effectiveness of solutions to be tested. Each hypothesis is given a status – confirmed, rejected, or requiring further research. This allows you to track progress and keep a history of decisions made.

A short experiment is created for each hypothesis. The results are stored in HMS with an indication of their status.

The fifth stage is refactoring IT project management, which is the basis of the method's adaptability. Here, areas for improvement are identified and directions for further research and recommendations for subsequent stages are determined. A cycle of invariant verification is initiated as a mechanism to ensure that the basic parameters of the project, such as the goal, main tasks and constraints, remain unchanged even after management changes are made.

Refactoring is the adaptation of management processes (not code). The invariant verification cycle ensures that the project's goal, key tasks, and constraints remain unchanged.

The sixth stage is updating the management structure. This involves transferring the results of refactoring to the operational project management model. The stage includes updating the backlog, sprint plans, communication schemes, and roles. All changes are documented and evaluated using comparative metrics.

All changes are recorded in the management system (Jira, Azure DevOps). The backlog is updated and sprint plans are adjusted automatically.

The final stage is cyclical HMS self-learning. The system accumulates data on hypotheses, research, and refactoring results and predicts new areas of uncertainty using machine learning methods. This creates a closed adaptive loop in which each cycle not only reduces uncertainty but also increases the maturity of the management system.

The developed method integrates scientific thinking, complex project management models, and automation into a single management structure and becomes the basis for the development of a management information system for complex IT projects.

5. Development of an IS for managing complex IT projects

The implementation of the information system is based on the concept of adaptive management of complex IT projects. The main idea is a cyclical process of identifying uncertainties, forming hypotheses for their elimination, verifying the proposed actions, and adapting the management plan based on the results obtained. This approach allows for a continuous reduction in the level of uncertainty, keeping the project in a predictable and controllable state.

To implement this vision, an information system structure has been proposed, the logical representation of which is shown in Figure 1. The structure includes the following modules:

– data collection and consolidation module;
– uncertainty and complexity identification module;
– module for forming management hypotheses;
– hypothesis evaluation and prioritisation module;
– hypothesis implementation (verification) module;
– module for evaluating results and controlling uncertainty reduction;
– module for adapting the management plan (refactoring);
– cyclicality and re-analysis module;
– manager's analytical panel.

ISSN 2076-2429 (print)
ISSN 2223-3814 (online)

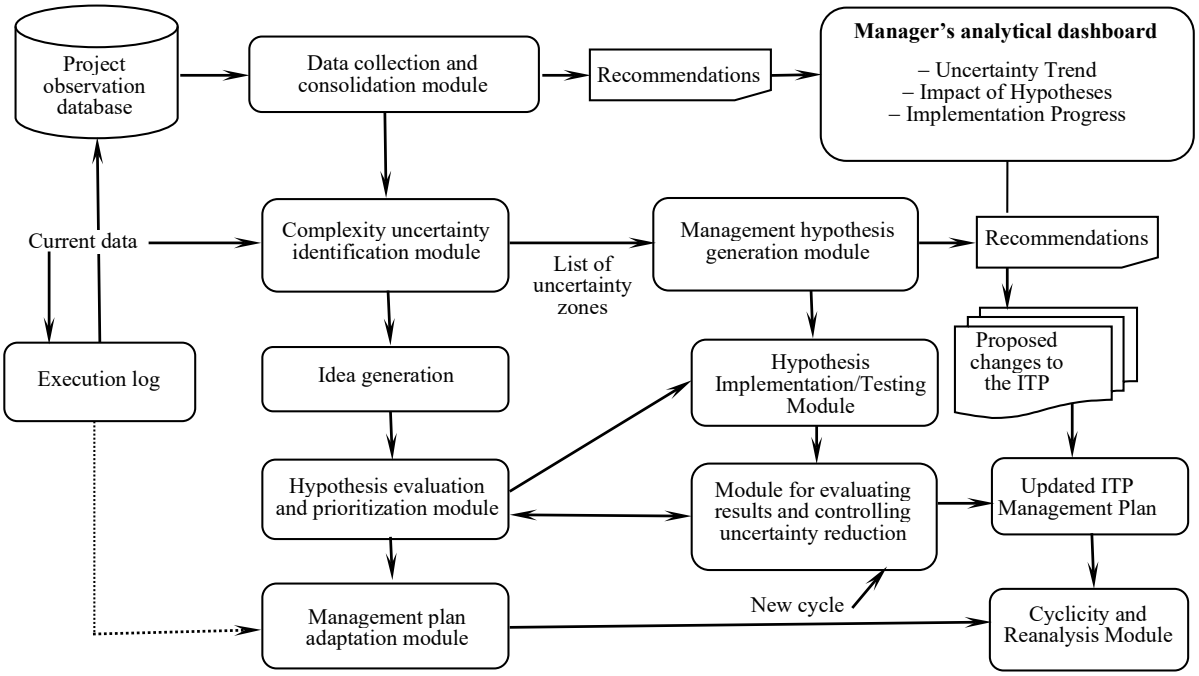

Fig. 1. Diagram of the logical representation of information system modules
The figure shows ITP as an IT project

The data collection module aggregates information from Jira, Git, Confluence, CI/CD logs, and QA reports in JSON format and forms a project observation database. Based on this, the uncertainty identification module uses NLP and clustering to identify problem areas – incomplete requirements, risky changes, unknown technology, or abnormal delays. These areas are transferred to the hypothesis formation module, which creates formalised records in the form of "if... then... because..." templates, suggesting options for action, such as Spike research or Proof of Concept. The next module evaluates and prioritises hypotheses using multi-criteria decision analysis (MCDA) methods, forming a list of the most important ones for implementation. The hypothesis implementation module tracks the execution of these actions, collecting data on resources used, time spent, and execution statuses. Next, the results evaluation module analyses whether uncertainty has decreased using the "Uncertainty Index" and "Risk Δ"metrics. If the changes have had a positive effect, the adaptation module automatically updates the management plan – backlog, roles, sprints, priorities. All changes are fed into the cyclicality module, which initiates a new management cycle for the next stage.

The project manager's analytical panel aggregates all results in the form of an interactive dashboard, which displays uncertainty trends, the impact of implemented hypotheses, and the current progress of the project. It is the main decision-making tool at the management level.

The figure shows the logical connections between the system modules. The data flow starts from the project observation base, from which information is sent to the uncertainty identification and analysis modules. The results are then transferred to the hypothesis formation, evaluation, and implementation blocks, after which the effectiveness of the actions is assessed. The updated management plan is submitted to the manager's analytical panel and returned to the system to start a new cycle. Thus, the IS structure implements a closed adaptive control loop for complex IT projects, in which each stage is a logical continuation of the previous one, ensuring a constant reduction in the level of uncertainty and increasing the manageability of the project.

6. Conclusions

Managing complex IT projects requires a new approach that goes beyond traditional methodologies. The complexity of modern IT projects is determined not only by technical or organisational factors, but above all by the dynamic relationships between people, technologies and the project environment, which has been interpreted as complexity of execution. Research shows that the key reason for failure in such projects is the accumulation of uncertainty arising from unstable requirements, lack of reliable estimates, limited team experience, or high technology novelty. It is uncertainty that is not

systematically controlled that becomes the main source of risk, complicating the prediction of results and reducing the likelihood of successful completion of such IT projects. Therefore, this article focused on reducing uncertainty as a central management goal.

A review of the literature showed that to overcome this problem in the management of complex IT projects, Spike, Proof of Concept, and research and development practices are being actively implemented. Spike allows you to quickly test a technical hypothesis or train a team, PoC demonstrates the viability of an idea, and R&D research ensures its practical implementation. At the same time, their independent use is usually episodic and not integrated into the management system, which reduces the effect of the knowledge gained. To ensure a cyclical and controlled reduction of uncertainty, a formalised approach is needed that can combine research activities with management processes.

Within the framework of this study, a method for managing complex IT projects has been developed, based on a conceptual model that covers the entire cycle: identifying uncertainties, forming hypotheses, testing their effectiveness, refactoring management processes, and adapting the plan. Refactoring is proposed as a separate element of the model, replacing the traditional stage of adapting the management plan. This allows for the continuous improvement of project organisational structures, communication schemes, and management approaches without losing project stability.

Based on this method, an information system for managing complex IT projects has been developed, which automates the processes of identifying, analysing, and eliminating uncertainties. The system includes nine interconnected modules that form a closed adaptive management loop. It combines natural language processing (NLP) tools, multi-criteria analysis (MCDA), machine learning, and predictive analytics algorithms that allow risks to be assessed before they actually occur. A key feature of the system is its ability to self-learn – after each management cycle, it accumulates experience and improves the accuracy of its forecasts and recommendations.

Thus, the proposed approach forms a new paradigm for managing complex IT projects, in which the main focus is not on fixing deviations, but on actively preventing risks through controlled reduction of uncertainty. Integrating the described model into project management practice will increase the predictability, adaptability, and sustainability of IT projects even in conditions of technological novelty and organisational turbulence.

Література

1. Putii I. D., Teslenko P. O. Analysis of modern approaches to managing complex IT projects. *Управління розвитком складних систем*. 2024. № 59. С. 81–89. URL: https://urss.knuba.edu.ua/zbirnyk-59 (дата звернення: 15.11.2025).
2. Guide to the Software Engineering Body of Knowledge. SWEBOK. URL: https://ieeecs-media.computer.org/media/education/swebok/swebok-v4.pdf. (дата звернення: 15.12.2025).
3. Putii I. D., Bondar O. A. Complexity of IT projects with research and development. *Information systems in project and program management* : international scientific and practical conference (Koblevo, 2024). KhNURE, 2024. P. 197–200.
4. Putii I. D., Teslenko P. O. Conceptual model of a complex IT project. *Таврійський науковий вісник. Серія: Технічні науки*. 2025. № 2. С. 148–154. DOI: https://doi.org/10.32782/tnv-tech.2025.2.16.
5. Putii I. D., Teslenko P. O. "Canvas" of the method of forming hypotheses for a complex IT project. *Управління розвитком складних систем*. 2025. № 64. С. 39–45.
6. Galushka V. Theoretical and methodological principles of project management. *Підприємництво, господарство і право*. 2020. № 7. С. 430–434. DOI: https://doi.org/10.32849/2663-5313/2020.7.72.
7. Bushuyev S. D., Kozyr B. Yu. Hybridization of methodologies for managing infrastructure projects and programs. *Вісник Одеського національного морського університету*. 2020. № 1. С. 187–207. DOI: 10.47049/2226-1893-2020-1-5-26.
8. Morozov V., Kulyk R. Building integration models of management efficiency of complex fixed-budget IT projects. *Управління розвитком складних систем*. 2025. № 62. С. 97–106.
9. Zachko O. B., Ivanusa A. I., Kobylkin D. S. Project management: theory, practice, information technologies. Lviv : LDU BZhD, 2019. 173 p.
10. Ankur Tak. Succeeding Against the Odds: Project Management in Complex IT Scenarios. *Journal of Technology and Systems*. 2023. Vol. 5, no. 2. P. 41–49. URL: https://ideas.repec.org/a/bhx/ojtjts/v5y2023i2p41-49id1544.html. (дата звернення: 15.11.2025).

11. The confluence of project and innovation management: A scientometric analysis of emerging trends and research frontiers / L. Zhang, S. Banihashemi, Y. Zhang, S. Chen. *Project Leadership and Society*. 2025. Vol. 6. Art. 100181. DOI: https://doi.org/10.1016/j.plas.2025.100181.
12. Chen M., Martins T. S., Zhang L., Dong H. Digital Transformation in Project Management: A Systematic Review and Research Agenda. *Systems*. 2025. Vol. 13, no. 625. DOI: https://doi.org/10.3390/systems13080625.
13. Stefan Morcov, Liliane Pintelon, Rob Kusters. Definitions, characteristics and measures of IT project complexity - a systematic literature review. *International Journal of Information Systems and Project Management*. 2020. Vol. 8, no. 2. P. 5–21. DOI: 10.12821/ijispm080201.
14. Research-Technology Management. Open Select: choose to publish open access. URL: https://www.tandfonline.com/journals/urtm20. (дата звернення: 15.11.2025).
15. A Hybrid Agent-Based and System Dynamics Framework for Modelling Project Execution and Technology Maturity in Early-Stage R&D / R. W. S. Pessoa et al. *Computer Science. Multiagent Systems*. Cornell University, 2025. DOI: https://doi.org/10.48550/arXiv.2510.09688.
16. ISO 21500:2021. Project, programme and portfolio management — Context and concepts. 2nd ed. 2021. URL: https://www.iso.org/standard/75704.html. (дата звернення: 15.11.2025).
17. A Guide to the Project Management Body of Knowledge (PMBOK® Guide). 7th ed. PMI, 2021. URL: https://www.pmi.org/standards/pmbok. (дата звернення: 15.11.2025).

References

1. Putii, I. D., & Teslenko, P. O. (2024). Analysis of modern approaches to managing complex IT projects. *Management of Complex Systems Development*, *59*, 81–89. https://urss.knuba.edu.ua/zbirnyk-59.
2. IEEE Computer Society. (2024). *Guide to the software engineering body of knowledge (SWEBOK)*. https://ieeecs-media.computer.org/media/education/swebok/swebok-v4.pdf.
3. Putii, I. D., & Bondar, O. A. (2024). Complexity of IT projects with research and development. In *Information systems in project and program management: Proceedings of the International Scientific and Practical Conference* (pp. 197–200). KhNURE.
4. Putii, I. D., & Teslenko, P. O. (2025). Conceptual model of a complex IT project. *Tavria Scientific Bulletin. Series: Technical Sciences*, (*2*), 148–154. https://doi.org/10.32782/tnv-tech.2025.2.16.
5. Putii, I. D., & Teslenko, P. O. (2025). “Canvas” of the method of forming hypotheses for a complex IT project. *Management of Complex Systems Development*, *64*, 39–45.
6. Galushka, V. (2020). Theoretical and methodological principles of project management. *Entrepreneurship, Economy and Law*, *7*, 430–434. https://doi.org/10.32849/2663-5313/2020.7.72.
7. Bushuyev, S. D., & Kozyr, B. Y. (2020). Hybridization of methodologies for managing infrastructure projects and programs. *Bulletin of the Odessa National Maritime University*, (*1*), 187–207. DOI: 10.47049/2226-1893-2020-1-5-26.
8. Morozov, V., & Kulyk, R. (2025). Building integration models of management efficiency of complex fixed-budget IT projects. *Management of Complex Systems Development*, (*62*), 97–106.
9. Zachko, O. B., Ivanusa, A. I., & Kobylkin, D. S. (2019). *Project management: Theory, practice, information technologies*. LDU BZhD.
10. Tak, A. (2023). Succeeding against the odds: Project management in complex IT scenarios. *Journal of Technology and Systems*, *5*(2), 41–49. https://ideas.repec.org/a/bhx/ojtjts/v5y2023i2p41-49id1544.html.
11. Zhang, L., Banihashemi, S., Zhang, Y., & Chen, S. (2025). The confluence of project and innovation management: A scientometric analysis of emerging trends and research frontiers. *Project Leadership and Society*, *6*, Article 100181. https://doi.org/10.1016/j.plas.2025.100181.
12. Chen, M., Martins, T. S., Zhang, L., & Dong, H. (2025). Digital transformation in project management: A systematic review and research agenda. *Systems*, *13*(8), Article 625. DOI: https://doi.org/10.3390/systems13080625.
13. Morcov, S., Pintelon, L., & Kusters, R. (2020). Definitions, characteristics and measures of IT project complexity - a systematic literature review. *International Journal of Information Systems and Project Management*, *8*(2), 5–21. DOI: 10.12821/ijispm080201.
14. Taylor & Francis Group. (n.d.). *Research-technology management*. https://www.tandfonline.com /journals/urtm20.

15. Pessoa, R. W. S., Næss, M. H., Bijos, J. C., Rebello, C. M., Colombo, D., Schnitman, L., & Nogueira, I. B. R. (2025). *A hybrid agent-based and system dynamics framework for modelling project execution and technology maturity in early-stage R&D*. arXiv. https://doi.org/10.48550/arXiv.2510.09688.
16. International Organization for Standardization. (2021). *Project, programme and portfolio management – Context and concepts* (ISO Standard No. 21500:2021). https://www.iso.org/standard/75704.html.
17. Project Management Institute. (2021). *A guide to the project management body of knowledge (PMBOK guide)* (7th ed.). https://www.pmi.org/standards/pmbok.

Путій Ілля Дмитрович; Illia Putii, ORCID: https://orcid.org/0009-0008-1111-4413
Тесленко Павло Олександрович; Pavlo Teslenko, ORCID: https://orcid.org/0000-0001-6564-6185

Received November 16, 2025
Accepted December 17, 2025

ISSN 2076-2429 (print)
ISSN 2223-3814 (online)

UDC 004.75:004.738.5:004.056

O. Streltsov, PhD, Assoc. Prof.,
M. Katrichenko,
Yu. Ornovetsky,
M. Hrynyov
Odessa Polytechnic National University, Shevchenko Ave. 1, Odesa, Ukraine, 65044, e-mail: streltsov.o.v@op.edu.ua

USING BLOCKCHAIN TECHNOLOGY TO IMPROVE SECURITY IN THE DISTRIBUTED INTERNET OF THINGS

О. Стрельцов, М. Катріченко, Ю. Орновецький, М. Гриньов. **Використання технології blockchain для покращення безпеки у розподіленому інтернеті речей.** Сучасний розвиток інформаційних технологій дедалі більше орієнтується на побудову розподілених систем, зокрема Інтернету речей (IoT), який об'єднує мільярди пристроїв у єдину глобальну інфраструктуру. Проте масштабне поширення IoT супроводжується зростанням ризиків у сфері кібербезпеки, оскільки централізовані підходи до зберігання та обробки даних часто виявляються вразливими до атак, маніпуляцій або відмов обладнання. У цьому контексті все більшої уваги набуває використання технології блокчейн, яка завдяки своїм ключовим характеристикам – децентралізації, прозорості та незмінності даних – відкриває нові можливості для підвищення рівня безпеки в розподіленому Інтернеті речей. У статті розглянуто проблематику забезпечення захисту інформації в IoT-системах, проаналізовано основні загрози, такі як несанкціонований доступ, підробка даних, витоки конфіденційної інформації та DDoS-атаки. Особлива увага приділяється аналізу того, як інтеграція blockchain здатна мінімізувати ці ризики шляхом децентралізованого управління доступом, автентифікації пристроїв, захищеного зберігання та передачі даних. Розглянуто можливості застосування смарт-контрактів для автоматизації процесів взаємодії між вузлами IoT-мережі, що підвищує довіру між учасниками та знижує потребу у посередниках. У результаті дослідження визначено, що поєднання IoT та blockchain створює передумови для побудови надійних, стійких до зловмисних впливів розподілених систем. Це може мати практичне застосування у таких сферах, як «розумні» міста, промисловий Інтернет речей, охорона здоров'я та енергетика. Водночас відзначено виклики, пов'язані з масштабованістю, затримками при обробці транзакцій та енергоспоживанням. Перспективними напрямами подальших досліджень є оптимізація протоколів консенсусу, використання гібридних архітектур та розробка спеціалізованих рішень для IoT-середовища.
Ключові слова: інтернет речей, блокчейн, однорангова мережа, доказ автентифікації, децентралізована мережа

O. Streltsov, M. Katrichenko, Yu. Ornovetsky, M. Hrynyov. **Using blockchain technology to improve security in the distributed internet of things**. The rapid development of information technologies increasingly focuses on building distributed systems, in particular the Internet of Things (IoT), which integrates billions of devices into a single global infrastructure. However, the large-scale adoption of IoT is accompanied by growing cybersecurity risks, since traditional centralized approaches to data storage and processing often prove to be vulnerable to attacks, manipulations, or equipment failures. In this context, the use of blockchain technology is gaining increasing attention. Owing to its key features – decentralization, transparency, and immutability of data – blockchain provides new opportunities to enhance security in distributed IoT environments. The article addresses the problem of information protection in IoT systems and analyzes major threats such as unauthorized access, data tampering, leakage of sensitive information, and DDoS attacks. Particular attention is given to how the integration of blockchain can minimize these risks through decentralized access management, device authentication, and secure storage and transmission of data. The use of smart contracts for automating interaction processes between IoT nodes is also examined, highlighting how they foster trust among participants and reduce the need for intermediaries. The findings suggest that combining IoT with blockchain technology creates the foundation for secure and resilient distributed systems that are resistant to malicious activities. Practical applications include smart cities, industrial IoT, healthcare, and energy management. At the same time, the paper outlines key challenges related to scalability, transaction latency, and energy consumption. Future research directions include optimizing consensus protocols, exploring hybrid architectures, and designing specialized blockchain solutions tailored to IoT environments.
Keywords: Internet of Things, blockchain, peer-to-peer network, proof of authentication, decentralized network

1. Introduction

In today's era of digital transformation, the Internet of Things (IoT) plays a key role in the development of information and communication technologies, allowing physical objects with built-in sensors, software and communication devices to be connected into a single network. The rollout of fifth-generation (5G) networks, which provide high bandwidth and reduced data transmission latency, has significantly accelerated the adoption of IoT in various areas, from smart home systems to critical infrastructure: smart cities, e-Health systems, industrial IoT (IIoT), automated agriculture, distributed control systems and intelligent transport [1, 2].

Although the introduction of IoT technologies contributes to process automation, resource optimisation and increased efficiency, it is accompanied by significant challenges in the field of cybersecurity. In particular, the scale of IoT infrastructure deployment, its heterogeneity, limited hardware resources of devices, and frequent disregard for proper protection mechanisms create numerous attack vectors [3].

DOI: 10.15276/opu.2.72.2025.14

One of the key threats is the possibility of remote takeover of IoT devices for use in botnets – networks of compromised devices controlled by an attacker. A typical scenario involves hacking poorly protected remote administration interfaces, in particular using default passwords or unpatched vulnerabilities in the firmware. Such botnets can be used to carry out distributed denial-of-service (DDoS) attacks, intercept or modify traffic, substitute data, attack the integrity of services, or interfere with the operation of critical facilities [4].

In centralised IoT architectures, there is an increased risk of compromising key nodes, such as central servers or microcontrollers that coordinate data exchange between devices. A successful attack on such an infrastructure element can lead to large-scale interference in the operation of the entire network, which highlights the need to develop mechanisms for redundancy, decentralisation, and protection of communication channels.

Thus, the security problem in the distributed Internet of Things is complex and requires an interdisciplinary approach, including the development of adaptive security protocols, authentication and authorisation mechanisms, software update strategies, and the application of artificial intelligence methods to detect anomalous behavior in network traffic. A blockchain-oriented Internet of Things architecture with smart contract-based data transfer can significantly improve integrity and trust in distributed Internet of Things systems [5].

2. Analysis of literature and statement of the problem

One of the main architectural models traditionally used to organise Internet of Things (IoT) systems is a centralised management model, in which the main processing, control and data storage are concentrated on a central server or in a cloud environment. This approach is relatively simple to implement, but has significant limitations in terms of attack resistance, scalability, and fault tolerance. The central point of control creates a critical vulnerability: if the server infrastructure is compromised, an attacker could potentially gain access to the entire network of IoT devices [6].

In contrast, decentralised architecture provides for distributed management, where each device in the network acts as an independent node capable of communicating without the need for a centralised intermediary. This means that compromising one device does not allow the attacker to control the entire network. To completely take over control of the system, an attacker would have to compromise a large number of nodes, which significantly complicates the attack [7].

An additional advantage of the decentralised model is provided by the implementation of blockchain technologies, which allow the creation of a secure communication environment between nodes by transmitting signed transactions stored in a distributed ledger. Such a ledger guarantees data immutability and message authenticity, and also provides the ability to verify each transaction by other nodes in the network [8]. Blockchain also eliminates the need for centralised trust, allowing the creation of trustless systems based on peer-to-peer (P2P) interaction. Smart contracts on blockchain create both opportunities and challenges in automation [9].

The key advantages of decentralised IoT include:

– decentralised management, which minimises the risks associated with centralised points of failure;

– high security through digital signatures, encryption and transaction verification mechanisms;

– device identification provided by public key authentication;

– network flexibility and scalability, allowing new nodes to be connected without rebuilding the infrastructure;

– autonomous operation, independent of the stability or performance of the central server;

– data reliability, as data is only recorded on the blockchain after verification, which prevents the creation or substitution of information.

Compared to centralised systems, decentralised IoT networks demonstrate a higher level of fault tolerance, which is particularly important for critical applications, such as in healthcare, energy, or transport infrastructure.

Therefore, a decentralised approach to building IoT systems is a promising direction that combines modern cryptographic methods, distributed computing and the concept of autonomous interaction, providing a new level of security, trust and stability in the context of a rapidly growing number of connected devices.

3. Purpose and objectives of the study

The purpose of this study is to analyse architectural approaches to building Internet of Things systems, with an emphasis on the advantages of a decentralised model compared to a centralised one. The paper examines the impact of decentralisation on the level of information security, resistance to

ISSN 2076-2429 (print)
ISSN 2223-3814 (online)

attacks, scalability and network autonomy. It also identifies the potential for integrating blockchain technologies to build trusted, secure and fault-tolerant distributed IoT systems.

4. Materials and methods

Based on a comparative analysis of centralised and decentralised IoT architectures in terms of key parameters of security, flexibility and resistance to attacks, scientific sources covering current approaches to ensuring security in IoT (in particular, using blockchain technologies), a logical communication diagram for a distributed IoT network with blockchain support is proposed (Fig. 1).

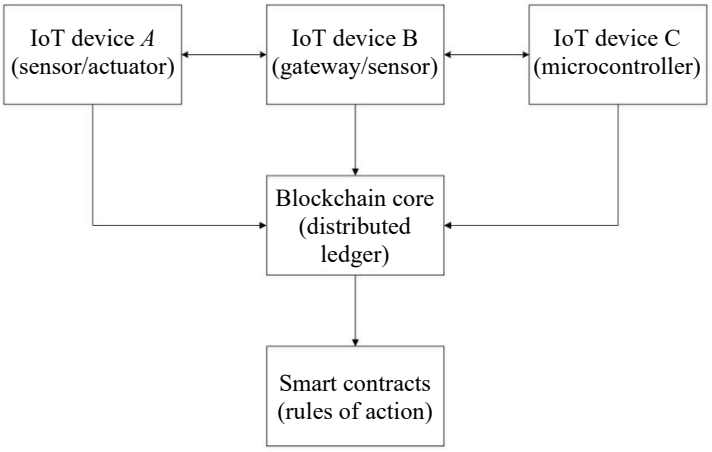

Fig. 1. Communication model in a distributed IoT network with blockchain support

The proposed model illustrates how nodes interact in a decentralised IoT network, where blockchain technology is used for data protection and access control.

Each IoT device (sensor, gateway, actuator, etc.) is a full-fledged network node with the following functions:

– data collection (temperature, pressure, movement, etc.);

– signing transactions with your own private key;

– sending messages to other nodes;

– validating transactions from a distributed ledger (partially or completely).

In some cases, nodes can be full nodes or light nodes, depending on resources.

The central element of decentralised logic is the blockchain core (distributed ledger).

Each node has a copy of the registry (complete or partial). Data sent by devices is recorded as transactions (in JSON format). Validation occurs through consensus (e.g., Proof-of-Authority, Delegated Proof-of-Stake, or IBFT for IoT). Recent advances in lightweight consensus and sharding techniques for IoT data exchange have demonstrated significant performance improvements under high transaction loads [10].

Smart contracts are software rules that automate actions in response to events:

– when a certain threshold value is reached or exceeded, the sensor activates the corresponding executive element;

– control access to data;

– process microtransactions between devices.

The communication process in the network occurs in the following sequence:

1. Data collection: The IoT device measures a parameter (e.g., temperature).

2. Transaction formation: The data is packaged into a transaction, which is signed with the device's private key.

3. Network transmission: the transaction is distributed via a P2P network to other nodes.

4. Validation: neighboring nodes check the signature, time, format and presence of conflicts.

5. Recording to the blockchain: once consensus is reached, the transaction is added to the next block.

6. Smart contract execution: if there is a corresponding trigger, an action is performed (e.g., a command to a relay).

7. Status update: all nodes synchronise their copies of the ledger.

5. Research results

This approach ensures data security – all transactions are signed and verified, and the data is immutable. The scheme has the advantage of autonomy: nodes operate without a central coordinator.

The proposed model is resistant to attacks because the failure of a single node does not affect the operation of the entire network. It has transparent access to data in an open registry that cannot be changed in an unauthorised manner. The network has good dynamic scalability and does not require additional configuration.

For the practical implementation of the logical model of a decentralised IoT network, the Ethereum platform was used – one of the most widespread blockchain ecosystems with built-in support for smart contracts.

When using this platform, each IoT device (or its gateway) interacts with the Ethereum network via an Ethereum light client node (e.g., via Geth, Infura, or Alchemy), which allows transactions to be transmitted without the need to store the entire blockchain on the device.

The implementation of the logical model consists of three main components:

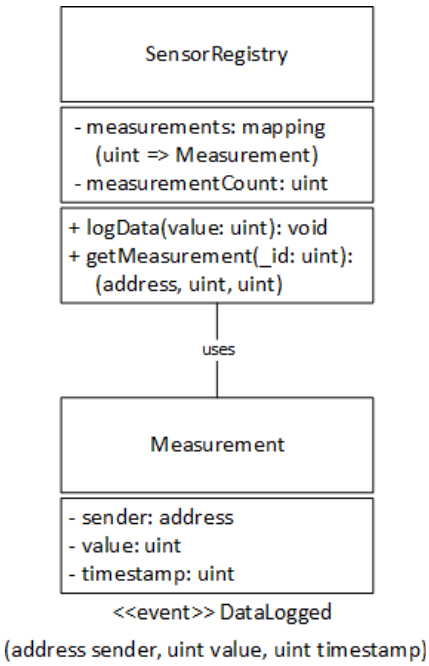

Fig. 2. Diagram of a smart contract fragment

1. An IoT device that generates key pairs (private/public), signs measured values (e.g., temperature) and transmits the transaction to the Ethereum gateway.

2. An Ethereum gateway connected to the Ethereum main net or test network (e.g., Sepolia, Goerli) that accepts transactions from multiple devices and forms calls to smart contracts.

3. The smart contract, which accepts parameters (sender, value, timestamp), stores the transaction history in event logs or arrays, and implements the logic for notification or triggering automated actions (Fig. 2).

Each IoT device (via a gateway) calls the logData() method, passing the measured value. The information is stored in a mapping with the possibility of further reading. The DataLogged event allows the system to respond to new measurements in real time (for example, in an external infrastructure via a Web3 connection).

Implementation on Ethereum determines storage reliability: all transactions are recorded in the blockchain and cannot be changed. Smart contracts enable the implementation of complex response logic, which provides certain opportunities for automation.

Integration with other systems is possible, for example, payment systems for micropayments for device services.

6. Conclusions

The proposed implementation of the model has certain limitations on the amount of storage in the smart contract. Transaction costs (gas fees) can complicate mass data recording.

For optimisation, only data hashes can be transferred to the blockchain, while the data itself is stored in external storage (IPFS, Filecoin).

To reduce transaction costs, Ethereum *L2* solutions (e.g., Arbitrum, Optimism) can be used.

As a result, this implementation allows for the creation of a reliable, distributed, scalable IoT system capable of autonomous operation, in which all transactions are confirmed by the Ethereum network consensus, and data is protected from unauthorised modification or falsification.

Література

1. Гриневич О. М., Ткачук А. В. Забезпечення кібербезпеки в системах Інтернету речей. *Наукові записки Українського науково-дослідного інституту зв'язку*. 2021. № 3(41). С. 54–60.
2. Шаров Ю. М., Бондар С. І. Проблеми інформаційної безпеки у розподілених IoT-системах. *Збірник наукових праць Харківського університету Повітряних Сил*. 2022. № 4(74). С. 112–117.

3. Sicari S., Rizzardi A., Grieco L. A., Coen-Porisini A. Security, privacy and trust in Internet of Things: The road ahead. *Computer Networks*. 2015. Vol. 76. P. 146–164. DOI: https://doi.org/10.1016/j.comnet.2014.11.008.
4. Kolias C., Kambourakis G., Stavrou A., Voas J. DDoS in the IoT: Mirai and other botnets. *Computer*. 2017. Vol. 50, No. 7. P. 80–84. DOI: https://doi.org/10.1109/MC.2017.201.
5. Albulayhi A. S., Alsukayti I. S. A Blockchain-Centric IoT Architecture for Effective Smart Contract-Based Management of IoT Data Communications. *Electronics*. 2023. Vol. 12, No. 12. Art. 2564. DOI: https://doi.org/10.3390/electronics12122564.
6. Пономаренко В. С., Кравченко О. О., Станіславенко В. А. Застосування блокчейн-технологій для підвищення захищеності IoT-мереж. *Інформаційні технології в освіті, науці та техніці*. 2021. № 1(20). С. 45–51.
7. Reyna A., Martín C., Chen J., Soler E., Díaz M. On blockchain and its integration with IoT. Challenges and opportunities. *Future Generation Computer Systems*. 2018. Vol. 88. P. 173–190. DOI: https://doi.org/10.1016/j.future.2018.05.046.
8. Novo O. Blockchain meets IoT: An architecture for scalable access management in IoT. *IEEE Internet of Things Journal*. 2018. Vol. 5, No. 2. P. 1184–1195. DOI: https://doi.org/10.1109/JIOT.2018.2812239.
9. Khan S. N. et al. Blockchain smart contracts: Applications, challenges, and future directions. *Peer-to-Peer Networking and Applications*. 2021. Vol. 14. P. 2151–2163. DOI: doi.org.
10. Haque E. U. et al. Performance enhancement in blockchain based IoT data sharing using lightweight consensus algorithm. *Scientific Reports*. 2024. Vol. 14. Art. 26561. DOI: https://doi.org/10.1038/s41598-024-77706-x.

References

1. Hrynevych, O. M., & Tkachuk, A. V. (2021). Ensuring cybersecurity in Internet of Things systems. *Naukovi zapysky Ukrainskoho naukovo-doslidnoho instytutu zv'iazku*, *3*(41), 54–60.
2. Sharov, Yu. M., & Bondar, S. I. (2022). Problems of information security in distributed IoT systems. *Zbirnyk naukovykh prats Kharkivskoho universytetu Povitrianykh Syl*, *4*(74), 112–117.
3. Sicari, S., Rizzardi, A., Grieco, L. A., & Coen-Porisini, A. (2015). Security, privacy and trust in Internet of Things: The road ahead. *Computer Networks*, *76*, 146–164. https://doi.org/10.1016/j.comnet.2014.11.008.
4. Kolias, C., Kambourakis, G., Stavrou, A., & Voas, J. (2017). DDoS in the IoT: Mirai and other botnets. *Computer*, *50*(7), 80–84. https://doi.org/10.1109/MC.2017.201.
5. Albulayhi, A. S., & Alsukayti, I. S. (2023). A blockchain-centric IoT architecture for effective smart contract-based management of IoT data communications. *Electronics*, *12*(12), Article 2564. https://doi.org/10.3390/electronics12122564.
6. Ponomarenko, V. S., Kravchenko, O. O., & Stanislavenko, V. A. (2021). Application of blockchain technologies to increase the security of IoT networks. *Informatsiini tekhnolohii v osviti, nautsi ta tekhnitsi*, *1*(20), 45–51.
7. Reyna, A., Martín, C., Chen, J., Soler, E., & Díaz, M. (2018). On blockchain and its integration with IoT: Challenges and opportunities. *Future Generation Computer Systems*, *88*, 173–190. https://doi.org/10.1016/j.future.2018.05.046.
8. Novo, O. (2018). Blockchain meets IoT: An architecture for scalable access management in IoT. *IEEE Internet of Things Journal*, *5*(2), 1184–1195. https://doi.org/10.1109/JIOT.2018.2812239.
9. Khan, S. N., Loukil, F., Ghedira-Guegan, C., Benharkat, A. N., & Bennani, E. (2021). Blockchain smart contracts: Applications, challenges, and future directions. *Peer-to-Peer Networking and Applications*, *14*, 2151–2163.
10. Haque, E. U., Abbasi, W., Almogren, A., Choi, J., Altameem, A., Ur Rehman, A., & Zaidi, S. A. R. (2024). Performance enhancement in blockchain based IoT data sharing using lightweight consensus algorithm. *Scientific Reports*, *14*, Article 26561. https://doi.org/10.1038/s41598-024-77706-x.

Стрельцов Олег Васильович; Oleh Streltsov, ORCID: https://orcid.org/0000-0002-4691-5703
Катріченко Михайло Олегович; Mykhailo Katrichenko, ORCID: https://orcid.org/0009-0004-2251-5600
Орновецький Юрій Васильович; Yuriy Ornovetsky, ORCID: https://orcid.org/0009-0006-2470-1559
Гриньов Максим Андрійович; Maksym Hrynyov, ORCID: https://orcid.org/0009-0007-7189-4485

Received September 29, 2025
Accepted November 01, 2025

UDC 004.93; 004.8; 004.942

V. Tigariev[1], PhD, Assoc. Prof.,
O. Lopakov[1],
V. Kosmachevskiy[1],
A. Liushenko[2]
[1] Odessa Polytechnic National University, Shevchenko Ave. 1, Odesa, Ukraine, 65044, e-mail: kedrodessa9@gmail.com
[2] Odesa I. I. Mechnikov National University, Dvoryanska St. 2, Odesa, 65082, Ukraine

DEVELOPMENT OF THE BASIC MODULE OF THE FUZZY ARTMAP ALGORITHM IN OPERATING SYSTEMS FOR DECISION MAKING AND INTELLIGENT DATA ANALYSIS

В. Тігарєв, О. Лопаков, В. Космачевський, А. Люшенко. **Розробка базового модуля алгоритму нечіткої логіки fuzzy artmap в операційних системах прийняття рішень та інтелектуального аналізу даних.** У системах підтримки прийняття рішень при управлінні організаціями на практиці часто застосовуються прості і зрозумілі моделі, як, наприклад, правила прийняття рішень на основі відомих методів нечіткої логіки, лінійна або логістична регресія, метод дерев класифікації і регресії. Цінність і практична значимість подібних алгоритмів полягає у важливій здатності цих алгоритмів розуміти і роз'яснювати їх внутрішню логіку прийняття рішення, але недоліком є їх невисока точність. Більш точні нейромережеві алгоритми, як правило, не мають властивості інтерпретованості. Однак пропонований в даному дослідженні алгоритм поєднує в собі досить високу точність при аналізі моніторингової інформації і, разом з тим, він добре пояснює отримані рішення. Для розробки методів і алгоритмів інтелектуальної підтримки прийняття управлінських рішень при обробці моніторингової інформації найкраще підходять нейронні мережі сімейства ART, оскільки вони відрізняються стабільною і швидкою атрибуцією даних, і разом з тим пластичністю для запам'ятовування нової інформації. На основі використання мереж сімейства ART запропоновано загальний підхід до вирішення завдань кластеризації моніторингових даних. Оскільки загальновідомим недоліком мереж сімейства ART є залежність від початкової ініціалізації гіперпараметрів, досліджено вид і характер даної залежності в завданнях кластеризації моніторингових даних. Запропоновано генетичний алгоритм для автоматичного налаштування гіперпараметрів мережі Fuzzy ARTMAP з метою подолання зазначеного недоліку. Такий алгоритм дозволяє вдосконалювати методи отримання та обробки інформації для завдань управління організаційними системами. Оскільки моніторингова інформація може породжувати потоки даних великого обсягу, запропоновано алгоритм використання ансамблю мереж Fuzzy ARTMAP для паралельної обробки та структурування потокових даних. Технологія паралельних і високопродуктивних обчислень розвивається, а обчислювальні ресурси стають все більш доступними, з'являються нові можливості для розпаралелювання моделей нейронних мереж, з точки зору кращої обробки обчислень і підвищення інтенсивності обробки даних, а, отже, і підвищення швидкості прийняття управлінських рішень на основі даних, які оперативно надходять , що особливо важливо в завданнях управління в організаційних системах. У статті розроблено та досліджено алгоритм навчання мережі Fuzzy ARTMAP для вирішення задачі класифікації в умовах пересічних класів. Така задача часто виникає при аналізі моніторингової інформації в системах підтримки прийняття управлінських рішень, оскільки при зборі оперативних даних часто зустрічаються шуми і помилки, що розмиває межі між класами, на які розбиваються значення вхідних моніторингових показників. Для цього алгоритму запропоновано модифіковану функцію вибору, що забезпечує подібну класифікацію, математично обґрунтовано її властивості.

Ключові слова: машинне навчання, алгоритми класифікації та кластеризації, нейро-нечіткі мережі (ANFIS), операційні системи (ОС), нормалізація вхідних векторів, препроцесинг, постпроцесинг, швидкість навчання мережі, метод комплементації, критерій подібності, фазіфікація даних

V. Tigarev, A. Lopakov, V. Kosmachevskiy, A. Liushenko. **Development of the basic module of the fuzzy artmap algorithm in operating systems for decision making and intelligent data analysis.** In decision support systems for organizational management, simple and understandable models are often used in practice, such as decision-making rules based on well-known fuzzy logic methods, linear or logistic regression, and classification and regression tree methods. The value and practical significance of such algorithms lie in their important ability to understand and explain their internal decision-making logic, but their disadvantage is their low accuracy. More accurate neural network algorithms, as a rule, do not have the property of interpretability. However, the algorithm proposed in this study combines a sufficiently high accuracy in the analysis of monitoring information and, at the same time, it explains the resulting decisions well. ART neural networks are best suited for developing methods and algorithms for intelligent support of management decision-making when processing monitoring information, as they are characterized by stable and fast data attribution, and at the same time are flexible for storing new information. Based on the use of ART family networks, a general approach to solving monitoring data clustering problems has been proposed. Since a well-known disadvantage of ART family networks is their dependence on the initial initialization of hyperparameters, the type and nature of this dependence in monitoring data clustering problems have been investigated. A genetic algorithm has been proposed for the automatic tuning of the hyperparameters of the Fuzzy ARTMAP network in order to overcome this drawback. Such an algorithm allows for the improvement of methods for obtaining and processing information for organizational system management tasks. Since monitoring information can generate large data flows, an algorithm for using an ensemble of Fuzzy ARTMAP networks for parallel processing and structuring of stream data is proposed. Parallel and high-performance computing technology is developing, and computing resources are becoming increasingly accessible, new opportunities are emerging for parallelizing neural network models in terms of better processing of calculations and increasing the intensity of data processing, and, consequently, increasing the speed of management decisions based on operational data, which is especially important in management tasks in organizational systems. This article develops and investigates an algorithm for training a Fuzzy ARTMAP network to solve classification problems in conditions of overlapping classes. Such a task often

DOI: 10.15276/opu.2.72.2025.15

ISSN 2076-2429 (print)
ISSN 2223-3814 (online)

arises when analyzing monitoring information in management decision support systems, since noise and errors often occur when collecting operational data, which blurs the boundaries between the classes into which the values of the input monitoring indicators are divided. A modified selection function that provides such classification is proposed for this algorithm, and its properties are mathematically justified.

Keywords: machine learning, classification and clustering algorithms, artificial neural fuzzy inverse systems (ANFIS), operating systems (OS), input vector normalization, preprocessing, postprocessing, network learning speed, complementation method, similarity criterion, data fuzzification

Introduction

Improving management processes in operating systems at the present stage requires the introduction of new information technologies, including methods of decision support based on operational monitoring data. In today's world, monitoring has become an integral part of various fields of activity. For example, it is actively used in ecology to control environmental pollution; in medicine to help monitor the health of patients; and in education to assess the effectiveness of educational institutions. The use of monitoring data to support management decision-making in operating systems has a number of advantages. First, monitoring provides continuous information about the status of objects and processes, which makes it possible to respond quickly to emerging problems when making management decisions. Second, monitoring contributes to more efficient use of resources, as processes can be optimized and losses reduced based on up-to-date data. However, despite all its advantages, monitoring also has its limitations. Existing methods of processing monitoring data are generally insufficiently effective due to the inability to quickly take into account large amounts of incoming information (including noisy data and data containing missing values collected from diverse sources). Incorrect processing and analysis of monitoring data often leads to wrong decisions. In general, the use of monitoring data in management requires not only its correct analysis, but also an understanding of how this data should influence changes in the organization. Machine learning technologies that have emerged in recent years, based on neural network and neuro-fuzzy approaches, allow management systems to process real-time data, including data containing missing, erroneous, or inaccurate values, and automatically generate examples of management decisions. A study of existing neural network and neuro-fuzzy architectures has revealed the feasibility of using adaptive resonance networks (ART) for processing monitoring data in decision support tasks. ART networks are stable, which means they can retain accumulated knowledge throughout the entire operating time of the system. In addition, they provide flexibility through the use of an incremental learning mechanism. Incremental learning allows you to take into account current information about the state of objects and respond quickly to changes in the situation. Cascade ARTMAP neuro-fuzzy models are good at processing noisy data and allow the development of a system for the automated construction of decision rules to support management decision-making based on monitoring data.

Analysis of recent publications and problem statement

Problems related to the development of management methods and mechanisms based on monitoring data were considered in the works of V.N. Burkov, D.A. Novikov, D.V. Gaskarov, A.V. Shchepkina, Ya. E. Lvovich, V.A. Irikov, V.D. Kondratiev, G.A. Ugolnitsky, and others. Modern neural network and neuro-fuzzy technologies used in the development of information support for control systems are discussed in the works of K. Broyden, D. Goldfarb, E. Mamdani, G.S. Pospelov, S. Haikin, D. Shanno, G. Carpenter, S. Grossberg, Y. Lecune, P. Flach, and Y. Goodfellow. However, issues related to the implementation of control methods based on real-time monitoring data using machine learning algorithms in the practice of decision support in control systems have not yet been sufficiently addressed in the literature. In this regard, the relevance of the topic of this article is dictated by the need for further development of intelligent decision support tools in organizational systems in the context of operational monitoring based on adaptive resonance neural networks.

The problem with using the neural ART system lies in the complexity of practical network use due to the lack of a generally accepted authorial formalization. The authors' publications reveal the concepts of functioning but do not pay attention to the training of structured algorithms [1 – 4]. Because of this, researchers using the system describe the structure of ART and training algorithms in different ways [4 – 6]. Therefore, it can be stated that there is no single standard for describing the ART family in scientific literature.

The purpose of the study

Development of means for algorithmizing the processes of management decision-making in OS based on incremental neural network methods of monitoring data analysis.

To achieve this study, the following tasks must be completed:

Conduct an analysis of management systems based on monitoring data in organizational systems, identify problems, and, on this basis, formulate relevant directions for the development of decision support systems.

Develop a structural and functional model for supporting management decision-making based on monitoring indicators in order to improve the information support for management processes in organizations.

Develop a modified algorithm for clustering monitoring data based on the Fuzzy ART neural network model to improve the cluster approach to management with the ability to select different control actions for different clusters of monitoring indicator values in the context of their operational analysis.

Subject of – methods for intellectualizing decision-making processes in OS based on monitoring data received in real time.

To solve the problems posed in the dissertation, methods of systems analysis, decision making, machine learning, big data processing, fuzzy logic, artificial neural network theory, and modern programming methods and tools were used.

Statement of the main material

Development of a clustering algorithm for operational analysis of monitoring data based on the FuzzyART neural-fuzzy network

There are several approaches to developing management information technologies based on monitoring data. Let's consider the main ones.

Real-time data analysis. This method involves continuous monitoring of various parameters and sensors to collect data in real time. The data obtained is analyzed to identify trends, patterns, and anomalies, which allows for quick management decisions.

Use of machine learning. This approach is based on the application of machine learning algorithms to analyze and process monitoring data.

Machine learning models can be trained to recognize certain patterns or predict future parameter values based on historical data.

Use of big data analytics. This approach involves collecting and analyzing large amounts of information using specialized tools and algorithms. Big data allows you to identify complex relationships and trends that can be used in management decision-making.

Using the Internet of Things (IoT). With the development of IoT technologies, monitoring capabilities have expanded significantly. IoT devices can collect and transmit data from various objects and sensors, enabling more accurate monitoring and control.

Process automation and optimization. This approach involves developing information technologies that enable the automation and optimization of various processes based on monitoring data. This may include automatic real-time parameter adjustment or the proposal of optimal management strategies based on the data obtained. The final choice of method for developing information technologies for management based on monitoring data depends on the specific task and requirements of the organization. However, machine learning methods are currently used as the main technology for the operational analysis of monitoring information. Let's consider the main reasons for this.

First, machine learning algorithms can quickly analyze and extract information from streaming data, which greatly simplifies working with large amounts of data.

Second, machine learning methods are capable of searching for and discovering hidden patterns and relationships in monitoring data that may be invisible even to an expert. This allows you to identify similar patterns in sets of monitoring indicators and predict future trends based on available data, which is valuable information for decision-making.

Third, machine learning methods allow you to create models that take into account complex nonlinear interactions and dependencies in data. Such models can be more accurate and of higher quality than linear approaches.

Fourth, machine learning methods can learn from new data and update model parameters, allowing them to adapt to changes and improve their performance. This is especially important for processing monitoring data, which can change significantly over time.

Fifth, machine learning methods can be used to automatically generate management actions based on previously accumulated knowledge.

ISSN 2076-2429 (print)
ISSN 2223-3814 (online)

Figure 1 shows a diagram of the decision support process based on machine learning methods using monitoring data.

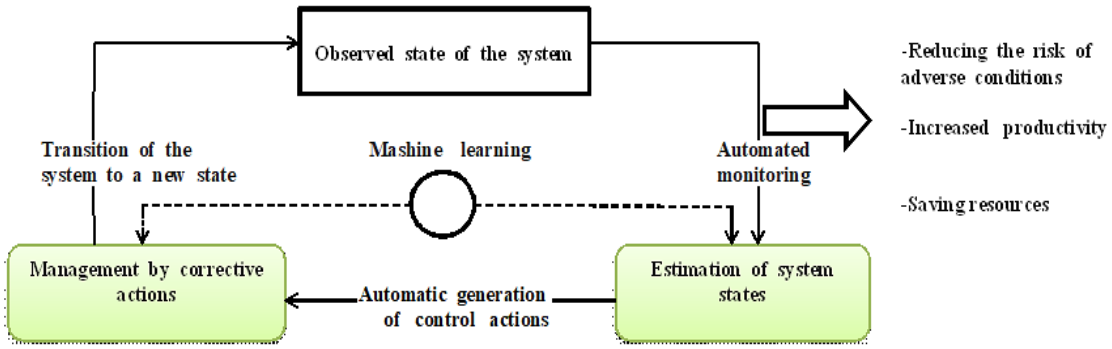

Fig. 1. Decision-making based on monitoring data using machine learning methods

Typically, methods for structuring monitoring data include clustering and classification algorithms. Clustering refers to a fundamental method of researching and processing indicators, widely used for:

− recognizing similar situations [7];
− identifying key features (characteristic features) of problematic situations [8 – 10];
− intelligent analysis, i.e., extracting knowledge from data [10].

Clustering identifies common structures present in a data set based on some measure of similarity.

Classification algorithms are used to systematize the information being processed. Classification can be binary or multi-class, produce overlapping or non-overlapping classes, and output a class label or a probability vector for each of the available classes. In any case, the classification algorithm structures the source data according to some feature.

The availability of modern capabilities for collecting and storing indicators helps to generate huge amounts of information for further use, searching for connections, interactions, and patterns. Information arrays demonstrate the need to include subprograms in comprehensive monitoring programs that conduct systematic information analysis using the characteristic features of indicators—multidimensionality and multirelationality. This contributes to difficulties in assessing and forecasting problematic situations. The decision-maker uses assessment methods, but they are not based on integration, so in practice, they are often considered ineffective and require more detailed elaboration on all strategies for responding to existing problems and damage caused. Particular attention should be paid to certain individual factors that influence their complex interaction. For example, aggregation is a traditional method of collecting and analyzing information based on the average monitoring value of indicators. Studies have shown that approaches to existing problems somewhat level out the differences between problematic situations that may be signaled by monitoring indicators [11]. To improve the accuracy and timeliness of management decisions, new intelligent technologies should be used in analysis. Such an intelligent approach to analysis will allow work to be carried out even in conditions of insufficient information. For example, studies [12 – 14] and [15] suggest using a scientific and methodological apparatus of a qualimetric approach based on fuzzy technologies when managing based on monitoring data. This will help to construct a non-additive integral assessment, which will serve as a weighted average “quasi-geometric” value. In order for system analysis to yield tangible results in problematic situations, it is necessary to build an integral assessment based on monitoring data by applying different approaches that establish structural links between the system’s monitoring indicators, as this will allow the most logical and consistent approach to be chosen when making important decisions.

In general, methods based on fuzzy logic are good at processing qualitative and imprecise indicator values, while also being highly interpretable. However, these methods require significant effort to configure their hyperparameters, involving subject matter experts. If such tuning were required only once, it would not be a significant limitation, but even a small change in the set of parameters being analyzed requires significant refinement of the system. Another group of methods used to process monitoring indicators are evolutionary modeling methods. The key to using genetic algorithms (GA)

in monitoring data processing is to frame the problem as an optimization task. Many monitoring data processing tasks are optimization tasks, for example, numerous applications of inverse models (i.e., tasks of finding such values of monitoring indicators that would lead to the desired effect in management). [16] describes a specific optimization problem in which GA proved useful – the use of pollutant concentration data in combination with a transport and dispersion model to reverse-calculate control actions based on meteorological information. Genetic algorithms (GA) can be used to optimize the parameters of monitoring data processing algorithms. However, this is an auxiliary tool, not a primary one. One of the main areas of computer monitoring technologies based on artificial intelligence is the use of neural networks, which greatly facilitate the analysis and prediction of problem situations. Today, artificial neural networks are one of the most advanced and modern methods of processing monitoring information and extracting knowledge from monitoring data. This is not surprising, since neural network algorithms have high potential for solving monitoring data processing tasks and are good at processing noisy and incomplete data. The only problem is that, as is well known, neural networks operate in a "black box" mode, i.e., they are not understandable and interpretable methods, which limits their applicability in many subject areas. In particular, in OS management tasks, situations sometimes arise that require urgent intervention, when the cost of an error can be very high. In such cases, experts cannot rely on the result predicted by the "black box." In such subject areas, in order to apply a decision support algorithm, it must not only be accurate, but also understandable to experts (decision makers) so that they can make adjustments to the resulting decision. Due to the inherent requirements for interpretability, experts often have to use a narrow range of models in practice: classification trees, fuzzy knowledge bases, or linear regression, while neglecting the low accuracy of the results obtained. Prior knowledge of the problem domain can help a neural network learn to solve the problem of insufficient interpretability. In particular, previously existing classification rules can be used to initialize the neural network architecture before training. The use of initial rules not only increases the efficiency of network training, but also allows you to obtain knowledge that cannot be obtained as a result of training or that cannot be easily learned by a neural network, thereby improving the predictive performance of the system. In addition, incomplete or partially correct knowledge formulated in the form of classification rules can be improved or expanded using neural network training algorithms. Thus, the introduction and refinement of rules into neural networks automates the expansion and restoration of expert knowledge. On the other hand, when there are high requirements for algorithm accuracy, experts are forced to resort to the use of deep learning algorithms [16 – 18]. Deep learning uses a backpropagation algorithm to learn to predict certain output vectors in response to processed input vectors [18]. However, deep learning can lead to information forgetting: at any stage of training, part of the neural network's memory may be destroyed [19]. The reason for this phenomenon is that all network input data is processed by the backpropagation algorithm through a common set of adjustable weights, while there is no mechanism within the algorithm for selectively buffering previous training that is predictively useful. Such forgetting can occur in any training algorithm in which weight updates are based on the use of the error gradient in response to the current input data packet.

Thus, one of the main problems with using backpropagation networks to improve rule-based knowledge is the preservation of accumulated knowledge. In the process of adjusting weights using the backpropagation algorithm, the initial rules quickly lose their original values. In fact, such training can result in large shifts in the values of the weights of hidden layers [20]. Another serious limitation of the backpropagation method is that the initial rule base must be almost complete, otherwise the initial network architecture created may not be accurate enough to process the entire data set. Since the standard backpropagation algorithm cannot dynamically create additional neurons or connections between them during training, a network initialized with a small set of rules may even have less chance of ultimately solving the classification problem. This problem was noted and partially solved in [21], which uses virtual rules to create potential connections for training. However, in general, it is difficult to determine the desired decision rules in advance. In [22], a learning algorithm is used that allows additional neurons to be created during the learning process. However, since this model consists only of rules that directly link input attributes to output predictions, the network is not versatile enough to work on a rule-based basis using intermediate attributes and rule chains. From all of the above, we can conclude that an effective adaptive decision support algorithm in an OS based on monitoring data must be capable of incremental learning, i.e., using all newly arriving data to retrain the existing model. As already noted, the specifics of management tasks in organizations based on monitoring indica-

ISSN 2076-2429 (print)
ISSN 2223-3814 (online)

tors include decision-making using data that contains noise and missing values. Input data may be partially incorrect due to faulty sensors. However, during training, such data should not "spoil" correctly configured weights. Thus, the peculiarities of management tasks in OS based on monitoring data dictate the need to use incrementally learning neural network algorithms. At the same time, the resulting data structuring results must be interpretable, that is, they must induce IF...THEN rules that explain which combinations of input features predict these particular results.

The first stage of processing incoming monitoring data is often clustering, which is used to perform preliminary systematization. The monitoring environment uses machine learning methods to perform cluster structuring of data across all aggregate indicators. The results determine the most appropriate alternative approach to structuring and enable the transition to the mathematical modeling stage. At the same time, such structuring methods of information processing allow focusing on specific goals.

By forming a cluster structure of the initial indicators, it is possible to understand the information they contain. The resulting clustering allows for the improvement of current approaches to management decision-making and the development of strategies for responding to deviations in the values of monitoring indicators. A special management technique can be applied to each cluster.

− During the clustering process, new and atypical data can be identified by detecting monitoring indicator values that do not belong to any of the clusters. These data require individual analysis to identify their characteristics.

− Clustering reduces the amount of information to be analyzed, allowing you to analyze not every set of monitoring indicator values, but only those combinations that are typical for individual clusters.

It is worth noting a particular pattern used to improve the assessment methodology. The widespread use of decision support systems in management based on monitoring data allows for the collection and processing of information, including the use of special sensors located at monitoring sites. Information from sensors is needed to conduct a full assessment and analysis of the functioning of facilities and the presence of man-made and negative natural phenomena. The quality of decisions made on the organization of further actions depends on a number of factors:

− timely receipt of information about all processes at the facilities;

− clear differentiation of processing results by clusters;

− objective processing of analytical data.

The indicators obtained from sensors are considered to be variants of more comprehensive indicators that require the application of intelligent control algorithms and processing of incoming analytical flows.

Thus, it is possible to formulate the characteristic features of monitoring data and the requirements for the algorithmic support for their processing.

As a rule, monitoring data is very large in volume, which requires its automatic processing (including in real time) and automated formation of control decisions.

Data for processing can be received in batch mode (for periodic monitoring) or in streaming mode (for continuous monitoring). Consequently, decision support methods are needed that can adapt to changing data flows and scale to their volume. Monitoring indicators are characterized by nonlinear interactions that affect the state of controlled objects, as well as inherent emergence. Consequently, decision support systems (DSS) require methods that take into account nonlinear relationships and at the same time form a structure that does not grow uncontrollably with the processing of large amounts of data.

Monitoring data usually contains noise, gaps, and inaccurate values (especially data transmitted from sensors). Therefore, methods are needed that can work with incomplete, fuzzy, and noisy information. Monitoring data used to support management decisions requires interpretive analysis. Therefore, methods are needed that can explain the results obtained. Practically all of the above requirements for algorithms for structuring monitoring data are met by the ART family of neural networks (based on adaptive resonance theory). The first networks of this family were proposed in the works of Carpenter and Grossberg [19-20]. However, these networks did not receive widespread application at that time, as they were inferior in accuracy to traditional networks when dealing with small amounts of data. In addition, ART networks have a more complex architecture than multilayer perceptron networks or Kohonen and Hopfield networks (proposed around the same time), and they are more difficult to configure (as they have a large number of hyperparameters). However, when solving big data processing tasks, especially those coming into the network as a continuous stream (such as monitoring

information from sensors), these networks have undeniable advantages over many traditional networks. These advantages are based on the use of a built-in incremental learning mechanism focused on solving the stability-plasticity dilemma: ANNs are retrained "on the fly," and new information does not erase accumulated knowledge. In addition, the ART network training algorithm is easily parallelized, making it suitable for big data processing. Most importantly, some subtypes of the ART family of networks are interpretable models, i.e., they allow the presentation of learning results in the format of "if-then" rules, similar to what can be done in the decision tree method. ART networks can solve both classification and data clustering tasks, and even when solving classification tasks, they divide the data into clusters (clusters) in an adaptive self-learning mode, with each resulting class corresponding to several categories.

The task of updating ART family networks in algorithms for structuring streaming monitoring data is of paramount importance, since there are currently no other architectures that are as suitable for solving this task. Table 1 provides a comparative analysis of the advantages and disadvantages of various methods of processing monitoring information, including ART family networks.

Table 1

Advantages and disadvantages of existing methods for processing monitoring information

Methods	Advantages	Disadvantages
Empirical-statistical methods	Well researched, long used, many of them interpretable	They do not have the ability to process incoming information (including noisy and incomplete information) in a timely manner, relying only on linear dependencies. They do not have the ability to process incoming information (including noisy and incomplete information) in a timely manner, relying only on linear dependencies.
Methods based on neural networks not belonging to the ART family	There are powerful learning algorithms that automatically generate features based on input indicators and allow nonlinear dependencies to be constructed, easily adapting to changes in the structure of the input data.	They do not have the property of incremental learning, are not interpretable, do not cope well with noisy and qualitative data, and require hyperparameter tuning.
Evolutionary, genetic algorithms	Allow automatic configuration of method parameters	They do not have the property of interpretability and do not cope well with noisy and qualitative data.
Methods based on fuzzy logic	They handle data containing gaps and erroneous or inaccurate values well, as well as qualitative data, which is important when processing monitoring data that may be partially incorrect due to faulty sensors. They have the property of interpretability.	Difficult to configure and train, requiring significant involvement of experts in developing methods and complete renewal of the entire system whenever the set of input indicators changes.
Neuro-fuzzy networks ANFIS (Adaptive Neuro-Fuzzy Inference System) and TSK (Takagi-Sugeno-Kang)	They have the ability to adapt to changes in data. They provide the ability to interpret results. They have learning algorithms for adjusting model parameters and combine the advantages of neural networks and fuzzy logic.	Training requires a large amount of data and computing resources, as well as the involvement of experts to select fuzzy membership functions. Prone to overfitting. Requires prior training.
Methods based on neural networks of the ART family	They are a hybrid approach combining neural network and fuzzy methods, retaining all their advantages. They possess the property of stability-plasticity: they are capable of incrementally memorizing new information without losing old information. They do not use explicit methods of fuzzification and defuzzification, which greatly facilitates their configuration.	They cannot fully cope with large flows of monitoring data, begin to form too many different categories in the data structure, and cannot cope with the task of classification in conditions of overlapping classes (this requires modification).

ISSN 2076-2429 (print)
ISSN 2223-3814 (online)

Structural and functional model for supporting management decision-making based on monitoring indicators When processing monitoring data, especially in the context of its operational analysis, the first step is to structure it, i.e., cluster or classify it. Clustering allows for a better "understanding" of the specifics of the incoming data and the identification of possible anomalies, while classification allows for the assignment of current measurements of indicators to one of the previously recorded classes of states of the monitored system. The structuring stage is followed by the decision-making stage, where the necessary corrective actions in a given situation are determined on the basis of the promptly received and already structured information. Neural network models can be used for the automated formation of control actions. Formally, such a system can be described as a tuple:

$$< P_t, K_t, R_t, U_t, N_t >, \quad (1)$$

where:

P_t – input set of monitoring indicator values at time *t*;

K_t – set of clusters into which the state of controlled objects is divided, taking into account the current values of monitoring indicators;

R_t – classification of possible system states depending on the clusters obtained;

U_t – a set of possible control actions depending on the class of the current state;

N_t – a set of neuro-fuzzy models that establish correspondences:

$P_t \to K_t$ (clustering model);

$K_t \to R_t$ (classification model);

$R_t \to U_t$ (decision rule construction model).

The ART neural network currently consists of 10 models based on the principle of stability-plasticity, the main ones being:

– ART-1 – this network processes binary input vectors;

– ART-2 – this network is designed for clustering continuous input vectors (demonstrates high quality performance);

– ART-2a – a faster version of ART-2, but inferior in quality;

– ARTMAP (combining two ART-1 or ART-2 networks into a single entity) – solves issues with the distribution of information across classes, i.e., it is designed for classification tasks;

– Fuzzy-ART and Fuzzy-ARTMAP – modify the architectures of ART-2 and ARTMAP networks by using fuzzy logic in the calculation process, which allows for better processing of incomplete and noisy data. To solve the problem of approaching the description of the system, it is necessary to formulate the functional principles of ART networks at general stages, namely the following:

All types of existing ART networks have at least one layer of neurons, which during operation are transformed into prototypes of corresponding clusters. The result of clustering is expressed in a specific "recognition" response by the neuron responsible for a certain cluster of the current input vector. If the input vector is not similar to any of the previously formed clusters, this leads to the creation of a new cluster corresponding to the input vector, which, in turn, leads to the addition of another neuron to the network structure, which will be the prototype of the new cluster. The cluster prototype is capable of "learning" and changing. The cluster prototype will not be modified if the input vector is not sufficiently similar to it (which solves the stability-plasticity problem). Input vectors that are not similar to previously processed data can lead to the formation of new clusters, but cannot destroy the accumulated memory of the network and "corrupt" previously formed clusters. To consider the general model of the ART family network, let us introduce several key definitions.

Definition 1 (initial sample). Let $X = \{x^1; x^2; \ldots; x^C\}$ – a set of data (vectors of features or objects). X – the initial sample of power C, each element of which is a vector in R^n type $x^k = (x_1; x_2; \ldots; x_n)$.

Definition 2 (cluster or cluster). A cluster (cluster) is a subset $Z \in X$. The result of clustering is a set of clusters that the clustering algorithm has detected in the dataset. *X.* "Hard" clustering is the division of X into mutually exclusive clusters, while "soft" (or overlapping) clustering allows a data element to belong to more than one cluster.

Definition 3 (prototype). Each j-th ART neural network $(j = \overline{1,M})$ has a vector associated with it $w^j = (w_{j1}; w_{j2}; \ldots; w_{jn})$, which consists of weighting factors w_{ji} on the connections of a neuron j. Such a vector w^j is called the prototype of the cluster, i.e., the internal representation of the cluster described by neuron j. The functionality of the network can be described using a general model, which can be used to analyze the training results of various ART networks. The results of this analysis can be conditionally divided into the following stages [20].

Setting the initial network parameters

In order for the ART network to work as planned, its initial parameters must be initialized in advance. Any network of the ART family includes at least one working layer that contains prototypes of the categories (clusters) created by the network in the input data. All network inputs are connected to each of the prototypes via a weight coefficient matrix $W = (w_{ij})$, which at this stage is usually filled with zeros, since the cluster prototypes are not yet known. At the initial stage, all the main network parameters must be initialized, including the learning rate coefficient β, the parameter regulating the similarity of vectors from the same cluster ρ, and the maximum number of iterations.

Preparation of input vectors (preprocessing)

Depending on the characteristics of the input data and the type of network, different processing of the input vector takes place at this stage. The procedure includes any changes to it: noise removal, normalization, dimension doubling (complementation), etc., without which the network cannot function correctly.

Primary data analysis (clustering)

At this point, each network in the ART family performs an initial evaluation of the input vector using a selection function designed to measure the distance between sets of input features based on one of the existing metrics. In Fuzzy-ART and Fuzzy-ARTMAP networks, fuzzy metrics are used to measure this distance.

Detailed compliance analysis

At this stage, a specific neuron belonging to the prototype layer is activated. It is determined using a special matching function. This function is responsible for the accuracy and non-linearity of the analysis in the recognition process concerning vector similarity. An important circumstance is taken into account here: if the vector and the prototype pass a successful check for functional correspondence with each other, a new stage will begin, in which the weights of the prototype vector will change, i.e., they will undergo training. If the check fails, the activated neuron will be temporarily deactivated. Thus, the selection function determines the cluster closest to the current input vector, and the matching function determines whether the input vector is sufficiently similar to the prototype of that cluster.

Training stage

During the training phase, the weights of the neuron, which is the prototype of the cluster selected in the previous phase, are changed. If none of the existing prototypes pass a detailed functional check for compliance, a new cluster will be created based on the vector that the network was unable to recognize. In this case, a new neuron is activated, the characteristics of which are determined by the coordinates of the unrecognized vector. At the same time, the size of the network increases. That is, the ART network has a growing architecture.

Post-processing (post-processing of results)

After the learning process is complete, the network provides for subsequent processing of the network output values. For example, if a limit on the quantitative composition of clusters is specified in advance, they are combined or separated from each other in accordance with the necessary conditions. Based on the above, we can conclude that in order to solve a specific problem related to the structuring of certain input data, it is necessary to determine the ART network model option depending on the required output structural elements and to complete the stages according to this algorithm. To do this, it is necessary to determine the list of network control parameters, fix the selection function, as well as the correspondence and training functions, and set two basic algorithms: pre- and post-processing. It should be noted that the architecture of the ART family network can include one or more basic modules consisting of three blocks: a learning block, a comparison block, and a recognition block. Figure 2 shows a diagram of the basic module of the ART family networks.

ISSN 2076-2429 (print)
ISSN 2223-3814 (online)

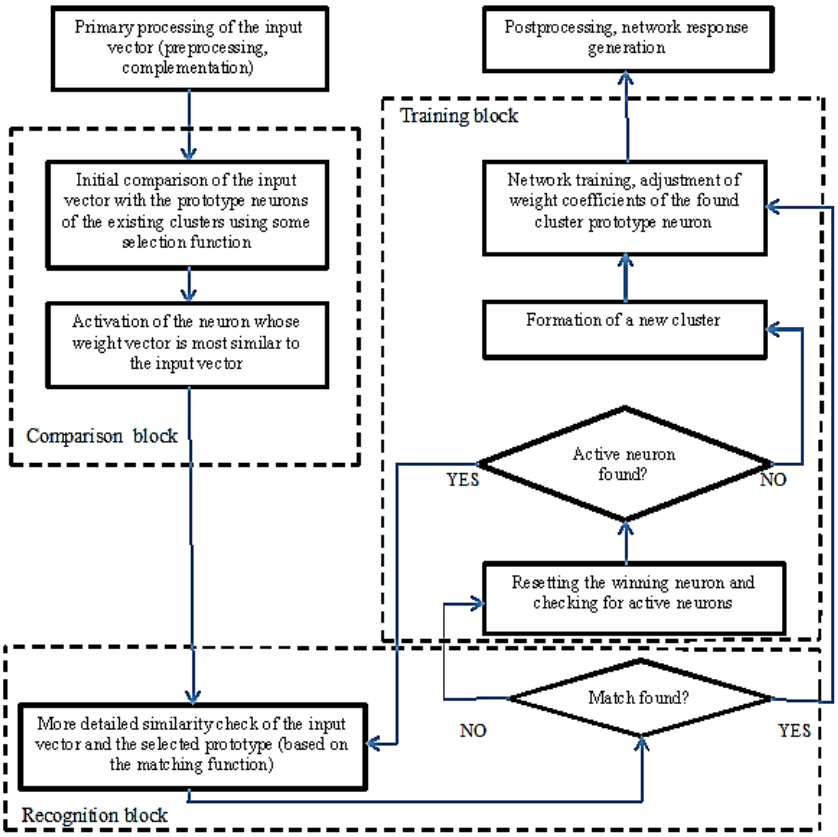

Fig. 2. Algorithm of the basic module of the ART family networks

Networks in the ART family can be trained either supervised or unsupervised. In any case, even if an ART network is supervised, it has a self-organizing module at its core, which divides all input vectors into clusters consisting of similar images. One class can correspond to multiple clusters. The converse is not true in the basic approach; each cluster can only correspond to one output class, which is not always convenient, as classes may overlap when processing real data. For example, the same set of input monitoring indicators may correspond to several problematic situations requiring management decisions, which obviously require modification. The above steps are common to all networks in the ART family, but their implementation varies across different networks in the family. Let us consider the content of the specified stages for two basic networks of this family that solve the clustering problem: the ART-2a network [23-24], which uses conventional arithmetic operations on real input data, and its modification, the Fuzzy ART network [25], which uses fuzzy logic operations in calculations (but does not require fuzzification of inputs). The use of fuzzy operations allows the network to be less sensitive to imprecise measurements and noise in the input data, and it is the neuro-fuzzy variations of ART models that are proposed in this study to be used as a basis for developing decision support systems in the OS in the context of operational analysis of monitoring data. However, to understand the features of the Fuzzy ART functioning, it is first necessary to describe the logic of the ART-2a network, of which Fuzzy ART is a modification.

B The list of parameters of the ART-2a network includes, in particular, the learning rate, which is a real number $\beta \in [0;1]$, normalization parameter θ, which is taken from the interval [0;0.01] and the boundary criterion similarities ρ, also belonging to the segment [0;1]. The ART-2a network requires mandatory normalization of input vectors to unit length before recognition:

$$x_{ij}^{new} = \frac{x_{ij}^{old}}{\sum_{j=1}^{J}(x_{ij}^{old})^2}, \qquad (2)$$

where through J the dimension of the next vector supplied to the input is indicated X^i, and through x_{ij} – his j-th component. Then the coordinates of the normalized vectors whose value became less

than the normalization parameter θ, are reset, after which the normalization procedure is repeated once more. This procedure is designed to suppress small random noise in the source data, which could negatively impact the resulting clustering quality. The ART-2a network uses the cosine distance between vectors as a similarity metric, which is calculated as the scalar product of corresponding unit-length vectors:

$$T^k = M_k = (X^i, w^k,) = \sum_{j=1}^{J} x_{ij} w_i^k, \tag{3}$$

where: through X^i again denotes the *i*-th input vector, via T_k the selection function is designated for *k*-th cluster, M_k – This is the value of the established conformity function, vector w^k – This is the currently existing prototype of the *k*-th cluster.

The ART-2a network's operating algorithm consists of the following steps. In the first step, using the cosine metric, the network selects a cluster with number s whose prototype has the greatest similarity to the original vector. X^i, i.e. $s = \arg\max_k T_k$. In the second step for the selected cluster k the matching condition is checked $M_s > \rho$, where ρ – the similarity criterion value, which sets the upper limit for the homogeneity of vectors in a cluster. If the selected cluster prototype satisfies the similarity condition, the original vector is assigned to that cluster. In this case, it is necessary to recalculate the coordinates of the cluster prototype so as to increase its similarity to the input vector in formula (4):

$$w^{k+1} = \frac{(1-\beta)w^k + \beta * X^i}{\left\|(1-\beta)w^k + \beta * X^i\right\|}, \tag{4}$$

where: β learning speed.

The weight vector modified according to formula (4) undergoes further normalization. Note that the choice of the speed parameter value β the requirement to identify long-term patterns or track data trends is influenced. In the first case, small parameter values are set, while in the second, larger ones are more appropriate. Regarding the parameter ρ (level of similarity), then choosing it is much more difficult. This is both from a theoretical and practical standpoint. Since the researcher does not always have an understanding of the data structure, the task of determining the largest angle at which vectors can be considered similar becomes labor-intensive. This is the reason for a serious drawback of the ART-2a network. Namely, high values ρ lead to an increase in the number of clusters, which is difficult to control. And small values lead to the formation of a single large cluster. A solution to this problem can be obtained by applying the following strategy: decrease the learning rate parameter while monitoring the number of clusters, and stop the process when this number stabilizes. The Fuzzy ART network [24 – 27] is based on a slightly different principle of processing continuous input data. This network uses fuzzy logic operations, but does not require explicit data fuzzification. To process the values of monitoring indicators using this network, scaling of all components of the input and output vectors within the interval [0;1] is required, rather than unit normalization:

$$x_{ij}^{new} = \frac{x_{ij}^{old} - x_i^{\min}}{x_i^{\max} - x_i^{\min}}, \tag{5}$$

where: through x_i^{min} denotes the minimum coordinate of the input vector X_i, and through x_i^{max} – its maximum coordinate.

The structure of this network is shown schematically in Figure 3.

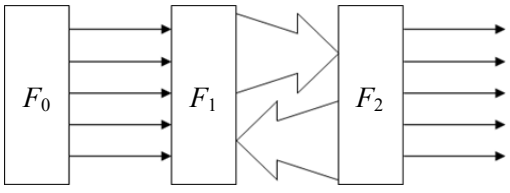

Fig. 3. Fuzzy ART network architecture

ISSN 2076-2429 (print)
ISSN 2223-3814 (online)

The Fuzzy ART network includes layer F_0, which represents the current input vector [28]; layer F_1, which processes both the input from layer F_0 and the feedback from layer F_2, which represents the recognized category (cluster).

Layer output F_0 is a vector $I=(a_1,\ldots a_{1M})$, each component of which belongs to a segment [0,1]. Layer F_1 generates a vector at the output $X=(x_1,\ldots,x_M)$, and the F_2 layer is a vector $Y=(y_1,\ldots,y_N)$. Weight matrix W connects layers together F_1 and F_2, and for each neuron $j(j=1,\ldots,N)$ layer F_2 corresponds to the weight vector $W^j=(w_{j1,\ldots}w_{jM})$, Initially it is assumed $w_{j1}=\ldots=w_{jM}=1$. At the stage of selecting the winning neuron of layer F_2 of the ART module (shown in Fig. 2. above), the task of finding the global maximum of the selection function can be divided into subtasks for each stream to find its local maximum, and then combined to generate the global maximum using the reduction function. The Fuzzy ART network has a number of hyperparameters α,β,ρ, where β and ρ have the same meaning as in the ART-2a network, and α – a small number (approximately 10^{-6}), responsible for the non-degeneracy of cluster prototypes. Any existing implementation of "fuzzy AND" can be used as the selection function, for example in formula (6):

$$T_k=\frac{\left|X^i\wedge w^k\right|}{\alpha+\left|w^k\right|}, \tag{6}$$

where: $\wedge$ – fuzzy multiplication operator, which is defined here and below as:

$$(p\wedge q)_j=\min(p_j,q_j),\ j=1,J\ ,$$

and the modulus sign denotes a fuzzy norm: $|p|=\sum_i p_i$. The Fuzzy ART network, if the similarity condition is not satisfied, applies a temporary cluster deactivation mechanism. Note that such a mechanism is not provided in the ART-2a network. Therefore, at the cluster determination stage, the cluster number will be determined by the maximum value of the function according to formula (6) across all active clusters, i.e. $s=\arg\max_k T_k, k\in Q$, where Q the set of numbers of clusters active at a given stage. Next, the *s*-th prototype is checked against the input vector. This check is performed using the following matching function in formula (7):

$$M_s=\frac{\left|X^i\wedge w^s\right|}{X^i}. \tag{7}$$

An input vector X belongs to cluster s only if: $M_s\geq\rho$, where ρ – similarity criterion [29]. If this inequality is not satisfied, the identified cluster s becomes temporarily inactive, and the selection function according to formula (6) is again applied to select a new candidate cluster. If, during the process, there are no more clusters to select (i.e., all clusters have become deactivated), a new cluster is created based on the input vector. The cluster weights are set equal to the weights of the input vector: $w=X^i$. After the cluster selection procedure [30], the learning function is applied, and the weights of the selected cluster (its prototype) are recalculated according to formula (8):

$$w^{t+1}=\left(1-\beta\right)w^t+\beta(X^i\wedge w^t). \tag{8}$$

In the Fuzzy ART network, weight vectors are not normalized to a unit length, so using this learning function causes a degeneration problem. The operator used, calculated as a coordinate minimum, contributes to a gradual decrease in the coordinates of the weight vectors. Their reduction will gradually lead to the degeneration of cluster prototypes when they forget the information learned earlier. In order to overcome this problem, complementary coding is applied to the input vectors at the preprocessing stage, thanks to which the dimension of the input vector is doubled by adding its components: $x_{i(J+j)}=1-x_{ij}$, which prevents all components of the weight vector *w* from degenerating to zero values. The main stages of the general scheme for solving the data clustering problem using the two considered networks of the ART family are described below.

Stage 1. Selection of the preprocessing algorithm. At this stage, input data preprocessing is implemented using a number of methods. Ranking of input variables. If information about the im-

portance of input variables is known in advance, they can be ranked, after which the inputs can be scaled according to the assigned ranks (for example, the most important variable is scaled to the interval [0;1], the next most important to the smaller interval [0; 0.9], and so on). This will significantly change the clustering result, as more significant variables will contribute more.

Normalization. In ART-2a and Fuzzy ART networks, normalized input vectors must be used. For Fuzzy ART networks, complementation is performed before normalization.

Noise removal. Noise in the input data can be eliminated by entering validation parameters that set upper and lower limits for each of the input parameters. If a value exceeds these limits, it will be truncated or discarded in accordance with the specified limits in order to remove erroneous values.

Complementation. This method increases the dimension of the input vector by doubling its size. As a result, instead of the input vector $\bar{a}$ the vector is considered:

$$I^a = [\overline{aa}^c] = [a_1,\ldots,a_n,a_1^c,\ldots,a_n^c], \text{ where } a_1^c = 1 - a_i .$$

Stage 2. Assigning selection, correspondence, and learning functions. After preprocessing, it is necessary to assign specific types of selection, correspondence, and learning functions. The generalized structure of the ART network family described above makes it possible to change these functions at any stage of network operation, since the architecture and general logic of the network do not depend on their specific type. However, the clustering results and characteristics of the clusters obtained strongly depend on the selected functions, so they must correspond to the task being solved.

Stage 3. Selection of the post-processing algorithm. This stage allows compensating for the shortcomings of the ART family model used after training is complete. For example, one of the main shortcomings of this family of networks is the complexity of calculations when selecting the similarity parameter ρ or its analogue proposed in this study–the integral similarity assessment of input vectors. An incorrect choice of the ρ parameter can lead to the merging of all available data into one large cluster or, conversely, to an uncontrolled increase in the number of clusters. To form a clustering algorithm, it is necessary to select preprocessing and postprocessing schemes. The problem of choosing a post-processing method is more complex, since if the ANN is used to cluster continuously incoming stream data, the number of clusters generated by the network will constantly grow over time, which complicates the analysis of incoming data and the making of management decisions based on it.

Research results

To solve the problem of management in an OS based on monitoring data, it is necessary to improve information support in terms of the ability to process large volumes of continuously incoming data. The first stage of processing is structuring based on cluster analysis. Algorithms for cluster structuring of stream data continuously process incoming input vectors, including in online mode. However, not all clustering algorithms can be used to solve this problem. As noted earlier, in order for the results to be reliable, such algorithms must meet certain conditions:

− display the final result in real time;
− instantly adapt to changing indicators;
− scale for an arbitrary number of objects;
− create a slightly expanding structure as more objects are processed;
− determine the presence of outliers in the data.

Based on this study, a computational experiment was conducted for the FuzzyART network, which involved processing a constantly incoming stream of input data. The stream was simulated using the scikit-learn library, designed to implement machine learning algorithms. This library contains random sample generators, whose data can be used to artificially create information of a controlled size and complexity [31]. The make blobs procedure used in this case helps to create multi-class data sets, each of which corresponds to one or more clusters. Based on the library procedure, a stream of 10-dimensional data consisting of three clusters of equal size was generated to analyze the possibility of using ART family networks for processing stream data. One of them was easily separable, while the other two were closely located. An illustration of this arrangement (for two-dimensional input vectors) is shown in Figure 4. Specific results were obtained during the computational experiment (Table 2). Errors in the operation of the networks under consideration are considered to be the discrepancy between the obtained result and the model classification of the initial data (the percentage of incorrect clustering).

ISSN 2076-2429 (print)
ISSN 2223-3814 (online)

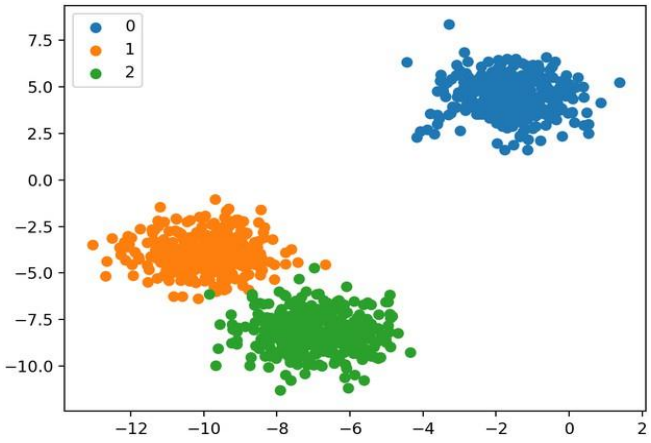

Fig. 4. Illustration of the mutual arrangement of generated clusters

Table 2

Dependence of the Fuzzy ART network operation on parameters.

0< ρ <0.68					
β	0.1	0.3	0.5	0.7	0.9
Errors, (%)	64%	60%	65%	66%	63%
Number of clusters	1	1	1	1	1
0.68≤ ρ<0.85					
β	0.1	0.3	0.5	0.7	0.9
Errors, (%)	33%	33%	6.6%	12%	12%
Number of clusters	2	2	3	4	4
0.85≤ ρ ≤ 0.9					
β	0.1	0.3	0.5	0.7	0.9
Errors, (%)	12%	12%	9.2%	6.6%	6.6%
Number of clusters	4	4	4	3	3

Conclusions

Based on the results of this experiment, the following conclusions were made regarding the applicability of the Fuzzy ART network for streaming clustering of monitoring data. Before obtaining the value ρ =0.68 the network connected the incoming vectors into a common cluster.

Meaning 0.68<ρ<0.85 indicates that the network divides the set into two clusters, one of which is easily separable, while the other consists of the remaining elements. Division into three clusters occurs when the value is 0.85≤ρ≤ 0.9. When there is a further increase ρ>0.9, the network begins to create an increasing number of clusters, i.e., the initial sample is divided into many small groups. It should be noted that Fuzzy ART has a number of positive functional characteristics, including stability, fast convergence, and clear dependence on the selected learning rate. However, during the experiment, it became clear that the functions used by Fuzzy ART for selection, learning, and matching can lead to high sensitivity to the order of the indicators provided. It was noted that if the data is fed into the input in a random order (shuffled) at the beginning of operation, the distribution across clusters will be much better. To solve the problem of uncontrolled growth in the number of clusters, this study proposes using the post-processing method [32 – 34], which allows the number of clusters to be limited to a specified value. However, it may not be known in advance what number to use to limit the number of clusters created. Therefore, this study proposes a special method for recalculating the similarity parameter ρ (which is responsible for the number of clusters). According to this method, it is proposed to set the maximum permissible number of clusters K at the initial stage of the algorithm and set the similarity parameter ρ very close to 1. If, during the execution of the next stage, the vector does not correspond to any of the existing clusters and the maximum possible number of clusters K has been reached, then a new cluster cannot be created. Thus, a new cluster will be created, but the total number of clusters will not change. The proposed approach to limiting the number of clusters is sufficiently versatile and can be easily applied to modify the training of any network of the ART family. Let us now present general recommendations obtained as practical results in the course of a computational

experiment concerning the FuzzyART network, which was engaged in processing a constant data stream. In each specific case, the network should be selected based on the type of indicators and the operating mode in which it functions. The Fuzzy ART network is very sensitive to the order of input data organization, based on which it is capable of generating and obtaining different results of the clustering process. Therefore, at the initial stage, it is recommended to perform several iterations in batch mode (not online).

Select or set training speed parameters β It depends on the type of task being performed in the process. Here, a low initial learning rate allows you to identify general patterns in the results obtained, while a high rate allows you to quickly catch and adapt to existing trends.

Apply the strategy of adjusting the similarity parameter ρ. Specifically, at the beginning of the algorithm, set the maximum number of clusters *K*, and set ρ=1. If it is necessary to create during the operation of the algorithm *(K*+1*)*-ht cluster (i.e., the algorithm cannot classify the input vector into existing clusters), it is necessary to reduce the parameter ρ and repeat the procedure again. The parameter will decrease until the input vector is assigned to one of the existing clusters. At the same time, if in the process of decreasing ρ the prototypes of any two of the existing clusters become similar in terms of the current value of the similarity criterion, then these two clusters should be merged into one common cluster. When the network has low indicators β it works slowly and has long cluster migration, so Fuzzy-ART is only used for data that comes in a large but discrete stream (like sensor readings taken a few times a day). In this case, the data can be processed in batch mode. In a scenario where noise spikes occur in the indicator stream, with the appearance of atypical input vectors that are remembered by new clusters, the cluster limit may be exceeded. Therefore, when analyzing the results, the expert will either study the small clusters that have appeared (if one of the goals of the analysis is to find anomalies in the data), or delete them (so that they do not create unnecessary noise), or reduce the requirements for the number of clusters. The latter approach, given the chaotic order of input data, will lead to the absorption of small clusters by the main clusters. The most commonly used quality metrics in clustering tasks are the average intracluster distance, which must be minimized, or the average intercluster distance, which is maximized. The silhouette coefficient metric [31] combines both of these approaches in a sense, which is why it is proposed for use in evaluating the quality of clustering. The silhouette coefficient is used to evaluate the difference between objects within clusters and objects in other clusters. The silhouette coefficient can range from –1 to 1. The higher the silhouette coefficient, the better the quality of the clustering. Negative values indicate poor or incorrect clustering, values close to zero indicate overlap and superimposition of clusters, and values close to 1 indicate tightly grouped clusters. In the future, the quality of the developed algorithms will be evaluated using this metric.

Література

1. Amis G. P., Carpenter G. A. Self-supervised ARTMAP. *Neural Networks*. 2010. № 23. P. 265–282.
2. Brito da Silva L. E., Elnabarawy I., Wunsch D. C. 2nd. Dual vigilance fuzzy adaptive resonance theory. *Neural Networks*. 2019. № 109. P. 1–5.
3. Nandwani P., Verma R. A review on sentiment analysis and emotion detection from text. *Social Network Analysis and Mining*. 2021. Vol. 11, № 81. DOI: https://doi.org/10.1007/s13278-021-00776-6.
4. Fuzzy ARTMAP: An adaptive resonance architecture for incremental learning of analog maps / G. A. Carpenter et al. *Proc. of the Int. Joint Conf. on Neural Network (Boston, 1992)*. 1992.
5. Acheampong F. A., Wenyu C., Nunoo-Mensah H. Text-based emotion detection: Advances, challenges, and opportunities. *Engineering Reports*. 2020. DOI: https://doi.org/10.1002/eng2.12189.
6. Challenges and opportunities of text-based emotion detection: A survey / A. A. Maruf et al. *IEEE Access*. 2024. Vol. 12. P. 18416–18450. DOI: https://doi.org/10.1109/ACCESS.2024.3356357.
7. Probabilistic ensemble Fuzzy ARTMAP optimization using hierarchical parallel genetic algorithms / K. L. Chu et al. *Neural Computing and Applications*. 2014. № 26. P. 263–276.
8. French R. M. Catastrophic forgetting in connectionist networks. *Trends Cogn. Sci.* 1999. № 3. P. 128–135.
9. Acheampong F. A., Nunoo-Mensah H., Chen W. Transformer models for text-based emotion detection: a review of BERT-based approaches. *Artificial Intelligence Review*. 2021. Vol. 54. P. 5789–5829. DOI: https://doi.org/10.1007/s10462-021-09958-2.

10. Zhang X., Mao R., Cambria E. Multilingual Emotion Recognition: Discovering the Variations of Lexical Semantics between Languages. *International Joint Conference on Neural Networks (IJCNN) (Yokohama, Japan, 2024)*. 2024. P. 1–9. DOI: https://doi.org/10.1109/IJCNN60899.2024.10651409.
11. Ghosh J., Acharya A. Cluster ensembles. *Wiley Interdisciplinary Reviews: Data Mining and Knowledge Discovery*. 2011. Vol. 1, № 4. P. 305–315.
12. Grossberg S. The resonant brain: how attentive conscious seeing regulates action sequences that interact with attentive cognitive learning, recognition, and prediction. *Atten. Percep. Psychophys.* 2019. № 81. P. 2237–2264.
13. De León Languré A., Zareei M. Improving text emotion detection through comprehensive dataset quality analysis. *IEEE Access*. 2024. Vol. 12. P. 70489–70500. DOI: https://doi.org/10.1109/ACCESS.2024.3491856.
14. Kharchenko V., Fesenko H., Illiashenko O. Quality models for artificial intelligence systems: characteristic-based approach, development and application. *Sensors*. 2022. Vol. 22, № 13. Art. 4865. URL: www.scopus.com. DOI: https://doi.org/10.3390/s22134865.
15. Optimizing deep learning inference on embedded systems through adaptive model selection / V. Marco et al. *ACM Transactions on Embedded Computing Systems*. 2020. Vol. 19, № 1. P. 1–28. DOI: https://doi.org/10.1145/3371154.
16. Haupt S. E., Pasini A., Marzban C. Environmental Optimization: Applications of Genetic Algorithms. *Artificial Intelligence Methods in the Environmental Sciences*. 2009. P. 379–395.
17. Keskin G. A., Ozkan C. An Alternative Evaluation of FMEA: Fuzzy ART Algorithm. *Quality and reliability engineering international*. 2009. Vol. 25, № 6. P. 647–661.
18. Overcoming catastrophic forgetting in neural networks / J. Kirkpatrick et al. *Proc. Natl. Acad. Sci. U.S.A.* 2017. № 114. P. 3521–3526.
19. Kuncheva L. I., Whitaker C. J. Measures of diversity in classifier ensembles and their relationship with the ensemble accuracy. *Machine Learning*. 2003. № 51. P. 181–207.
20. Le Cun Y., Bengio Y., Hinton G. Deep learning. *Nature*. 2015. № 521. P. 436–444.
21. Massey L. Real-world text clustering with adaptive resonance theory neural networks. *Proceedings of 2005 international joint conference on neural network (Montreal, Canada, July 31–August 4, 2005)*. 2005.
22. Fuzzy ART Neural Network Parallel Computing on the GPU / M. Martinez-Zarzuela et al. *Computational and Ambient Intelligence*. 2007. P. 463–470.
23. Meng L., Tan A.-H., Wunsch D. C. Vigilance adaptation in adaptive resonance theory. *In Proc. IEEE International Joint Conference on Neural Networks (IJCNN)*. 2013. P. 1–7.
24. Oong T. H., Isa N. A. M. Feature-Based Ordering Algorithm for Data Presentation of Fuzzy ARTMAP Ensembles. *IEEE Transactions on Neural Networks and Learning Systems*. 2014. № 25. P. 812–819.
25. Rosenberg A., Hirschberg J. Detecting pitch accent using pitch-corrected energy-based predictors. *In Interspeech*. 2007. P. 2777–2780.
26. Rousseeuw P. Silhouettes: A Graphical Aid to the Interpretation and Validation of Cluster Analysis. *Computational and Applied Mathematics*. 1987. № 20. P. 53–65.
27. Pedregosa F. et al. Scikit-learn: Machine Learning in Python. *Journal of Machine Learning Research*. 2011. № 12. P. 2825–2830.
28. Seto K., Liu W. Comparing ARTMAP neural network with the maximum-likelihood classifier for detecting urban change. *Photogrammetric Engineering & Remote Sensing*. 2003. № 69(9). P. 981–990.
29. Solyanik S. A., Kravets O. JA. Development of distributed management complexes for territorial information systems data flows. Yelm, WA, USA : Science Book Publishing House LLC, 2020.
30. Skovajsova L., Rojcek M. Soft clustering algorithms based on neural networks. *IEEE 12th International Symposium on Computational Intelligence and Informatics (Budapest, 2011)*. 2011. P. 439–442.
31. Wasserman P. D. Neural Computing: Theory and Practice. Van Nostrand Reinhold Co., 1989. 230 p.
32. Versace M., Kozma R. T., Wunsch D. C. Adaptive Resonance Theory Design in Mixed Memristive-Fuzzy Hardware. *Advances in Neuromorphic Memristor Science and Applications*. 2012. P. 133–153.
33. Xu R., Wunsch D. C. 2nd. Survey of Clustering Algorithms. *IEEE transactions on neural networks*. 2005. Vol. 16, № 3. P. 645–678.
34. Calibrated learning for online distributed power allocation in small-cell networks / X. Zhang et al. *IEEE Transactions on Signal Processing*. 2019. Vol. 67, № 11. P. 8124–8136.

References

1. Amis, G. P., & Carpenter, G. A. (2010). Self-supervised ARTMAP. *Neural Networks*, *23*, 265–282.
2. Brito da Silva, L. E., Elnabarawy, I., & Wunsch, D. C., 2nd. (2019). Dual vigilance fuzzy adaptive resonance theory. *Neural Networks*, *109*, 1–5.

3. Nandwani, P., & Verma, R. (2021). A review on sentiment analysis and emotion detection from text. *Social Network Analysis and Mining*, *11*(81). https://doi.org/10.1007/s13278-021-00776-6.
4. Carpenter, G. A., Grossberg, S., Markuzon, N., Reynolds, J. H., & Rosen, D. B. (1992). Fuzzy ARTMAP: An adaptive resonance architecture for incremental learning of analog maps. *Proceedings of the International Joint Conference on Neural Networks*, 1992.
5. Acheampong, F. A., Wenyu, C., & Nunoo-Mensah, H. (2020). Text-based emotion detection: Advances, challenges, and opportunities. *Engineering Reports*. https://doi.org/10.1002/eng2.12189.
6. Maruf, A. A., Khanam, F., Haque, M. M., Jiyad, Z. M., Mridha, M. F., & Aung, Z. (2024). Challenges and opportunities of text-based emotion detection: A survey. *IEEE Access*, *12*, 18416–18450. https://doi.org/10.1109/ACCESS.2024.3356357.
7. Chu, K. L., Liew, W., Seera, M., & Lim, E. (2014). Probabilistic ensemble Fuzzy ARTMAP optimization using hierarchical parallel genetic algorithms. *Neural Computing and Applications*, *26*, 263–276.
8. French, R. M. (1999). Catastrophic forgetting in connectionist networks. *Trends in Cognitive Sciences*, *3*, 128–135.
9. Acheampong, F. A., Nunoo-Mensah, H., & Chen, W. (2021). Transformer models for text-based emotion detection: A review of BERT-based approaches. *Artificial Intelligence Review*, *54*, 5789–5829. https://doi.org/10.1007/s10462-021-09958-2.
10. Zhang, X., Mao, R., & Cambria, E. (2024). Multilingual emotion recognition: Discovering the variations of lexical semantics between languages. *International Joint Conference on Neural Networks (IJCNN)*, 1–9. https://doi.org/10.1109/IJCNN60899.2024.10651409.
11. Ghosh, J., & Acharya, A. (2011). Cluster ensembles. *Wiley Interdisciplinary Reviews: Data Mining and Knowledge Discovery*, *1*(4), 305–315.
12. Grossberg, S. (2019). The resonant brain: How attentive conscious seeing regulates action sequences that interact with attentive cognitive learning, recognition, and prediction. *Attention, Perception, & Psychophysics*, *81*, 2237–2264.
13. De León Languré, A., & Zareei, M. (2024). Improving text emotion detection through comprehensive dataset quality analysis. *IEEE Access*, *12*, 70489–70500. https://doi.org/10.1109/ACCESS.2024.3491856.
14. Kharchenko, V., Fesenko, H., & Illiashenko, O. (2022). Quality models for artificial intelligence systems: Characteristic-based approach, development and application. *Sensors*, *22*(13), 4865. https://doi.org/10.3390/s22134865.
15. Marco, V., Taylor, B., Wang, Z., & Elkhatib, Y. (2020). Optimizing deep learning inference on embedded systems through adaptive model selection. *ACM Transactions on Embedded Computing Systems*, *19*(1), 1–28. https://doi.org/10.1145/3371154.
16. Haupt, S. E., Pasini, A., & Marzban, C. (2009). Environmental optimization: Applications of genetic algorithms. In *Artificial Intelligence Methods in the Environmental Sciences* (pp. 379–395).
17. Keskin, G. A., & Ozkan, C. (2009). An alternative evaluation of FMEA: Fuzzy ART algorithm. *Quality and Reliability Engineering International*, *25*(6), 647–661.
18. Kirkpatrick, J., Pancanu, R., Rabinowitz, N., Veness, J., Desjarkins, G., Rusu, A. A., ... & Hadsell, R. (2017). Overcoming catastrophic forgetting in neural networks. *Proceedings of the National Academy of Sciences*, *114*, 3521–3526.
19. Kuncheva, L. I., & Whitaker, C. J. (2003). Measures of diversity in classifier ensembles and their relationship with the ensemble accuracy. *Machine Learning*, *51*, 181–207.
20. LeCun, Y., Bengio, Y., & Hinton, G. (2015). Deep learning. *Nature*, *521*, 436–444.
21. Massey, L. (2005). Real-world text clustering with adaptive resonance theory neural networks. *Proceedings of 2005 International Joint Conference on Neural Networks*.
22. Martinez-Zarzuela, M., Diaz Pernas, F. J., Diez Higuera, J. F., & Rodriguez, M. A. (2007). Fuzzy ART neural network parallel computing on the GPU. In *Computational and Ambient Intelligence* (pp. 463–470).
23. Meng, L., Tan, A.-H., & Wunsch, D. C. (2013). Vigilance adaptation in adaptive resonance theory. *2013 IEEE International Joint Conference on Neural Networks (IJCNN)*, 1–7.
24. Oong, T. H., & Isa, N. A. M. (2014). Feature-based ordering algorithm for data presentation of Fuzzy ARTMAP ensembles. *IEEE Transactions on Neural Networks and Learning Systems*, *25*, 812–819.
25. Rosenberg, A., & Hirschberg, J. (2007). Detecting pitch accent using pitch-corrected energy-based predictors. *Interspeech 2007*, 2777–2780.
26. Rousseeuw, P. J. (1987). Silhouettes: A graphical aid to the interpretation and validation of cluster analysis. *Journal of Computational and Applied Mathematics*, *20*, 53–65.
27. Pedregosa, F., Varoquaux, G., Gramfort, A., Michel, V., Thirion, B., Grisel, O., ... & Duchesnay, E. (2011). Scikit-learn: Machine learning in Python. *Journal of Machine Learning Research*, *12*, 2825–2830.

ISSN 2076-2429 (print)
ISSN 2223-3814 (online)

28. Seto, K. C., & Liu, W. (2003). Comparing ARTMAP neural network with the maximum-likelihood classifier for detecting urban change. *Photogrammetric Engineering & Remote Sensing*, *69*(9), 981–990.
29. Solyanik, S. A., & Kravets, O. J. (2020). *Development of distributed management complexes for territorial information systems data flows*. Science Book Publishing House LLC.
30. Skovajsova, L., & Rojcek, M. (2011). Soft clustering algorithms based on neural networks. *2011 IEEE 12th International Symposium on Computational Intelligence and Informatics*, 439–442.
31. Wasserman, P. D. (1989). *Neural computing: Theory and practice*. Van Nostrand Reinhold Co.
32. Versace, M., Kozma, R. T., & Wunsch, D. C. (2012). Adaptive resonance theory design in mixed memristive-fuzzy hardware. In *Advances in Neuromorphic Memristor Science and Applications* (pp. 133–153).
33. Xu, R., & Wunsch, D. C., 2nd. (2005). Survey of clustering algorithms. *IEEE Transactions on Neural Networks*, *16*(3), 645–678.
34. Zhang, X., Nakhai, M. R., Zheng, G., Lambotharan, S., & Ottersten, B. (2019). Calibrated learning for online distributed power allocation in small-cell networks. *IEEE Transactions on Signal Processing*, *67*(11), 8124–8136.

Тігарєв Володимир Михайлович; Volodymyr Tigariev, ORCID: https://orcid.org/0000-0001-8492-6633
Лопаков Олексій Сергійович; Oleksii Lopakov, ORCID: https:// orcid.org/0000-0001-6307-8946
Космачевський Володимир Володимирович; Volodymir Kosmachevskiy, ORCID: https://orcid.org/0000-0002-3234-2297
Люшенко Андрій Миколайович; Andrii Liushenko, ORCID: https://orcid.org/0009-0004-0410-3100

Accepted October 05, 2025

Accepted November 11, 2025

UDC 005.8 : 004.94

E. Zabarna, DSc, Prof.,
O. Timchinsky,
O. Bondar, PhD, Assoc. Prof.,
V. Ovsiychuk
Odessa Polytechnic National University, Shevchenko Ave. 1, Odesa, Ukraine, 65044, e-mail: e.m.zabarna@op.edu.ua

COMPLEXITY OF CYBER-PHYSICAL DIGITAL MARKETING PRODUCT DEVELOPMENT PROJECTS

Е. Забарна, О. Тімчинский, О. Бондар, В. Овсійчук. **Складність проєктів розробки кіберфізичних продуктів цифрового маркетингу.** В статті показано, що актуальність дослідження зумовлена зростанням складності ІТ-проєктів, спрямованих на розробку кіберфізичних продуктів у сфері цифрового маркетингу, які поєднують апаратні компоненти, датчики, програмне забезпечення, аналітичні модулі та елементи штучного інтелекту. Обґрунтовано, що такі проєкти характеризуються високим рівнем інтеграції між фізичним і цифровим середовищами та мультикомандною структурою, що ускладнює процес управління. Виявлено, що ключовою проблемою є забезпечення ефективної міжкомандної комунікації та синхронізації дій між групами розробників, маркетологів і аналітиків, оскільки будь-які зміни у технічних чи програмних компонентах без своєчасного узгодження створюють ризики асинхронності, втрат даних, вимог та порушення строків завершення ІТ-проєкту. Сформульовано мету дослідження, яка полягає в обґрунтуванні підходів до вдосконалення управління комунікаціями в ІТ-проєктах розробки кіберфізичних систем цифрового маркетингу шляхом створення інтегрованої інтелектуальної моделі інформаційних взаємодій між командами. Для досягнення мети проаналізовано сучасні наукові підходи до управління складними мультидисциплінарними ІТ-проєктами, виділено особливості комунікацій у кіберфізичних системах. Запропоновано модель системи комунікацій, що включає три рівні – інфраструктурний, інформаційно-комунікаційний та аналітичний. Розроблено принцип побудови мережевої карти взаємодій між командами, у якій кожен зв'язок характеризується частотою, затримкою та якістю обміну. Побудовано математичну модель графа комунікацій G(V,E,W) з урахуванням вагових коефіцієнтів, що відображають інтенсивність інформаційних потоків. Запроваджено застосування методів інтелектуального аналізу даних та штучного інтелекту для автоматичного виявлення ризикових зв'язків, аналізу стану інформаційних потоків і формування управлінських рекомендацій. Проаналізовано можливості використання побудованої системи для автоматизації управління мультикомандними ІТ-проєктами, прогнозування ризиків асинхронності та підвищення ефективності прийняття рішень в процесі розробки складних кіберфізичних продуктів.

Ключові слова: кіберфізичний продукт проєкту, складний ІТ-проєкт, мультикомандна розробка, комунікації, цифровий маркетинг, міжкомандна взаємодія, штучний інтелект

E. Zabarna, O. Timchinsky, O. Bondar, V. Ovsiychuk. **Complexity of cyber-physical digital marketing product development projects.** The article shows that the relevance of the study is due to the increasing complexity of IT projects aimed at developing cyber-physical products in the field of digital marketing, which combine hardware components, sensors, software, analytical modules and elements of artificial intelligence. It is substantiated that such projects are characterised by a high level of integration between the physical and digital environments and a multi-team structure, which complicates the management process. It is revealed that the key problem is ensuring effective inter-team communication and synchronisation of actions between groups of developers, marketers and analysts, since any changes in technical or software components without timely coordination create risks of asynchrony, loss of data, requirements and violation of the deadlines for completing the IT project. The research objective is formulated, which is to substantiate approaches to improving communications management in IT projects for the development of cyber-physical digital marketing systems by creating an integrated intellectual model of information interactions between teams. To achieve the goal, modern scientific approaches to managing complex multidisciplinary IT projects are analysed, and the features of communications in cyber-physical systems are highlighted. A model of the communications system is proposed, which includes three levels: infrastructure, information-communication, and analytical. The principle of constructing a network map of interactions between teams is developed, in which each connection is characterised by the frequency, delay and quality of exchange. A mathematical model of the communications graph G (V, E, W) is constructed, taking into account weight coefficients reflecting the intensity of information flows. The application of methods of intelligent data analysis and artificial intelligence for automatic detection of risk relationships, analysis of the state of information flows and formation of management recommendations was introduced. The possibilities of using the constructed system for automating the management of multi-team IT projects, forecasting asynchrony risks and increasing the efficiency of decision-making in the process of developing complex cyber-physical products were analysed.

Keywords: cyber-physical product of the project, complex IT project, multi-team development, communications, digital marketing, inter-team interaction, artificial intelligence

Introduction

The product of digital marketing IT projects is often a cyber-physical system that combines physical devices, sensors, digital models, artificial intelligence algorithms, and network interaction. Examples include interactive AR shop windows and "smart mirrors". Such a system allows the user to interact with the product in real time – for example, to "try on" clothes or cosmetics using augmented reality, observing the integration of their own reflection with virtual models. A cyber-physical product consists of hardware, which includes a mirrored touchscreen display, RGB and depth cameras, lighting, motion sen-

DOI: 10.15276/opu.2.72.2025.16

ISSN 2076-2429 (print)
ISSN 2223-3814 (online)

sors, controllers, and a microcomputer (e.g., NVIDIA Jetson or Raspberry Pi), and software, which includes computer vision modules, AR visualisation systems, product model databases, user behavior tracking and analytics algorithms, as well as APIs for integration with the brand's e-commerce platforms.

It is important to distinguish between the concepts of a hardware-software complex and a cyber-physical system. The first term refers to the technological integration of hardware and software that performs a specific function. A cyber-physical system, on the other hand, is a more complex entity with elements of AI, as it involves the interaction of physical processes with digital models in real time, state analytics, and the adaptation of system behaviour to external conditions, as shown in [1]. In the following discussion, the term *cyber-physical system* is used, as it more accurately reflects the intellectual nature of the product.

Three main teams are involved in the IT project to develop such a cyber-physical system: a hardware development team responsible for assembling the housing, sensors, electronic modules, connections, and creating prototypes; a software development team that implements computer vision, AR visualisation and analytics; and a brand marketing team that develops user interaction scenarios, visual product models and content strategy.

The complexity of such projects lies in the high level of integration between different technological domains – from electronics and brand marketing to artificial intelligence – and the need to ensure the synchronised work of several interdisciplinary teams. Any change in technical design or visualisation algorithm can affect the marketing concept or hardware interface requirements. An additional complexity is created by the need for continuous coordination between these teams, as all changes must be promptly recorded, agreed upon, and communicated to other project participants for the correct updating of decisions and continued development based on current data.

This is a complex and non-trivial task, as it requires simultaneous management of technical, communication and time dependencies. To solve this problem, it is advisable to develop a project communication management model that will ensure automated synchronisation of interaction between teams. Such a model should use intelligent data analysis methods and artificial intelligence systems to monitor information flows, identify critical messages, warn of inconsistencies, and support real-time decision-making.

Analysis of literature data and problem statement

Articles on the management of IT projects for the development of cyber-physical systems pay particular attention to the complexity of their organisation and team coordination. The paper "Enhancing Project Management for Cyber-Physical Systems Development" [2] identifies that the main problem with such projects is the combination of different domains – hardware, software, communication, and analytics – within a single life cycle. The authors note that classic IT project management methodologies, focused solely on software, do not take into account the physical part of the system, which leads to conflicts in planning, integration, and testing. The complexity is compounded by the different work rhythms of the teams: electronics engineers work with longer production cycles, while software developers use agile approaches. To address this imbalance, a hybrid management model has been proposed that combines elements of PMBOK [3] and Agile, creating a unified plan for integrating the hardware and digital parts of the system.

The same authors, in [4], emphasise that managing projects to create cyber-physical systems requires modifying classic PMI processes. The authors highlight the problem of communication between teams from different domains – software, hardware and analytical. Information barriers arise due to differences in terminology, testing methods, and reporting formats. To overcome this, a communication integration model is proposed in which all teams use a common management platform that synchronises changes in requirements and automatically updates project documentation. Such a platform effectively acts as the "digital core" of a CPS project, preventing information loss between teams and increasing process transparency.

The study [5] describes the practical difficulties that arise when creating complex cyber-physical products. The authors emphasise that the difference between such projects and conventional IT projects lies in the need for the synchronous development of three layers of the system – physical, software and network – each of which has its own dynamics of change. The main difficulty lies in ensuring the coherence of the architecture and managing the interdependencies between these layers. The paper describes the automation of management through the implementation of a "Digital Thread" – an end-to-end digital model that tracks changes at all stages of the CPS life cycle. The use of artificial intelligence elements, in particular machine learning methods, allows predicting integration risks and optimising the testing process of hardware and software components.

The analysed articles note that IT projects for the development of cyber-physical systems are characterised by increased complexity due to their multidisciplinary nature, the synchronisation of different types of teams, and the need to integrate physical and digital environments. The complexity of an IT project may be determined by the need for additional research to reduce uncertainty, as shown in [6]. At the same time, automation of management and the use of AI are considered key factors in improving the efficiency of such projects and reducing both risks and uncertainties in their implementation.

Therefore, the issue of communication management in complex IT projects was further considered. In article [7], communication is defined as a fundamental process that builds trust, mutual understanding, and motivation within a team. The authors emphasise that in the context of distributed and virtual IT teams, the complexity lies in maintaining a single information space when team members are in different time and cultural contexts. The main problem is identified as fragmented communication, which leads to information loss and destabilisation of processes. To overcome this, a two-component communication management model is proposed: interpersonal (human) and organisational, covering information flows, tools, exchange structure and feedback control. The authors analyse a number of communication management models, from the classic one based on communication planning to modern integration approaches that involve the use of Jira, Trello, Slack or Confluence platforms. It is important to emphasise the capabilities of artificial intelligence, which can automate the analysis of communication flows and identify information gaps to improve team coordination.

Another point of view is presented in the work of V. Bannikov [8], which focuses on the practical aspects of coordinating communications in complex projects. The author describes communication as a multi-level mechanism that includes the collection, systematisation, analysis, and transfer of information between all participants. The problem is identified as the lack of a systematic approach to communication management, where each team acts autonomously. The solution proposed is to develop a structured communication management plan covering the stages of initiation, planning, control, analysis, and closure. The plan involves the creation of an information and technology model of communication with a clear distribution of responsibilities. To avoid errors and data loss, it is recommended to use communication matrices and electronic message logs. The author believes that only on the basis of a detailed communication system is it possible to effectively coordinate complex IT projects.

In the article “The Role of Communication Management Within the Virtual Team in an International Projects-Based Organisation” [9], researchers analyse the problem of information asymmetry, which is particularly acute in international distributed teams. The complexity lies in uneven access to information due to time zones and cultural differences. To solve this problem, they propose the implementation of a “Communication Governance Framework” – a digital communication management system that includes a monitoring panel, automatic logging of discussions, and activity analytics. Such a system acts as a central hub that synchronises data exchange between teams and allows managers to identify information delays in real time.

Research [10] highlights the relationship between communications and risk management. The authors note that the lack of integrated channels between parallel teams creates hidden risks. To minimise them, they propose introducing a continuous data exchange mechanism between projects based on a centralised knowledge base. This allows for the synchronisation of management decisions and reduces task duplication.

In article [11], the authors focus on the cultural aspect of communications and the role of a manager’s “soft skills”. The authors emphasise that even with digital tools, communication remains primarily a human process, where emotional intelligence and the ability to build trust are critically important.

All of the articles analysed share the common idea that communication is a system-forming factor for complex IT projects. Their complexity lies not only in technical barriers, but also in interpersonal interaction. The authors point to the need for automation of communication management, development of integrated digital platforms, and use of intelligent message analysis algorithms to predict information gaps and improve team coordination. Such a solution is a necessary condition for the success of modern IT projects, especially in the context of multi-team interaction and a highly dynamic environment.

Purpose and objectives of the study

The purpose of the study is to justify communication measures in projects for the development of complex cyber-physical digital marketing products in order to ensure effective multi-team interaction. Achieving the stated goal will ensure the fulfilment of tasks related to the development of the structure

ISSN 2076-2429 (print)
ISSN 2223-3814 (online)

and content of the communication system for IT projects for the development of complex cyber-physical products.

Justification of the approach to managing the information environment of IT projects for the development of cyber-physical digital marketing products

As revealed by the review and analysis of literature sources, the complexity of managing projects for the development of cyber-physical products lies in their multi-team nature, namely in the complexity and inefficiency of communication between all teams. Therefore, the effectiveness of managing such projects directly depends on a high-quality communication system [12].

The communication system for an IT project to develop a cyber-physical system in the field of digital marketing should be an integrated intelligent communication and analytical platform that not only ensures the transfer of information between teams, but also the automatic collection, structuring and analytical interpretation of data from the project environment. Its structure consists of three levels: infrastructure, information and communication, and analytical (intellectual).

At the infrastructure level, the system provides physical interaction between teams through a centralised data transfer environment. All teams – hardware, software, and marketing – connect to a single network infrastructure that supports both wired and cloud connections. This level is responsible for unifying data formats, synchronising file storage, maintaining change logs, and ensuring secure access to project information.

The information and communication level is the central part of the system, which performs the functions of collecting, filtering, and routing messages. All data generated in team environments (Jira, Git, Figma, Slack, Confluence, CAD systems) is automatically transferred to a centralised communication repository. Here, the system classifies content by type (technical changes, marketing decisions, graphic updates, defects, requirements, etc.) and establishes links between different types of messages [13].

A general view of such a network map is shown in Fig. 1. To ensure traceability, all communications are visualised in the form of a network map of interactions, showing the links between teams, the frequency of exchange, and the degree of information saturation of each node. The physical interaction between teams in the figure is graphically presented as directed lines. The direction indicates where and to whom the information is sent. The thickness of the lines indicates the intensity of such interactions; the thicker the line, the more intense the interaction. The dotted line indicates the discontinuity and instability of such interaction. The color indicates which department formed the corresponding communication. Additionally, on the network map of interactions, “alarmist” yellow or red marks may be provided near the lines of interaction between departments to signal a conflict of the information provided, or its critical delay. For a specific project, together with the network map, an appropriate dictionary of conventional symbols and images is created.

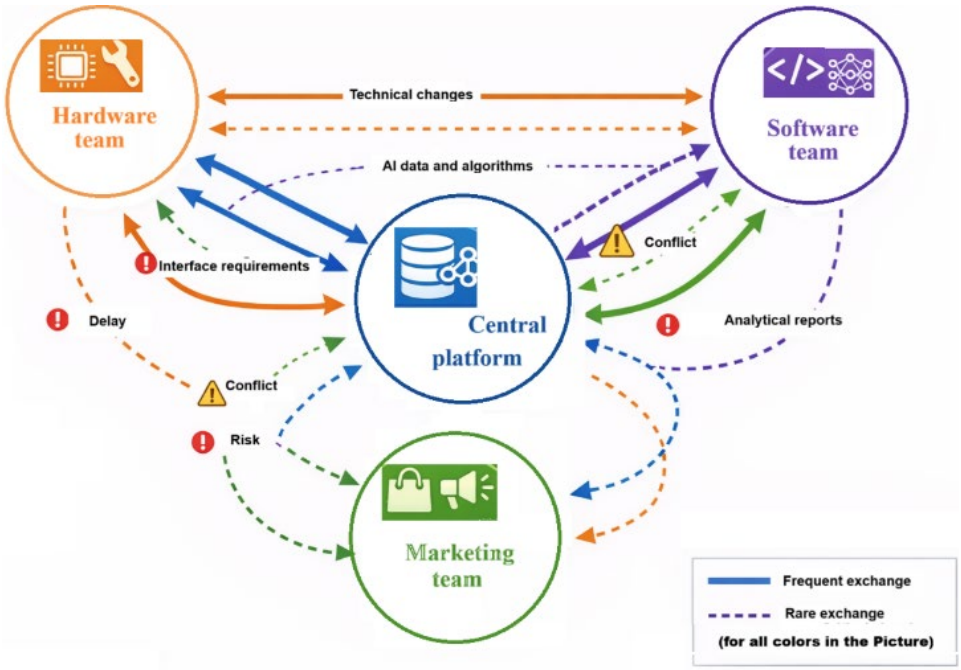

Fig. 1. General view of the network map of interactions between teams in a cyber-physical digital marketing product development project

Based on *the network map*, it is possible to calculate the necessary metrics of information interaction for a multi-team project, which are presented in Table 1.

Table 1

Key metrics of information interaction in a multi-team project

Metric	What it shows
Degree Centrality	Number of connections for each participant (how active they are in terms of communication)
Betweenness Centrality	how much a participant acts as an "intermediary" in communications between others
Closeness Centrality	how quickly information from a participant can reach others
Edge Weight	the intensity of communication between pairs
Density	overall level of interaction within the team (0–1)
Modularity / Clusters	how "sub-teams" or "interest clubs" are formed
Information Flow Index	speed of information transfer between teams (calculated based on time logs)

Based on this, the following management issues can be identified:
– find isolated nodes (teams that interact little);
– identify overloaded nodes (where there is too much communication and a risk of loss);
– reveal gaps in connections between key domains (e.g., Hardware ↔ Marketing);
– find time lags in communications (delays between a change and notification of it).

To build a network map of interactions in an IT project for the development of a cyber-physical digital marketing product, data on communications between teams and their members is required. This does not necessarily have to be correspondence; it can be any form of interaction that can be recorded as an event in the space "who ↔ *with whom* ↔ *about what* ↔ *when*". Such data is recorded in a communication table, an example of which is given in Table 2.

Table 2

Typical data from the "Project Communications Table"

Category	Source	Format	Example
Task	Jira / Trello	JSON / CSV	Task ID, Author, Assignee, Time, Comments
Code	GitLab / GitHub	Logs	Commit author, reviewers, merge requests
Documents	Confluence / Google Docs	API export	Co-authorship, comments, edit times
Communications	Slack / Teams / Email	Chat logs	From, To, Timestamp, Message text
Meetings	Google Meet / Zoom	Calendar logs	Participants, Duration, Agenda
Testing / analytics	CI/CD, QA logs	CSV	Pipeline triggers, responsible team

In a real IT project, such a table is filled from project management systems (Jira, GitLab, MS Teams, Confluence, Slack) [14].

Metadata collection plugins can be used that do not violate confidentiality and only record metrics: *who, when, with whom, through which channel, how often.*

For the study, a synthetic dataset was created based on simulation (simulation data for 3 teams, 15 participants, 500 communications). This made it possible to demonstrate the principle of the model without interfering with real processes.

As a result, the interaction graph is not just a "picture" but an analytical model in which each edge has a mathematical weight.

That is, graph G can be represented as:

$$G = (V, E, W), \tag{1}$$

where:

V is a set of vertices, in our case, *teams or key project participants*, for example:
$V = \{HardwareTeam, SoftwareTeam, MarketingTeam\}$;

E is a set of *edges*, i.e. pairs of vertices between which there is communication, for example:
$E = \{(Hardware, Software), (Software, Marketing), (Hardware, Marketing)\}$;

W – a set of *weights* characterising the intensity, delay or quality of communication.

ISSN 2076-2429 (print)
ISSN 2223-3814 (online)

Thus, each edge E_{ij} has its own weight W_{ij}, which can be one-dimensional or a vector depending on the complexity and depth of the analysis.

The graph can also be overlaid (as shown in Fig. 1) with:

– colors – type of communication (technical, managerial, marketing);

– line thickness – frequency or volume of exchange;

– node size – level of communication activity;

– centrality indices – importance in the network (who is the "bottleneck").

In addition to visualisation, you can calculate:

–Communication Density – how integrated the team is;

– Information Delay Index – average response time between teams;

– Dependency Entropy – degree of uncertainty in connections (variation in exchange frequency);

– Centrality Index – who actually controls the information flow, even if they are not formally a manager.

Note that *a verbal description* of communications (for example, "the marketing team agrees on changes with the programmers") only provides the logic of the process. It does not show:

– the actual intensity of the exchange;

– who is actually the center of influence (rather than the formal manager);

– where there are gaps or delays in the transmission of information;

– whether there is excessive communication that slows down work;

– which nodes become risk points for information overload.

In contrast, *a graph model* provides a quantitative picture that can be measured, compared, and predicted. It allows you to:

– see the "real state of interaction" rather than the one described in the documentation;

– predict the risks of communication gaps (based on a decrease in communication intensity);

– track team synchronisation;

– receive automatic recommendations from AI, for example:

"The intensity of communication between Hardware Team and Marketing Team has decreased by 40%. The probability of an asynchronous release has increased to 0.7".

At the analytical (intellectual) level, artificial intelligence modules perform intelligent analysis of communication content. Using natural language processing (NLP) technologies and analytical models, the system automatically identifies potential conflicts between teams, task duplication, coordination delays, or conflicting requirements. To do this, it uses a multi-layer neural network that analyses text messages, code comments, documentation updates, and test reports. The result of the analysis is intelligent signals – automatically generated recommendations to the IT project manager on the need to coordinate, prioritise changes, or adjust the team interaction plan.

To implement this, the following system functionality was proposed:

– real-time communication monitoring with automatic identification of critical messages and risky exchange nodes;

– a system of notifications about detected inconsistencies or information gaps between teams;

– an intelligent assistant to the IT project manager, which generates recommendations based on statistical analysis and machine learning (for example, "the delay in synchronising the hardware design with the AR module exceeds the acceptable threshold – it is recommended to convene an inter-team session");

– a communications control panel that displays the status of team interaction in the form of interactive graphs, data exchange dynamics, and consistency indicators.

This system eliminates the human factor in terms of losing or ignoring important messages and creates a closed loop of information management, where any change in one part of the project (team) is automatically reflected in all others. The use of artificial intelligence models allows us to go beyond passive data storage and ensure active communication management – to anticipate risks, identify inconsistencies, and support the IT project manager in making timely and informed project decisions.

Development of a network interaction map as an element of complex IT project management

As mentioned earlier, the information and communication level is the central part of the cyber-physical product development management system of a multi-team IT project. The project tasks involve the participation of three independent but interrelated teams: hardware, software, and marketing.

The main task of the analysis is to identify the effectiveness of communication between these teams and to formulate management recommendations to reduce the risks of asynchronous work [15].

A network communication map allows formalising relationships, measuring their intensity, identifying central nodes, and identifying weaknesses in interaction.

To build the interaction map, a mathematical model based on graph theory is used, where the project communication network is defined as (1).

The weight of each connection is determined by the formula:

$$W_{ij} = \alpha f_{ij} - \beta l_{ij} + \gamma q_{ij}, \quad (2)$$

where:

f_{ij} is the average frequency of communications between teams i and j (messages/day);

l_{ij} – average delay in responses (hours);

q_{ij} – interaction quality (0 – 1), and the coefficients α, β, γ are set experimentally: for example, $\alpha = 1.0$, $\beta = 0.5$, $\gamma = 2.0$.

Communication parameters taken into account in the model:

– frequency (f_{ij}) – reflects the intensity of exchange between teams;

– delay (l_{ij}) – average time between request and response;

– quality (q_{ij}) – subjective assessment of the completeness and accuracy of responses;

direction – oriented communication (from source to receiver).

Based on these parameters, a synthetic dataset (Table 3) was created for communication modelling.

Table 3

Synthetic dataset of project communications

Day	Sender	Recipient	Messages	Delay (hours)	Quality (0 – 1)
1	Hardware	Software	1	2.1	0.92
1	Software	Marketing	3	8.5	0.60
1	Hardware	Marketing	1	10.2	0.55
2	Software	Hardware	7	3.1	0.88
2	Marketing	Software	2	7.4	0.65

The data undergoes preliminary processing: cleaning, normalisation and aggregation to average the parameters over time intervals.

A relationship matrix is constructed based on the processed data:

Command →	HW	SW	MKT
HW	–	8.5	0.7
SW	7.9	–	3.5
MKT	0.9	1.2	–

Next, the weights of the connections between nodes are calculated using the above formula. For example, for the Hardware–Software connection, where $f_{ij} = 8.5$, $l_{ij} = 2.1$, $q_{ij} = 0.92$:

$$W_{\text{HW,SW}} = 1.0 \times 8.5 - 0.5 \times 2.1 + 2.0 \times 0.92 = 9.79.$$

Sets of nodes, edges, and weights are formed:

$$V = \{\text{HW}, \text{SW}, \text{MKT}\}, \quad (3)$$

$$E = \{(\text{HW}, \text{SW}), (\text{SW}, \text{MKT}), (\text{HW}, \text{MKT})\}, \quad (4)$$

$$W = \{9.79, 2.10, -1.85\}.$$

The analytical model of the graph allows network metrics to be calculated.

Centrality determines which team has the most connections.

Clustering coefficient shows the degree of node grouping in a subnetwork.

Density characterises the degree of network connectivity:

ISSN 2076-2429 (print)
ISSN 2223-3814 (online)

$$D = \frac{2\,|E\,|}{|V\,|\left(|V\,|-1\right)}, \tag{5}$$

where:

$|V|$ is the number of nodes (participants or project teams);

$|E|$ is the number of connections (actual channels of interaction between them).

The multiplier 2 in the numerator takes into account that the connections are bilateral (for example, "Hardware ↔ Software").

Network density is one of the basic indicators in sociometry, organisational structure analysis, and project communications. It shows how fully all project participants actually interact with each other. In our case (an IT project for the development of a cyber-physical product), this metric measures: "*what proportion of possible connections between teams is actually used for communication*". In other words, if three teams (hardware, software, marketing) could have three bilateral connections but actively communicate only through two, the density will be less than 1, meaning there is a "gap" in communications within the system.

The value of D always belongs to the interval from 0 to 1:

– $D \approx 1.0$ – the network is fully connected: all participants interact with each other regularly;

– $D \approx 0.5$ – partial communication: half of the possible connections actually work;

– $D < 0.3$ – weak connectivity: information circulates only through individual intermediaries;

For example: "The current communication density between IT project teams is 0.58. Recommendation: increase interaction between Software Team and Marketing Team through joint stand-ups or short synchronisation sessions". Thus, D is a quantitative measure that transforms "invisible" communication problems into a measurable management indicator.

Centrality analysis may show that the marketing team has only weak inbound connections, and is therefore a peripheral node and a potential source of asynchrony.

Based on the metrics, critical ties are identified – those with a weight below the threshold value (e.g., $W < 2.0$). Such ties are subject to managerial intervention.

For clarity, the graph is visualised: the thickness of the edge is proportional to the weight value, the color indicates the status of the link (green – stable, yellow – risky, red – critical), and the direction of the arrow corresponds to the initiator of communication.

The critical state can be specified by the system by subtypes:

– unsatisfactory – the connection does not provide data exchange or distorts information;

– dysfunctional – formally exists but does not perform its functions (messages do not arrive, long delays);

– ineffective – communication is of low quality or frequency;

– faulty – communication is unstable over time.

Based on the simulated synthetic dataset, all the necessary indicators were calculated to build a network map of IT project interactions, which are summarised in Table 4.

Table 4

Calculated indicators of communication activity in the project environment

No. No.	Sender	Recipient	Number of messages	Average delay, hours	Communication quality rating (0–1)	Intensity
1	HardwareTeam	SoftwareTeam	36	1.2	0.9	0.82
2	HardwareTeam	MarketingTeam	15	4.5	0.6	0.41
3	SoftwareTeam	HardwareTeam	32	1.0	0.92	0.85
4	SoftwareTeam	MarketingTeam	48	2.8	0.8	0.67
5	MarketingTeam	SoftwareTeam	20	3.6	0.75	0.55
6	MarketingTeam	Hardware Team	12	5.0	0.5	0.3
7	ProductManager	Hardware Team	18	1.8	0.88	0.76
8	ProductManager	Software Team	25	2.0	0.9	0.78
9	ProductManager	Marketing Team	30	1.5	0.95	0.84

After that, based on Table 4, a network map of the project was formed, which is presented in Fig. 2.

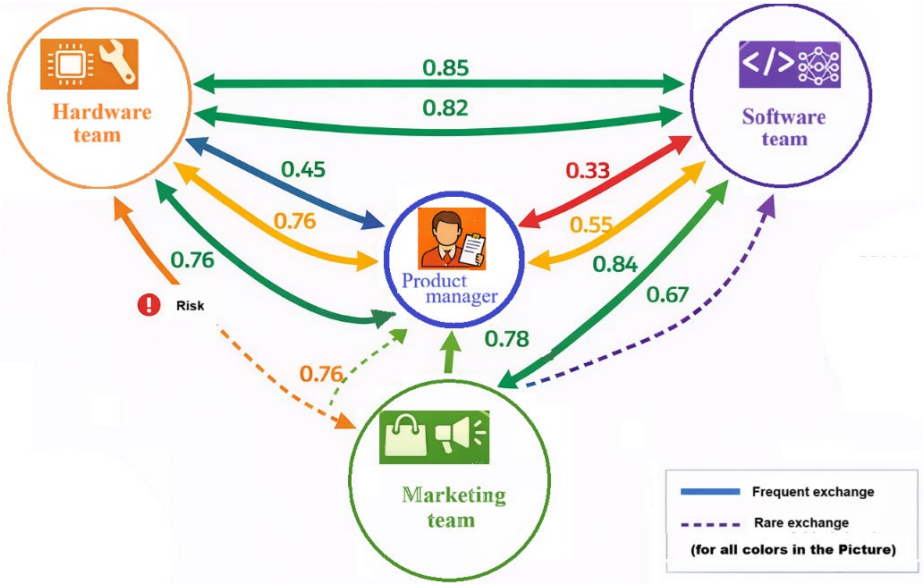

Fig. 2. Calculated network map of the IT project (the symbols and interaction lines shown correspond to Fig. 1**)**

The interaction network map (Fig. 2) was built for an IT project to develop a cyber-physical digital marketing product. It reflects the intensity and directions of information exchange between three teams: software and hardware development, marketing, and the Product Manager, who coordinates their interaction. The Product Manager is at the center of the map because this project is distinctly product-oriented, as the end result is not just a system but a commercial interactive product (AR showcase or "smart mirror") that integrates technology, design, marketing and user experience. Therefore, it is the Product Manager who is the link that coordinates the requirements of the market, the marketing team, and the hardware and software development teams. They define the product vision, functionality, usage scenarios, and priorities. The Project Manager is still present in such a system, but they manage deadlines, resources, risks, and plans, and in this case, they are not the center of communication between teams. Their role is organisational.

The number of arrows on the map corresponds to the number of fixed communication directions in Table 3. Each arrow shows the existence of real information exchange between two teams. Where the exchange is mutual, the arrows are bidirectional, indicating active two-way communication, for example between the hardware and software teams. If the arrow is unidirectional, this indicates asymmetry in the interaction, where one team initiates the exchange more often or transmits more information than it receives, which may be a sign of communication imbalance.

The color of the arrows reflects the status and quality of the connection. Green lines indicate stable connections with high-quality information exchange and minimal delays, such as between hardware and software teams. Yellow arrows indicate risky communications – delays in response, low frequency of contact, or partial loss of context, which is typical for communication between software and marketing teams. Red lines indicate unsatisfactory or failed communication, for example between the marketing and hardware teams, where the frequency of interactions is low and delays are significant. This color signals the need for project manager intervention to restore full communication.

The numbers on the arrows reflect the weight of the connection – a calculated communication intensity coefficient that combines message frequency, exchange quality, and average delay time. A value close to one indicates high intensity and stability of exchange, while low values signal weak or unstable interaction. These values are calculated automatically based on data from corporate communication platforms such as Jira, Slack or Teams.

For a project manager, such a map is an analytical tool that allows them to quickly identify bottlenecks in the interaction between teams. If, for example, the connections between the marketing and hardware teams have a low weight or are colored red, it means that changes in software logic or AR content are not synchronised with marketing scenarios. In this case, the manager can quickly schedule a short inter-team meeting or appoint a coordination specialist.

ISSN 2076-2429 (print)
ISSN 2223-3814 (online)

It is advisable to calculate such a map regularly – at least once per sprint, and in intensive projects with parallel development of hardware and software – weekly, in order to record the dynamics of changes in communication links. It is not necessary to show the map directly to the teams, as it performs an analytical function for the manager. However, aggregated results, such as a decrease in intensity or an increase in delays, can be demonstrated at retrospectives as objective indicators of team interaction. Thus, the network map is not only a visualisation but also a tool for managing the quality of communication in a complex IT project.

The resulting graph allows the IT manager to immediately identify weak communication channels, assess the level of interaction between teams, and determine the need for synchronisation actions (additional meetings, clarification of technical requirements, or automatic notification via IS). Thus, the communication network map transforms subjective team interaction processes into a formalised analytical model suitable for monitoring, risk forecasting, and supporting management decisions in complex IT projects.

Conclusions

The study found that the complexity of IT projects for the development of cyber-physical digital marketing products is due to the high level of integration of various technological components, the multi-team development structure, and the need to maintain constant synchronisation between the physical, software, and marketing parts of the product. Unlike classic IT projects, which are dominated by software development, cyber-physical systems combine hardware devices, sensors, analytical modules, artificial intelligence algorithms, and elements of real-time user interaction. This creates fundamentally new requirements for information flow management, transforming communication between teams from a supporting process to a central element of the entire project's effectiveness.

The main factor complicating such IT projects is the need to ensure coherence between teams with different profiles that use different tools, methodologies, and languages to describe results. Any change in one of the subsystems, for example, in the design of a perception sensor block or in AR visualisation, instantly affects other components of the system, creating cascading risks for the entire project. Therefore, the key area for management optimisation is the development of an intelligent communication system that provides automated monitoring, analysis and visualisation of interactions between teams.

The practical implementation of the network communication map has demonstrated that the transition from descriptive management methods to analytical and visual ones allows complex communication processes to be transformed into an objectively measurable system. The constructed map reflects the actual intensity, frequency, delays, and quality of information exchange between teams, and also allows identifying central nodes and weak links that require intervention. In particular, the application of a formalised graph model $G(V, E, W)$ made it possible to calculate the weight coefficients of connections and network metrics such as communication density, centrality, and clustering coefficient. This provides the ability to quantitatively analyse interactions that were previously assessed only intuitively.

The system's intelligent modules, based on machine learning and natural language analysis technologies, provide automatic detection of risks of asynchrony, information gaps, and potential conflicts between teams. The analytical data obtained allows for the generation of management recommendations in real time — for example, on the need for urgent coordination of changes or a synchronisation session. Thus, the network map of interactions not only performs a visualisation function, but also becomes an integrated component of the management decision support system.

An important advantage of the developed approach is the transition to proactive communication management, where the system not only records the facts of communication, but also predicts possible failures and provides analytical signals to the manager about the need for intervention. This significantly increases the resilience of multi-team IT projects to dynamic changes in the environment and reduces the risks of asynchrony in development. Thus, the construction of a network communication map and the implementation of an intelligent analytical system become an effective tool for improving the manageability, coordination, and adaptability of IT projects for the development of cyber-physical digital marketing products, which is a necessary condition for their successful implementation in the digital economy.

Література

1. Zabarna E., Liubchenko V. To the issue of digitization of the service sector in Ukraine. *Proceedings of Odessa Polytechnic University*. 2024. Vol. 69, Issue 1. P. 134. DOI: 10.15276/opu.1.69.2024.14.
2. Enhancing Project Management for Cyber-physical Systems Development / F. E. Palma et al. *Proceedings of the Federated Conference on Computer Science and Information Systems*. 2018. Vol. 15. P. 747–750. DOI: 10.15439/2018F258.
3. PMBOK Guide. The Standard for Project Management and a Guide to the Project Management Body of Knowledge. Seventh Edition. USA : Project Management Institute, 2021. 250 p.
4. CPS-PMBOK: How to Better Manage Cyber-Physical System Development Projects / F. Palma et al. *Enterprise Information Systems : Lecture Notes in Business Information Processing*. 2020. P. 154–181. DOI: 10.1007/978-3-030-40783-4_9.
5. Experiences and challenges from developing cyber-physical systems in industry-academia collaboration / J. Cederbladh et al. *Software: Practice and Experience*. 2024. Vol. 54, Issue 6. P. 1193–1212. DOI: https://doi.org/10.1002/spe.3312.
6. Путій І., Тесленко П. Аналіз сучасних підходів до управління складними IT-проєктами. *Управління розвитком складних систем*. 2024. Вип. 59. С. 81–88. DOI: https://doi.org/10.32347/2412-9933.2024.59.81-88.
7. Kosmala K., Marszalek A., Rudawska E. Communication in Project Team Management - Identification of Research Gaps and Direction for Future Research. *European Research Studies Journal*. 2024. Vol. XXVII, Special Issue A. P. 732–751. DOI: 10.35808/ersj/3746.
8. Банніков В. Вдосконалення процесу управління комунікаціями при виконанні проекту: інструменти та методи. *Економіка та суспільство*. 2022. Вип. 41. DOI: 10.32782/2524-0072/2022-41-20.
9. Abdul O., Kozlovski E. The Role of Communication Management Within the Virtual Team in an International Projects-Based Organisation. *Archives of Business Research*. 2023. Vol. 11, No. 9. P. 205–218. DOI: https://doi.org/10.14738/abr.119.15534.
10. Simon D., Reicher R. The role of inter-project communication and continuous risk management strategy in a maintenance facility: A case study. *Corporate & Business Strategy Review*. 2025. Vol. 6, No. 1. P. 75–84. DOI: https://doi.org/10.22495/cbsrv6i1art7.
11. Effective Project Communication: Navigating Stakeholder Engagement in the AI-Powered Era / M. Pirozzi et al. *PM World Journal*. 2025. Vol. XIV, Issue I. URL: https://pmworldlibrary.net/wp-content/uploads/2025/01/pmwj148-Jan2025-Pirozzi-Apponi-Liburdi-Quagliarini-Remediani-Effective-Project-Communication.pdf.
12. Marqués A. Communication in IT: Strategies for Managing Teams, Stakeholders and Successful Projects (Workplace Mastery Series). Independently published, 2024. 218 p.
13. Мільська К. О. Проєктування інтерфейсу взаємодії з користувачем у системах із надання послуг. *Інформаційні технології і системи в документознавчій сфері*. 2024. С. 88–89.
14. Кордунов С. Ю. Автоматизація управління IT-проєктами за допомогою сучасних інструментів (Jira, Trello, Monday). *Здобутки економіки: перспективи та інновації*. 2025. Вип. 20. DOI: https://doi.org/10.5281/zenodo.16480693.
15. Ровенська В., Смирнова І., Латишева О. Комунікації та управління конфліктами в операційних та IT проєктах. *Вісник Приазовського державного технічного університету. Серія: Економічні науки*. 2023. Вип. 1(38). С. 12–20. DOI: https://doi.org/10.31498/2225-6725.1(38).2023.280727.

References

1. Zabarna, E., & Liubchenko, V. (2024). To the issue of digitization of the service sector in Ukraine. *Proceedings of Odessa Polytechnic University*, *69*(1), 134. DOI : 10.15276/opu.1.69.2024.14.
2. Palma, F. E., Fantinato, M., Rafferty, L., & Hung, P. C. (2018). Enhancing project management for cyber-physical systems development. *Proceedings of the Federated Conference on Computer Science and Information Systems*, *15*, 747–750. DOI: 10.15439/2018F258.
3. Project Management Institute. (2021). *A guide to the project management body of knowledge (PMBOK guide) and the standard for project management* (7th ed.).
4. Palma, F., Fantinato, M., Rafferty, L., & Hung, P. C. (2020). CPS-PMBOK: How to better manage cyber-physical system development projects. In *Enterprise Information Systems* (pp. 154–181). Springer. DOI:10.1007/978-3-030-40783-4_9.
5. Cederbladh, J., Kamburjan, E., Manrique-Negrin, D. A., Mittal, R., & Weber, T. (2024). Experiences and challenges from developing cyber-physical systems in industry-academia collaboration. *Software: Practice and Experience*, *54*(6), 1193–1212. DOI: https://doi.org/10.1002/spe.3312.

6. Putii, I., & Teslenko, P. (2024). Analysis of modern approaches to managing complex IT projects. *Management of Complex Systems Development*, (59), 81–88. DOI: https://doi.org/10.32347/2412-9933.2024.59.81-88.
7. Kosmala, K., Marszalek, A., & Rudawska, E. (2024). Communication in project team management - Identification of research gaps and direction for future research. *European Research Studies Journal*, *27*(Special Issue A), 732–751. DOI: 10.35808/ersj/3746.
8. Bannikov, V. (2022). Improving the communications management process during project implementation: Tools and methods. *Economy and Society*, (41). DOI: https://doi.org/10.32782/2524-0072/2022-41-20.
9. Abdul, O., & Kozlovski, E. (2023). The role of communication management within the virtual team in an international projects-based organisation. *Archives of Business Research*, *11*(9), 205–218. DOI: https://doi.org/10.14738/abr.119.15534.
10. Simon, D., & Reicher, R. (2025). The role of inter-project communication and continuous risk management strategy in a maintenance facility: A case study. *Corporate & Business Strategy Review*, *6*(1), 75–84. DOI: https://doi.org/10.22495/cbsrv6i1art7.
11. Pirozzi, M., Apponi, F., Liburdi, E., Quagliarini, A., & Remediani, E. (2025). Effective project communication: Navigating stakeholder engagement in the AI-powered era. *PM World Journal*, *14*(1). Retrieved from https://pmworldlibrary.net/wp-content/uploads/2025/01/pmwj148-Jan2025-Pirozzi-Apponi-Liburdi-Quagliarini-Remediani-Effective-Project-Communication.pdf.
12. Marqués, A. (2024). *Communication in IT: Strategies for managing teams, stakeholders and successful projects*. Independently published.
13. Milska, K. O. (2024). Designing the user interface in service delivery systems. *Information Technologies and Systems in the Document Science Sphere*, 88–89.
14. Kordunov, S. Y. (2025). Automation of IT project management using modern tools (Jira, Trello, Monday). *Achievements of the Economy: Prospects and Innovations*, (20). DOI: https://doi.org/10.5281/zenodo.16480693.
15. Rovenska, V., Smirnova, I., & Latysheva, O. (2023). Communications and conflict management in operational and IT projects. *Bulletin of the Azov State Technical University. Series: Economic Sciences*, (1/38), 12–20. DOI: https://doi.org/10.31498/2225-6725.1(38).2023.280727.

Забарна Елеонора Миколаївн; Eleonora Zabarna, ORCID: http://orcid.org/0000-0002-2659-5909
Тімчинський Олексій Олександрович; Oleksiy Timchinsky, ORCID: https://orcid.org/ 0009-0009-6416-5430
Бондар Олександр Анатолійович; Oleksandr Bondar, ORCID: https://orcid.org/0000-0001-7132-6057
Овсійчук Віталій Петрович; Vitaliy Ovsiychuk, ORCID: https://orcid.org/ 0009-0005-9049-4060

Received November 17, 2025

Accepted December 16, 2025

UDC 004.93

D. Koshutina
Odessa Polytechnic National University, Shevchenko Ave. 1, Odesa, Ukraine, 65044, e-mail: d.v.koshutina@op.edu.ua

KAN-TYPE NEURAL NETWORK MODEL FOR ECG SIGNAL ANALYSIS AND CLASSIFICATION

Д. Кошутіна. **Нейромережева модель KAN-типу для аналізу та класифікації сигналів ЕКГ.** Дослідження електрокардіограм має критичне значення для діагностики серцево-судинних патологій, оскільки точне виділення локальних особливостей сигналу забезпечує надійність класифікації аритмій. Актуальність роботи обумовлена потребою підвищення точності автоматизованих систем, здатних працювати із сегментами сигналів різної довжини та в умовах шумового впливу. Метою роботи є розробка моделі на основі багатошарового перцептрона з додатковим шаром, що комбінує радіальні базисні функції та вейвлет-перетворення для точного виявлення локальних особливостей сигналу. Завдання включали підготовку та нормалізацію сегментів сигналів, експериментальне порівняння різних типів вейвлетів і рівнів їх декомпозиції, вибір числа функцій у додатковому шарі та оцінку впливу архітектурних параметрів на точність класифікації та швидкодію моделей. Методи дослідження передбачали обробку сигналів із відкритої бази даних, нормалізацію значень сегментів у визначеному діапазоні, побудову моделей із застосуванням багатокласової функції втрат і методів оптимізації градієнтного спуску, а також оцінку ефективності через точність класифікації і показники збалансованої точності для сегментів зі шлуночковими порушеннями ритму. Результати показали, що інтеграція додаткового шару з радіальними базисними функціями і вейвлет-перетворенням підвищує точність класифікації аритмій, забезпечує стабільність моделей при зміні параметрів сегментації та наявності шуму, а також дозволяє ефективно виділяти локальні особливості сигналу. Застосування різних типів вейвлетів і рівнів декомпозиції дозволяє досягти оптимального співвідношення точності та швидкодії моделей. Наукова новизна полягає у поєднанні радіальних базисних функцій із вейвлет-перетворенням для покращеного виділення локальних ознак сигналів електрокардіограми, що забезпечує підвищену стійкість до шуму. Практичне значення роботи полягає у створенні ефективної методики для автоматизованого аналізу електрокардіограм із високою точністю класифікації аритмій.

Ключові слова: електрокардіограма, багатошаровий перцептрон, MLP-KAN, вейвлет-перетворення, радіальні базисні функції, класифікація, точність

D. Koshutina. **KAN-Type Neural Network Model for ECG Signal Analysis and Classification.** Electrocardiogram analysis is critically important for the diagnosis of cardiovascular pathologies, as precise identification of local signal features ensures reliable arrhythmia classification. The relevance of this work is determined by the need to improve the accuracy of automated systems capable of processing signal segments of varying length under noisy conditions. The objective of the study is the development of a model based on a multilayer perceptron with an additional layer that combines radial basis functions and wavelet transformation for accurate detection of local signal characteristics. The tasks included preparation and normalization of signal segments, experimental comparison of different types of wavelets and their decomposition levels, selection of the number of functions in the additional layer, and assessment of the impact of architectural parameters on classification accuracy and computational performance. The research methods involved processing signals from an open database, normalizing segment values within a defined range, constructing models using a multiclass loss function and gradient descent optimization, and evaluating performance through classification accuracy and balanced accuracy metrics for segments with ventricular rhythm disturbances. The results demonstrated that integrating an additional layer with radial basis functions and wavelet transformation increases arrhythmia classification accuracy, ensures model stability under variations in segmentation parameters and noise presence, and allows effective extraction of local signal features. The use of different wavelet types and decomposition levels enables achieving an optimal balance between accuracy and computational efficiency. The scientific novelty lies in combining radial basis functions with wavelet transformation to enhance the detection of local electrocardiogram signal features, providing increased noise robustness. The practical significance of the study is the creation of an effective methodology for automated electrocardiogram analysis with high arrhythmia classification accuracy.

Keywords: electrocardiogram, multilayer perceptron, MLP-KAN, additional layer, wavelet transformation, radial basis functions, classification, accuracy

1. Introduction

Electrocardiographic (ECG) signals are a primary diagnostic tool for monitoring cardiac activity and detecting rhythm disturbances. Accurate analysis of ECG signals is crucial for early identification of cardiovascular pathologies, as subtle variations in wave morphology can indicate serious conditions [1]. Traditional signal processing techniques, such as digital filtering, morphological feature extraction, and R-peak detection algorithms – including the Pan-Tompkins approach and wavelet transforms – have provided reliable tools for feature extraction; however, their performance heavily depends on preprocessing quality and careful parameter tuning [1].

The rise of high-performance computing has enabled the adoption of machine learning methods, such as support vector machines, decision trees, and ensemble models, which allow partial automation of feature extraction. Yet, these models often struggle to capture the complex nonlinear dependencies and inter-patient variability inherent in ECG signals [2]. Recent developments in deep learning, in-

DOI: 10.15276/opu.2.72.2025.17

ISSN 2076-2429 (print)
ISSN 2223-3814 (online)

cluding convolutional, recurrent, and hybrid architectures, have demonstrated remarkable performance in ECG classification tasks [3]. Despite these advances, classical multilayer perceptron (MLP) models and their extensions remain relevant due to their structural simplicity, stability during training, and precise control over architectural parameters.

An emerging approach involves Knowledge-Augmented Networks (KAN), which integrate MLP architectures with radial basis functions (RBFs) to enhance the network's ability to approximate local signal features [4]. Such models generate localized responses to morphological variations, improving detection of pathological contractions while preserving overall network stability.

The present study aims to investigate the effectiveness of a KAN-type neural network for ECG classification, comparing it to conventional MLP models. The research focuses on analyzing the impact of RBF components and wavelet-based preprocessing on model performance, robustness, and sensitivity to rare pathological events.

2. Literature Review and Problem Statement

Electrocardiographic (ECG) signals are a central tool for diagnosing cardiac rhythm and conduction disorders. The diagnostic value of ECG relies not only on the morphology of individual waves but also on subtle variations in their duration, amplitude, wavefront slopes, and interval ratios, which are critical for detecting early stages of arrhythmias and ischemic changes [5, 6]. Preservation of these features depends on high-quality preprocessing, making filtering and normalization stages essential for maintaining diagnostically relevant characteristics [7].

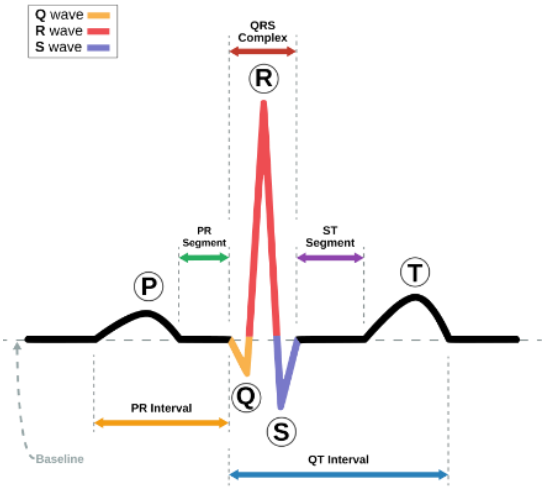

Fig. 1. QRS complex visualization

Classical ECG processing methods, developed in the foundational works of Pan and Tompkins (1985), Tompkins (1993), and studies associated with the MIT-BIH Arrhythmia Database (2001), established the basis for QRS complex detection, noise removal, and standardization of analysis approaches [8, 9]. Sörnmo and Laguna further systematized filtering strategies, artifact models, and baseline drift correction techniques [10]. Despite these advances, traditional filters – including low-pass, high-pass, band-pass, and adaptive types – remain limited when applied to real clinical data containing motion artifacts, myogenic noise, sudden baseline shifts, and uneven sampling frequency, particularly in long-term Holter recordings [5, 6].

Adaptive filtering methods, such as LMS- and RLS-based algorithms (Widrow, Haykin), enable real-time spectral adaptation [6]. Kalman filtering and its nonlinear extensions (Extended and Unscented Kalman Filters) have been successfully applied to reconstruct P-waves and suppress biomechanical noise while preserving QRS complex and ST-segment morphology, as illustrated in Figure 1 [5]. Unlike static filters, these approaches reduce the loss of diagnostically critical features, which is especially important for long-duration and noisy recordings [1].

Wavelet transforms have been widely adopted for ECG preprocessing due to their ability to represent signals at multiple scales [7, 11, 12]. Wavelets such as Db4, Db6, or Symlet enable multilevel extraction of the QRS complex, while adaptive thresholding of coefficients suppresses high-frequency noise [11, 12]. Multilevel decomposition with subsequent reconstruction preserves small P-wave components often lost during classical filtering [7].

Statistical and clustering approaches, including Gaussian Mixture Models (GMM), Hidden Markov Models (HMM), DBSCAN, and Spectral Clustering, facilitate grouping of cardiac cycles and identification of pathological rhythm patterns, such as atrial extrasystoles or fibrillation episodes [13, 14]. These methods reduce noise influence and structure large datasets, preparing segments for machine learning models like CNNs, LSTMs, and hybrid architectures [15, 2]. Adaptive clustering combined with dimensionality reduction methods such as UMAP has demonstrated high effectiveness in analyzing large clinical ECG streams [14, 1].

The introduction of deep learning has significantly advanced automated ECG analysis. Classical classifiers (SVM, kNN, naïve Bayes) were limited in capturing complex nonlinear dependencies in

high-dimensional ECG time series [15, 16]. CNNs efficiently extract local QRS patterns, while LSTM and CNN-LSTM hybrids preserve long-term dependencies [17, 18].

Knowledge-Augmented Networks (KAN) integrate MLP architectures with radial basis functions (RBF), compensating for limitations in modeling local nonlinearities [17, 18, 19]. RBF components allow the network to adapt to variations in individual complexes, reducing dependence on specific patients or recording devices. KAN models show improved arrhythmia recognition on noisy datasets such as MIT-BIH Noise Stress Test Database and real-world clinical streams [17, 20]. Wavelet-based preprocessing further enhances KAN models by providing a multilevel time–frequency representation of ECG segments, preserving local morphology and improving robustness to noise while maintaining computational efficiency [7].

Despite these advances, several challenges remain. Segmentation and normalization parameters strongly influence QRS morphology, amplitude ratios, and temporal intervals, affecting classification accuracy and model stability across different devices and patient populations. Real-world ECG signals often contain electromagnetic interference, motion artifacts, and electrode-related distortions, yet the robustness of modern neural network architectures – including MLP, RBF-KAN, and wavelet-KAN models – under such conditions is insufficiently studied. Comparisons between architectures are necessary to determine which approach best balances artifact resistance, training efficiency, and classification accuracy.

Thus, the present study addresses the following objectives:

– Evaluate the impact of segmentation, normalization, and noise parameters on model performance;

– Compare the effectiveness of MLP, RBF-KAN, and wavelet-KAN models for ECG classification;

– Improve the reliability of automated cardiac diagnostics;

– Develop practical guidelines for model configuration and preprocessing across clinical scenarios.

3. Aim and Objectives of the Study

The aim of this study is the development and systematic evaluation of a KAN-type neural network for ECG signal classification, taking into account the influence of segmentation parameters, normalization methods, and architectural configurations, including RBF and wavelet components. The research focuses on identifying configurations that provide an optimal balance between classification accuracy, the network's ability to capture local time–frequency patterns of the signal, robustness to noisy data, and training efficiency.

The objectives of the study include:

– preparation of the ECG dataset, including segmentation of signals of varying lengths (100…250 samples), normalization, and class balancing to ensure a stable foundation for model training;

– development and tuning of the baseline MLP model, the MLP-KAN architecture with varying numbers of radial basis functions (RBF: 4, 6, 8), and integration of wavelet preprocessing (MLP-KAN-WT) for subsequent performance comparison;

– analysis of the impact of segmentation and normalization parameters on model accuracy and stability;

– investigation of model effectiveness in detecting rare classes (extrasystoles, class V) through data balancing and F1-score evaluation;

– visualization and assessment of classification results using confusion matrices to compare baseline MLP, MLP-KAN, and MLP-KAN-WT;

– evaluation of model training time to determine the trade-off between computational efficiency and processing speed.

4. Materials And Methods

The study utilized the MIT-BIH Arrhythmia Database [9], a standard dataset for ECG-based arrhythmia classification tasks. This database contains recordings of various cardiac rhythms, allowing modeling of both normal and pathological signals.

Signal segmentation was performed based on R-peaks, as the R-peak represents the most prominent part of the QRS complex, serving as a reliable reference point for defining the start and end of each cardiac cycle. Segmenting by R-peaks standardizes the length of input signal windows, reduces

ISSN 2076-2429 (print)
ISSN 2223-3814 (online)

the impact of interbeat variability, and facilitates the extraction of local morphological ECG features. Figure 1 illustrates an example ECG signal with highlighted R-peaks used for segmentation.

Class labels N (normal rhythm) and V (extrasystoles / premature ventricular contractions) were converted into numeric format to ensure compatibility with machine learning algorithms. Normal rhythm (*N*) includes QRS complexes without arrhythmic signs, characterized by regular heart rates and stable amplitude-time characteristics. Extrasystoles (*V*) are premature ventricular beats differing in shape, amplitude, or RR interval. Although rare, these events are clinically significant. This labeling approach enables models to learn normal patterns while simultaneously evaluating their ability to detect pathological signals, which is critical for automated diagnostic applications [21].

The dataset was split into training and testing sets while preserving class proportions to provide representative evaluation of model performance and reduce overfitting risk. To ensure training stability and comparability across different signal segments, data normalization was applied. This preprocessing step scales input features to a uniform range, improving convergence during training and the reliability of performance evaluation.

4.1. Data Preprocessing

Normalization is a critical step for the operation of multilayer perceptrons (MLPs) and KAN-type neural networks, as these models are sensitive to the scale of input data. ECG signals vary in amplitude due to patient-specific characteristics, sensor placement, and recording conditions. Without normalization, larger amplitude signals could dominate the learning process, leading to biased or unstable model behavior.

In this study, each ECG segment $x = [x_1, x_2, ..., x_n]$ was rescaled to the range $[0,1]$ using min-max normalization:

$$x_i' = \frac{x_i - x_{\min}}{x_{\max} - x_{\min}},$$

where: x is the original signal value, $x_{\min}$ and $x_{\max}$ are the minimum and maximum values of the segment, respectively, and x' is the normalized value [22].

Normalization ensures that models consistently capture both local and global features of ECG signals. It also improves the comparability of results across experiments, reduces training time, and enhances generalization to unseen data, which is particularly important for clinical applications.

In addition to amplitude normalization, the dataset was structured to maintain class balance. Ventricular extrasystoles (class *V*) are less frequent than normal beats (class *N*), and an unbalanced dataset can bias the model toward the majority class. The training set was constructed to provide sufficient representation of rare pathological events, ensuring the model learns to detect clinically significant anomalies.

4.2. Model Architectures

The multilayer perceptron (MLP) is a fundamental neural network architecture commonly used for classification tasks due to its ability to model nonlinear relationships between input features and target classes [23]. The network consists of fully connected layers, where each neuron receives input from all neurons of the previous layer, applies learned weights, passes the result through an activation function, and forwards the signal to subsequent layers.

ECG signals were divided into fixed-length windows of 200 samples, each corresponding to an individual cardiac cycle centered on the R-peak. Such segmentation standardizes the input length, reduces interbeat variability, and enables the model to effectively capture both local morphological features and temporal patterns of the QRS complex.

In this study, the MLP processes one-dimensional ECG segments of 200 samples, representing individual cardiac cycles. Input normalization to the 0…1 range standardizes amplitudes across different patients and segments, promoting stable training and consistent feature representation [22].

The network comprises two hidden Dense layers. The first layer contains 128 neurons with ReLU activation, responsible for extracting local morphological features of the ECG, including wave peaks, slopes, and the overall shape of the QRS complex. A Dropout layer with 0.2 probability follows to reduce overfitting. The second hidden Dense layer has 64 neurons, also with ReLU activation, and is followed by a Dropout layer with 0.1 probability for additional regularization.

The output layer consists of two neurons corresponding to *N* (normal rhythm) and *V* (ventricular extrasystoles) classes, with a Softmax activation function to generate class probabilities:

$$P(y=i)=\frac{e^{z_i}}{\sum_j e^{z_j}},$$

where: z_i represents the linear combination of weighted inputs for the i-th output neuron.

Figure 2 presents the schematic of the MLP architecture, showing the sequential processing of ECG segments from input normalization through hidden layers to class probability outputs. The design ensures comprehensive capture of local and global morphological features for accurate classification of normal and pathological cardiac events.

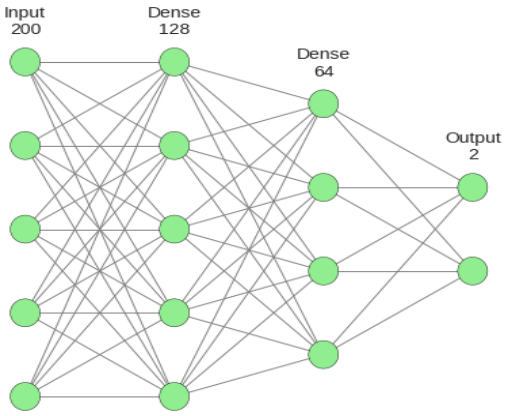

Fig. 2. Schematic of basic MLP

The MLP-KAN (Knowledge-Augmented Network) model represents an extension of the classical multilayer perceptron through the integration of a KAN layer [24]. This layer enhances the network's ability to capture local variations and subtle morphological patterns in ECG signals, which are often critical for detecting rare or irregular events. The KAN layer incorporates radial basis functions (RBFs) to supplement the fully connected structure of the MLP, enabling the modeling of complex nonlinear relationships that standard dense layers alone may not adequately represent [25].

The input layer processes normalized ECG segments of 200 samples, consistent with the baseline MLP [26]. Within the KAN layer, each neuron corresponds to a Gaussian RBF, and in this study, four RBF units are used to capture localized morphological features. These functions generate selective responses to specific ECG characteristics, such as sharp peaks or deviations in wave slopes, increasing the network's sensitivity to clinically significant variations [27]. The output of the i-th RBF neuron is defined as:

$$\varphi_i(x)=\exp\left(-\frac{(x-c_i)^2}{2\sigma^2}\right),$$

where: x is the input segment value, c_i is the center of the i-th RBF, and σ is the width parameter controlling the locality of the function's influence [28, 29, 30]. Figure 3 illustrates the four Gaussian RBF functions applied to a representative ECG segment, with each function labeled $\varphi_0, \varphi_1, \varphi_2, \varphi_3$.

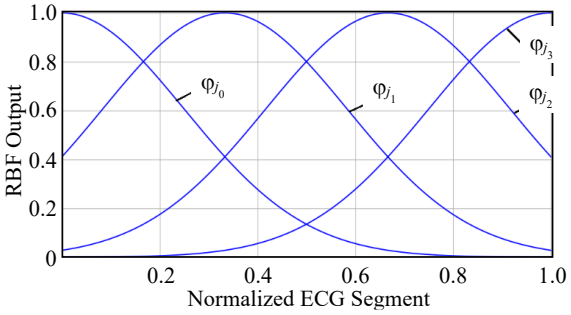

Fig. 3. Typical form of functions φ_i for $m = 4$

The outputs of the RBF neurons are then fed into a fully connected Dense layer, where each output is combined with trainable weights optimized during training [31]. This produces a condensed representation of the local morphological features detected by the RBFs. Subsequently, the representation is processed through two hidden Dense layers with 128 and 64 neurons, applying ReLU activation and Dropout regularization to enhance feature integration, nonlinearity, and generalization [32].

Finally, the output Dense layer contains two neurons with a Softmax activation function, yielding probabilities for classification into N (normal rhythm) and V (extrasystoles). This layered organization allows the network to combine localized feature extraction via RBFs with global pattern integration, ensuring that subtle variations in ECG signals, including rare or irregular events, contribute effectively to the classification decision.

The overall MLP-KAN architecture, showing the RBF layer in parallel with the fully connected hidden layers and the final output layer, is presented in Figure 4. This schematic highlights how local signal characteristics are extracted and integrated to improve classification performance on both typical and atypical ECG patterns.

The MLP-KAN-WT (Multilayer Perceptron with Knowledge-Augmented and Wavelet Transform) model extends the classical MLP-KAN architecture by replacing the radial basis functions in the KAN lay-

ISSN 2076-2429 (print)
ISSN 2223-3814 (online)

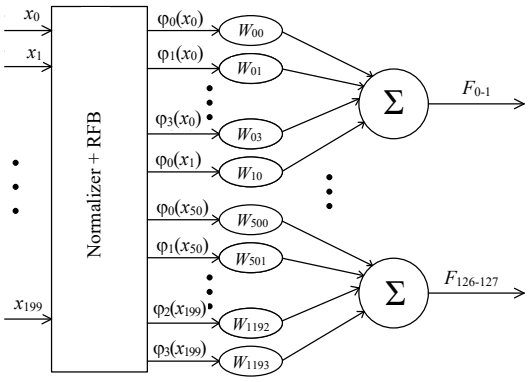

Fig. 4. Example of KAN layer

er with wavelet functions. This modification enhances the network's ability to capture local and time–frequency features of ECG signals, enabling precise detection of short-term anomalies, abrupt spikes, and transient events characteristic of arrhythmogenic episodes. Wavelet functions effectively highlight localized patterns of the QRS complex, premature ventricular depolarizations, and other subtle morphological variations, while providing robustness to noise, amplitude fluctuations, and segmentation variability.

Within the KAN-Wavelet layer, multiple parameterized wavelet functions are applied to each ECG segment of 200 samples to generate a multidimensional vector of local time–frequency features. The selected wavelet functions include Haar (level 1), Daubechies 4 (level 4), Symlet 4 (level 4), and Coiflet 5 (level 5), providing diverse basis functions capable of representing a range of ECG signal characteristics. Each wavelet function $\psi_j(t)$ transforms the input segment $x(t)$ into a feature representation:

$$\varphi_j(x) = \sum_{t=1}^{n} x(t) \cdot \psi_j(t),$$

where: n is the number of samples in the segment. The trainable parameters of each wavelet allow the network to adapt to variations in signal morphology and inter-patient differences.

The outputs of the wavelet functions are subsequently fed into two fully connected Dense layers for feature integration. The first Dense layer contains 128 neurons with ReLU activation and a Dropout probability of 0.2, while the second layer has 64 neurons with ReLU and Dropout 0.1. This structure aggregates the extracted time-frequency features, introduces nonlinearity, and supports stable model training.

Figure 5 illustrates the typical forms of the five shifted Daubechies 4 wavelet functions applied to a representative ECG segment. The graph demonstrates how these wavelets localize and detect subtle signal variations. Figure 6 presents the complete schematic of the MLP-KAN-WT architecture, showing the integration of the KAN-Wavelet layer with the subsequent Dense layers and output classification layer. This architecture ensures effective extraction of local and time–frequency features, increases robustness to noise and inter-patient variability, and improves arrhythmia classification accuracy compared to the classical MLP-KAN model.

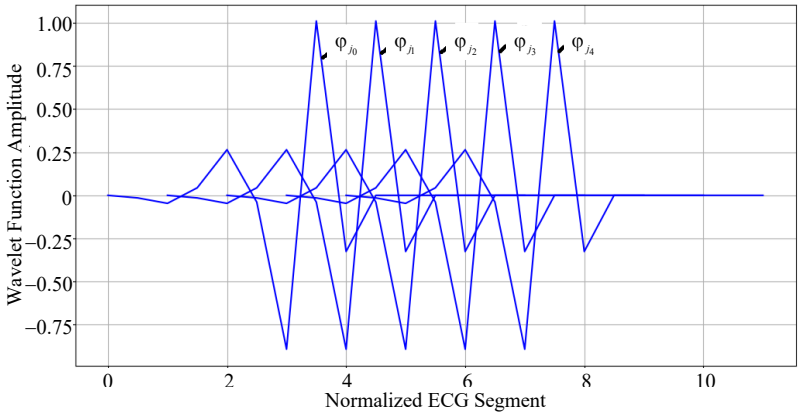

Fig. 5. Typical form of wavelet functions Daubechies 4 φ_i for $m = 5$

4.3. Experiments

The experimental part of the study focused on a comprehensive evaluation of three distinct architectures: the baseline MLP, the MLP-KAN model incorporating a kernel layer for local nonlinear approximation, and the modified MLP-KAN-WT, which combines the KAN approach with multiscale features ob-

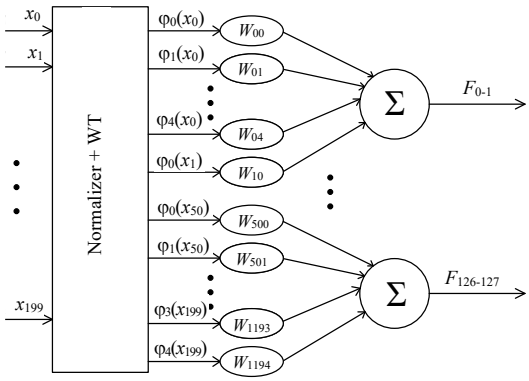

Fig. 6. Examzple of KAN layer with WT

tained through discrete wavelet transforms. For MLP-KAN-WT, Haar wavelets with decomposition level 1, Daubechies 4 with level 4, Symlet 4 with level 4, and Coiflet 5 with level 5 were selected.

The choice of decomposition levels was guided by energy and entropy criteria as proposed in [7, 33]. Signal energy reflects the concentration of information at a particular scale, while entropy measures the disorder of the coefficients. Selecting levels that maximize energy and minimize entropy allows automatic identification of scales that best capture both local and frequency characteristics of ECG signals.

All models were trained under a unified optimization scheme using the Adam optimizer with a learning rate of 0.001, fixed-size mini-batches, and categorical cross-entropy as the loss function. Initial weights were identical across runs to minimize variability and allow reliable statistical comparison. Evaluation was performed on an independent test set, recording performance metrics such as overall accuracy, class-specific $F1$-score, precision, recall, and training time.

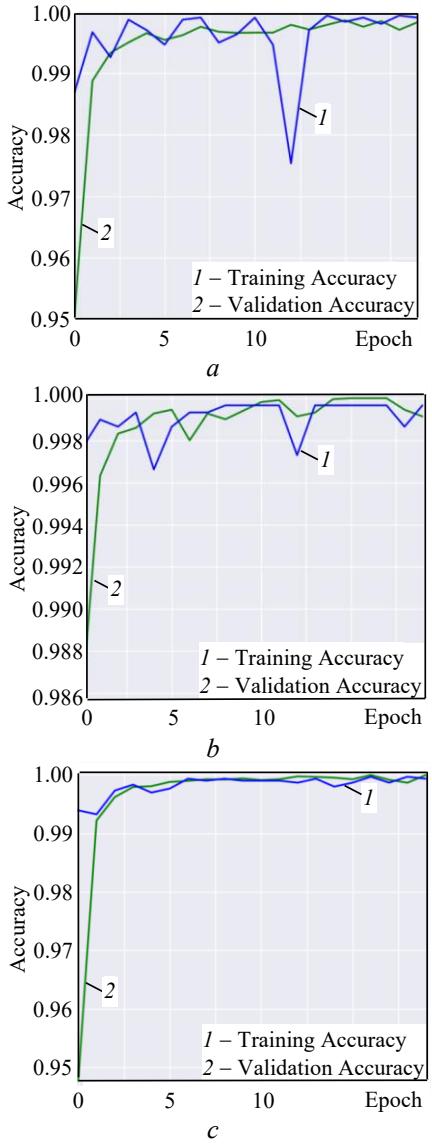

Fig. 7. Learning curves: *a* – for MLP; *b* – for MLP-KAN; *c* – for MLP-KAN-WT, showing both training and validation loss and accuracy over epochs

A substantial portion of the experiments examined the impact of input window size. ECG signals were divided into fixed-length segments of 200 samples, corresponding to individual cardiac cycles centered on the R-peak. This interval provides sufficient morphological information to capture characteristic QRS features while reducing interbeat variability. Additional segment lengths of 100, 150, and 250 samples were tested to assess sensitivity to available temporal context.

Class imbalance was explicitly addressed: the dataset contained a majority of normal beats (class *N*) and a relative scarcity of ventricular ectopic beats (class *V*). Oversampling of class *V* was applied during training to ensure sufficient representation, mitigating bias toward the dominant class and enabling accurate evaluation of models' ability to detect clinically relevant anomalies.

For MLP-KAN, the capacity of the kernel layer was varied by adjusting the number of radial basis functions (4, 6, or 8 RBF) to evaluate the effect of increased nonlinear space complexity on the detection of subtle morphological changes. In MLP-KAN-WT, wavelet transforms represent ECG signals across multiple levels, preserving local variations such as short impulses, abrupt transitions, and fine-grained features that conventional dense layers or RBFs may smooth out.

Learning curves illustrating loss and accuracy on training and validation sets were generated for all architectures. These curves provide insight into convergence speed, stability, and the influence of the KAN layer and wavelet-based feature extraction on regularization and generalization. Figure 7 presents the loss curves, while Figure 8 shows accuracy progression.

Confusion matrices were analyzed in detail to reveal characteristic misclassifications, such as ventricular ectopic beats labeled as normal. These patterns highlight how the integration of local nonlinear processing in the KAN layer and multiscale wavelet features in MLP-KAN-WT improve recognition of complex morphological structures.

Overall, these experiments provide a holistic understanding of the functional advantages and limitations of each model, demonstrating how architectural choices, input segmentation, and class

ISSN 2076-2429 (print)
ISSN 2223-3814 (online)

balancing influence classification performance, robustness to noisy or variable signals, and computational efficiency.

5. Research Results

The evaluation of the baseline MLP and its KAN-augmented variants was performed using three primary metrics: overall classification accuracy, *F*1-score for class *V* (ventricular ectopic beats), and training time. Given that class *V* occurs far less frequently than class *N* (normal rhythm), the *F*1-score serves as a critical measure of the model's ability to correctly identify rare pathological segments. Training time provides insight into computational efficiency and highlights the trade-off between learning speed and classification performance, which is especially important in real-time clinical scenarios.

All models were trained on normalized ECG segments of 200 samples each, scaled to the [0,1] range. Normalization ensures uniform signal amplitude across different patients and segments, promoting stable training and consistent feature representation. To mitigate class imbalance, additional class V segments from multiple records in the MIT-BIH dataset were included, ensuring a representative number of examples for both classes and reducing overfitting toward the dominant class *N*. Specifically, the training set contained approximately 90% class *N* and 10% class *V* segments, reflecting the natural prevalence of these rhythms while providing sufficient samples for robust learning of rare events.

Test results, summarized in Table 1, show the performance of the baseline MLP, the MLP-KAN models with RBF layers, and the MLP-KAN-WT variants using wavelet preprocessing. The data indicate that the integration of a KAN layer and wavelet transforms improves both overall classification accuracy and the *F*1-score for the underrepresented class *V* compared to the standard MLP. This confirms the advantages of combining local nonlinear modeling with multiscale time-frequency feature extraction.

The baseline MLP achieved an overall accuracy of 0.9993, but its ability to detect rare class V segments was limited, as reflected by an *F*1-score of 0.9951. The addition of the KAN layer with 8 RBF units (MLP-KAN-RBF8) increased the *F*1-score to 0.9976, at the expense of higher training time (61.07 s). The MLP-KAN-WT model with Haar wavelet preprocessing (level 1) achieved a comparable *F*1-score of 0.9976 while maintaining lower computational cost (41.46 s), demonstrating that wavelet preprocessing efficiently enhances detection of rare pathological events without compromising performance for the main class *N*:

$$\text{F1-score} = 2 \cdot \frac{\text{Precision} \cdot \text{Recall}}{\text{Precision} + \text{Recall}},$$

$$\text{Precision} = \frac{\text{TP}}{\text{TP} + \text{FP}}, \text{Recall} = \frac{\text{TP}}{\text{TP} + \text{FN}},$$

where: TP, FP, and FN represent true positives, false positives, and false negatives for class *V*, respectively.

Table 1

Comparative Results

Model	Accuracy	*F*1_*V*	Precision_*V*	Recall_*V*	Time_s
MLP	0.999324	0.995146	0.990338	1.000000	32.36
MLP-KAN-RBF4	0.999324	0.995146	0.990338	1.000000	46.12
MLP-KAN-RBF6	0.999324	0.995122	0.995122	0.995122	66.43
MLP-KAN-RBF8	0.999662	0.997555	1.000000	0.995122	61.07
MLP-KAN-WT-haar_1	0.999662	0.997555	1.000000	0.995122	41.46
MLP-KAN-WT-db4_4	0.998648	0.990243	0.990243	0.990243	43.24
MLP-KAN-WT-sym_4	0.998648	0.990243	0.990243	0.990243	52.01
MLP-KAN-WT-coif_5	0.998648	0.990148	0.990148	0.990148	51.64

Training dynamics were assessed through learning curves for each model, showing both accuracy and loss over epochs (Figure 8). These curves confirm that the baseline MLP quickly reaches high accuracy but exhibits fluctuations late in training, indicating some instability in detecting class *V*. In contrast, the modified architectures with KAN and wavelet preprocessing exhibit smoother, more stable learning, maintaining peak accuracy around 0.9997:

$$\text{Accuracy} = \frac{\text{TP} + \text{TN}}{\text{TP} + \text{TN} + \text{FP} + \text{FN}}.$$

Confusion matrices further illustrate model performance. For the MLP-KAN-RBF8 model (Figure 9), class *N* achieved 2,743 correct predictions with 10 misclassified as class V, while class *V* had 189 correct predictions with 16 misclassified as class *N*. For the MLP-KAN-WT with Haar wavelet preprocessing (Figure 10), class *N* had 2.754 correct predictions with zero misclassifications, and class *V* had 204 correct predictions with only 7 misclassifications. These results highlight the improved sensitivity and stability provided by wavelet preprocessing combined with the KAN layer.

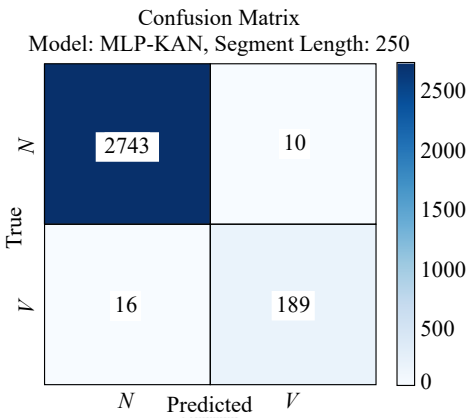

Fig. 8. Confusion Matrix: MLP-KAN- RBF8

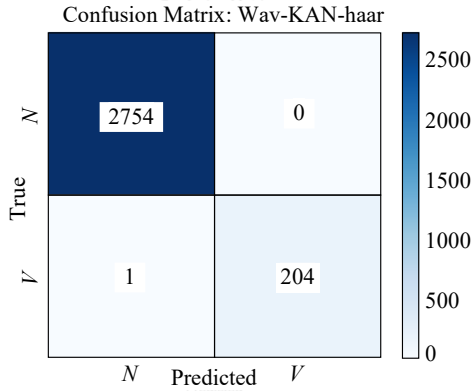

Fig. 9. Confusion Matrix: MLP -KAN-WT-haar_1

6. Conclusions

The experiments demonstrated that integrating the KAN layer into the baseline MLP architecture significantly improves ECG segment classification accuracy. The baseline MLP achieved an accuracy of 0.9993, whereas the modified MLP-KAN-RBF8 reached 0.9997, with the *F*1-score for the rare class V increasing from 0.9951 to 0.9976.

The model with Haar wavelet preprocessing– MLP-KAN-WT (Haar wavelet, level 1) – achieved comparable results: accuracy of 0.9997 and *F*1-score for class *V* of 0.9976, with relatively lower computational costs. This indicates that wavelet preprocessing maintains high model performance while reducing training time.

MLP-KAN exhibited higher training stability and better robustness to segment variations. Validation accuracy for the modified models remained at 0.9997, whereas the baseline MLP showed larger fluctuations in later epochs. Increasing the number of RBFs from 4 to 8 improved classification accuracy for class *V* by approximately 0.2…0.3 %, although training time increased by 32…35 s. Wavelet preprocessing ensures an optimal balance between high accuracy and computational efficiency.

Analysis of confusion matrices confirmed that MLP-KAN substantially reduces misclassifications of class V segments compared to the baseline MLP while maintaining high accuracy for class *N*. Overall results indicate model stability and effective capture of local nonlinearities in the signal, enhancing generalization on test data.

These findings support the use of the KAN layer for automated ECG classification tasks, providing a balance between accuracy, *F*1-score, and computational cost, making this approach promising for practical medical applications. Using wavelet preprocessing, as in the MLP-KAN-WT model with Haar wavelet (level 1), achieves high performance at an optimal computational complexity.

Thus, combining wavelet preprocessing with the KAN layer offers the best compromise between classification accuracy, sensitivity to rare segments, and computational efficiency, making this approach particularly suitable for practical automated ECG analysis.

Література

1. Hemanth D. J., Gupta D., Balas V. E. Intelligent Data Analysis for Biomedical Applications. Academic Press, 2019. 420 p. DOI: https://doi.org/10.1016/C2017-0-03676-5.
2. Deep learning-based ECG arrhythmia classification: A systematic review / Q. Xiao et al. *Applied Sciences*. 2023. Vol. 13, Issue 8. Art. 4964. DOI: https://doi.org/10.3390/app13084964.

3. The applications of deep learning in ECG classification for disease diagnosis: A systematic review and meta-data analysis / M. Khalid et al. *Engineering Journal*. 2024. Vol. 28, Issue 8. P. 45–77. DOI: https://doi.org/10.4186/ej.2024.28.8.45.
4. MLP-K AN: implementation of the Kolmogorov-Arnold layer in a multilayer perceptron / O. Galchonkov et al. *Eastern-European Journal of Enterprise Technologies*. 2025. Vol. 3/4 (135). P. 34–41. DOI: https://doi.org/10.15587/1729-4061.2025.328928.
5. Ahmed A. F., Al-Obaidi M. K. A review of ECG signal filtering approaches. *Global Journal of Engineering and Technology Advances*. 2022. Vol. 11, Issue 3. P. 093–097. DOI: https://doi.org/10.30574/gjeta.2022.11.3.0099.
6. Sharma N., Sidhu J. S. Removal of noise from ECG signal using adaptive filtering. *Indian Journal of Science and Technology*. 2016. Vol. 9 (48). DOI: https://doi.org/10.17485/ijst/2016/v9i48/106424.
7. Shcherbakova G., Koshutina D. Development of a criterion for selecting the level of wavelet decomposition for QRS detection in electrocardiogram signals using energy and entropy. *Proceedings of Odessa Polytechnic University*. 2025. Issue 1 (71). P. 157–166. DOI: https://doi.org/10.15276/opu.1.71.2025.18.
8. Pan J., Tompkins W. J. A Real-Time QRS Detection Algorithm. *IEEE Transactions on Biomedical Engineering*. 1985. Vol. BME-32, Issue 3. P. 230–236. DOI: 10.1109/TBME.1985.325532.
9. MIT-BIH Arrhythmia Database / PhysioNet. URL: https://www.physionet.org/content/mitdb/1.0.0/ (дата звернення: 16.11.2025).
10. Sörnmo L., Laguna P. Electrocardiogram Signal Processing. Wiley, 2005. 680 p.
11. He H., Tan Y., Wang Y. Optimal base wavelet selection for ECG noise reduction using a comprehensive entropy criterion. *Entropy*. 2015. Vol. 17, Issue 9. P. 6093–6109. DOI: https://doi.org/10.3390/e17096093.
12. Agrawal P., Arun V., Basu A. Artificial Neural Network Based ECG Feature Extraction Using Wavelet Transform. *Emerging Wireless Technologies and Sciences. ICEWTS 2024*. Cham: Springer, 2025. P. 8–22. (CCIS; vol. 2399). DOI: https://doi.org/10.1007/978-3-031-87886-2_2.
13. Scalable clustering of complex ECG health data: Big data clustering analysis with UMAP and HDBSCAN / V. Kaverinskiy et al. *Computation*. 2025. Vol. 13, Issue 6. Art. 144. DOI: https://doi.org/10.3390/computation13060144.
14. Adaptive clustering for distribution parameter estimation in technical diagnostics / G. Shcherbakova et al. *12th International Conference on Applied Innovations in IT (ICAIIT)*, Köthen, Germany, 2024. DOI: https://doi.org/10.25673/115650.
15. ECG analysis using consensus clustering / A. Lourenço et al. *2014 22nd European Signal Processing Conference (EUSIPCO)*, Lisbon, Portugal, 2014. P. 511–515.
16. Evaluating binary classifiers for cardiovascular disease prediction: Enhancing early diagnostic capabilities / P. Iacobescu et al. *Journal of Cardiovascular Development and Disease (JCDD)*. 2024. Vol. 11, Issue 12. Art. 396. DOI: https://doi.org/10.3390/jcdd11120396.
17. Guo C., Ahmed S., Alouini M.-S. Machine learning-based automatic cardiovascular disease diagnosis using two ECG leads. 2023. DOI: https://doi.org/10.48550/arXiv.2305.16055.
18. Wu Z., Guo C. Deep learning and electrocardiography: Systematic review of current techniques in cardiovascular disease diagnosis and management. *BioMed Eng OnLine*. 2025. Vol. 24. Art. 23. DOI: https://doi.org/10.1186/s12938-025-01349-w.
19. Savalia S., Emamian V. Cardiac arrhythmia classification by multi-layer perceptron and convolution neural networks. *Bioengineering*. 2018. Vol. 5, Issue 2. Art. 35. DOI: https://doi.org/10.3390/bioengineering5020035.
20. Li Z. Kolmogorov-Arnold networks are radial basis function networks. 2024. arXiv:2405.06721. URL: https://arxiv.org/abs/2405.06721.
21. Classification of arrhythmia based on convolutional neural networks and encoder-decoder model / J. Liu et al. *Computer Systems Science and Engineering*. 2022. DOI: https://doi.org/10.32604/cmc.2022.029227.
22. Mavaddati S. ECG arrhythmias classification based on deep learning methods and transfer learning technique. *Biomedical Signal Processing and Control*. 2024. DOI: https://doi.org/10.1016/j.bspc.2024.107236.
23. Multi-layer perceptron-based data-driven multiscale modelling of granular materials with a novel Frobenius norm-based internal variable / M. Wang et al. *Journal of Rock Mechanics and Geotechnical Engineering*. 2024. DOI: https://doi.org/10.1016/j.jrmge.2024.02.003.
24. Hadj Kilani B. Kolmogorov-Arnold networks: Key developments and uses. 2024. DOI: https://doi.org/10.32388/7NNCAA.
25. Yu R., Yu W., Wang X. KAN or MLP: A fairer comparison. 2024. DOI: https://doi.org/10.48550/arXiv.2407.16674.

26. KAN: Kolmogorov-Arnold Networks / Z. Liu et al. 2024. arXiv:2404.19656. URL: https://arxiv.org/abs/2404.19756.
27. Ismayilova A., Ismayilov M. On the universal approximation property of radial basis function neural networks. 2023. arXiv:2304.02220. URL: https://arxiv.org/abs/2304.02220.
28. Ta T. H. BSRBF-KAN: A combination of B-splines and radial basis functions in Kolmogorov-Arnold networks. 2024. DOI: https://doi.org/10.13140/RG.2.2.16755.54562.
29. Hollósi J. Efficiency analysis of Kolmogorov–Arnold networks for visual data processing. *SMTS 2024 Conference Proceedings*. 2024. DOI: https://doi.org/10.3390/engproc2024079068.
30. Seghouane A.-K., Shokouhi N. Adaptive learning for robust radial basis function networks. *IEEE Transactions on Cybernetics*. 2021. Vol. 51, Issue 5. P. 2847–2856. DOI: https://doi.org/10.1109/TCYB.2019.2951811.
31. Panda S., Panda G. On the development and performance evaluation of improved radial basis function neural networks. *IEEE Transactions on Systems, Man, and Cybernetics: Systems*. 2022. Vol. 52, Issue 6. P. 3873–3884. DOI: https://doi.org/10.1109/TSMC.2021.3076747.
32. Bozorgasl Z., Chen H. Wav-KAN: Wavelet Kolmogorov-Arnold networks. 2024. arXiv:2405.12832. URL: https://arxiv.org/abs/2405.12832.
33. Koshutina D. V., Shcherbakova H. Yu. Automated selection of wavelet decomposition level based on energy and entropy for QRS complex detection in ECG. *Modern Information Technologies – 2025: proc. 15th Int. Sci. Conf. for Students and Young Scientists*, Odesa, Ukraine, May 15–16, 2025. Odesa: Nauka i Tekhnika, 2025. P. 21–23. DOI: https://doi.org/10.5281/zenodo.15521809.

References

1. Hemanth, D. J., Gupta, D., & Balas, V. E. (2019). *Intelligent data analysis for biomedical applications*. Academic Press. DOI: https://doi.org/10.1016/C2017-0-03676-5.
2. Xiao, Q., Lee, K., Mokhtar, S. A., Ismail, I., Md Pauzi, A. L., Zhang, Q., & Lim, P. Y. (2023). Deep learning-based ECG arrhythmia classification: A systematic review. *Applied Sciences, 13*(8), Article 4964. DOI: https://doi.org/10.3390/app13084964.
3. Khalid, M., Pluempitiwiriyawej, C., Wangsiripitak, S., & Abdulkadhem, A. A. (2024). The applications of deep learning in ECG classification for disease diagnosis: A systematic review and meta-data analysis. *Engineering Journal, 28*(8), 45–77. DOI: https://doi.org/10.4186/ej.2024.28.8.45.
4. Galchonkov, O., Baranov, O., Maslov, O., Babych, M., & Baskov, I. (2025). MLP-K AN: Implementation of the Kolmogorov-Arnold layer in a multilayer perceptron. *Eastern-European Journal of Enterprise Technologies, 3/4*(135), 34–41. DOI: https://doi.org/10.15587/1729-4061.2025.328928.
5. Ahmed, A. F., & Al-Obaidi, M. K. (2022). A review of ECG signal filtering approaches. *Global Journal of Engineering and Technology Advances, 11*(3), 093–097. DOI: https://doi.org/10.30574/gjeta.2022.11.3.0099.
6. Sharma, N., & Sidhu, J. S. (2016). Removal of noise from ECG signal using adaptive filtering. *Indian Journal of Science and Technology, 9*(48). DOI: https://doi.org/10.17485/ijst/2016/v9i48/106424.
7. Shcherbakova, G., & Koshutina, D. (2025). Development of a criterion for selecting the level of wavelet decomposition for QRS detection in electrocardiogram signals using energy and entropy. *Proceedings of Odessa Polytechnic University, 1*(71), 157–166. DOI: https://doi.org/10.15276/opu.1.71.2025.18.
8. Pan, J., & Tompkins, W. J. (1985). A real-time QRS detection algorithm. *IEEE Transactions on Biomedical Engineering, BME-32*(3), 230–236. DOI: 10.1109/TBME.1985.325532.
9. PhysioNet. (n.d.). *MIT-BIH Arrhythmia Database*. Retrieved from https://www.physionet.org/content/mitdb/1.0.0.
10. Sörnmo, L., & Laguna, P. (2005). *Electrocardiogram signal processing*. Wiley.
11. He, H., Tan, Y., & Wang, Y. (2015). Optimal base wavelet selection for ECG noise reduction using a comprehensive entropy criterion. *Entropy, 17*(9), 6093–6109. DOI: https://doi.org/10.3390/e17096093.
12. Agrawal, P., Arun, V., & Basu, A. (2025). Artificial neural network based ECG feature extraction using wavelet transform. In *Emerging Wireless Technologies and Sciences. ICEWTS 2024* (CCIS, Vol. 2399, pp. 8–22). Springer, Cham. DOI: https://doi.org/10.1007/978-3-031-87886-2_2.
13. Kaverinskiy, V., Chaikovsky, I., Mnevets, A., & Malakhov, K. S. (2025). Scalable clustering of complex ECG health data: Big data clustering analysis with UMAP and HDBSCAN. *Computation, 13*(6), Article 144. DOI: https://doi.org/10.3390/computation13060144.
14. Shcherbakova, G., Antoshchuk, S., Koshutina, D., & Sakhno, K. (2024). Adaptive clustering for distribution parameter estimation in technical diagnostics. *12th International Conference on Applied Innovations in IT (ICAIIT)*, Köthen, Germany. DOI: https://doi.org/10.25673/115650.

ISSN 2076-2429 (print)
ISSN 2223-3814 (online)

15. Lourenço, A., Carreiras, C., Bulò, S. R., & Fred, A. (2014, August 25–29). *ECG analysis using consensus clustering* [Paper presentation]. 2014 22nd European Signal Processing Conference (EUSIPCO), Lisbon, Portugal.
16. Iacobescu, P., Marina, V., Anghel, C., & Anghele, A. (2024). Evaluating binary classifiers for cardiovascular disease prediction: Enhancing early diagnostic capabilities. *Journal of Cardiovascular Development and Disease (JCDD), 11*(12), Article 396. DOI: https://doi.org/10.3390/jcdd11120396.
17. Guo, C., Ahmed, S., & Alouini, M.-S. (2023). *Machine learning-based automatic cardiovascular disease diagnosis using two ECG leads*. arXiv. DOI: https://doi.org/10.48550/arXiv.2305.16055.
18. Wu, Z., & Guo, C. (2025). Deep learning and electrocardiography: Systematic review of current techniques in cardiovascular disease diagnosis and management. *BioMed Eng OnLine, 24*, Article 23. DOI: https://doi.org/10.1186/s12938-025-01349-w.
19. Savalia, S., & Emamian, V. (2018). Cardiac arrhythmia classification by multi-layer perceptron and convolution neural networks. *Bioengineering, 5*(2), Article 35. DOI: https://doi.org/10.3390/bioengineering5020035.
20. Li, Z. (2024). *Kolmogorov-Arnold networks are radial basis function networks*. arXiv. Retrieved from https://arxiv.org/abs/2405.06721.
21. Liu, J., Xia, X., Han, C., Hui, J., & Feng, J. (2022). Classification of arrhythmia based on convolutional neural networks and encoder-decoder model. *Computer Systems Science and Engineering*. DOI: https://doi.org/10.32604/cmc.2022.029227.
22. Mavaddati, S. (2024). ECG arrhythmias classification based on deep learning methods and transfer learning technique. *Biomedical Signal Processing and Control*. DOI: https://doi.org/10.1016/j.bspc.2024.107236.
23. Wang, M., Feng, Y. T., Guan, S., & Qu, T. (2024). Multi-layer perceptron-based data-driven multiscale modelling of granular materials with a novel Frobenius norm-based internal variable. *Journal of Rock Mechanics and Geotechnical Engineering*. DOI: https://doi.org/10.1016/j.jrmge.2024.02.003.
24. Hadj Kilani, B. (2024). *Kolmogorov-Arnold networks: Key developments and uses*. Qeios. DOI: https://doi.org/10.32388/7NNCAA.
25. Yu, R., Yu, W., & Wang, X. (2024). *KAN or MLP: A fairer comparison*. arXiv. DOI: https://doi.org/10.48550/arXiv.2407.16674.
26. Liu, Z., Wang, Y., Vaidya, S., Ruehle, F., Halverson, J., Soljačić, M., Hou, T. Y., & Tegmark, M. (2024). *KAN: Kolmogorov–Arnold Networks*. arXiv. Retrieved from https://arxiv.org/abs/2404.19756.
27. Ismayilova, A., & Ismayilov, M. (2023). *On the universal approximation property of radial basis function neural networks*. arXiv. Retrieved from https://arxiv.org/abs/2304.02220.
28. Ta, T. H. (2024). *BSRBF-KAN: A combination of B-splines and radial basis functions in Kolmogorov-Arnold networks*. ResearchGate. DOI: https://doi.org/10.13140/RG.2.2.16755.54562.
29. Hollósi, J. (2024). Efficiency analysis of Kolmogorov–Arnold networks for visual data processing. *SMTS 2024 Conference Proceedings*. DOI: https://doi.org/10.3390/engproc2024079068.
30. Seghouane, A.-K., & Shokouhi, N. (2021). Adaptive learning for robust radial basis function networks. *IEEE Transactions on Cybernetics, 51*(5), 2847–2856. DOI: https://doi.org/10.1109/TCYB.2019.2951811.
31. Panda, S., & Panda, G. (2022). On the development and performance evaluation of improved radial basis function neural networks. *IEEE Transactions on Systems, Man, and Cybernetics: Systems, 52*(6), 3873–3884. DOI: https://doi.org/10.1109/TSMC.2021.3076747.
32. Bozorgasl, Z., & Chen, H. (2024). *Wav-KAN: Wavelet Kolmogorov-Arnold networks*. arXiv. Retrieved from https://arxiv.org/abs/2405.12832.
33. Koshutina, D. V., & Shcherbakova, H. Y. (2025, May 15–16). *Automated selection of wavelet decomposition level based on energy and entropy for QRS complex detection in ECG* [Paper presentation]. 15th International Scientific Conference for Students and Young Scientists "Modern Information Technologies – 2025", Odesa, Ukraine. DOI: https://doi.org/10.5281/zenodo.15521809.

Кошутіна Дар'я Валеріївна; Daria Koshutina ORCID: https://orcid.org/0009-0004-1326-8775

Received November 17, 2025

Accepted December 15, 2025

UDC 004.94

V. Tigariev, PhD, Assoc. Prof.,
O. Lopakov,
V. Kosmachevskiy,
V. Dotsenko, PhD, Assoc. Prof.
Odessa Polytechnic National University, Shevchenko Ave. 1, Odesa, Ukraine, 65044, e-mail: volodymyr_t@ukr.net

USING COMPUTER-AIDED DESIGN AND TECHNOLOGY TO AUTOMATE THE CREATION OF DRAWINGS FROM 3D MODELS

В. Тігарєв, О. Лопаков, В. Космачевський, В. Доценко. **Використання комп'ютерного проектування виробів та технологій при автоматизованому формуванні креслеників з 3d моделей.** Впровадження використання комп'ютерного проектування виробів та технологій для автоматизації створення креслеників полягає в тому, щоб заощадити час і надати інженерам і дизайнерам можливість зосередитися на завданнях високої цінності. Автоматизуючи створення креслень, Fusion звільняє команди дизайнерів, щоб вони могли витрачати більше часу на інновації та вирішення проблем, а не на повторювані завдання. Автоматизація комп'ютерного проектування виробів та технологій на основі штучного інтелекту дозволяє їм задовольняти ці вимоги без шкоди для якості. Можливість швидко створювати 2D-креслення також допомагає забезпечити точне донесення задуму про проект до виробничих команд. Це зменшує потенційні затримки та непорозуміння під час виробництва. Ключовою перевагою можливостей штучного інтелекту Autodesk Fusion є її безперешкодна інтеграція з хмарним середовищем платформи. Fusion служить центральним центром для даних, дозволяючи командам дизайнерів і виробничих компаній працювати з найактуальнішою інформацією. Це надзвичайно важливо в той час, коли дані є одним з найцінніших ресурсів у галузі. Для більш досконалого розуміння процесу та технології автоматизованого формування креслеників нами запропоновано блок схему автоматизованого формування креслеників у Fusion. Блок схема автоматизованого формування креслеників у Fusion складається із трьох основних частин: формування креслеників окремих деталей, формування креслеників складань, створення шаблонів. Кожна частина блок схеми складається з окремих елементів, які пояснюють сутність кожного з блоків. Наведені приклади використання блок схеми для автоматизованого формування як окремих креслеників різного типу так і креслеників складального вузлу повністю.

Ключові слова: комп'ютерне проектування виробів та технологій, автоматизація формування креслеників, штучний інтелект, Autodesk Inventor, Fusion

V. Tigariev, O. Lopakov, V. Kosmachevskiy, V. Dotsenko. **Using computer-aided design and technology to automate the creation of drawings from 3D models.** The adoption of computer-aided design and technology to automate the creation of drawings is to save time and allow engineers and designers to focus on high-value tasks. By automating the creation of drawings, Fusion frees design teams to spend more time innovating and solving problems, rather than on repetitive tasks. AI-based computer-aided design and technology automation allows them to meet these demands without compromising quality. The ability to quickly create 2D drawings also helps ensure that the design vision is accurately communicated to production teams. This reduces potential delays and misunderstandings during production. A key advantage of Autodesk Fusion's AI capabilities is its seamless integration with the platform's cloud environment. Fusion serves as a central hub for data, allowing design teams and manufacturing companies to work with the most up-to-date information. This is extremely important at a time when data is one of the most valuable resources in the industry. For a better understanding of the process and technology of automated drawing generation, we have proposed a block diagram of automated drawing generation in Fusion. The block diagram of automated drawing generation in Fusion consists of three main parts: drawing generation of individual parts, drawing generation of assemblies, and template creation. Each part of the block diagram consists of separate elements that explain the essence of each of the blocks. Examples of using the block diagram for automated generation of both individual drawings of various types and drawings of the assembly unit as a whole are given.

Keywords: computer-aided design of products and technologies, automation of drawing generation, artificial intelligence, Autodesk Inventor, Fusion

Introduction

In today's fast-paced world of engineering and design, efficiency is everything. Computer-aided design (CAD) tools have evolved rapidly, and with them comes a powerful revolutionary tool: CAD automation. Whether you are an architect, mechanical engineer, or product designer, CAD automation can significantly reduce manual tasks, increase accuracy, and optimize your entire workflow. Currently, the industry is undergoing a process of active integration of automated solutions for creating technical documentation, in particular drawings, based on three-dimensional models. Such tasks are driven by the ever-increasing demands for speed of project execution, high accuracy of technical information, and the need to minimize human error. CAD automation involves the use of scripts, macros, or software tools that automatically generate or modify CAD drawings and models. Instead of manually

DOI: 10.15276/opu.2.72.2025.18

ISSN 2076-2429 (print)
ISSN 2223-3814 (online)

drawing each line, curve, or component, CAD automation allows repetitive or complex tasks to be performed with minimal human intervention. The development of computer-aided design tools and technologies has greatly simplified and accelerated the design process. Automation can include anything from automatically updating part numbers on a drawing to creating complete assemblies based on predefined parameters. This not only saves time but also increases accuracy. However, there are serious challenges associated with adapting software to work with complex geometric shapes and ensuring flexible configuration of drawings in accordance with various standards and requirements of a specific project.

The problem lies in the need to develop a clear understanding among specialists of the functionality of automated drawing generation tools for optimal and well-informed selection and use in work on projects of various types.

Analysis of recent studies and publications

The topic of automating the creation of drawings from three-dimensional models is relevant both in industry and in scientific research. Recent publications in this field focus on improving algorithms for processing geometric shapes, optimizing design processes, and integrating artificial intelligence to solve complex technical problems.

The study [1,2] examines the features of solid modeling and the creation of technical drawings in the Autodesk AutoCAD and Autodesk Inventor software environments. A comparative analysis of the processes of modeling and drawing design is provided, emphasizing the advantages of Inventor in creating volumetric models with threaded connections, automating the construction of drawings, and applying dimensions in accordance with standards. Autodesk Inventor provides a higher level of automation and convenience when working with complex models. Work [3] investigates the effectiveness of modern software for automating the creation of drawings from three-dimensional models, which is a relevant task for the engineering and architectural industries. The main focus is on analyzing the capabilities of AutoCAD, SolidWorks, and Fusion. The work [4, 5] considers the issues of expanding the capabilities of computer modeling and adapting the tools of the corresponding software packages for the development of design documentation in accordance with standards, in particular, in the Autodesk Inventor package environment. In the work [6, 7, 8], one of the most important results is the creation of 2D drawings. It can be sent and distributed using various output options, such as printed and digital formats (DWG, PDF, DWF, etc.). Creating a 2D drawing in the Autodesk Inventor environment can be done manually by the user, programmatically using codes, or using a combination of manual data entry and automation. The latter option is very common, where codes perform some repetitive tasks and the user completes what is missing in the drawing. Source [9] is dedicated to the Autodesk Inventor ADC software application. ADC (Automatic Drafting Constructor) introduces innovative concepts to the drafting process, extending the capabilities of Inventor and enabling creators to reach new heights. When ADC is used with an assembly node, it is possible to choose to create drawings for all assembly levels. This means that it is possible to include every document in the assembly, only the first level of the assembly, or only the current assembly document. ADC understands the specification, guiding the creation of the necessary drawings and providing the freedom to adjust settings according to the task. Work [10] discusses the creation of technical drawings. Autodesk Fusion revolutionizes the creation of drawings with automated dimensioning, view generation, and artificial intelligence features that optimize the process, reduce errors, and improve collaboration between teams.

Source [11] is a Fusion system reference element. Drawing automation is a powerful automated process that quickly generates 2D drawings from your designs in the Fusion Drawing workspace. To get the most out of drawing automation, you need to configure templates. Sources [12 – 15] are dedicated to three AI-based features that have appeared in Autodesk Fusion: Sketch AutoConstrain, Automated Drawings, and Autodesk Assistant. Autodesk Assistant is currently a product support chatbot. Fusion Automated Drawings takes a 3D model and generates 2D drawings of the entire assembly and each of its parts. This core functionality is based on user templates and heuristics, but Autodesk has now included some AI-based features. The tool now includes an artificial intelligence model that scans geometry to classify standard fasteners and exclude them from drawings. Work [16-18] is dedicated to customization features in the Autodesk Fusion automatic drawing template file. The system creates drawings with corresponding views and dimensions based on the 3D model of the project. By default, they will include a drawing sheet with an ISO view and a parts list (if it is an assembly), as well as a

sheet with orthographic views and dimensions. It is also possible to create drawing sheets for each component of the assembly.

Based on the analysis, we conclude that the use of computer-aided design technologies and technologies for automating the process of creating 2D drawings from 3D models is highly relevant and strategically important for the further development of engineering design and related industries.

The purpose of the study

The purpose of this study is to conduct a comparative analysis of the capabilities of AutoCAD, Autodesk Inventor, Fusion software, and algorithms used in the automation of flat drawing creation based on three-dimensional models. The study aims to determine their level of efficiency based on key parameters such as processing speed, adaptation to complex shapes, and flexibility in drawing configuration. The results obtained will allow us to form a block diagram of automated drawing generation in Fusion for performing various types of tasks depending on the requirements for geometric complexity, accuracy, and ease of adaptation of technical documentation.

Materials and methods of the research

Modern computer-aided design of products and technologies in industry is increasingly focused on automating the process of creating drawings of various objects. These objects can be both engineering structures and architectural units. The need for faster project execution, minimization of the human factor, and increased efficiency in working with large volumes of technical information are among the priority requirements of industry. Nowadays, engineers, designers, and architects first develop a three-dimensional model of an object and then use it as a basis for developing technical documentation, including the corresponding drawings. This has become possible with the development of computer modeling tools.

The process of converting three-dimensional models into flat drawings depends not only on the features of the software itself, but also on the algorithms implemented in these systems. Our study evaluates the capabilities of AutoCAD, Autodesk Inventor, Fusion, and algorithms for performing such tasks.

AutoCAD uses basic algorithms for converting three-dimensional objects into two-dimensional projections based on the principles of projection geometry. These algorithms enable the rapid creation of drawings with clear lines and simple geometric shapes. This tool is best used for creating drawings of a single part, but AutoCAD's functionality is not sufficiently developed for converting assembly units. Limitations in working with curved surfaces or complex polygonal objects significantly narrow the scope of AutoCAD's application in tasks where detailed complex shapes are required.

Autodesk Inventor uses more advanced algorithms for generating projections, including spline interpolation algorithms, which allow for accurate representation of curved elements and roundings. In addition, the system integrates methods for automatically creating cross-sections and displaying the internal geometry of the model, which significantly increases the accuracy and detail of flat drawings. Thanks to its support for parametric models, Autodesk Inventor adapts to changes in a three-dimensional object, automatically updating the corresponding drawings.

Fusion combines the advantages of projection geometry algorithms and cloud computing. Using computer graphics methods to create two-dimensional views, Fusion can quickly process even complex models. The system's algorithms are optimized for working with curved and organic shapes, making Fusion a versatile tool for a variety of tasks. Autodesk Fusion's AI-powered automated drafting feature automates what used to be a tedious and time-consuming part of the design process. After analyzing a 3D model, the AI system automatically generates the necessary 2D views, dimensions, and other details required to manufacture the part. This speeds up the workflow and reduces the likelihood of errors that often occur due to manual input. AI doesn't just generate drawings; it intelligently decides which details are necessary and which can be omitted. It can identify fasteners or other components that do not need to be included in the final set of drawings. The result is an optimized set of drawings ready for production, without the need for excessive manual editing. The software's ability to work with complex shapes in the context of converting three-dimensional models into flat drawings is determined by its ability to accurately and efficiently process models with complex geometry. Such shapes include objects with complex curved surfaces, multi-layered structures, detailed textures, internal structural elements, and irregular organic contours. Effective software for such tasks uses modern algorithms, such as curve interpolation, surface approximation, or volumetric sectioning. In particular, Autodesk Inventor uses spline algorithms to create accurate projections of curved surfaces, while Fu-

ISSN 2076-2429 (print)
ISSN 2223-3814 (online)

sion provides high-quality processing of organic shapes through the use of powerful computational methods. AutoCAD, on the other hand, has limited capabilities when working with complex shapes, as its functionality is primarily focused on processing basic geometric elements.

Flexibility in drawing customization is defined as the ability of software to provide users with advanced capabilities for adapting two-dimensional graphics to specific project requirements. This includes customizing the appearance, style, and format of drawings in created templates, as well as modifying parameters created automatically based on a three-dimensional model. One important aspect is the ability to change drawing standards, which allows the software to support a variety of technical standards and adapt to the requirements of a specific project. Flexibility also includes control over the level of detail, in particular the adjustment of the visibility of drawing elements such as hidden or axis lines, as well as cross-sections. Another important factor is the support for exporting drawings to various formats, such as DWG, DXF, or PDF, which ensures convenient data transfer for further work. Software solutions such as Autodesk Inventor and Fusion demonstrate high flexibility thanks to the ability to automatically create standard drawings with subsequent manual editing, such as changing the scale, projection location, or adding text notes or specification tables.

However, less flexible systems, such as AutoCAD in its basic configuration, limit the user's capabilities, which often leads to the need to perform a significant amount of manual work to adapt drawings to the requirements of a specific task. As part of research into the use of computer-aided design of products and technologies in automated drawing generation, a block diagram for automated drawing generation in Fusion using AI was developed. The block diagram allows you to analyze the processes of generating drawings of varying complexity and creating templates to accelerate and expand the capabilities of automated drawing generation. The proposed block diagram is shown in Fig. 1.

The block diagram of automated drawing generation in Fusion consists of three main parts:

1. Generation of drawings for individual parts;
2. Creation of templates;
3. Generation of assembly drawings.

Each part of the block diagram consists of separate elements that explain the essence of each block.

Let's look at each part of the block diagram separately.

The creation of drawings for individual parts is discussed in the first part of the block diagram:

a) automatic placement and scaling of views;

b) automatic rotation of components to the best orientation;

c) automatic breaking of long components;

d) application of center lines and marks;

e) automatic scaling of views and placing them on a sheet;

f) moving overlapping dimensions and changing their order;

g) placement of flat sheet metal templates, bend tables, and identifiers.

These features allow you to create drawings of individual parts of various types and levels of complexity.

The creation of assembly drawings is explained in the third part of the block diagram:

a) automatic placement of drawing sheets for each component in the model and scaling of views;

b) shows dimension strategies in a "generative" style. These dimensions are categorized into broad categories: Base Line, Chain, Symmetrical, and Ordinate;

c) generation of parts lists and positions for assemblies;

d) automatic ignoring of components from the skip list;

e) use artificial intelligence to identify fasteners: nuts, bolts, and washers in assemblies and exclude them from the drawing package;

f) components modeled "in place" require named views for easy detailing using traditional workflows;

g) drawing automation allows you to ignore standard fasteners from the Autodesk fastener library and also ignores components in the "Skip" list (based on the component name);

h) uses advanced artificial intelligence to identify nuts, bolts, and washers in assemblies and excludes them from the drawing package;

i) the use of computer-aided product design and technologies in automating the creation of a set of individual drawings and an assembly drawing performs 60…80% of the work on documenting.

The steps required to create and configure a template file are explained in the second part of the flowchart.

A template file with preconfigured drawing standards, basic inscriptions, and basic views saves time on reconfiguration:

a) create multiple templates for different models or production processes.

b) forming placeholder views, browser nodes, and additional sheets.

c) deleting placeholder views, browser nodes, and additional sheets to convert a "Smart Template" to a "Drawing Template."

d) create multiple templates with different omission lists.

e) use the omission list to ignore components that do not need to be detailed.

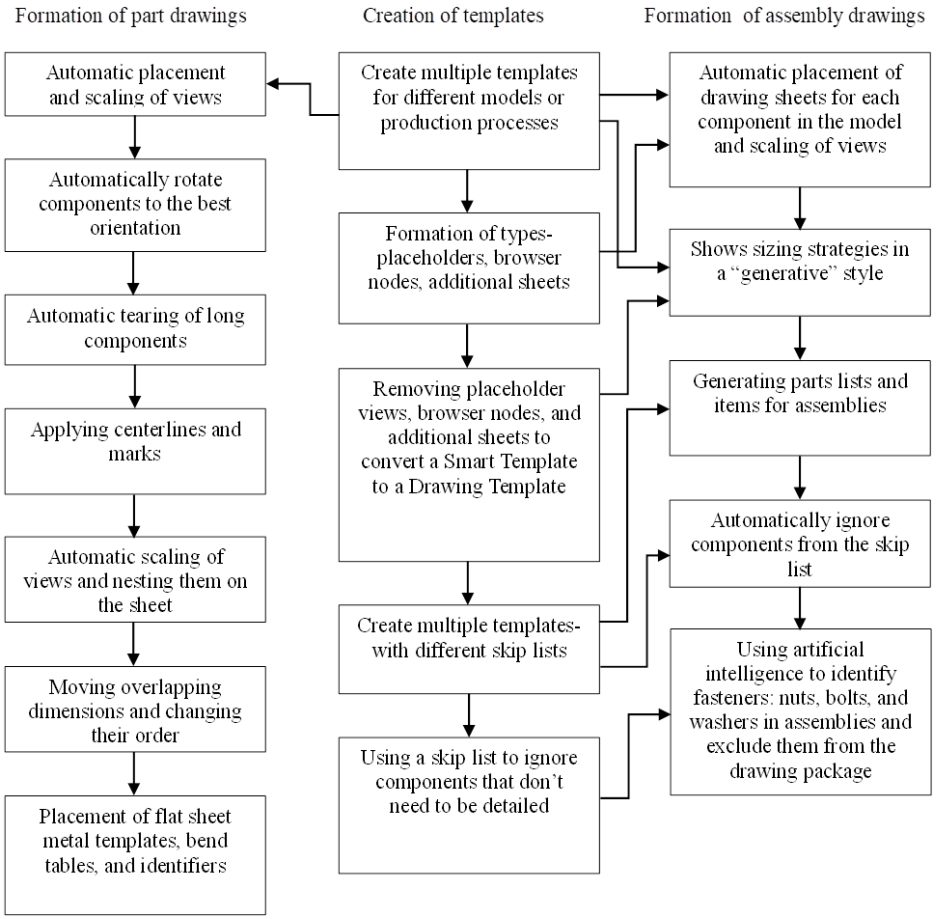

Fig. 1. Block diagram of automated chair formation in Fusion

There are three types of templates: From scratch (Out of the box), Drawing template (user-modified template), Templates based on work processes.

Let's take a look at each type of template.From scratch. Uses Autodesk default settings. Designed to allow you to "try out" the automation of drawing creation. Drawing templates or Smart templates (outdated – not very suitable for automation). Any template with placeholder views, browser node entries (links or part lists), or additional sheets is considered a smart template. Templates that take into account work processes. They take into account the desired work processes when creating templates, drawing templates, and take into account the template document settings.

Practical implementation

Within the scope of the study, we use the proposed block diagram when testing the specified tools for creating a drawing of a separate part and an assembly node in Fusion. In both examples, the capabilities of automation for creating and designing drawings were used.

Let's look at the use of computer-aided design and technologies in the automated creation of a drawing from a 3D model of a plate part. To do this, we use the first part of the block diagram. The drawing will be created in accordance with the ISO standard. We use the standard Fusion configura-

ISSN 2076-2429 (print)
ISSN 2223-3814 (online)

tion template. The three-dimensional model of the Plate part is shown in Fig. 2. It was created in a three-dimensional solid modeling environment. We select to create a drawing in the Settings window and set it to Automatic (Fig. 3).

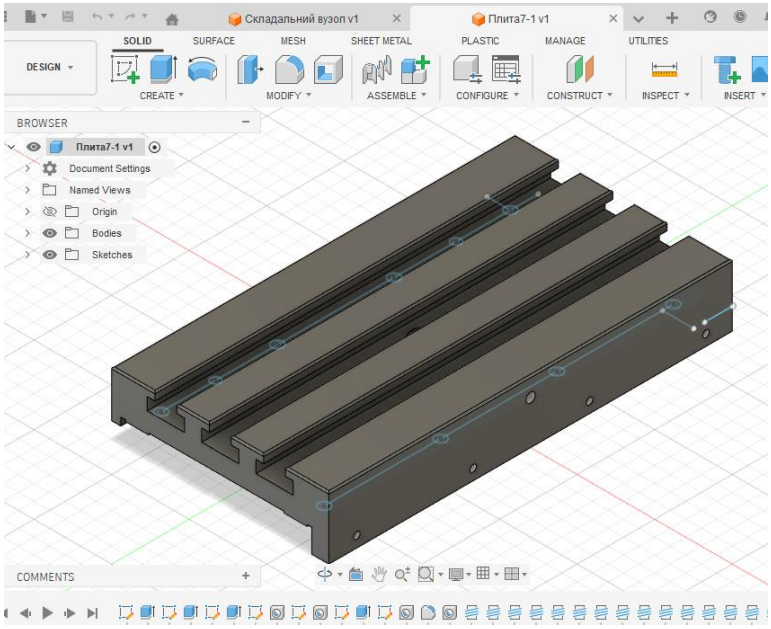

Fig. 2. Three-dimensional model of a part Plate

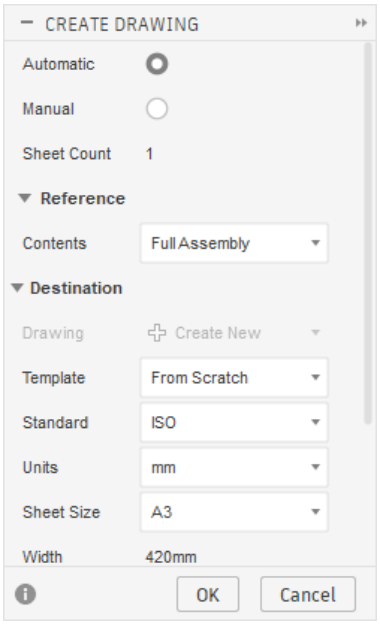

Fig. 3. Setting the parameters

Fusion generates a drawing and offers to select the required type of dimensioning from the table of options. Fig. 4 shows an example of selecting the type of dimensioning on a drawing.

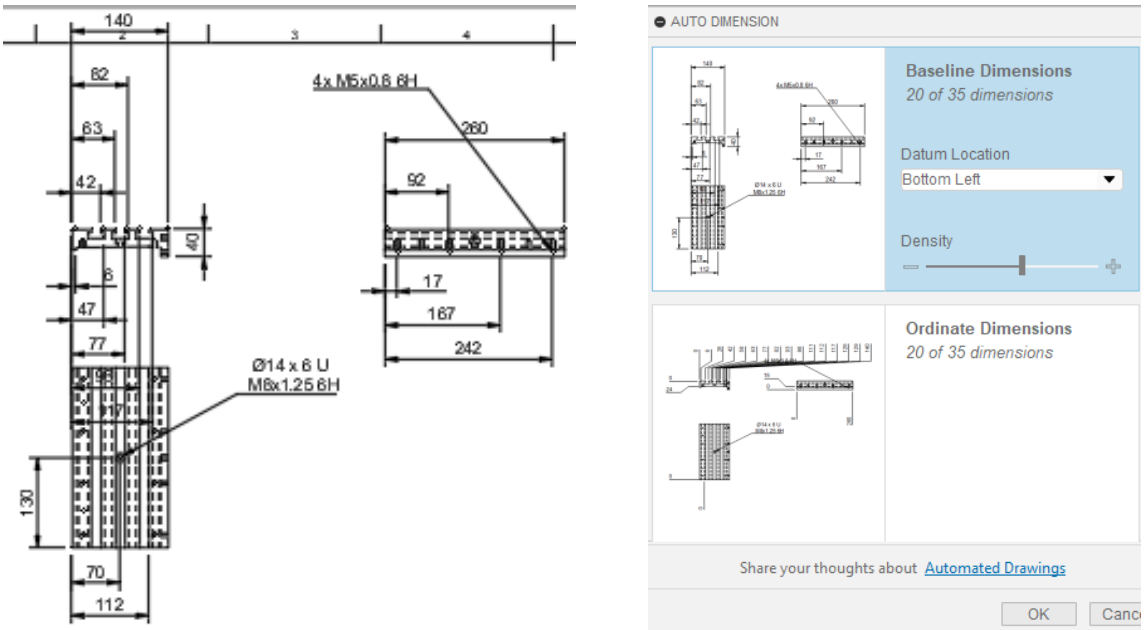

Fig. 4. Selecting the type of dimension formation on the drawing

After selecting the type of dimensions, the final version of the drawing is formed (Fig. 5).

If necessary, you can edit the drawing by adding new types or sections. The automated option for creating drawings significantly speeds up the process and increases the accuracy of document creation.

This procedure can be repeated for other settings and using various templates. If you choose to create the drawing manually, you will need to perform all the actions that the AI performs yourself. Let's consider the option of automated drawing generation from an assembly node based on the third part of the block diagram. When solving this task, it is possible to perform three options for forming

drawings: a drawing of a separate part of your choice, an assembly drawing with specifications, or a complete set of drawings for all assembly parts, except for standard and typical parts specified in separate settings. As an example, let's consider the assembly model of a valve pneumatic device. The assembly model of the valve pneumatic device was created from separate part models in a solid modeling environment. After that, all parts were assembled into a separate assembly node. The solid assembly model of the pneumatic valve device is shown in Fig. 6.

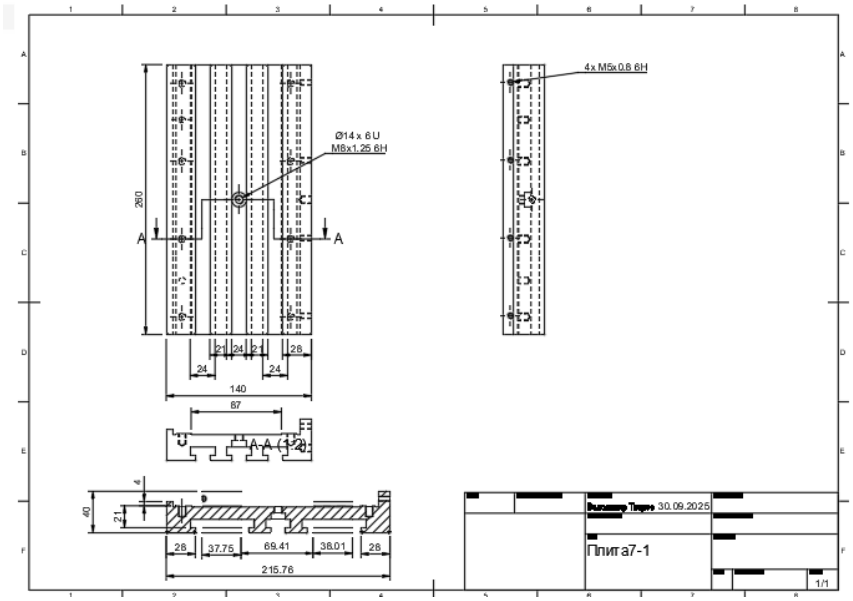

Fig. 5. Drawing of the part Plate

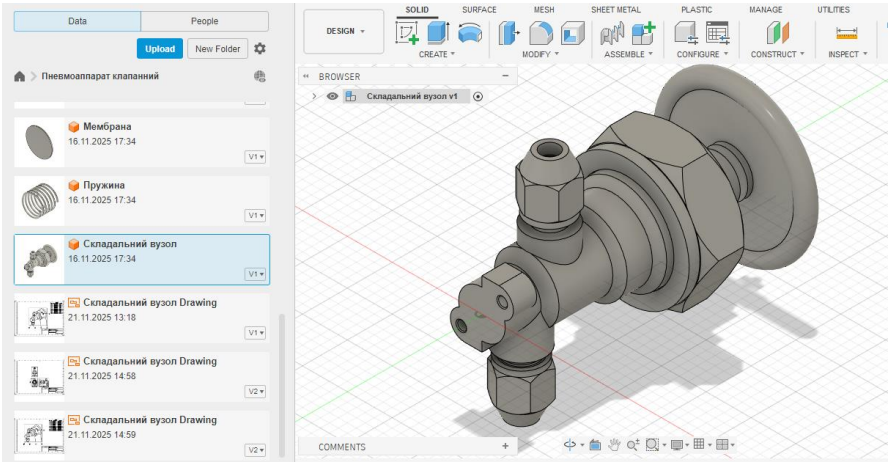

Fig. 6. Solid assembly model of a pneumatic valve device

Fig. 6 shows images of individual parts of the assembly unit in the browser (left side). To select an individual part, select the required part in the graphic area of the assembly tree. It will then be highlighted in a different color, as shown in Fig. 7.

Then repeat the steps as when creating a drawing of a separate part. The drawing of the body part is shown in Fig. 8.

The next task is to create a drawing of the assembly unit from the model. To do this, select the All Assembly and First Level settings, i.e., the entire assembly is shown in Fig. 9. The program generates two drawings: the first is an isometric image with specifications, and the second is a complete drawing of the assembly unit (Fig. 10, Fig. 11). When generating specifications, you need to configure the design template according to the required standard.

ISSN 2076-2429 (print)
ISSN 2223-3814 (online)

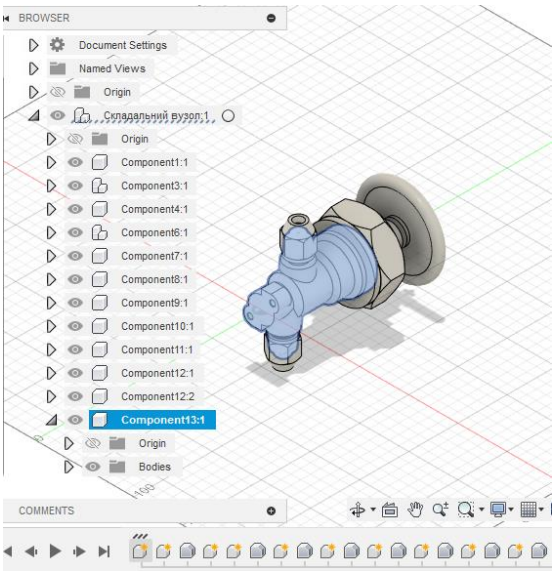

Fig. 7. Highlighting a separate detail in an assembly

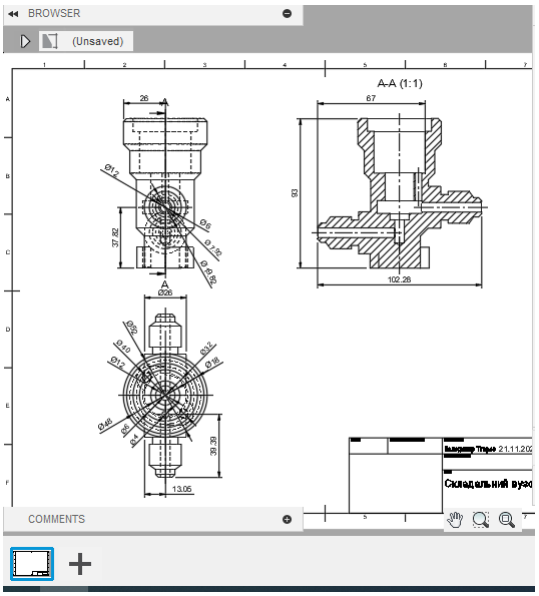

Fig. 8. Detail drawing of the housing

The last option for generating design documentation from an assembly model creates assembly drawings and drawings of all non-standard parts. When configuring the template, you must specify which parts do not need to be drawn; these can be standard parts or typical parts for which drawings already exist. After creating a set of drawings, a row of icons for the created drawings appears at the bottom of the assembly model screen. This allows you to select the desired drawing (Fig. 12) and, if necessary, correct and print it.

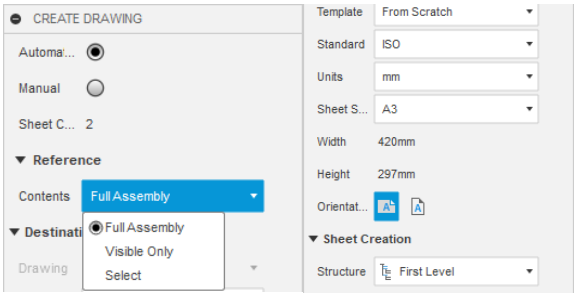

Fig. 9. Settings

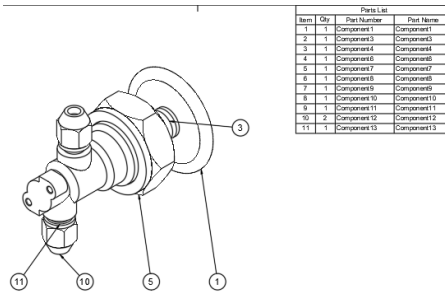

Fig. 10. Isometric image of the assembly with specifications assembly parameters

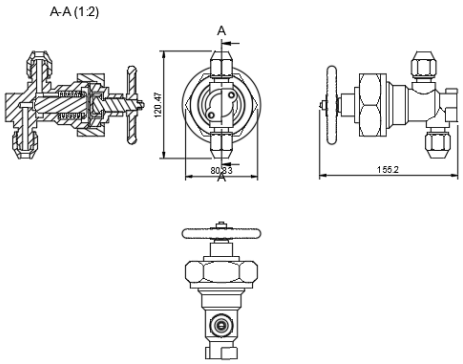

Fig. 11. Drafting of the assembly unit

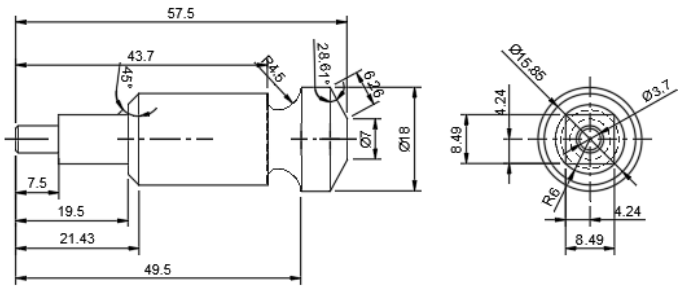

Fig. 12. Detail drawing with a row of pictograms of created drawings

Research results

When analyzing the effectiveness of using the proposed block diagram to accelerate the creation of drawings using automation and AI, the time required to generate documents in automated and man-

ual modes was recorded. The following results were obtained. The drawing of a separate part, the plate, was generated in 32.5 seconds. It took 4 minutes and 25 seconds to create the drawing in manual mode. An assembly drawing consisting of two drawings and specifications was created in 15.6 seconds. In manual mode, it took 3 minutes and 12 seconds. The drawing of a separate simple part from the assembly was obtained in 22.2 seconds, and in manual mode in 1 minute and 35 seconds. A complete set of documentation consisting of 12 drawings of parts and an assembly drawing was generated in 2 minutes and 4 seconds. It took 29 minutes and 34 seconds in manual mode to obtain this set of drawings. The results of the study confirmed the effectiveness of using block diagrams and automating the drawing generation mode.

Conclusions

The paper analyzes the possibility of automated drawing generation from a three-dimensional model in modern CAD systems. The features of drawing generation in AutoCAD, Inventor, and Fusion are considered. Fusion has the greatest capabilities for automated drawing generation. It uses artificial intelligence and a cloud environment to process results for this class of tasks. For a more complete explanation of the technology of automated drawing generation, a block diagram of automated drawing generation in Fusion is proposed. It consists of three parts, which are designed to explain the generation of drawings of individual parts, the generation of assembly drawings, and the creation of templates. The interconnection between the individual elements of the block diagram is shown. An important part is the configuration of templates for high-quality drawing generation, especially for working with assembly units. Using the proposed block diagram, examples of automated drawing generation for a single part and options for working with an assembly node are given. A study was conducted to calculate the time required to generate drawings in automated and manual modes. As a result, a reduction in the time required to generate drawings in automated mode was confirmed. The block diagram can be used to train engineers who use Fusion to speed up the generation of design documentation. Gradually, with the development of new opportunities for using AI to automate work with Fusion, the block diagram will be improved.

Література

1. Пустовой Д. С. Особливості використання 3d-моделювання і побудови асоціативних креслеників машинобудівних деталей в системі Autodesk AutoCAD та Autodesk Inventor. *Інноваційні технології підготовки кадрів для промисловості та транспорту 2025* : зб. наук. праць міжнар. конф. (м. Дніпро, 25–26 квітня 2025 р.). Дніпро, 2025. URL: https://ir.nmu.org.ua/entities/publication/9b012a48-ea1c-492a-890e-38a041ec5fe4. (дата звернення: 24.01.2026).
2. Гурковська С. С., Міхєєнко Д. Ю. Автоматизована побудова 2d-креслень з 3d-моделей із використанням інструментів комп'ютерної графіки. *Вісник Херсонського національного технічного університету*. 2024. № 4. DOI: https://doi.org/10.35546/kntu2078-4481.2024.4.34.
3. Черніков О. В., Назарько О. О., Усенко І. С. Розробка та впровадження бібліотеки додатків до пакету Autodesk Inventor. *Прикладна геометрія та інженерна графіка*. Київ : КНУБА, 2023. Вип. 104. С. 190–200. DOI: https://doi.org/10.32347/0131-579X.2023.104.190-200.
4. Черніков О. В., Усенко В. Г., Усенко І. С. Моделювання та оформлення креслеників деталей з елементами шліцьових з'єднань у пакеті Autodesk Inventor. *Прикладна геометрія та інженерна графіка*. Київ : КНУБА, 2024. Вип. 107. С. 182–191. DOI: https://doi.org/10.32347/0131-579X.2024.107.182-191.
5. Duran S. Drawing Automation with API and New iLogic Snippets in Inventor 2021. *Autodesk University*. 2020. URL: https://www.autodesk.com/autodesk-university/class/Drawing-Automation-API-and-New-iLogic-Snippets-Inventor-2021-2020. (дата звернення: 24.10.2025).
6. Автоматизація оформлення конструкторської документації пружин розтягання в пакеті Autodesk Inventor / Є. Іванов та ін. *Сучасні проблеми моделювання*. 2022. № 23. С. 90–97. DOI: https://doi.org/10.33842/2313-125X-2023-23-90-97.
7. Хомин М. Т., Сторожук О. Л. Метод структуризації геометричних елементів креслення для CAD/CAM-систем. *Науковий вісник НЛТУ України*. 2025. Т. 35, № 4. С. 166–171. DOI: https://doi.org/10.36930/40350419.
8. Automatic 3D CAD Model and 2D Drawings Generation in Construction Engineering / S. Jin et al. *Journal of Physics: Conference Series*. 2021. Vol. 1827. 012115. DOI: 10.1088/1742-6596/1827/1/012115.

9. ADC (Automatic Drawing Creator) / Blue Mech. *Autodesk App Store*. 2025. URL: apps.autodesk.com. (дата звернення: 24.10.2025).
10. Кресленики в Autodesk Fusion: Переваги єдиного середовища та прискорення штучного інтелекту у створенні листів. *Autodesk Community Blog*. 2025. URL: https://forums.autodesk.com/t5/community-blog/kresleniki-v-autodesk-fusion-perevagi-edinogo-seredovishcha-ta/ba-p/13754003. (дата звернення: 24.10.2025).
11. Drawing Automation. *Autodesk Fusion Help*. URL: https://help.autodesk.com/view/fusion360/ENU/?guid=DWG-AUTO-DRAWING. (дата звернення: 24.10.2025).
12. Alba M. AI takes on sketching and drawings in Autodesk Fusion. *Engineering.com*. 2025. URL: https://www.engineering.com/ai-takes-on-sketching-and-drawings-in-autodesk-fusion/. (дата звернення: 24.10.2025).
13. Alba M. 3 new AI features in Autodesk Fusion. *Engineering.com*. 2025. URL: https://www.engineering.com/3-new-ai-features-in-autodesk-fusion/. (дата звернення: 24.10.2025).
14. Still T. AI in Manufacturing: Automated Drawings in Autodesk Fusion. *Autodesk Blog*. 2024. URL: https://www.autodesk.com/products/fusion-360/blog/ai-in-manufacturing-automated-drawings-in-autodesk-fusion/. (дата звернення: 24.01.2025).
15. Still T. AI in Manufacturing: Auto Constrain in Fusion Automated Sketching. *Autodesk Blog*. 2024. URL: https://www.autodesk.com/products/fusion-360/blog/ai-in-manufacturing-sketch-auto-constrain/. (дата звернення: 24.10.2025).
16. MacKenzie C. Autodesk Fusion Automatic Drawings Template. *Man and Machine*. 2025. URL: https://www.manandmachine.co.uk/autodesk-fusion-automatic-drawings-template/. (дата звернення: 24.10.2025).
17. Buktar R. Multiple novel generative design solutions for various mechanical engineering related products using Autodesk Fusion 360 software. *International Journal of Design Engineering*. 2022. DOI: https://doi.org/10.1504/IJDE.2022.127058.
18. Fusion Drawing Automation Template Options. *Clint Brown Blog*. 2024. URL: https://clintbrown.co.uk/2024/02/26/fusion-drawing-automation-template-options/. (дата звернення: 24.10.2025).

References

1. Pustovoi, D. (2025). *Features of using 3d modeling and construction of associative drawings of mechanical engineering parts in autodesk autocad and autodesk inventor systems*. Innovative technologies for training personnel for industry and transport 2025: Collection of scientific papers of the international conference, (2025, April 25–26), Dnipro, Ukraine. Retrieved from https://ir.nmu.org.ua/entities/publication/9b012a48-ea1c-492a-890e-38a041ec5fe4.
2. Gurkovska, S. S., & Mikheenko, D. Y. (2024). Automated construction of 2D drawings from 3D models using computer graphics tools. *Visnyk of Kherson National Technical University*, (4). DOI: https://doi.org/10.35546/kntu2078-4481.2024.4.34.
3. Chernikov, O. V., Nazarko, O. O., & Usenko, I. S. (2023). Development and implementation of an application library for the Autodesk Inventor package. *Applied Geometry and Engineering Graphics*, (104), 190–200. DOI: https://doi.org/10.32347/0131-579X.2023.104.190-200.
4. Chernikov, O. V., Usenko, V. G., & Usenko, I. S. (2024). Modeling and design of drawings of parts with spline connection elements in the Autodesk Inventor package. *Applied Geometry and Engineering Graphics*, (107), 182–191. DOI: https://doi.org/10.32347/0131-579X.2024.107.182-191.
5. Duran, S. (2020). *Drawing automation with API and new iLogic snippets in Inventor 2021*. Autodesk University. Retrieved from https://www.autodesk.com/autodesk-university/class/Drawing-Automation-API-and-New-iLogic-Snippets-Inventor-2021-2020.
6. Ivanov, E., Alefirov, O., Kulish, M., & Ovsyannikov, V. (2022). Automation of design documentation for tension springs in Autodesk Inventor. *Modern Problems of Modeling*, (23), 90–97. DOI: https://doi.org/10.33842/2313-125X-2023-23-90-97.
7. Khomin, M. T., & Storozhuk, O. L. (2025). Method of structuring geometric elements of drawings for CAD/CAM systems. *Scientific Bulletin of UNFU, 35*(4), 166–171. DOI: https://doi.org/10.36930/40350419.
8. Jin, S., Zhang, Y., Yamazaki, T., & Jiang, Z. (2021). Automatic 3D CAD model and 2D drawings generation in construction engineering. *Journal of Physics: Conference Series, 1827*(1), Article 012115. DOI: 10.1088/1742-6596/1827/1/012115.

9. Blue Mech. (2025). *ADC (Automatic Drawing Creator)* [Software help document]. Autodesk App Store. Retrieved from apps.autodesk.com.
10. Autodesk. (2025). *Autodesk Fusion drafting: Benefits of a unified environment and AI acceleration in sheet creation*. Autodesk Community Blog. Retrieved from https://forums.autodesk.com/t5/community-blog/kresleniki-v-autodesk-fusion-perevagi-edinogo-seredovishcha-ta/ba-p/13754003.
11. Autodesk. (n.d.). *Drawing automation*. Fusion Help. Retrieved from https://help.autodesk.com/view/fusion360/ENU/?guid=DWG-AUTO-DRAWING.
12. Alba, M. (2025). *AI takes on sketching and drawings in Autodesk Fusion*. Engineering.com. Retrieved from https://www.engineering.com/ai-takes-on-sketching-and-drawings-in-autodesk-fusion.
13. Alba, M. (2025). *3 new AI features in Autodesk Fusion*. Engineering.com. Retrieved from https://www.engineering.com/3-new-ai-features-in-autodesk-fusion.
14. Still, T. (2024). *AI in manufacturing: Automated drawings in Autodesk Fusion*. Autodesk Blog. Retrieved from https://www.autodesk.com/products/fusion-360/blog/ai-in-manufacturing-automated-drawings-in-autodesk-fusion.
15. Still, T. (2024). *AI in manufacturing: Auto constrain in Fusion automated sketching*. Autodesk Blog. Retrieved from https://www.autodesk.com/products/fusion-360/blog/ai-in-manufacturing-sketch-auto-constrain.
16. MacKenzie, C. (2025). *Autodesk Fusion automatic drawings template*. Man and Machine. Retrieved from https://www.manandmachine.co.uk/autodesk-fusion-automatic-drawings-template.
17. Buktar, R. (2022). Multiple novel generative design solutions for various mechanical engineering related products using Autodesk Fusion 360 software. *International Journal of Design Engineering, 11*(1). DOI: https://doi.org/10.1504/IJDE.2022.127058.
18. Brown, C. (2024). *Fusion drawing automation template options*. Clint Brown Blog. Retrieved from https://clintbrown.co.uk/2024/02/26/fusion-drawing-automation-template-options.

Тігарєв Володимир Михайлович; Volodymyr Tigariev, ORCID: https://orcid.org/0000-0001-8492-6633
Лопаков Олексій Сергійович; Oleksii Lopakov, ORCID: https:// orcid.org/0000-0001-6307-8946
Космачевський Володимир Володимирович; Volodymir Kosmachevskiy, ORCID: https://orcid.org/0000-0002-3234-2297
Доценко Вадим Павлович; Vadym Dotsenko, ORCID: https://orcid.org/0000-0001-6066-2047

Received November 01, 2025
Accepted November 29, 2025

Праці Одеського політехнічного університету, 2025. Вип. 2(72)
ISSN 2076-2429 (print)
ISSN 2223-3814 (online)

UDC 004.056

V. Khamitov,
S. Antoshchuk. DSc, Prof.
Odessa Polytechnic National University, Shevchenko Ave. 1, Odesa, Ukraine, 65044, e-mail: asg@op.edu.ua

APPLICATION OF NONLINEAR DISCRETE MAPS TO CONSTRUCT PSEUDO-CHAOTIC CRYPTOSYSTEMS

В. Хамітов, С. Антощук. **Використання нелінійних дискретних відображень для побудування псевдохаотичних криптосистем**. Стаття присвячена використанню нелінійних дискретних динамічних систем у комп'ютерній криптографії. Основою багатьох потокових схем шифрування є псевдохаотичні послідовності, що генеруються за допомогою деякої обраної траєкторії дискретної динамічної системи. Основна проблема використання псевдохаотичних динамічних систем у комп'ютерних обчисленнях полягає в тому, що кількість різноманітних станів у комп'ютері скінчено, отже, кожна побудована траєкторія є періодичною, причому довжина періоду може бути невеликою. Крім того, різні платформи (апаратні та програмні) використовують різні алгоритми обчислення математичних функцій та зберігають проміжні результати з різною точністю, тому результати, отримані на різних платформах, можуть суттєво відрізнятися. Для подолання зазначених проблем пропонується використати нову динамічну систему, а саме узагальнене відображення Тент з керуванням, яке стабілізує цикли заданої довжини. Ці цикли залежать від параметрів системи та початкового значення; ці величини є коротким ключем для генерації довгої псевдохаотичної послідовності. У статті наводиться найпростіший статистичний аналіз перевірки некорелювання ключової послідовності, а також графічний тест. Експерименти показують відсутність значної кореляції. Також досліджено чутливість елементів ключової послідовності до варіації параметрів ключа. Як приклад роботи алгоритму розглянуто завдання шифрування зображень.

Ключові слова: псевдохаотичні послідовності, шифрування зображень, криптосистеми, захист інформації від несанкціонованого доступу, апаратно-програмна платформа, статистичний аналіз, дискретні динамічні системи, нестійкі періодичні орбіти, стабілізація періодичних орбіт

V. Khamitov, S. Antoshchuk. **Application of nonlinear discrete maps to construct pseudo-chaotic cryptosystems**. The article is devoted to the application of nonlinear discrete dynamical systems in computer cryptography. The basis of many stream encryption schemes is pseudo-chaotic sequences, which are generated using a certain selected trajectory of a discrete dynamical system. The main problem with using pseudo-chaotic dynamical systems in computer calculations is that the number of all possible states in a computer is finite, therefore, every constructed trajectory is periodic, and the period length can be small. In addition, different platforms (hardware and software) use different algorithms for calculating mathematical functions and store intermediate results with different precision, so the results obtained on different platforms can differ significantly. To overcome these problems, it is proposed to use a new dynamical system, namely the generalized Tent map with control, which stabilizes cycles of a given length. These cycles depend on the system parameters and the initial value; these values are a short key (seed) for generating a long pseudo-chaotic sequence. The article provides a simple statistical analysis to check the uncorrelation of the key sequence, as well as a graphical test. The experiments show the absence of significant correlation. The sensitivity of the elements of the key sequence to the variation of the key parameters was also investigated. As an example of the algorithm's operation, the problem of image encryption is considered.

Keywords: pseudo-chaotic sequences, image encryption, cryptosystems, protection of information from unauthorized access, hardware-software platform, statistical analysis, discrete dynamical systems, unstable periodic orbits, stabilization of periodic orbits

Introduction

One of the main problems of digital data processing is the problem of unauthorized access to information. To protect data in a digital environment, cryptographic methods are used. Cryptographic transformations can be conditionally divided into two types: classical methods or alphabetic ciphers, and arithmetic transformations, in which transformation operations occur on the bit (decimal) representation of data. In modern cryptography, methods of the second type are used. Symmetric and asymmetric encryption schemes are distinguished. Another well-known classification distinguishes between block and stream ciphers. A stream cipher converts a stream of text characters into a stream of ciphertext, and the transformation depends on the state of the system. Identical text characters will be encrypted into different ciphertext characters. There is extensive literature on various aspects of cryptography, for example, [1, 2, 3].

Many stream encryption schemes can be viewed from the point of view of nonlinear dynamics. A feature of these schemes is the use of the values of a certain selected trajectory of a discrete dynamical system, i.e., constructed for some given initial conditions and system parameters. A similar way can be used to obtain a sequence of decimal digits or a bit sequence. This sequence is then used as a key to transform the original sequence (the source message) into an encrypted one (ciphertext). The process is

DOI: 10.15276/opu.2.72.2025.19

ISSN 2076-2429 (print)
ISSN 2223-3814 (online)
Proceedings of Odessa Polytechnic University, Issue 2(72), 2025

carried out by linear operations modulo (for example, two or ten) of the elements of the source and key sequences. The simplest stream cipher is the Vernam cipher [4].

A stream encryption scheme is considered secure if the key sequence is truly random and its length is equal to the length of the original message [5]. However, in practice, it is difficult to generate and transmit such keys. Instead, pseudo-random (pseudo-chaotic) sequences are used, generated by some deterministic generator from a short key (seed), using a discrete dynamical system [6-9].

However, at the stage of modeling dynamical systems on modern computers, fundamental problems arise. For example, in [10] it is noted that computer calculations necessarily require additional special confirmation of the results. The main computational problem is that in computers, numbers are stored in registers and memory cells with a limited number of bits, as a result of which the system of real numbers representable in a machine is discrete and finite. To trace what consequences may arise as a result of this, let's consider the simplest example of calculating an iterated sequence using the standard Tent function $f(x) = 2(1/2 - |x - 1/2|)$ in the EXEL software environment. Let's choose the starting point $x_0 = 2/3$. Then theoretically it should be $f^{(k)}(x_0) = x_0$, $k = 1, 2, \ldots$ (here and below the notation $f^{(1)}(x) = f(x)$, $f^{(k}(x) = f(^{(k-1)}(x))$ is used). However, the calculations give different results: $f^{(53)}(x_0) = 1$, $f^{(54)}(x_0) = 0$. One can choose other initial values for x_0, and again we will get $f^{(54)}(x_0) = 0$. The reason for such incorrect calculations is explained by the fact that a number from the interval $[0, 1]$ is represented in a computer in the binary number system by a finite sum of numbers of the form $\alpha_j / 2^j$ ($\alpha_j \in \{0,1\}$), i.e., they are binary-rational numbers, it is equal to $A/2^m$ (A is an integer and $0 \le A \le 2^m$). The number m is called the order. But then $f(A/2^m) = A_1/2^{m-1}$ (A_1 is an integer and $0 \le A_1 \le 2^{m-1}$), $f^{(2)}(A/2^m) = A_2/2^{m-2}$, … , $f^{(m+1)}(A/2^m) = 0$. On computers where the iterated sequence was calculated, the maximum order was 53.

Let's turn again to the Tent map. We will carry out the calculations in the MAPLE package with a decimal representation with the value of the variable *Digits*:=25. We generate the sequences $\{x_k = f^{(k)}(x_0)\}$, $\{y_k = f^{(k)}(y_0)\}$, $k = 1, 2, \ldots$, where $x_0 = 1/1001$, $y_0 = evalf(1/1001)$, and construct the sequence $\{x_k - y_k\}$. It can be seen that, starting from the 80th step, the behavior of this sequence is quasi-chaotic.

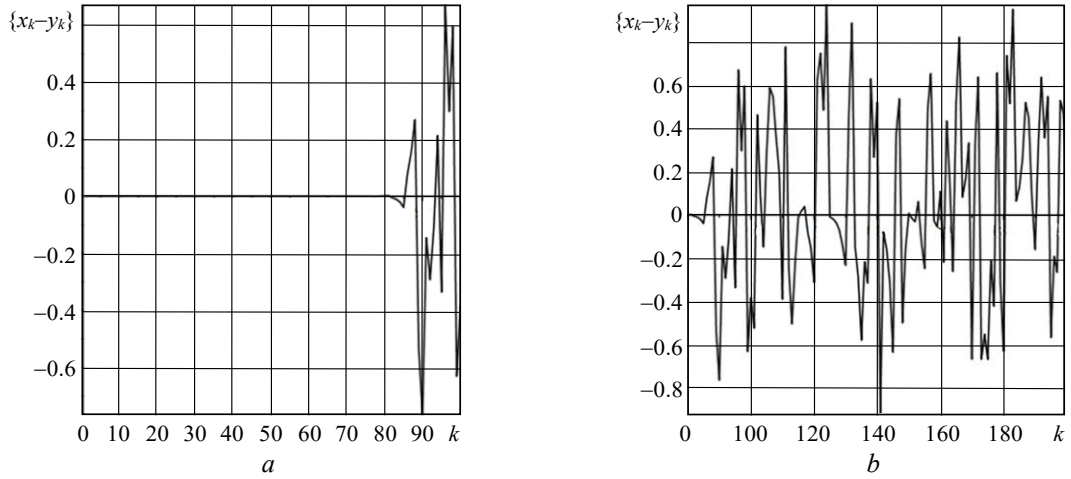

Fig. 1. Graphical representation of the sequence $\{x_k - y_k\}$: *a – for* $k = 1, \ldots, 100$; *b – for* $k = 80, \ldots, 200$

Similar examples can be constructed further. However, the examples given above clearly show that a researcher can never be sure of the correctness of calculations performed on a computer. That is, to the question of *R. Lozi* [10] (about trust in numerical results), the answer is,

ISSN 2076-2429 (print)
ISSN 2223-3814 (online)

unfortunately, negative. This once again proves the need to develop mathematical methods that allow correcting computer calculations.

Another problem may arise when the orbit of a discrete dynamical system becomes cyclic, and the cycle length turns out to be quite small, for example, due to an unsuccessfully chosen initial value. It is also possible that as a result of rounding values, the trajectory will become cyclic, again, with a small cycle length. The point here is that the variables that determine the state of the system can have close, but not equal values; and when rounded, the chaotic behavior ceases. In these cases, it is impossible to construct a correct key sequence.

The next problem is related to the fact that different platforms (hardware and software) use different algorithms for calculating mathematical functions and store intermediate results with different precision. Since chaotic generators are extremely sensitive to precision and error, it is very likely that the same encryption algorithms implemented on different platforms will lead to different results.

Thus, the property of chaoticity of dynamical systems turns out to be dual: on the one hand, it provides the properties of confusion and diffusion absolutely necessary for cryptography (relative to the text and the key) [11], on the other hand, it causes inconvenience of use associated with high sensitivity to disturbances and rounding.

The purpose of this article is to construct a new discrete dynamical system with which you can generate long pseudo-chaotic sequences; in this case, the system parameters and initial values are used as a seed (key). Requirements for the seed: the seed should consist of a small number of elements. Requirements for the algorithm: the algorithm should not depend on the hardware and software.

Literature Review

A significant number of works are devoted to the use of chaotic systems in cryptanalysis, for example, [12 – 15]. The importance of the problem of the performance of chaotic cryptosystems is noted [17, 18, 19]. Discrete dynamic systems of small dimensions have obvious advantages over high-dimensional systems: these systems are easier to implement in software, and the time costs for generating a pseudo-chaotic sequence are less, which allows encrypting large amounts of data in real time [20]. Therefore, the development of effective models of one-dimensional discrete chaotic systems for constructing encryption algorithms is an actual task [21, 22, 23].

Preliminary results

The mathematical basis for constructing new algorithms for generating pseudo-chaotic cryptosystems is the one-dimensional Tent mapping with additional predictive control.

Following [24], let's consider a nonlinear equation with discrete time:

$$x_{n+1} = f(x_n), \quad n = 1, 2, \dots , \tag{1}$$

where:

$$f(x) = H(1/2 - |x - 1/2|) = \begin{cases} H\,x, x \le 1/2; \\ H(1-x), x > 1/2, \end{cases} \tag{2}$$

$x \in (-\infty, +\infty)$, $H \ge 2$.

The map (2) is called the generalized Tent map.

A set U is called invariant for equation (1) if for any $x_0 \in U$ it follows that $f^{(k)}(x_0) \in U$, $k = 1, 2, \dots$. It can be shown that for $H > 2$ in equation (1) the invariant set will be a *Cantor*-type set: closed, continuum power, with zero *Lebesgue* measure. Note that each point of the invariant set is representable in the form $\sum_{j=1}^{\infty} \frac{\alpha_j}{H^j}$, where $\alpha_j \in \{0, H-1\}$. This set includes a countable subset of all periodic points of the map (2). If x_0 does not belong to the invariant set, then

ISSN 2076-2429 (print)
ISSN 2223-3814 (online)
Proceedings of Odessa Polytechnic University, Issue 2(72), 2025

the corresponding sequence $\{f^{(k)}(x_0)\}_{k=1}^{\infty}$ tends to $-\infty$. Such invariant sets are called repellers of the map (2).

The set $\{\eta_1, \dots, \eta_T\}$ is called a T - cycle of the map (2) if the numbers $\eta_1, \dots, \eta_T$ are different and $\eta_{j+1} = f(\eta_j)$, $j = 1, \dots, T-1$, $\eta_1 = f(\eta_T)$, while each point of the T – cycle is called a T – periodic point. The multiplier of the cycle of equation (1) is determined by the formula $\mu = f'(\eta_T) \cdot \ldots \cdot f'(\eta_1)$, i.e. $\mu = \pm H^T$.

As is known [25], the local asymptotic stability of a cycle is determined by the condition (sufficient): the multiplier in absolute value is less than one. Since $|\mu| = H^T > 1$, any cycle of equation (1) is unstable. In addition, if $H > 2$, then for almost any initial point, the corresponding trajectory goes to infinity.

Along with equation (1), let's consider the equation:

$$x_{n+1} = F(x_n), \quad n = 1, 2, \dots, \tag{3}$$

where: $F(x) = f(\vartheta x + (1-\vartheta) f^{(T)}(x))$, ϑ – is some real number, called the control parameter and subject to determination. Equation (3) is called the control system for equation (1). Let $\{\eta_1, \dots, \eta_T\}$ be a cycle of equation (1).

Since $\vartheta \eta_k + (1-\vartheta) f^{(T)}(\eta_k) = \eta_k$, then $F(\eta_k) = f(\eta_k)$, this means that the cycle of equation (1) will also be a cycle of equation (3). Note that the converse is not true in the general case.

The multiplier λ of this same cycle $\{\eta_1, \dots, \eta_T\}$ but for equation (3) can be found from [26]:

$$\lambda = \mu(\vartheta + (1-\vartheta)\mu)^T.$$

Two cases are possible: $\mu > 0$ and $\mu < 0$. The condition for local asymptotic stability of a T - cycle of equation (3) for $\mu = H^T$: $|\lambda| = \left|H^T (\vartheta + (1-\vartheta) H^T)^T\right| < 1$, whence:

$$\frac{H^T - \frac{1}{H}}{H^T - 1} < \vartheta < \frac{H^T + \frac{1}{H}}{H^T - 1}. \tag{4}$$

If $\mu = -H^T$, then the condition for local asymptotic stability of the cycle of equation (5): $|\lambda| = \left|H^T (\vartheta - (1-\vartheta) H^T)^T\right| < 1$, whence:

$$\frac{H^T - \frac{1}{H}}{H^T + 1} < \vartheta < \frac{H^T + \frac{1}{H}}{H^T + 1}. \tag{5}$$

***Theorem* 1** [24]. If inequalities (4) are satisfied, then any solution of equation (3) is bounded (i.e., for any initial point $x_0 \in (-\infty, +\infty)$ the corresponding trajectory is bounded). Moreover, any T – cycle $\{\eta_1, \dots, \eta_T\}$ of this equation, for which the value $\mu = f'(\eta_T) \cdot \ldots \cdot f'(\eta_1)$ is positive, is locally asymptotically stable.

***Theorem* 2** [24]. If inequalities (5) are satisfied, then the set $[0, H/2]$ is an invariant set of equation (1) (i.e., for any initial point the corresponding trajectory is bounded by the values 0 and $H/2$). Moreover, any T – cycle $\{\eta_1, \dots, \eta_T\}$ of this equation, for which the value $\mu = f'(\eta_T) \cdot \ldots \cdot f'(\eta_1)$ is negative, is locally asymptotically stable.

Main result

To generate a pseudo-chaotic sequence, it is proposed to use a dynamical system (3), in which ϑ satisfies condition (4) or (5). In this case, the sequence itself is determined through the T periodic points $\{\eta_1, \dots, \eta_T\}$. Here T – is a sufficiently large number. In order to exclude

ISSN 2076-2429 (print)
ISSN 2223-3814 (online)

short subcycles, the number T must be taken to be simple. In total, there are $\frac{2^{T-1}-1}{T}$ cycles of length T, i.e., for sufficiently large lengths T the total number of cycles will be very large (exponential growth in T), i.e., the probability of guessing a specific cycle that is realized is negligible. Due to the chaotic nature of the dynamical system (1), a long cycle will be practically indistinguishable from an arbitrary bounded non-cyclic trajectory. Note, however, that in practice for $H > 2$ any trajectory of equation (1) will go to infinity due to rounding of results. Fig. 2 shows typical T - periodic trajectories of equation (1) for $T = 223$, $H = 2.070801$, $x_0 = 0.9$.

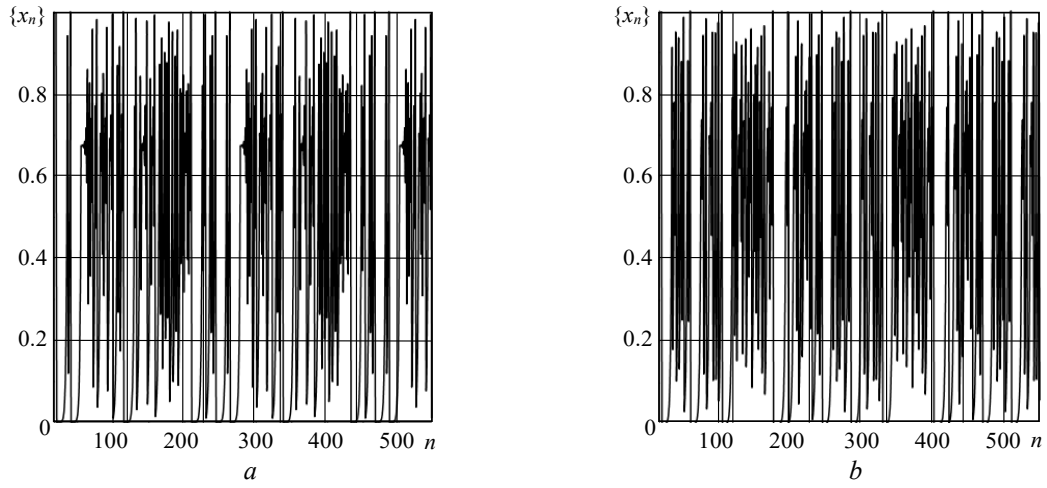

Fig. 2. T – periodic trajectories of equation (1) for $T = 223$, $H = 2.070801$, $x_0 = 0.9$: a – the value $\mu = f'(\eta_T)\cdot\ldots\cdot f'(\eta_1)$ is negative; b – the value $\mu = f'(\eta_T)\cdot\ldots\cdot f'(\eta_1)$ is positive

For things to work practically, you need to use equation (3). Then the found cycle will depend on the initial point $x_0 \in (0,1)$, on the number T and on the parameters H and ϑ, which may contain a sufficient number of decimal places. Such a complex dependence will in fact make the cycle parameters non-obvious for a cryptanalyst.

This cycle is locally asymptotically stable. This means that the resulting trajectory does not depend on minor disturbances, inaccuracies in calculations and rounding. Moreover, one can expect that for different but close values of x_0, T, H, ϑ different cycles will be obtained on the same computers. The main question is the speed of convergence (i.e., the number of correct decimal places). Roughly speaking, this speed must be sufficient for the length of the cycle. Experiments show [24] that the accuracy should be chosen at least $1.05 \cdot T \lg(H)$.

However, the sequence $\{\eta_1, \ldots, \eta_T\}$ is not pseudo-random –the order of elements is fully determined. So an extra trick is needed. The point is that as a result of the calculation, we need to guarantee q correct decimal places in the cycle $\{\eta_1, \ldots, \eta_T\}$, where q denotes the number of decimal places. In this case, we have $T \cdot q$ decimal digits, from which we can build a pseudo-chaotic sequence. For example, in the following way: let's take the numbers T_0, T_1, and computational precision should be taken $q = T_1 + 2T_0$ ($T_1 + 2T_0 > 1.05 \cdot T \lg(H)$).For each number η_j take decimal digits of the fractional part starting from digit number $T_0 + 1$, ending with number $T_1 + T_0$. Denote these sets $\{\eta_{j1}, \ldots, \eta_{jT_1}\}$, $j = 1, \ldots, T$. For the formation of the key sequence, we obtained $T \cdot T_1$ decimal digits. The key sequence itself can have, for example, the form:

$$I_1 = \{\eta_{11}, \eta_{12}, \ldots, \eta_{1T_1}, \eta_{21}, \ldots, \eta_{2T_1}, \ldots, \eta_{T1}, \ldots, \eta_{TT_1}\} \quad (6)$$

or

$$I_2 = \{\eta_{11}, \eta_{21} \ldots, \eta_{T1}, \eta_{12}, \ldots, \eta_{T2}, \ldots, \eta_{1T_1}, \ldots, \eta_{TT_1}\}. \quad (7)$$

ISSN 2076-2429 (print)
ISSN 2223-3814 (online)
Proceedings of Odessa Polytechnic University, Issue 2(72), 2025

You can form the sequence in other ways.

Choice of key parameters

The seed for generating a pseudo-chaotic sequence is the key $Key = [T, H, \pm\alpha, x_0]$. Here the numbers α or $-\alpha$ are used to calculate the control parameter $\vartheta = \dfrac{H^T + \alpha\dfrac{1}{H}}{H^T - 1}$ or $\vartheta = \dfrac{H^T - \alpha\dfrac{1}{H}}{H^T + 1}$ respectively.

The closer α is to zero, the closer the cycle multiplier is to zero, the faster the initial point will be attracted to this cycle. Therefore, it is advisable to take $0 < \alpha < 0.005$. Practical experiments show that with such α , the initial point falls into the cycle in no more than 20 iterations. This means that the number T_0 in the formula $q = T_1 + 2T_0$ can be taken equal to 20. In this case, the number T_1 can be taken simply equal to T. The period T must be a prime number in the range between 100 and 500. Large numbers lead to a sharp increase in calculation time. The initial point x_0 must be chosen from the interval $(0, 1)$.

Periodic trajectories are sensitive to changes in key parameters. Let's take, for example, $x_0 = 0.9$, $T = 223$, $\vartheta = \dfrac{H^T + 0.001 \cdot 1/H}{H^T - 1}$, $H \in \{2.070801, 2.0708011\}$, i.e. $Key = [223, \{2.070801, 2.0708011\}, 0.001, 0.9]$. Let's calculate the two corresponding periodic trajectories and their difference z_n. Let's plot the resulting trajectory in Fig. 3.

Due to the high sensitivity, the parameter H can be chosen quite close to two, for example, $H \in (0, 2.2)$, and the whole uncertainty can be put into the following significant decimal places.

Let's take the key: $Key = [223, 2.0708011, \{0.001, -0.001\}, 0.9]$. Let's calculate the two corresponding periodic trajectories and their difference z_n. Let's plot the resulting trajectory in Fig. 4.

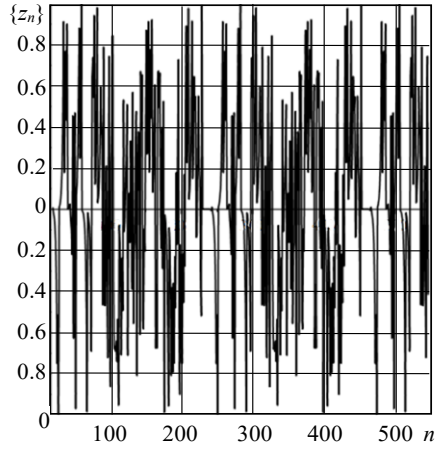

Fig. 3. The difference of two T – periodic trajectories of equation (3) for $Key = [223, \{2.070801, 2.0708011\}, 0.001, 0.9]$

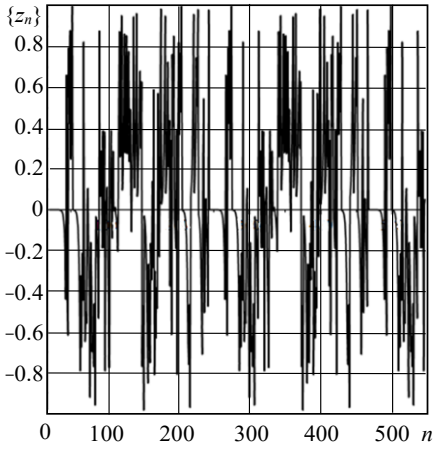

Fig. 4. The difference of two T – periodic trajectories of equation (3) for $Key = [223, 2.0708011, \{0.001, -0.001\}, 0.9]$

Similarly, we construct the difference of trajectories for $Key = [223, 2.0708011, \{0.001, 0.0011\}, 0.9]$ (Fig.5), $Key = [223, 2.0708011, 0.001, \{0.9, 0.9001\}]$ (Fig.6)

ISSN 2076-2429 (print)
ISSN 2223-3814 (online)

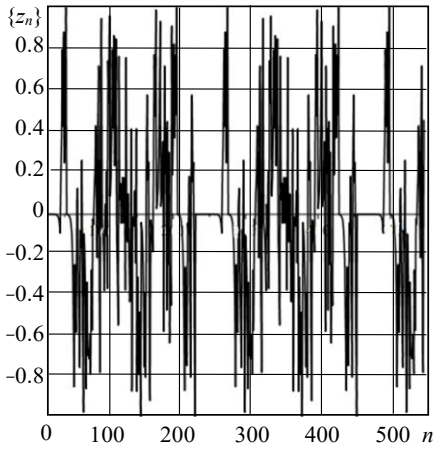

Fig. 5. The difference of two T – periodic trajectories of equation (3) for $Key = [223,\ 2.0708011,\ \{0.001,\ 0.0011\},\ 0.9]$

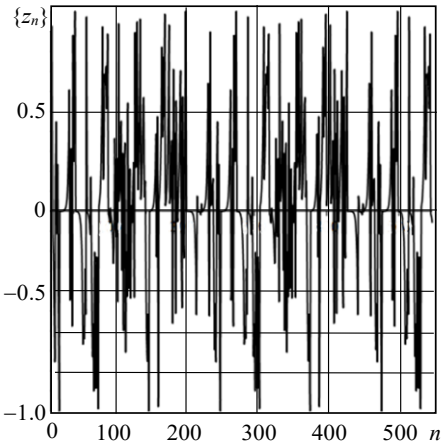

Fig. 6. The difference of two T – periodic trajectories of equation (3) for $Key = [223, 2.0708011,\ 0.001,\ \{0.9,\ 0.9001\}]$

Let's consider the sensitivity of the key sequence to the parameter T (period), i.e., let's calculate two corresponding periodic trajectories x_n and y_n (constructed for $T = 223$ and $T = 227$ respectively) and their difference z_n for the key: $Key = [\{223,\ 227\}, 2.0708011,\ 0.001,\ 0.9]$. Let's plot the resulting trajectory in Fig. 7-*a*). In Fig. 7-*b*) we plot the points of the sequence $\{\ln(|z_n|)\}$.

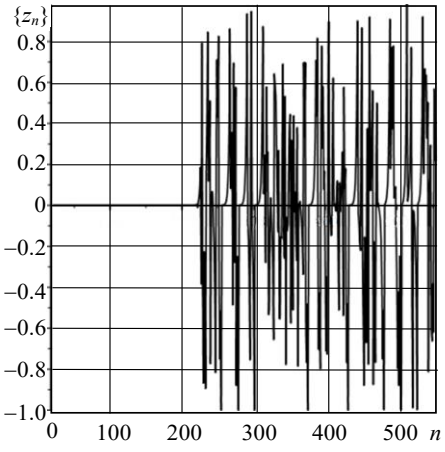

a

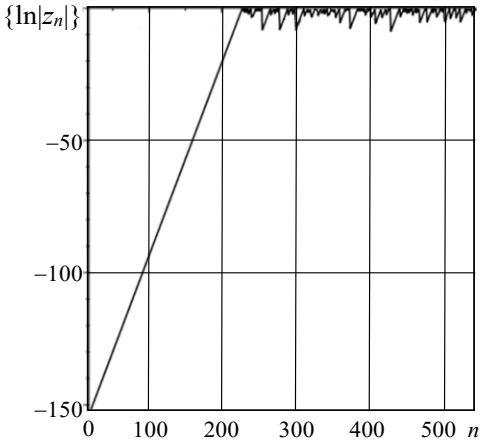

b

Fig. 7. The difference of two periodic trajectories of equation (3) for $Key = [\{223,\ 227\}, 2.0708011,\ 0.001,\ 0.9]$: *a* – the sequence $\{z_n\}$; *b* – the sequence $\{\ln(|z_n|)\}$

Analysis of the results shows that for $n < 210$ the values of the two trajectories x_n and y_n are close to each other, in particular $|z_n| < 10^{-50}$ for $n < 74$. For $230 < n < 440$ the values x_n and y_{n+4} will be close; further, for $460 < n < 670$ the values x_n and y_{n+8}, will be close, and so on. Conclusion: variation of the parameter T does not give the necessary divergence of the key sequences.

The essential parameters of the key are the values $H,\ \alpha,\ x_0$. If these parameters are determined by at least ten decimal places, then the number of all possible variants of the keys will be of the order of 10^{30}, i.e., about 100 bits. If necessary, you can increase the cryptographic strength of the algorithm by using several keys in series.

ISSN 2076-2429 (print)
ISSN 2223-3814 (online)
Proceedings of Odessa Polytechnic University, Issue 2(72), 2025

Statistical analysis

Let's investigate some statistical characteristics of pseudo-chaotic sequences (6) and (7) for the $Key = [223, 2.070811, 0.001, 0.9]$. Let's construct a histogram and determine the mean and standard deviation. Let's start with sequence (6). The sequence contains T^2 elements. In our case, 49729 elements. The mean is $S = 4.4795...$, which deviates insignificantly from the theoretical mean of 4.5 of a uniformly distributed discrete random variable. The standard deviation is the theoretical one is 2.8722... Let's construct histograms for the first 1000 elements of the sequence, for elements with numbers from 2000 to 3000, for all elements (Fig. 8).

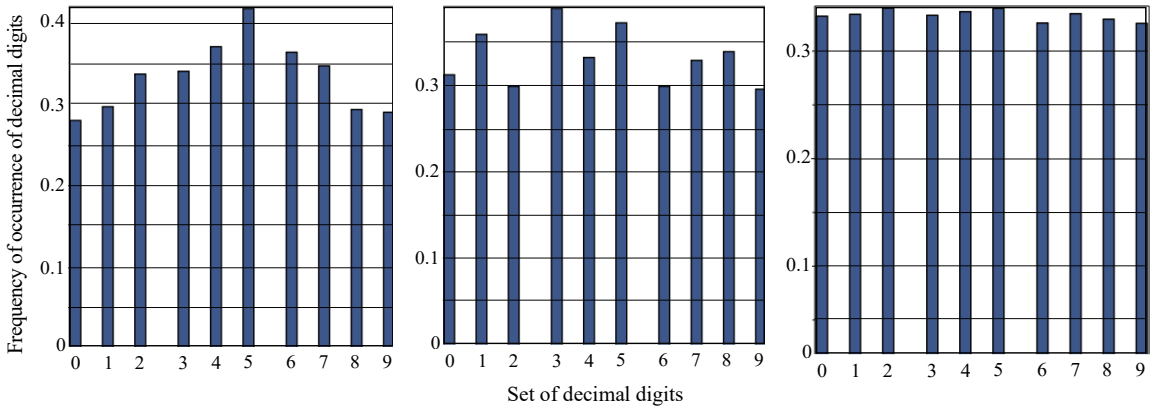

Fig. 8. Histogram for the sequence: $a - [I_1[j]: j = 1..1000]$; $b - [I_1[j]: j = 2000..3000]$; $c - [I_1[j]: j = 1..49729]$, constructed for $T = 223$, $H = 2.0708011$, $\vartheta = \dfrac{H^T + 0.001 \cdot 1/H}{H^T - 1}$, $x_0 = 0.9$

We see that individual sections of the sequence do not have a strictly uniform distribution, although their distributions are close to uniform.

For further analysis of the properties of the sequence $[I_1[j]: j = 1..49729]$ let's define three quantities: the cumulative mean $\overline{I}_1(k) = \dfrac{1}{k}\sum_{j=1}^{k} I_1[j]$, $k = 1, \ldots, T^2$; the cumulative standard deviation $\delta_1(k) = \dfrac{1}{k-1}\sum_{j=1}^{k} (I_1[j] - \overline{I}_1(k))^2$; the cumulative variance $\sigma_1(k) = \sqrt{\delta_1(k)}$, $k = 2, \ldots, T^2$. It is clear that the usual sample mean is equal to $\overline{I}_1(T^2)$, and the sample variance is $\sigma_1(T^2)$.

To construct graphs of the cumulative mean and variance, we derive recurrent formulas for these quantities. Since $\overline{I}_1(k) = \dfrac{k-1}{k}\dfrac{1}{k-1}\sum_{j=1}^{k-1} I_1[j] + \dfrac{1}{k} I_1[k]$, then

$$\overline{I}_1(k) = \frac{k-1}{k}\overline{I}_1(k-1) + \frac{1}{k} I_1[k], \quad \overline{I}_1(1) = I_1[1]. \tag{8}$$

Further, $(I_1[j] - \overline{I}_1(k))^2 = (I_1[j])^2 - 2I_1[j]\overline{I}_1(k) + (\overline{I}_1(k))^2$, whence

$$\delta_1(k) = \frac{1}{k-1}\sum_{j=1}^{k} (I_1[j])^2 - \frac{2}{k-1}\overline{I}_1(k)\sum_{j=1}^{k} I_1[j] + \frac{k}{k-1}(\overline{I}_1(k))^2 = \frac{1}{k-1}\sum_{j=1}^{k} (I_1[j])^2 - \frac{k}{k-1}(\overline{I}_1(k))^2.$$

Let's denote:

$$\overline{I}_1^{(2)}(k) = \frac{1}{k-1}\sum_{i=1}^{k} (I_1[j])^2,$$

Праці Одеського політехнічного університету, 2025. Вип. 2(72)
ISSN 2076-2429 (print)
ISSN 2223-3814 (online)

then $\overline{\mathrm{I}}_1^{(2)}(k)=\frac{k-2}{k-1}\frac{1}{k-2}\sum_{j=1}^{k-1}(\mathrm{I}_1[j])^2+\frac{1}{k-1}(\mathrm{I}_1[k])^2=\frac{k-2}{k-1}\overline{\mathrm{I}}_1^{(2)}(k-1)+\frac{1}{k-1}(\mathrm{I}_1[k])^2$. Thus, the following recursive relation is valid:

$$\begin{cases}\delta_1(k)=\overline{\mathrm{I}}_1^{(2)}(k)-\frac{k}{k-1}(\overline{\mathrm{I}}_1(k))^2;\\ \overline{\mathrm{I}}_1^{(2)}(k)=\frac{k-2}{k-1}\overline{\mathrm{I}}_1^{(2)}(k-1)+\frac{1}{k-1}(\mathrm{I}_1[k])^2.\end{cases} \tag{9}$$

In this case, $k=3,\ldots,N$, and $\overline{\mathrm{I}}_1^{(2)}(2)=(\mathrm{I}_1[1])^2+(\mathrm{I}_1[2])^2$.

The graphs of the quantities $\{\overline{\mathrm{I}}_1(j)\}_{j=1}^{500}$, $\left\{\overline{\mathrm{I}}_1(j)\right\}_{j=1}^{T^2}$ are shown in Fig. 9. The graphs of the quantities $\left\{\sigma_1(j)\right\}_{j=1}^{500}$, $\{\sigma_1(j)\}_{j=1}^{T^2}$ are shown in Fig. 10.

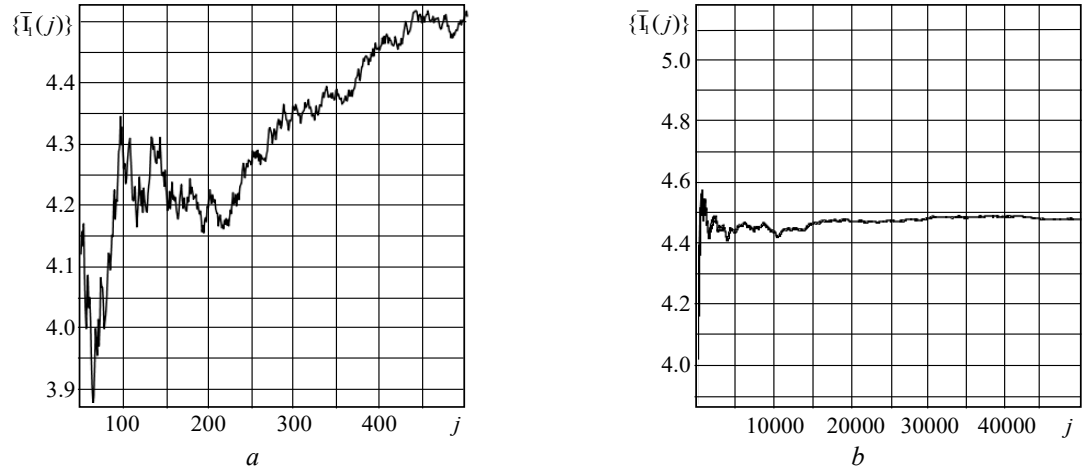

Fig. 9. Graphs of the quantities: *a* – $\{\overline{\mathrm{I}}_1(j)\}_{j=1}^{500}$; *b* – $\{\overline{\mathrm{I}}_1(j)\}_{j=1}^{T^2}$

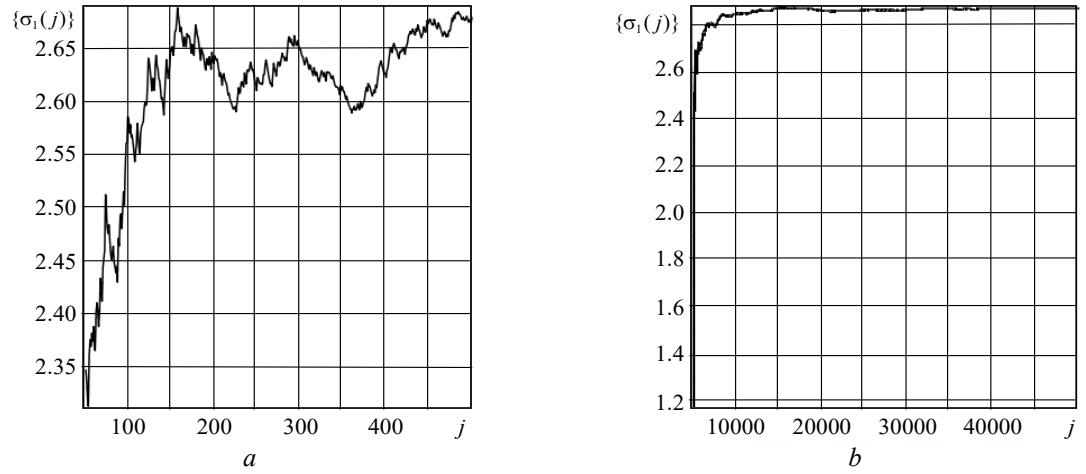

Fig. 10. Graphs of the quantities: *a* – $\{\sigma_1(j)\}_{j=1}^{500}$; *b* – $\{\sigma_1(j)\}_{j=1}^{T^2}$

The absence of periodicity in the behavior of the graphs of the cumulative mean and variance indicates the absence of regularities between individual parts of the sequence, which may indicate its pseudo-stochastic nature.

Let's carry out a similar analysis for sequence (7). In this case, we note that in formulas (8), (9) the index 1 must be replaced by 2. The corresponding graphs are given below (Fig. 11–13).

ISSN 2076-2429 (print)
ISSN 2223-3814 (online)

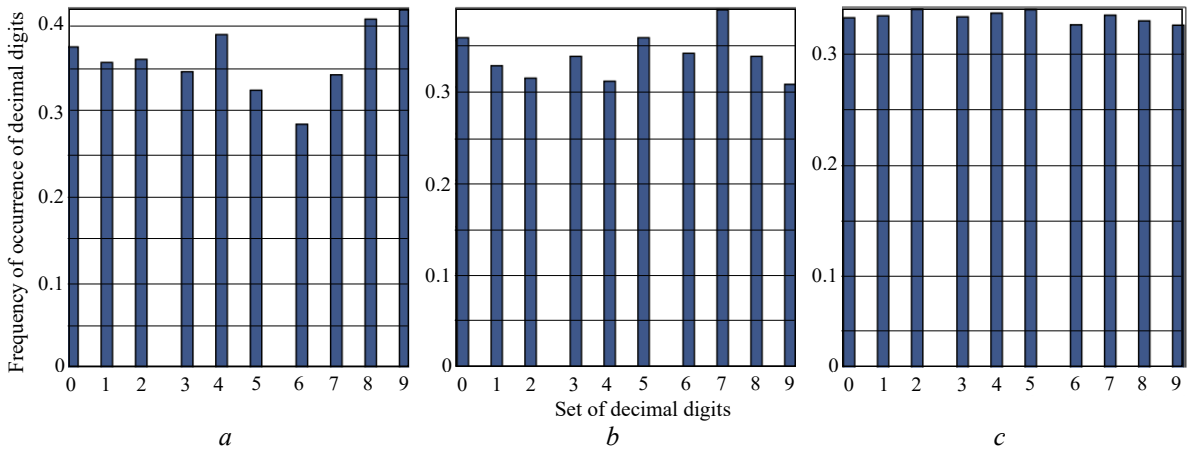

Fig. 11. Histogram for the sequence: a – $[\mathrm{I}_2[j]: j=1..1000]$; b – $[\mathrm{I}_2[j]: j=2000..3000]$; c – $[\mathrm{I}_2[j]: j=1..49729]$, constructed for $T=223$, $H=2.0708011$, $\vartheta=\dfrac{H^T+0.001\cdot 1/H}{H^T-1}$, $x_0=0.9$

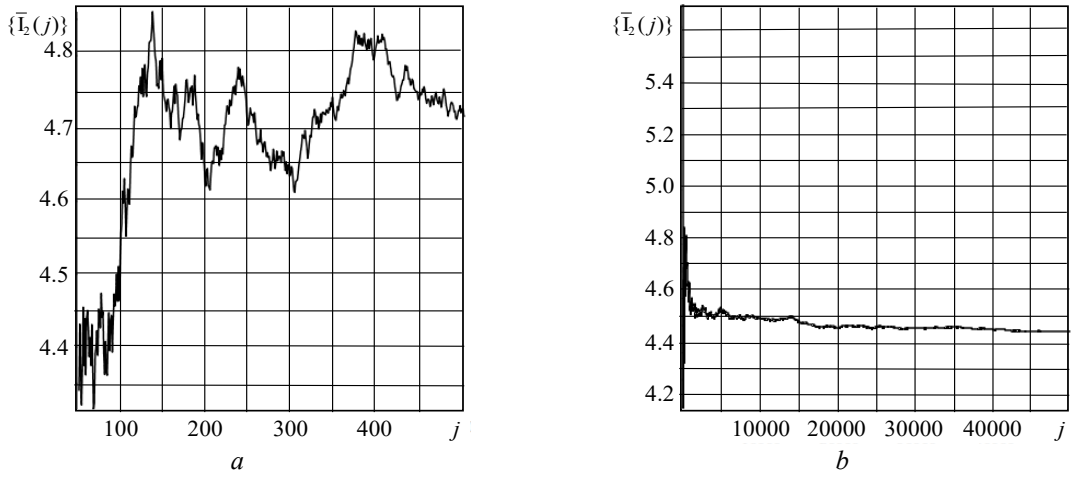

Fig. 12. Graphs of the quantities: a – $\{\bar{\mathrm{I}}_2(j)\}_{j=1}^{500}$; b – $\{\bar{\mathrm{I}}_2(j)\}_{j=1}^{T^2}$

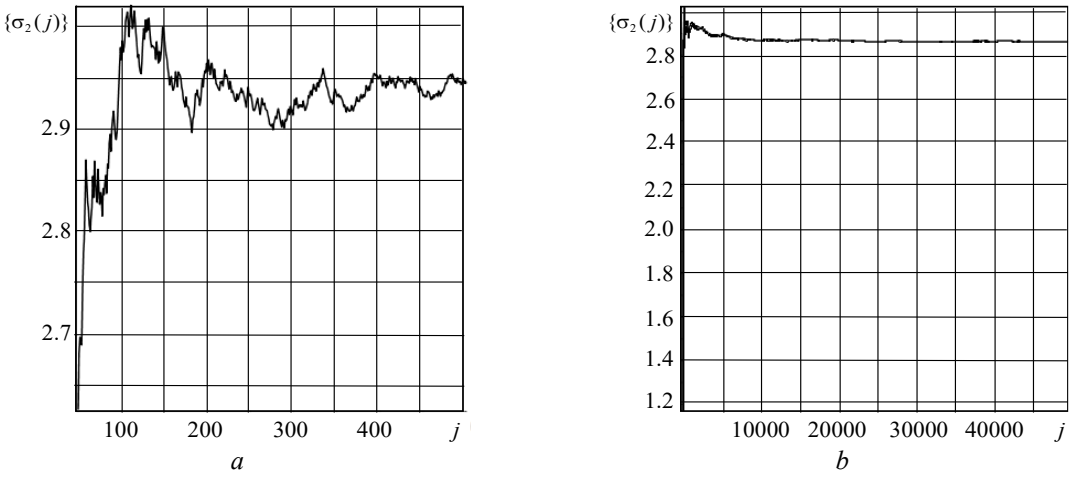

Fig. 13. Graphs of the quantities: a – $\{\sigma_2(j)\}_{j=1}^{500}$; b – $\{\sigma_2(j)\}_{j=1}^{T^2}$

Праці Одеського політехнічного університету, 2025. Вип. 2(72)
ISSN 2076-2429 (print)
ISSN 2223-3814 (online)

Graphical testing method

There is a known problem in testing a pseudo-chaotic sequence for uncorrelation, which is that the use of point characteristics (mean, variance), as well as correlation functions or even functions that depend on higher-order moments, can be ineffective.

Therefore, we will additionally apply a graphical testing method. Let's break down the sequence $[\mathrm{I}_1[j]: j = 1..49729]$ into elements consisting of consecutive triples of decimal numbers, and divide the resulting three-digit numbers by 10^3. We get a new sequence:

$$[\mathrm{I}_1[j]\cdot 10^{-1} + \mathrm{I}_1[j+1]\cdot 10^{-2} + \mathrm{I}_1[j+2]\cdot 10^{-3} : j = 1..49727],$$

consisting of decimal numbers, which are determined by the first three digits. Let's plot the points with coordinates on the plane:

$$\{\mathrm{I}_1[j]\cdot 10^{-1} + \mathrm{I}_1[j+1]\cdot 10^{-2} + \mathrm{I}_1[j+2]\cdot 10^{-3}, \mathrm{I}_1[j+3]\cdot 10^{-1} + \mathrm{I}_1[j+4]\cdot 10^{-2} + \mathrm{I}_1[j+5]\cdot 10^{-3}\}. \quad (10)$$

The resulting image will allow us to assess the chaotic nature of consecutive triples of numbers. In Fig. 14, the points with coordinates (10) are shown for $j = 1..3000$ and $j = 5000..20000$.

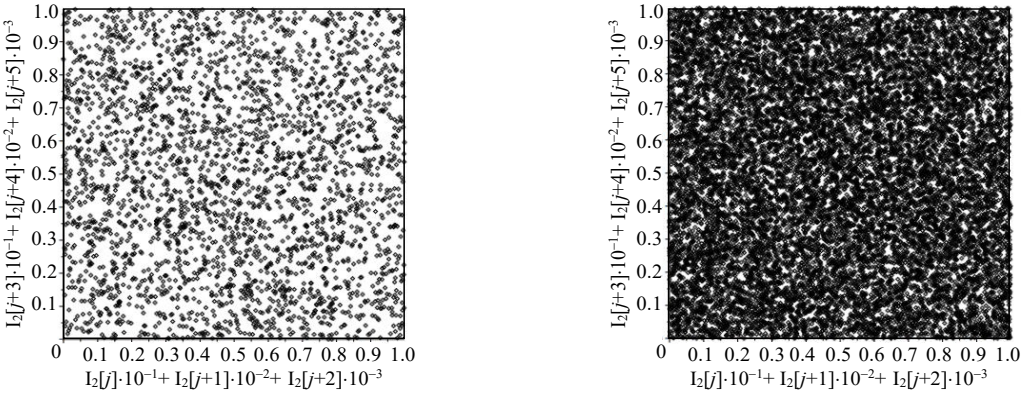

a *b*

Fig. 14. Points with coordinates (10) for: *a* – $j = 1..3000$ and *b* – $j = 5000..20000$, generated by sequence (6)

for $T = 223$, $H = 2.0708011$, $\vartheta = \dfrac{H^T + 0.001\cdot 1/H}{H^T - 1}$, $x_0 = 0.9$

One can see the absence of explicit correlation in sequence (6). For sequence (7), the results of the corresponding constructions are shown in Fig. 15.

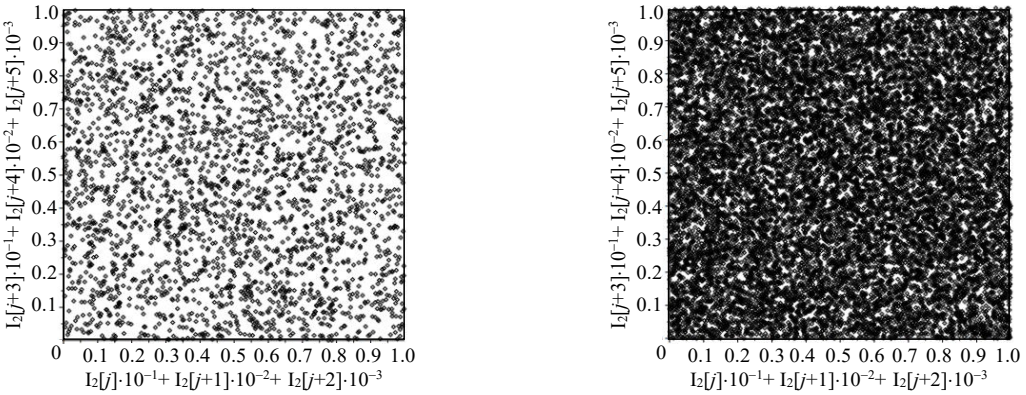

a *b*

Fig. 15. Points with coordinates (10) (with the replacement of index 1 by 2) for: *a* – ; *b* – $j = 5000..20000$, generated by sequence (6) for $T = 223$, $H = 2.0708011$, $\vartheta = \dfrac{H^T + 0.001\cdot 1/H}{H^T - 1}$

ISSN 2076-2429 (print)
ISSN 2223-3814 (online)
Proceedings of Odessa Polytechnic University, Issue 2(72), 2025

Visual analysis of the corresponding graphs shows that sequence (7) may be more uncorrelated than (6). However, sequence (6) is constructed sequentially with the calculation of the cycle points $\{\eta_1, \ldots, \eta_T\}$, while for the construction of sequence (7) it is necessary to know the entire cycle at once, which leads to a decrease in the speed of the algorithm and an increase in the memory used.

The graphical test used above can be modified. For a more effective check of the correlation of the sequence, instead of a two-color image, one can consider a color one. To do this, three sequences are generated from the sequence $[\mathrm{I}[j]: j = 1..N]$: $R = [0.1 \cdot \mathrm{I}[j]: j = 1..N]$, $G = [0.1 \cdot \mathrm{I}[j+1]: j = 1..N]$, $B = [0.1 \cdot \mathrm{I}[j+2]: j = 1..N]$. Further, for each pixel, the color in RGB format is determined using the generated sequences R, G, B.

Let's take, for example, an image height of $h = 438$ pixels, a width of $w = 648$ pixels. A total of 279936 pixels are used. Let's generate the sequence $[j \bmod 10: j = 1..N]$ (the number N must be chosen not less than 279938), which is clearly correlated. In this case, the histogram, mean and variance of this sequence will be, as for a uniformly distributed one. For comparison, let's generate a sequence of the first digits of the fractional part of the expression $\sin(j^2 + 1)$, $j = 1..N$. Let's construct images of these sequences in RGB format (Fig. 12).

Since any correlation should manifest itself in the form of visual regularity, it can be argued that the sequences that generate the images in Fig. 16 are strongly correlated.

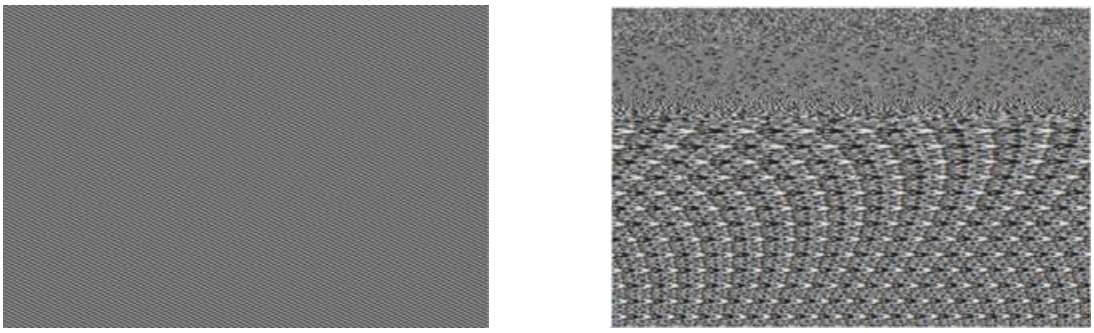

a *b*

Fig. 16. Images in RGB format for the sequences: *a* – $[j \bmod 10: j = 1..N]$;
b – $[trunc(10 \cdot \sin(j^2 + 1)) : j = 1..N]$

Let's construct a similar image for sequences (6) and (7) (Fig. 17).

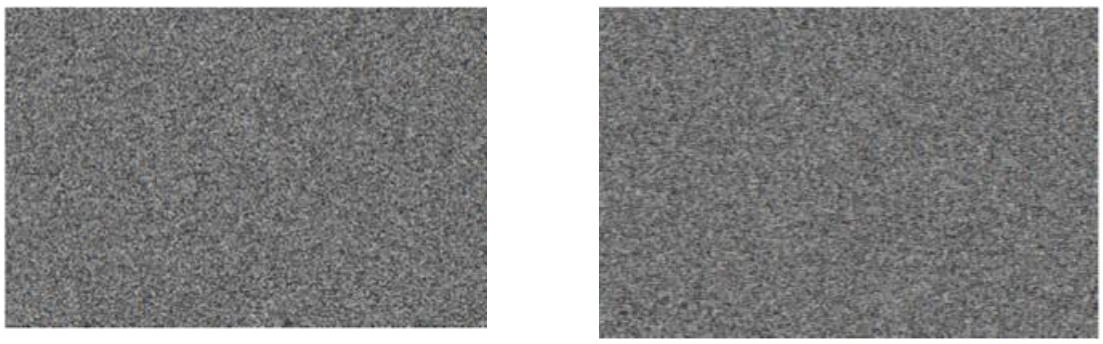

a *b*

Fig. 17. Image in RGB format for sequences (6) (case *a*) and (7) (case *b*)

For these sequences, the regular structure is not visually traced.

For comparison, we give an image in RGB format for the sequence of the first 286000 decimal digits of the numbers π and e (Fig. 18).

ISSN 2076-2429 (print)
ISSN 2223-3814 (online)

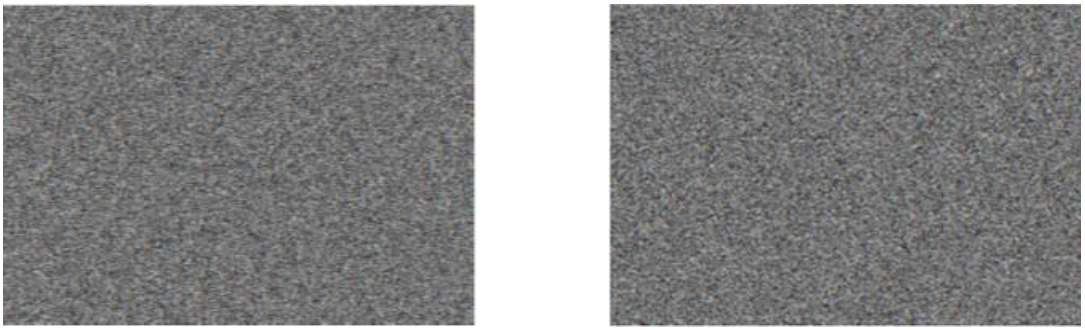

a *b*

Fig. 18. Image in RGB format for the sequence of the first 286000 decimal digits of the numbers: $a - \pi$; $b - e$

Image encryption

Let's apply the above algorithm to image encryption. An image with a height of h pixels and a width of w pixels consists of $n = h \cdot w$ pixels. That is, it is considered as an array of n elements, to each of which a three-dimensional vector of decimal numbers is assigned. These numbers have 15 digits and are enclosed between zero and one. The vector (0, 0, 0) defines a black pixel, and the vector (1, 1, 1) a white pixel. The coordinates characterize the shades of red, green and blue, respectively. Sometimes a fourth coordinate is also considered, which characterizes the transparency of the color.

To encrypt an image, you need to generate a pseudo-chaotic sequence whose elements are enclosed between zero and one, and add it element-wise modulo 1 with the sequences R, G and B. It is clear that instead of one pseudo-chaotic sequence, you can generate three different similar sequences.

Let the sequence $[\mathrm{I}[j]: j = 1..N]$ be generated according to rule (6) or (7) with the corresponding key: $Key = [T, H, \pm\alpha, x_0]$. Let's define the sequence:

$$[\sum_{k=1}^{p} \mathrm{I}[j+k-1] \cdot 10^{-k} : j = 1..N+1-p], \tag{11}$$

where $1 \le p \le 15$ (experiments show that it is sufficient to take $p = 2$ or 3). If T is such that N is less than n, then it is necessary to generate several key sequences (with different keys). Let r – i-th element of the sequence R, α – i-th element of the key sequence. Then the encrypted element $\hat{r}$ in the simplest case will be calculated by the formula:

$$\hat{r} = \{r + \alpha\}, \tag{12}$$

where the function $\{\cdot\}$ means the integer part of the number.

Formula (12) allows for the reverse:

$$r = \begin{cases} \hat{r} - \alpha, & \hat{r} - \alpha > 0; \\ 1 + \hat{r} - \alpha, & \hat{r} - \alpha < 0. \end{cases} \tag{13}$$

Formula (13) allows you to uniquely restore the value of the original pixel from the encrypted value in all cases, except for $\hat{r} - \alpha = 0$. In this case, two options are possible $r = 0$ or 1. In order to exclude ambiguity, you can perform rescaling of the sequences R, G and B: $X \to (1 - \varepsilon)X$, where ε — is a small number, greater than 10^{-15}. Then in the case of $\hat{r} - \alpha = 0$ it is necessary that $r < 1$, i.e. $r = 0$. Physically, rescaling means the absence of pure white. For small ε, this fact practically does not change anything. It is clear that if necessary, you can perform the reverse rescaling $X \to X/(1 - \varepsilon)$.

Let's consider the image presented in Fig. 19. It consists of 238572 pixels ($h = 423$, $w = 564$). For encryption, let's take the key $Key = [223, 2.070811, 0.001, 0.9]$ and generate the key

ISSN 2076-2429 (print)
ISSN 2223-3814 (online)
Proceedings of Odessa Polytechnic University, Issue 2(72), 2025

sequence. It contains 49729 elements. It is necessary to generate additional sequences. Let's do this by choosing the keys $Key_j = [223, 2.07081j,\ 0.001,\ 0.9]$, $j = 2..6$. The combined key sequence contains $49729 \cdot 6 = 298374$ elements, which is sufficient to perform the encryption process. The results of the encryption process using sequences (6), (7). The image encrypted in this way is presented in Fig. 20.

Fig. 19. Test image for encryption

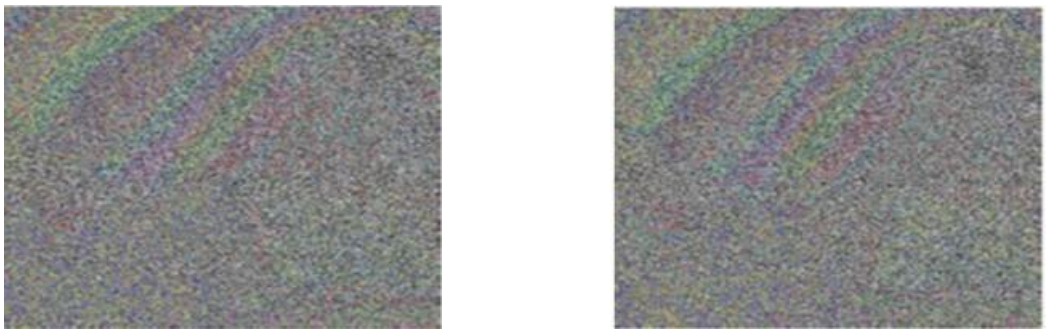

a *b*

Fig. 20. Encrypted test image using sequence (6) (case *a*) and (7) (case *b*)

A regular structure is traced on the encrypted images. If you use a modified version (14), then already for $p = 2$ the encrypted images look without a visible regular structure (Fig. 21).

a *b*

Fig. 21. Encrypted test image using modification (14) for $p = 2$ for sequences: (6) (case *a*) and (7) (case *b*)

Let's consider one more example (the test image is shown in Fig. 22).

ISSN 2076-2429 (print)
ISSN 2223-3814 (online)

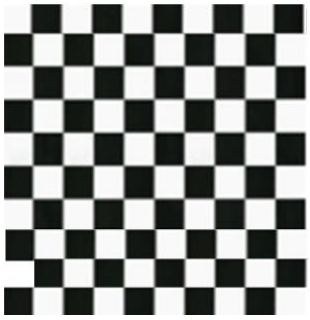

Fig. 22. Test image for encryption

The encryption results are presented in Fig. 23. It can be seen that the simple use of sequences (6) and (7) leads to a regular structure (cases *a*) and *b*). With modification (14) ($p = 2$), the visible regularity of the encrypted image disappears.

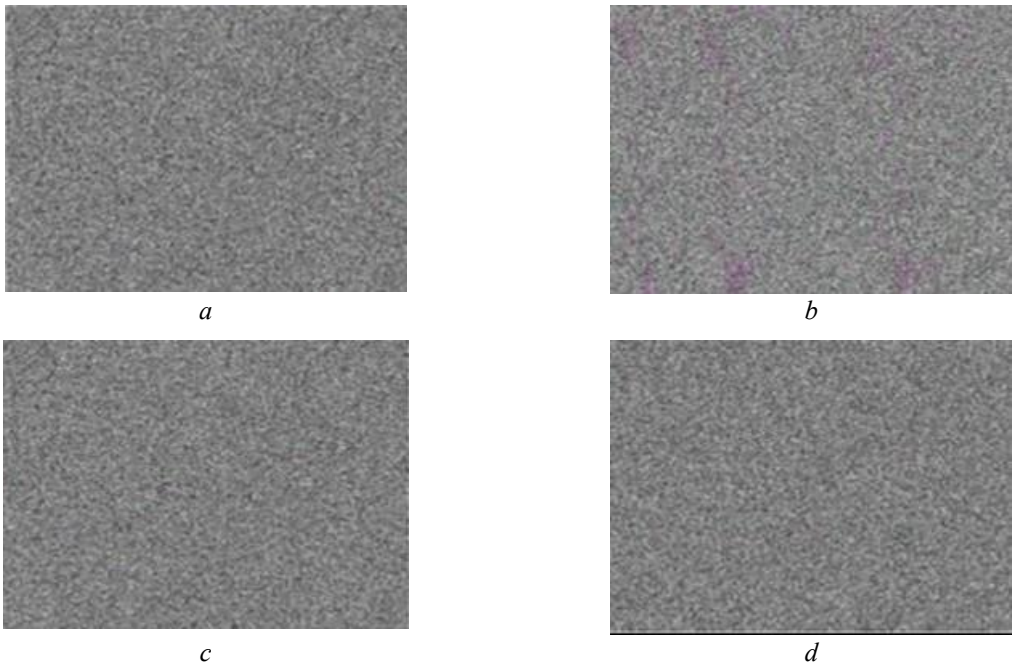

Fig. 23. Encrypted test image for sequences (6) and (7): without modification (cases *a* and *b*); with modification (14) for $p = 2$ (cases *c* and *d*)

Concluding remarks

This paper proposes a new discrete dynamical system for generating long pseudo-chaotic sequences. The system can be used for data encryption, for example, images and information protection from unauthorized access. The advantage of the proposed solution is the short key length and the independence of the algorithm from the hardware and software platform used.

The algorithm for constructing pseudo-chaotic sequences proposed in the article, of course, needs further testing. It is necessary to conduct a detailed correlation analysis of the sequence, an approximate entropy analysis, a statistical test (National Institute of Standards and Technology, USA), etc. It is necessary to additionally conduct an analysis of the security of the keys, an analysis of the statistical histograms of encrypted messages (images), an analysis of sensitivity, an analysis of robustness, an analysis of complexity, etc. [27].

It is also interesting to consider other schemes for stabilizing cycles, for example, [28, 29, 30] and compare them with the scheme proposed in the article.

These are all tasks for further research.

ISSN 2076-2429 (print)
ISSN 2223-3814 (online)
Proceedings of Odessa Polytechnic University, Issue 2(72), 2025

Література

1. Stinson D. R. Cryptography: Theory and Practice. 3rd ed. Boca Raton : Chapman and Hall/CRC, 2006. 593 p.
2. Mao W. Modern Cryptography: Theory and Practice. Upper Saddle River : Pearson Education, 2003. 755 p.
3. Bauer F. L. Decrypted Secrets: Methods and Maxims of Cryptology. 4th ed. Berlin : Springer, 2007. 487 p. DOI: https://doi.org/10.1007/978-3-540-48121-8.
4. Menezes A. J., van Oorschot P. C., Vanstone S. A. Handbook of Applied Cryptology. Boca Raton : CRC Press, 1996. 780 p. URL: https://cacr.uwaterloo.ca/hac.
5. Shannon C. E. A mathematical theory of communication. *Bell System Technical Journal*. 1948. Vol. 27, no. 4. P. 379–423, 623–656. DOI: https://doi.org/10.1002/j.1538-7305.1948.tb01338.x.
6. Zhu C. X. A novel image encryption scheme based on improved hyperchaotic sequences. *Optics Communications*. 2012. Vol. 285, no. 1. P. 29–37. DOI: https://doi.org/10.1016/j.optcom.2011.08.079.
7. Lu Q., Yu L., Zhu C. Symmetric Image Encryption Algorithm Based on a New Product Trigonometric Chaotic Map. *Symmetry*. 2022. Vol. 14, no. 2. Art. 373. DOI: https://doi.org/10.3390/sym14020373.
8. Zhang W., Zhu Z., Yu H. A symmetric image encryption algorithm based on a coupled logistic-Bernoulli map and cellular automata diffusion strategy. *Entropy*. 2019. Vol. 21, no. 5. Art. 504. DOI: https://doi.org/10.3390/e21050504.
9. An Intelligent Session Key-Based Hybrid Lightweight Image Encryption Algorithm Using Logistic-Tent Map and Crossover Operator for Internet of Multimedia Things / M. Gupta et al. *Wireless Personal Communications*. 2021. Vol. 121. P. 1857–1878. DOI: https://doi.org/10.1007/s11277-021-08713-3.
10. Lozi R. Can we trust in numerical computations of chaotic solutions of dynamical systems? *Topology and Dynamics of Chaos* / eds. Ch. Letellier, R. Gilmore. World Scientific, 2013. Vol. 84. P. 63–98. DOI: https://doi.org/10.1142/9789814434928_0003.
11. Shannon C. E. Communication Theory of Secrecy Systems. *Bell System Technical Journal*. 1949. Vol. 28, no. 4. P. 656–715. DOI: https://doi.org/10.1002/j.1538-7305.1949.tb00928.x.
12. Malik D. S., Shah T. Color multiple image encryption scheme based on 3D-chaotic maps. *Mathematics and Computers in Simulation*. 2020. Vol. 178. P. 646–666. DOI: https://doi.org/10.1016/j.matcom.2020.07.011.
13. Öztürk İ., Kılıç R. Utilizing true periodic orbits in chaos-based cryptography. *Nonlinear Dynamics*. 2021. Vol. 103. P. 2805–2818. DOI: https://doi.org/10.1007/s11071-021-06275-w.
14. Image encryption scheme based on blind signature and an improved Lorenz system / G. Ye et al. *Expert Systems with Applications*. 2022. Vol. 205. Art. 117709. DOI: https://doi.org/10.1016/j.eswa.2022.117709.
15. Zhu S., Wang G., Zhu C. A Secure and Fast Image Encryption Scheme based on Double Chaotic S-Boxes. *Entropy*. 2019. Vol. 21, no. 8. Art. 790. DOI: https://doi.org/10.3390/e21080790.
16. An image encryption scheme based on multi-objective optimization and block compressed sensing / X. Chai et al. *Nonlinear Dynamics*. 2022. Vol. 108. P. 2671–2704. DOI: https://doi.org/10.1007/s11071-022-07331-5.
17. Liu L., Wang J. A cluster of 1D quadratic chaotic map and its applications in image encryption. *Mathematics and Computers in Simulation*. 2023. Vol. 204. P. 89–114. DOI: https://doi.org/10.1016/j.matcom.2022.07.027.
18. Dynamic analysis and image encryption application of a sinusoidal-polynomial composite chaotic system / H. Zhu et al. *Mathematics and Computers in Simulation*. 2022. Vol. 198. P. 188–210. DOI: https://doi.org/10.1016/j.matcom.2022.02.027.
19. A New One-Dimensional Compound Chaotic System and Its Application in High-Speed Image Encryption / S. Zhu et al. *Applied Sciences*. 2021. Vol. 11, no. 23. Art. 11206. DOI: https://doi.org/10.3390/app112311206.
20. Complexity analysis of chaotic pseudo-random sequences based on spectral entropy algorithm / K. H. Sun et al. *Acta Physica Sinica*. 2013. Vol. 62, no. 1. Art. 010501. DOI: https://doi.org/10.7498/aps.62.010501.
21. A new hybrid digital chaotic system with applications in image encryption / M. Alawida et al. *Signal Processing*. 2019. Vol. 160. P. 45–58. DOI: https://doi.org/10.1016/j.sigpro.2019.02.016.
22. Adleman L. M. Molecular computation of solutions to combinatorial problems. *Science*. 1994. Vol. 266, no. 5187. P. 1021–1024. DOI: https://doi.org/10.1126/science.7973651.
23. Midoun M. A., Wang X., Talhaoui M. Z. A sensitive dynamic mutual encryption system based on a new 1D chaotic map. *Optics and Lasers in Engineering*. 2021. Vol. 139. Art. 106485. DOI: https://doi.org/10.1016/j.optlaseng.2020.106485.
24. Search for invariant sets of the generalized tent map / K. Ayers et al. *Journal of Difference Equations and Applications*. 2023. Vol. 29, no. 9-12. P. 1156–1183. DOI: https://doi.org/10.1080/10236198.2024.2307521.

ISSN 2076-2429 (print)
ISSN 2223-3814 (online)

25. Elaydi S. N. Discrete Chaos: With Applications in Science and Engineering. 2nd ed. Boca Raton : Chapman & Hall/CRC, 2007. 440 pDmitrishin D., Stokolos A., and Iacob J., Average predictive control for nonlinear discrete dynamical systems, Adv. Syst. Sci. Appl. 20(1) (2020), pp. 27 – 49.
26. Dmitrishin D., Stokolos A., Iacob J. Average predictive control for nonlinear discrete dynamical systems. *Advances in Systems Science and Applications*. 2020. Vol. 20, no. 1. P. 27–49. DOI: https://doi.org/10.25728/assa.2020.20.1.848.
27. Teh J. S., Alawida M., Sii Y. C. Implementation and practical problems of chaos-based cryptography revisited. *Journal of Information Security and Applications*. 2020. Vol. 50. Art. 102421. DOI: https://doi.org/10.1016/j.jisa.2019.102421.
28. Biham O., Wenzel W. Characterization of Unstable Periodic Orbits in Chaotic Attractors and Repellers. *Physical Review Letters*. 1989. Vol. 63, no. 8. P. 819–822. DOI: https://doi.org/10.1103/PhysRevLett.63.819.
29. A new method for finding cycles by semilinear control / D. Dmitrishin et al. *Physics Letters A*. 2019. Vol. 383, no. 16. P. 1871–1878. DOI: https://doi.org/10.1016/j.physleta.2019.03.018.
30. Miller J. R., Yorke J. A. Finding all periodic orbits of maps using Newton methods: sizes of basins. *Physica D: Nonlinear Phenomena*. 2000. Vol. 135, no. 3-4. P. 195–211. DOI: https://doi.org/10.1016/S0167-2789(99)00114-1.

References

1. Stinson, D. R. (2006). *Cryptography: Theory and Practice* (3rd ed.). Chapman and Hall/CRC.
2. Mao, W. (2003). *Modern Cryptography: Theory and Practice*. Pearson Education.
3. Bauer, F. L. (2007). *Decrypted Secrets: Methods and Maxims of Cryptology* (4th ed.). Springer. https://doi.org/10.1007/978-3-540-48121-8.
4. Menezes, A. J., van Oorschot, P. C., & Vanstone, S. A. (1996). *Handbook of Applied Cryptology*. CRC Press. https://cacr.uwaterloo.ca/hac/.
5. Shannon, C. E. (1948). A mathematical theory of communication. *Bell System Technical Journal*, *27*(4), 379–423, 623–656. https://doi.org/10.1002/j.1538-7305.1948.tb01338.x.
6. Zhu, C. X. (2012). A novel image encryption scheme based on improved hyperchaotic sequences. *Optics Communications*, *285*(1), 29–37. https://doi.org/10.1016/j.optcom.2011.08.079.
7. Lu, Q., Yu, L., & Zhu, C. (2022). Symmetric Image Encryption Algorithm Based on a New Product Trigonometric Chaotic Map. *Symmetry*, *14*(2), 373. https://doi.org/10.3390/sym14020373.
8. Zhang, W., Zhu, Z., & Yu, H. (2019). A symmetric image encryption algorithm based on a coupled logistic-Bernoulli map and cellular automata diffusion strategy. *Entropy*, *21*(5), 504. https://doi.org/10.3390/e21050504.
9. Gupta, M., Gupta, K. K., Khosravi, M. R., Shukla, P. K., Kautish, S., & Shankar, A. (2021). An Intelligent Session Key-Based Hybrid Lightweight Image Encryption Algorithm Using Logistic-Tent Map and Crossover Operator for Internet of Multimedia Things. *Wireless Personal Communications*, *121*, 1857–1878. https://doi.org/10.1007/s11277-021-08713-3.
10. Lozi, R. (2013). Can we trust in numerical computations of chaotic solutions of dynamical systems? In Ch. Letellier & R. Gilmore (Eds.), *Topology and Dynamics of Chaos* (Vol. 84, pp. 63–98). World Scientific. https://doi.org/10.1142/9789814434928_0003.
11. Shannon, C. E. (1949). Communication Theory of Secrecy Systems. *Bell System Technical Journal*, *28*(4), 656–715. https://doi.org/10.1002/j.1538-7305.1949.tb00928.x.
12. Malik, D. S., & Shah, T. (2020). Color multiple image encryption scheme based on 3D-chaotic maps. *Mathematics and Computers in Simulation*, *178*, 646–666. https://doi.org/10.1016/j.matcom.2020.07.011.
13. Öztürk, İ., & Kılıç, R. (2021). Utilizing true periodic orbits in chaos-based cryptography. *Nonlinear Dynamics*, *103*, 2805–2818. https://doi.org/10.1007/s11071-021-06275-w.
14. Ye, G., Wu, H., Liu, M., & Shi, Y. (2022). Image encryption scheme based on blind signature and an improved Lorenz system. *Expert Systems with Applications*, *205*, 117709. https://doi.org/10.1016/j.eswa.2022.117709.
15. Zhu, S., Wang, G., & Zhu, C. (2019). A Secure and Fast Image Encryption Scheme based on Double Chaotic S-Boxes. *Entropy*, *21*(8), 790. https://doi.org/10.3390/e21080790.
16. Chai, X., Fu, J., Gan, Z., Lu, Y., & Zhang, Y. (2022). An image encryption scheme based on multi-objective optimization and block compressed sensing. *Nonlinear Dynamics*, *108*, 2671–2704. https://doi.org/10.1007/s11071-022-07331-5.

ISSN 2076-2429 (print)
ISSN 2223-3814 (online)
Proceedings of Odessa Polytechnic University, Issue 2(72), 2025

17. Liu, L., & Wang, J. (2023). A cluster of 1D quadratic chaotic map and its applications in image encryption. *Mathematics and Computers in Simulation*, *204*, 89–114. https://doi.org/10.1016/j.matcom.2022.07.027.
18. Zhu, H., Ge, J., Qi, W., Zhang, X., & Lu, X. (2022). Dynamic analysis and image encryption application of a sinusoidal-polynomial composite chaotic system. *Mathematics and Computers in Simulation*, *198*, 188–210. https://doi.org/10.1016/j.matcom.2022.02.027.
19. Zhu, S., Deng, X., Zhang, W., & Zhu, C. (2021). A New One-Dimensional Compound Chaotic System and Its Application in High-Speed Image Encryption. *Applied Sciences*, *11*(23), 11206. https://doi.org/10.3390/app112311206.
20. Sun, K. H., He, S. B., He, Y., & Yin, L. Z. (2013). Complexity analysis of chaotic pseudo-random sequences based on spectral entropy algorithm. *Acta Physica Sinica*, *62*(1), 010501. https://doi.org/10.7498/aps.62.010501.
21. Alawida, M., Samsudin, A., Teh, J. S., & Alkhawaldeh, R. S. (2019). A new hybrid digital chaotic system with applications in image encryption. *Signal Processing*, *160*, 45–58. https://doi.org/10.1016/j.sigpro.2019.02.016.
22. Adleman, L. M. (1994). Molecular computation of solutions to combinatorial problems. *Science*, *266*(5187), 1021–1024. https://doi.org/10.1126/science.7973651.
23. Midoun, M. A., Wang, X., & Talhaoui, M. Z. (2021). A sensitive dynamic mutual encryption system based on a new 1D chaotic map. *Optics and Lasers in Engineering*, *139*, 106485. https://doi.org/10.1016/j.optlaseng.2020.106485.
24. Ayers, K., Dmitrishin, D., Radunskaya, A., Stokolos, A., & Stokolos, K. (2023). Search for invariant sets of the generalized tent map. *Journal of Difference Equations and Applications*, *29*(9-12), 1156–1183. https://doi.org/10.1080/10236198.2024.2307521.
25. Elaydi, S. N. (2007). *Discrete Chaos: With Applications in Science and Engineering* (2nd ed.). Chapman & Hall/CRC.
26. Dmitrishin, D., Stokolos, A., & Iacob, J. (2020). Average predictive control for nonlinear discrete dynamical systems. *Advances in Systems Science and Applications*, *20*(1), 27–49. https://doi.org/10.25728/assa.2020.20.1.848.
27. Teh, J. S., Alawida, M., & Sii, Y. C. (2020). Implementation and practical problems of chaos-based cryptography revisited. *Journal of Information Security and Applications*, *50*, 102421. https://doi.org/10.1016/j.jisa.2019.102421.
28. Biham, O., & Wenzel, W. (1989). Characterization of Unstable Periodic Orbits in Chaotic Attractors and Repellers. *Physical Review Letters*, *63*(8), 819–822. https://doi.org/10.1103/PhysRevLett.63.819.
29. Dmitrishin, D., Skrinnik, I., Lesaja, G., & Stokolos, A. (2019). A new method for finding cycles by semilinear control. *Physics Letters A*, *383*(16), 1871–1878. https://doi.org/10.1016/j.physleta.2019.03.018.
30. Miller, J. R., & Yorke, J. A. (2000). Finding all periodic orbits of maps using Newton methods: sizes of basins. *Physica D: Nonlinear Phenomena*, *135*(3-4), 195–211. https://doi.org/10.1016/S0167-2789(99)00114-1.

Хамітов Віталій Миколайович; Vitalii Khamitov, ORCID: https://orcid.org/0009-0005-3494-8304,
Антощук Світлана Григорівна; Svitlana Antoshchuk, ORCID: https://orcid.org/0000-0002-9346-145X

Received October 03, 2025

Accepted November 21, 2025

Ministry of Education, Science of Ukraine

Odessa Polytechnic

National University

PROCEEDINGS OF ODESSA POLYTECHNIC UNIVERSITY

(Language: ENG-UKR)

Edition periodicity: two issues annually

Scientific, science and technology collected articles

Issue 2(72), 2025

NATIONAL COUNCIL OF TELEVISION AND RADIO BROADCASTING OF UKRAINE
Assigned Media ID R30-01905
Decision No. 1575 of 12/04/2023
Kyiv, Protocol No. 29

Included in the list of scientific professional titles **category "B"** of Ukraine where the results of PhD and DSc dissertations in the field of technical sciences can be published, by the order of the Ministry of Education, Science of Ukraine dated February 24, 2025, No. 349

A double-blind review method is mandatory for processing of all scientific manuscripts submitted to the editorial board of *"Proceedings of Odessa Polytechnic University"*.

Міністерство освіти і науки України

Національний університет
«Одеська політехніка»

ПРАЦІ ОДЕСЬКОГО ПОЛІТЕХНІЧНОГО УНІВЕРСИТЕТУ

(англійською та українською мовами)

Виходить два рази на рік

Науковий та науково-виробничий збірник

2025, Вип. 2(72)

НАЦІОНАЛЬНОЇ РАДОЙ УКРАЇНИ З ПИТАНЬ ТЕЛЕБАЧЕННЯ І РАДІОМОВЛЕННЯ
Присвоєно Ідентифікатор медіа R30-01905
Рішення № 1575 від 04.12.2023,
м. Київ, Протокол № 29

Внесений до переліку наукових фахових видань **категорія «Б»** України, в яких можуть публікуватися результати дисертаційних робіт на здобуття наукових ступенів доктора і кандидата наук з технічних галузей науки, наказом Міністерства освіти і науки України від 24 лютого 2025 р. № 349

Всі наукові статті, які надійшли до редакції збірника *«Праці Одеського політехнічного університету»,* проходять обов'язкове подвійне сліпе рецензування (ні автори, ні рецензенти не знають один одного).

Editors	Dmytrenko K. Radovska O.	Редактори	Дмитренко К.М. Радовська О.С.
Layout	Prokopovych I.	Комп'ютерне верстання	Прокопович І.В.

Editorial board address:

Odessa Polytechnic
National University,
1 Shevchenko Avenue,
65044 Odesa,
Ukraine.
Tel./fax: +38(048) 705-83-11;
tel.: +38(048)705-83-27; +38(048)705-85-30.
E-mail: pratsi@op.edu.ua
pratsi.opu@gmail.com

Адреса редакції:

Національний університет
«Одеська політехніка»,
пр-т Шевченка, 1,
Одеса, 65044.
Україна
Тел./факс +38(048) 705-83-11;
Тел. +38(048)705-83-27; +38(048)705-85-30.
Електронна адреса: pratsi@op.edu.ua
pratsi.opu@gmail.com

Здано у виробництво 25.12.2025. Підписано до друку 26.12.2025. Формат 60x88/8. Папір офсетн. Гарнітура "TimesNewRoman". Друк цифровий. Ум. др. арк. 23,25. Тираж 300 прим. Зам. № 115/25

Надруковано з готових оригінал-макетів
Національним університетом «Одеська політехніка»

Printed using the layouts prepared at the Odessa Polytechnic National University